Terms and Conditions of Use of Digitised Theses from Trinity College Library Dublin

Copyright statement

All material supplied by Trinity College Library is protected by copyright (under the Copyright and Related Rights Act, 2000 as amended) and other relevant Intellectual Property Rights. By accessing and using a Digitised Thesis from Trinity College Library you acknowledge that all Intellectual Property Rights in any Works supplied are the sole and exclusive property of the copyright and/or other IPR holder. Specific copyright holders may not be explicitly identified. Use of materials from other sources within a thesis should not be construed as a claim over them.

A non-exclusive, non-transferable licence is hereby granted to those using or reproducing, in whole or in part, the material for valid purposes, providing the copyright owners are acknowledged using the normal conventions. Where specific permission to use material is required, this is identified and such permission must be sought from the copyright holder or agency cited.

Liability statement

By using a Digitised Thesis, I accept that Trinity College Dublin bears no legal responsibility for the accuracy, legality or comprehensiveness of materials contained within the thesis, and that Trinity College Dublin accepts no liability for indirect, consequential, or incidental, damages or losses arising from use of the thesis for whatever reason. Information located in a thesis may be subject to specific use constraints, details of which may not be explicitly described. It is the responsibility of potential and actual users to be aware of such constraints and to abide by them. By making use of material from a digitised thesis, you accept these copyright and disclaimer provisions. Where it is brought to the attention of Trinity College Library that there may be a breach of copyright or other restraint, it is the policy to withdraw or take down access to a thesis while the issue is being resolved.

Access Agreement

By using a Digitised Thesis from Trinity College Library you are bound by the following Terms & Conditions. Please read them carefully.

I have read and I understand the following statement: All material supplied via a Digitised Thesis from Trinity College Library is protected by copyright and other intellectual property rights, and duplication or sale of all or part of any of a thesis is not permitted, except that material may be duplicated by you for your research use or for educational purposes in electronic or print form providing the copyright owners are acknowledged using the normal conventions. You must obtain permission for any other use. Electronic or print copies may not be offered, whether for sale or otherwise to anyone. This copy has been supplied on the understanding that it is copyright material and that no quotation from the thesis may be published without proper acknowledgement.

Mathematical Modelling of Diffusion in Physico-Chemical Systems

by

Judith Murphy

B.A. (Mod.)

A Thesis Submitted to
The University of Dublin
for the Degree of

Doctor of Philosophy

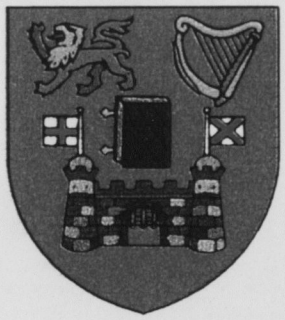

UNIVERSITY CHEMICAL LABORATORY
TRINITY COLLEGE
UNIVERSITY OF DUBLIN

October 1999

Declaration

This thesis has not been submitted as an exercise for a degree at any other University.

Except where otherwise stated, the work described herein has been carried out by the author alone.

Signature of Author ....Judith Murphy.....

Judith Murphy

October 1999

To my parents: Fergus and Margot

Acknowledgements

To begin, I thank my supervisors Prof. J. Corish and Dr. M. E G. Lyons for their good advice, help and encouragement throughout the course of my studies. I am also grateful to Mr. Danny Boyle who initiated this project. A multi-disciplinary project requires help from many disciplines! I am grateful to Dr. J. Greer and Dr. D. Mc Donaill of the Chemistry Department, Dr. J. Sexton and Dr. R. Timoney of the Maths Department, Dr. P. J. Prendergast and Dr. J. Monaghan from Mechanical Engineering and especially Dr. E. Cahill from Hitachi, for both teaching me and then allowing me to use their various pieces of equipment!

The first year of my research brought me to Athlone I.T. Thanks to the many friends I made there - postgrads, staff and flatmates. Back to TCD, thanks to all the residents of G30 – Conor, Des, Geoff, Joe, Marc, Marco, Michael, Paul, Sadikah, Simon C., Stefan and Stuart– for all the 'in-lab' entertainment and for answering my questions time and time again. Thanks also to the other supervisors of our lab: Dr. C. Patterson, Prof. D. Weaire and Dr. S. Bates for social discussions. Thanks to the gang at the Arches –especially Dara for his amazing database of information and Tom for good advice on personal and financial matters! I thank Igor's group for organising the best barbecues!

Thanks to the Graduate Student's Union - especially the committee of 1998/99 (David, Sarah, Treasa, Geoff & Co.) who worked hard to keep the stress levels low and for organising the best social events of the year. Now there is something that I will really miss! Thanks to Prof. J. M. Kelly and to all the academic, technical and administrative staff of the chemistry department for solving my day-to-day hiccoughs. Thanks to all the postgrads in the physics and chemistry departments and to Liz and Catriona for good craic. Special thanks to Robert for technical support as well as everything else...and to Keelin and Ciaran for

listening to me when I was irrational(?) and putting up with all my moaning.

Finally –and most importantly– thanks to my family. Special thanks to Mam and Dad for their moral and financial support during the past twenty two years of my education. (I hope it was worth it.) Thanks also to Keelin, Marita, Nichola, Jeff and Robert have always helped out in times of crisis.

I acknowledge the generosity of Elan, Du Pont and the Krieble fund for providing me with financial assistance.

Summary

The purpose of this thesis was to investigate the usefulness of mathematical modelling as an aid to understanding the physico chemcial processes of iontophoresis in transdermal drug delivery and electrochemical sensor technology. We begin by presenting a general introduction to mathematical modelling. In chapter one we show how it was used in the early stages of mathematics and how it has developed as a powerful tool for a industrial, economic and social disciplines of the modern world. From this we discuss one of our physical systems, paying particular attention to the complexity of the system and the difficulties associated with modelling this.

Chapter 2 outlines the theory of the numerical methods used in solving the systems. We discuss both the finite difference and the finite element method, and show how these methods are implemented in practice. Chapter 3 describes how the finite element package ANSYS was used to simulate the process of transdermal drug delivery. We point out the limitations of this system. and conclude with a general discussion on possible future work that could be carried out in this area.

Chapters 4, 5 and 6 contain the bulk of the simulation work. In each chapter we begin by discussing the system of interest, show how the relevant partial differential equations (PDEs) and boundary conditions are applied, and solve the system either analytically or, if this is not possbile, numerically. We present the results as three dimensional plots of concentration over distance and time as a function of the additional parameters such as migration and reaction which were included in the original PDE. Finally we make some concluding remarks on possible future work that could be carried out in this area.

Contents

List of Figures

List of Tables

Chapter 1

Introduction

1.1 Mathematical Modelling

Mathematical modelling has its origins in the beginning of mathematics, where it was perceived as a practical science. It was used to assist in agricultural endeavours and engineering problems such as surveying methods for canal and reservoir construction. Further advances were made in representing and investigating natural phenomena with the development of calculus in the latter half of the seventeenth century (for an historical review see Eve (1969)). Later, theories to explain complex physical phenomena such as gravitation by Newton, Maxwell's theory of electromagnetic waves and Einstein's theory of relativity were all developed using mathematical models. As the models have become more complex, analytical solutions to the relevant mathematical equations have not been developed and numerical modelling has arisen. Contemporary numerical modelling is performed using computer simulations, and this has advanced greatly in the past twenty years. The reasons for the recent advances in modelling stem from the development of more easily accessible high-level computer languages and the large variety of robust numerical methods available, but most of all from the relatively small (and ever decreasing) cost of computer power. Examples of current

problems where mathematical modelling is useful range from the mechanism of transdermal drug delivery, which is the concern of this thesis, to stock market volatility.

Numerical models can be used to aid understanding of complex physical processes or systems. The system might be economic, social, industrial (Burghes *et al.* (1982)) or, in the case of this thesis, physiochemical. In essence mathematical modelling is the transformation of an idealised form of a real-world situation into mathematical terms and numerical modelling is the practical realisation and approximation of the solution using a computer.

1.1.1 Why use models ?

The usual motivation for modelling a system is to answer a question from one of the following categories:

- system understanding
- system design
- process optimisation
- control

In terms of understanding, biologists may wish to gain an understanding of the interactions between cells in the body. For both ethical and practical reasons, they cannot simply observe the procedure in humans so they make a few observations for a small system and then build a full scale mathematical model based on these. Engineers may wish to improve the design of a plant. In this case, it is cheaper to develop a mathematical model rather than build a physical model and it is also easier to modify the mathematical model. By modifying their mathematical model they can obtain the necessary information to improve the system design and efficiency. Similarly with process engineering - the parameters

in a model process can be varied and their effects can be observed without risk. In the case of a nuclear reactor, it is too dangerous to use trial and error so mathematical modelling is necessary. Furthermore, exhaustive modelling can be used to reduce or eliminate the risk of unforeseen problems occurring. A similar argument holds for process control. Engineers can model extreme variation of the control parameters, observe the results and hence devise safety limits.

The results of modelling are evident in our everyday lives. A topical example of this is the problem of preventing grid-lock in the city traffic (Dym and Ivey (1980)). Maximising traffic flow rates depends on factors such as traffic speed, separation between vehicles, average length of vehicle and number of traffic lights in a given distance. If we use these factors to develop a model to measure flow rate for different switching sequences, we can then maximise the flow rate thereby making the traffic flow more efficient.

1.1.2 Modelling Procedure

The standard procedure involved in modelling is to form a set of mathematical equations to represent the system. For continuous systems, these equations are usually ordinary differential equations (ODEs) and partial differential equations (PDEs). The equations are solved subject to certain boundary/initial conditions and the result is carefully interpreted in order to obtain some physical meaning. Therefore, modelling requires not only the ability to solve complex equations, but also the ability to translate the system description into mathematics and *vice versa.*

There are two classifications of models - steady state and dynamic. A system with spatial complexities is usually modelled at steady state and, if insufficient information is obtained from this, it is then modelled over time. In this work, we will see that the static model is insufficient and therefore our models include time dependencies.

1.1.3 Diffusion Models

This thesis is focussed on macroscopic models of diffusion and their applications to transdermal drug delivery and electrochemical sensor technology. The diffusion equation is a partial differential equation relating change of material flux with respect to distance to rate of change of material concentration with respect to time. This type of system also describes phenomena such as weather variations. In addition to the numerous applications in physics and chemistry, another area of current interest is financial modelling. Diffusion models have provided the basic statistical models for financial research in the past 25 years. In particular the Black-Scholes model (Black and Scholes (1973), used to value options, is based on microscopic diffusion via Brownian motion and a random walk behaviour (Rossi (1996)). The main result of the Black-Scholes model is that the stock price, S_t, is governed by the following equation:

$$dS_t = \alpha(t)S_t dt + \sigma(t)S_t dB_t \tag{1.1}$$

This illustrates that the growth rate $\frac{dS_t}{S_t}$ is the sum of a deterministic term $\alpha(t)dt$ and a random term $\sigma(t)dB_t$. The function $\sigma(t)$ is known as the volatility of the stock and the random term dB_t is Brownian motion. This example serves to illustrate the scope and diversity of diffusion models.

1.1.4 Conclusion

Mathematical modelling is primarily the use of abstractions as an aid in understanding the behaviour of complex systems. Providing that these abstractions represent a good approximation to the system, a wealth of useful information can be obtained. However, it must not be forgotten that models are *abstractions* and must not be confused with reality. It is important to be aware of the limitations of modelling. For example, the classic model of the solar system describing cir-

cular paths of the planets with the earth as centre was successful in explaining phenomena such as day and night, and the seasons. However, when Copernicus modified this model and explained the solar system as we know it today, his theory was not accepted. In this case the existing model had become confused with the truth and it served to retard rather than progress knowledge.

There are two systems of interest to us in this work. The first is a transdermal drug delivery system, and the second is mediated electrocatalysis. As has been mentioned above, the solution of the differential equations is as important as the ability to translate the physical system into the mathematical equations. Therefore, we must start by understanding the physical systems. These will be discussed at length in the relevant chapters but we will continue now by briefly introducing both systems and showing how the pertinent differential equations are developed.

1.2 Transdermal Drug Delivery

The recent development of the transdermal patch as a means of controlled release of a drug into the body through the skin is marked as a major advance in the field of drug delivery (Sanders (1985)). Extensive research, development and marketing by commercial companies such as ELAN Corporation plc and Ciba Geigy have ensured that products such as the nicotine patch have, by now, become a common household name.

However, despite that fact that it is known what happens as a drug migrates from an external source into the skin, and why these processes occur, relatively little is understood about their detailed mechanisms. There are a number of reasons for this which range from the failure to develop adequate mathematical models to the pressure always apparent in the development of commercial products.

One purpose of this thesis is to add to such knowledge and, in particular,

to pay attention to the processes that occur when drug transport is assisted by an applied electric potential *i.e.* when the drug transport is iontophoretically assisted.

The model will consist of a vehicle containing the drug and the skin onto which the drug is applied. The PDE describes movement of the drug from the vehicle into the skin. If we are interested in the amount of drug entering the skin, then the most useful information comes from time-lag and transient kinetic studies on which the experimental research in the literature has been focussed. This will be discussed in detail in chapter 5.

1.3 Chemical Sensors

The term chemical sensor defines the general class of self-contained, reversible devices that are used to quantify specific analytes within a complex sample milieu. In the simplest configuration, a chemical recognition element is used in conjunction with some form of transducer system. When the immobilized recognition element (*e.g.* a biomolecule) interacts with the target analyte, a change is induced in the recognition element that is measured by the transducer (Bright (1999)).

Chemical sensors are being used in many applications ranging from manufacturing, industrial and automotive processing, and combustion control, to environmental and personal space monitoring. They are based on the principle of converting a chemical reaction into a measurable physical property -usually an electrical signal. They are particularly advantageous because of their low cost and are therefore seen as alternatives to large analytical tools such as optical spectrometers (Post (1999)). The integration of electrochemically active thin films with conventional integrated circuits creates integrated circuit chemical microsensors which have advantages of the minimization and robustness of solid-state devices. The addition of real-time monitoring to these attributes,

make chemical sensors particularly attractive for bio-medical applications.

In chapter 6 of this thesis we will look at the process of diffusion, migration and reaction in polymer thin films. We will see how the concentration of a substrate changes across the width of the film and develop expressions for the experimentally measurable quantity - the current response - as a function of concentration.

1.4 Theoretical Analysis of Diffusion

In this final section we take a look at the theory of diffusion. We start with a very general description of matter transport in condensed media. We will see how the flux analysis leads us to a partial differential equation (PDE) and we will then discuss the best method of solving this PDE. Finally we will look at the analogies between this diffusion equation and that relating to heat conduction and then conclude with a brief discussion on the use and application of diffusion in other branches of physics and chemistry. We begin therefore with an *ab initio* derivation of the diffusion equation.

1.4.1 Matter transport in Condensed media

Consider the motion of particles contained within a specified volume Ω as shown in figure 1-1.

The flux of the particles - rate of transport - is described by the following equation

$$\vec{J} = -\frac{cD}{RT}\nabla\tilde{\mu} \tag{1.2}$$

where c is the concentration of the species, D is its diffusion coefficient, R is the universal gas constant ($= 8.314\ J\ mol^{-1}\ K^{-1}$), T is temperature and $\tilde{\mu}$ is the electrochemical potential of the diffusant. This is known as the Nernst-Planck equation first described by Planck (1890).

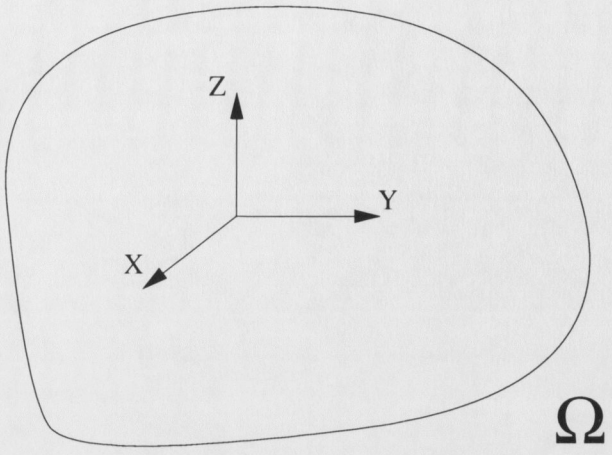

Figure 1-1: Schematic representation of particle motion

In the presence of both a chemical potential and an electrostatic potential, $\tilde{\mu}$ is the sum of the two potentials as follows

$$\tilde{\mu} = \mu + zF\psi \tag{1.3}$$

In this case μ denotes the chemical potential and the electrostatic potential is given by the product of the valency z the Faraday constant F and the galvanic potential ψ.

Therefore equation (1.2) becomes

$$\vec{J} = -\frac{cD}{RT}(\nabla\mu + zF\nabla\psi) \tag{1.4}$$

For ideal-dilute solutions, μ may be related to the activity of diffusant, a, by invoking Henry's Law (Atkins (1994)) as follows:

$$\mu = \mu^0 + RT\ln a \tag{1.5}$$

where μ^0 is the chemical potential of the pure substance.

The activity is related to the concentration c by $a = \gamma c$ where $0 < \gamma < 1$ and

therefore $a \to c$ as $\gamma \to 1$. We will therefore make the approximation that activity can be replaced by concentration. It should be noted that, in fact, Henry's law is not valid for charged species since there will always be solute solvent interactions. These calculations, therefore, while strictly no valid for the conditions described, are useful to get a handle on the process.

The expression for the flux therefore becomes

$$\vec{J} = -cD\nabla \ln c - \frac{zFcD}{RT}\nabla\psi \tag{1.6}$$

If we assume that the electric field is constant within the volume, then $-\nabla\psi$ can be set equal to a constant (E_0) and the noting that $c\nabla \ln c = \nabla c$, equation (1.6) is simplified to

$$\vec{J} = D\nabla c + \frac{zFcD}{RT}E_0 \tag{1.7}$$

Applying continuity requirements, we see that the rate of change of concentration is equal to the gradient of the flux.

$$\frac{\partial c}{\partial t} = -\nabla\vec{J} \tag{1.8}$$

The negative sign is accountable by the fact that we are looking at the transport of particles out of rather than into a region of interest Ω. In terms of measurable quantities therefore, the rate of change of concentration is

$$\frac{\partial c}{\partial t} = \nabla[D\nabla c - \frac{zFcD}{RT}E_0] \tag{1.9}$$

If, in addition to migration, the particles also undergo chemical reaction within the volume Ω, then an extra term $-k\ c$ must be added to equation (1.9) where k is the reaction rate constant. For simple first order reactions, k is a constant and this gives us a linear differential equation. For higher order reactions, k can be a polynomial function of c, thereby leading to a more difficult non-linear

differential equation. This enables us to describe mathematically any diffusion reaction system such as those described by Ludloph *et al.* (1979) and Lyons *et al.* (1996, 1999).

In most cases, the diffusion coefficient D is constant across the substance so for diffusion-migration and chemical reaction, the diffusion equation is

$$\frac{\partial c}{\partial t} = D\nabla^2 c - \frac{zFDE_0}{RT}\nabla c - kc \tag{1.10}$$

We note that this is a co-ordinate free representation and the particular form of ∇ will depend on whether the geometry is planar, cylindrical or spherical. For a planar diffusion, we see that equation (1.10) becomes

$$\frac{\partial c}{\partial t} = D[\frac{\partial^2 c}{\partial x^2} + \frac{\partial^2 c}{\partial y^2} + \frac{\partial^2 c}{\partial z^2}] - \frac{zFDE_0}{RT}[\frac{\partial c}{\partial x} + \frac{\partial c}{\partial y} + \frac{\partial c}{\partial z}] - kc \tag{1.11}$$

This is a partial differential equation, the solution of which gives the concentration of the particles at a particular time at any point in space.

For the purposes of this thesis, we will examine diffusion-migration and reaction in one dimension only. This situation will pertain for material transport through membranes and thin films. It can be seen that even at this simple level the equations and solutions are very complex. For this case equation (1.11) reduces to a more manageable

$$\frac{\partial c}{\partial t} = D\frac{\partial^2 c}{\partial x^2} - \frac{zFDE_0}{RT}\frac{\partial c}{\partial x} - kc \tag{1.12}$$

This partial differential equation can be solved to obtain an expression for the concentration profile of the diffusant as a function of time. This expression may then be manipulated to obtain a closed form expression for the total quantity of material entering or exiting the membrane at any given time, and therefore the lag time and the permeability can be determined. Typically there will be a lag time before steady state conditions are reached. The permeability is a measure

of the steady state rate of material transport through the membrane. Both of these quantities in addition to the total amount entering or exiting may, of course be determined by experiment. The solution of such a PDE is the main topic of the next chapter. We will continue here by drawing an analogy between heat conduction and diffusion.

1.4.2 Heat conduction/Diffusion Analogy

The first law of thermodynamics states than energy is conserved. Heat transport in solids is described essentially by the following general equation (Incropera and DeWill (1996)) which is derived from this law:

$$\frac{\partial T}{\partial t} = \frac{K}{\rho c}\nabla^2 T + v_x \nabla T - \frac{q'''}{\rho c} \tag{1.13}$$

where T is the temperature, t is the time, K is the thermal conductivity, ρ is the density, c is the heat capacity of the solid and x is the distance from the heat source. The velocity of mass transfer is v_x, and the heat generation rate per unit volume is denoted by q'''. Equation (1.13) describes heat transport via conduction and convection. If however, there is no convection, equation (1.13) reduces to

$$\frac{\partial T}{\partial t} = \frac{K}{\rho c}\nabla^2 T \tag{1.14}$$

Reducing this to one-dimension it becomes

$$\frac{\partial T}{\partial t} = \frac{K}{\rho c}\frac{\partial^2 T}{\partial x^2} \tag{1.15}$$

In considering *passive* diffusion of matter (*i.e.* without electrical assistance or chemical reactions –the diffusion equation is

$$\frac{\partial c}{\partial t} = D\frac{\partial^2 c}{\partial x^2} \tag{1.16}$$

It is clear that the temperature in equation (1.15) corresponds to concentration in equation (1.16) while the diffusion constant D is analogous to $\frac{K}{\rho c}$. By assigning a constant value of 1 to both ρ and c, D can then equated with K. It is therefore possible to simulate passive electrical diffusion using a package designed for heat conduction where the diffusion constant is input as the thermal conductivity of the material.

The case of electrically assisted diffusion is more complicated. The diffusion equation associated with this is

$$\frac{\partial c}{\partial t} = D\frac{\partial^2 c}{\partial x^2} - \frac{ZFDE_0}{RT}\frac{\partial c}{\partial x} \tag{1.17}$$

The terms Z, F, D, E_0, R and T have already been defined. For simplicity, the term $\frac{ZFDE_0}{RT}$is denoted by a constant β. Equation (1.17) then becomes

$$\frac{\partial c}{\partial t} = D\frac{\partial^2 c}{\partial x^2} - \beta\frac{\partial c}{\partial x} \tag{1.18}$$

The general heat transfer equation, equation (1.13), reduces to one dimension as:

$$\frac{\partial T}{\partial t} = \frac{K}{\rho c}\frac{\partial^2 T}{\partial x^2} + v_x\frac{\partial T}{\partial x} - \frac{q'''}{\rho c} \tag{1.19}$$

Comparing with equation (1.18) it is clear that β is analogous to v_x and the term $\frac{q'''}{\rho c}$ is zero. Since we have already defined ρ and c as having a value 1, that means that q''' in this case is zero. In the mathematics at least, v_x, the velocity of mass transfer should equate with β. Therefore in simulating electrically assisted diffusion using a thermal analysis package, the simulation is carried out as for the case of simple diffusion. An additional parameter, v_x, was included in this simulation to account for the electrical parameter β.

1.4.3 Measuring Diffusion Coefficients

The choice of method for measuring the diffusion coefficient of a substance depends on the physical state of the diffusant and the medium through which it is diffusing. Diffusion of matter in solid media can be measured by monitoring the change in conductivity of the substance migrates through the solid. The diffusion coefficient of gases can be measured by the flow method (Harteck and Schmidt (1933)) or by optical methods (Klotz and Miller (1947)). The diffusion coefficients of liquids may be measured using the diaphragm cell method (Northrup and Anson (1929)), the Lamm's scale method (Lamm (1939)) or optical methods among others. Dennis (1968) has shown how diffusion coefficients can be determined by changes in concentration of a solution placed above a gel.

1.5 Scope of diffusion studies

Other work in the general area of diffusion includes that by Mysels and co-workers (Mysels (1982), Frisch and Mysels (1983)) who model adsorption from solution. In addition to scientific interest, this field is of practical importance in that it plays a role in detergency, flotation and drug administration. The mechanism of adsorption from solution is not fully understood. Early models were based on adsorption on a plane in a quiescent solution. From these models, numerical solutions were obtained describing the concentration changes over time. For ideal adsorption isotherms, it was possible to obtain exact solutions for the change in concentration. Later, Mysels and Frisch (1984) refined the model by including a film of liquid at the surface of the adsorbent and solving the system for ideal adsorption isotherm.

Some researchers have looked at passive diffusion in non-homogeneous media, (non-ideal membrane diffusion) where there is a gradation in diffusion properties along the axis of diffusion (Grztwna and Pertropoulos (1983a,b)). In accordance

with diffusion in heterogeneous media the most useful studies of these systems are done using time lag (Pertropoulos and Roussis (1967)) and transient state kinetic analysis (Tsimillis and Pertropoulos (1967)). Higuchi and Higuchi (1960) have done some theoretical analysis on diffusion through heterogeneous barriers in an attempt to more accurately model drug delivery into the skin. They consider however a simple case of a two phase mixture, each phase having a characteristic diffusion coefficient rather than the more complicated case mentioned above where the diffusion coefficient is continuously varying through the medium.

A non-linear diffusion equation must be used to describe certain phenomena such as heat conduction in solid H_2 (Rosen (1979)). The solutions to such equations are as expected, a good deal more complex than the linear case, as demonstrated by several reports in the literature (Berryman (1980); Berryman and Holland (1982); Stephenson (1995)).

1.6 Overview

The purpose of this thesis is to investigate the usefulness of mathematical modelling as an aid to understanding the physico chemical processes of iontophoresis in transdermal drug delivery and electrochemical sensor technology. In this chapter we have set the scene by showing how mathematical modelling has developed and how its applications cover a broad range of disciplines. In chapter two we will outline the theory of the numerical methods used in solving the systems. We discuss both the finite difference and the finite element method, and show how these methods are implemented in practice.

Chapter three traces initial work done at the beginning of the project, discussing the attempts to model electro-transdermal drug delivery using a finite element package designed for modelling heat conduction. We point out the limitations of this system and indicate how the work could be expanded in the future. The aim was to examine drug migration from an external patch and into the in-

dividual layers of the skin. We therefore present a detailed discussion on the physical nature of the skin and its electrical properties, before illustrating and analysing the results. It soon became apparent that ANSYS was not as versatile or as well equipped as was necessary to solve our diffusion problems and a new direction was therefore taken. The problems of diffusion solved analytically where possible, and, where necessary by the finite difference method and the finite difference package DEQSOL.

Chapters four five and six contain the bulk of the simulation work. Each chapter begins with a discussion of the system of interest and a review the work to date. We then show how the relevant partial differential equations (PDEs) and boundary conditions are applied, and solve the system either analytically or, if this is not possible, numerically. The results are presented as three dimensional plots of concentration over distance and time as a function of the additional parameters such as migration and reaction which were included in the original PDE.

In chapter seven the general conclusions that can be drawn from the study and their implications for further study and understanding of the system are discussed.

Chapter 2

Theory

2.1 Introduction

This chapter explores two different methods of solving the diffusion equation numerically. We discuss the use of Finite Difference and Finite Element Methods. Specific reference is made to the accuracy of the numerical techniques in terms of justifying the results obtained. We begin with a review on the classification of partial differential equations.

2.1.1 Classification of PDE's

The diffusion equation is a second order Partial Differential Equation (PDE). Partial differential Equations (PDE's) are divided into one of three classes according to their characteristic. The *characteristics* are defined by the roots of the *characteristic* equation. Hyperbolic equations have two real roots, parabolic equations have one real root and elliptical equations have complex roots or characteristics.

The generic second order PDE is as follows:

$$A\frac{\partial^2 c}{\partial x^2} + B\frac{\partial^2 c}{\partial x \partial y} + C\frac{\partial^2 c}{\partial y^2} = f(x, y, c, \frac{\partial c}{\partial x}, \frac{\partial c}{\partial y}) \tag{2.1}$$

and its characteristic equation is

$$A\left(\frac{\partial y}{\partial x}\right)^2 + B\frac{\partial y}{\partial x} + C = 0 \tag{2.2}$$

In the case of the diffusion equation, A has a value of 1, B has a value of zero and C has a value of zero or 1, depending on whether the problem is in one or two dimensions.

There is one characteristic for the diffusion equation : $\frac{\mathrm{d}y}{\mathrm{d}x} = w$ where w is a constant. Therefore, based on its characteristics, the diffusion equation is parabolic.

PDE's are also classified into initial value problems and boundary value problems. Initial value problems describe how the solution $c(x,t)$ propagates itself forward in time. In contrast boundary value problems aim to find a static function $c(x,y)$ which has some desired behaviour on the boundary. The diffusion problem is therefore an initial value problem.

2.1.2 General considerations

It is always preferable to find an analytical solution rather than a numerical solution to a PDE. Analytical solutions are exact whereas numerical solutions, no matter how advanced or accurate, will always remain as approximations. In many cases it is not possible to obtain an analytical solution to a particular problem and in such a case numerical methods can be powerful tools. Several general mathematics textbooks (*e.g.*Kreyzig (1993)) describe in detail the methods used for obtaining analytical solutions of PDE's. These include the methods of Separation of Variables, Laplace Transforms and Fourier transforms - all of which are used in this work and outlined in detail in Appendix B.

Depending on the class of the PDE, different numerical methods will suit more than others. For example, finite difference methods are used for initial value problems whereas the finite element method is more suitable for boundary

value problems. A variety of textbooks discuss the numerical methods of solving ordinary and partial differential equations (Prenter (1975); Sewell (1988)). In the following sections we discuss the Finite Difference Method and details of the finite difference package DEQSOL which was used in calculations. Then there is a description of the finite element method (FEM). Finally, as a benchmark experiment we look at a comparison of the numerical solution of the simple diffusion equation obtained using the finite difference method with the analytical solution (obtained using Laplace transforms) to illustrate the accuracy of this numerical method.

2.2 The Finite Difference Method

All numerical methods involve simplifying and discretising the problem. Of these, the Finite Difference Method is the simplest and the easiest to program. Because of its simplicity, it is the most widely used numerical method by electrochemists (Britz (1981); Pons (1984)) having been introduced by Feldberg (1969) in the 1960's. In the finite difference method, Taylor's theorem is used to rewrite the partial differential equations that govern the behaviour of the system in terms of difference equations. The initial and boundary conditions pertaining to the PDE are applied to the difference equations which are then solved. The solutions to these difference equations are analytical and provided that they are close to the differential equation, their solution will represent a good approximation to the solution of the differential equation. We will now show how typical finite difference equations are developed.

2.3 Forward, Backward and Central Difference

Consider an arbitrary function $f(x)$ shown in figure 2-1. If $f(x)$ and its derivatives f_x, f_{xx} etc. are finite continuous and single valued, then we may do a Taylor

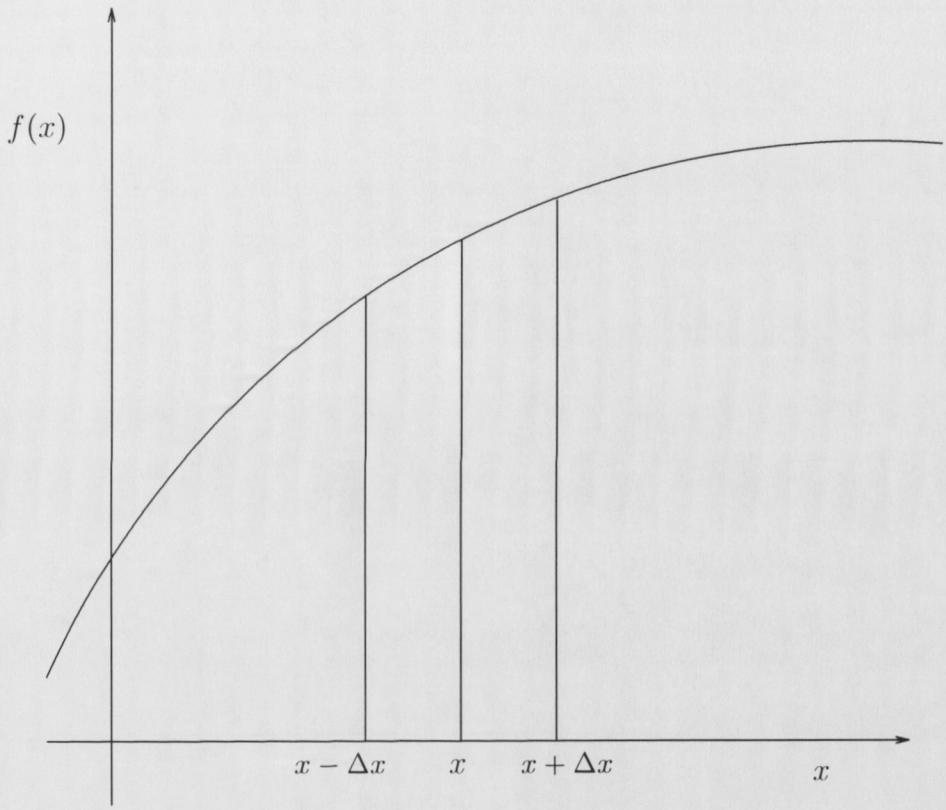

Figure 2-1: Graph of an arbitrary function $f(x)$

expansion and express $f(x + \Delta x)$ as a sum of its derivatives as follows:

$$f(x + \Delta x) = f(x) + \Delta x f'(x) + \frac{\Delta x^2}{2!} f''(x) + ... + \frac{\Delta x^n}{n!} f^n(x) + ... \quad (2.3)$$

In this way we have expressed the derivatives of x in terms of the the value of the function $f(x)$ at x and at a step Δx ahead of x.

The Taylor expansion for the backward step is

$$f(x - \Delta x) = f(x) - \Delta x f'(x) + \frac{\Delta x^2}{2!} f''(x) + ... + (-1)^n \frac{\Delta x^n}{n!} f^n(x) + ... \quad (2.4)$$

If we take the first two terms in either of the expansions and ignore the rest some algebraic manipulation leads to an approximation for f_x. The first equation yields a forward difference approximation since we have used the value of the function at a point in front of f_x in order to find the derivative at x. The second equation leads to the backward difference approximation.

Both of these approximations are only first order. To get a second order approximation for f_x we can add the equations and get the central difference. Expressions for the second and subsequent derivatives are obtained in a similar manner. They are summarised in table 2.1. We will now illustrate the use of the finite difference method in solving the diffusion equation.

2.4 The diffusion equation as a difference equation

The simple Fick diffusion equation (Atkins (1994)) is as follows:

$$\frac{\partial c(x,t)}{\partial t} = D \frac{\partial^2 c(x,t)}{\partial^2 x} \quad (2.5)$$

Approximation	Equation	Accuracy
Forward difference (First derivative)	$f_x = \frac{f(x+\Delta x)-f(x)}{\Delta x}$	1^{st} order
Backward difference	$f_x = \frac{f(x)-f(x-\Delta x)}{\Delta x}$	1^{st} order
Central difference	$f_x = \frac{f(x+\Delta x)-f(x-\Delta x)}{2\Delta x}$	2^{nd} order
Central difference (Second derivative)	$f_{xx} = \frac{f(x+\Delta x)+2f(x)-f(x-\Delta x)}{\Delta x^2}$	2^{nd} order

Table 2.1: Summary of various finite difference approximations

Since the concentration c is a function of two variables (i.e. space and time), a two dimensional grid is made up of distance and time coordinates. If the time interval is Δt, and the distance interval Δx, then the spacings between adjacent points on the grid are Δt and Δx. The distance and time coordinates are then given by

$$x_j = x_0 + j\Delta x \qquad \text{and} \qquad t_n = t_0 + n\Delta t$$

Each point on the grid may then be defined by

$$c_j^n = c(j\Delta x, n\Delta t) \tag{2.6}$$

To perform the discretisation, we use a forward difference in time and a central difference in space, as shown in table 2.1 The discrete form of the diffusion equation is

$$\frac{c_j^{n+1} - c_j^n}{\Delta t} = \frac{D(c_{j+1}^n - 2c_j^n + c_{j-1}^n)}{\Delta x^2} \tag{2.7}$$

2.5 Analysis of Numerical Schemes

The accuracy of a numerical scheme depends on three concepts. These are consistency, stability and convergence. By consistency we mean that in the limit of small step size, the difference equation should tend to the differential equation. Stability requires that difference between the computed solution and the exact solution to the difference equation does not diverge or grow without bound. Convergence requires that in the limit of small step size, the computed solution should tend to the analytical solution of the differential equation.

In the case of the diffusion equation, Lax's Fundamental Equivalence theorem allows stability to be a sufficient condition for convergence. By taking limits as the step size approaches zero, it is easy to show that the diffusion equation is consistent. The discussion here will therefore focus on the stability of this numerical scheme.

2.5.1 Stability Analysis

In analysing the stability of the scheme, one first of all finds the round-off error - the difference between the exact solution of the discrete equation and the computed solution. If the error satisfies the discrete equation, the scheme will be stable on the condition that the error does not grow without bound. The diffusion equation is a linear equation with constant coefficients and is therefore suitable for von Neumann stability analysis. This technique involves decomposing the error into a Fourier series. One harmonic of the Fourier series is then substituted into the discrete equation. If we require that any harmonic is not amplified by the scheme, the requirements for stability are satisfied.

To illustrate how the error is dependent on the time-step we look at the discrete form of the time derivative

$$\frac{\partial c}{\partial t} = \frac{c_j^{n+1} - c_j^n}{\Delta t} + O(\Delta t) \tag{2.8}$$

The difference between the derivative and the discrete form is an error term to the order of Δt. Therefore, minimizing the time-step will minimize the error.

The discretised form of the diffusion equation equation (2.7) is forward difference in time (FT) and central difference in space (CS). The FTCS scheme is first order in time, second order in space and is a fully explicit scheme since all information about c_j^{n+1} comes from points preceding it. However, von Neumann stability analysis shows that this is unstable for time steps larger than approximately $\frac{\Delta x^2}{D}$. These time steps are both prohibitively small and too computationally expensive so a new scheme - Crank-Nicholson (Press *et al.* (1992))- is used.

2.5.2 Crank-Nicholson Scheme

In the Crank-Nicholson scheme, the discretised spatial equations are moved one time step forward relative to the discretised time equations. The resulting discretised equation is as follows:

$$\frac{c_j^{n+1} - c_j^n}{\Delta t} = \frac{D(c_{j+1}^{n+1} - 2c_j^{n+1} + c_{j-1}^{n+1})}{\Delta x^2} \tag{2.9}$$

The advantage of this is that we now have no restrictions on the size of the time step. This is because it can be shown (Press *et al.* (1992)) that absolute value of the amplification factor (the condition for stability) is always less than 1, consequently the scheme is unconditionally stable. However, there is a trade-off. The Crank-Nicholson scheme is fully implicit which means that the details of small-scale evolution from the initial conditions are inaccurate for large time steps.

For a two-dimensional analysis, a more generalised form of Crank Nicholson is necessary. The alternating direct implicit method (ADI) involves splitting the time step in two thereby creating two sub-steps. In each sub-step, a different dimension is treated implicitly.

2.5.3 DEQSOL

DEQSOL is an acronym for Differential EQuation SOlver Language. It is a software package developed by HITACHI for the purpose of solving Partial differential equations by means of either the Finite Difference or the Finite Element method. On presentation of an input file, the DEQSOL translator generates a FORTRAN program which is then compiled and run in the usual way. The input file must have the following structure:

Statement of: the beginning of the program the method used (FDM or FEM)
Statement of: the spatial domain the spatial grid size the time the time-step
Statement of: the region used for the calculation the variables to be used the values of constants the boundary conditions the initial conditions
Statement of: the beginning of the solver procedure the solver procedure the end of the solver procedure
Statement of: writing or printing the output data the end of the program

The DEQSOL system therefore offers problem definition, solver description, result manifestation, program connection and file input and output.

The problem definition function allows the user to define the problem region, the variable to which a solution is to be obtained, and the conditions for problem resolution based on user supplied data (*e.g.*space, time co-ordinates, physical constants, variables, partial differential equations boundary and initial conditions). The solver description function enables a solution to be obtained by dividing the computational region automatically and solving the discretised equation according to the predefined procedure (*e.g.* Gaussian elimination). The result manifestation allows the data to be printed or passed to a graphics program. The program connection facility allows DEQSOL programs to be changed to subroutines and so the DEQSOL program may be connected to a user created main program. A sample DEQSOL file is included in Appendix A.1.

2.5.4 Applications of Numerical Methods in Electrochemistry

In addition to being useful for solving PDE's related to drug diffusion, the finite difference method has many other interesting applications especially in the general area of electrochemistry. Lasia (1985) has looked at applications of FDM to cyclic voltammetry. In an earlier publication (Lasia (1983)), he used the Crank-Nicholson method for examining dimerisation.

Orthogonal collocation has been used for characterising diffusion at microelectrodes (Cassidy *et al.* (1983)) and in other electroanalytical problems (Speiser and Pons (1983, 1982a,b); Cassidy *et al.* (1985)). This technique involves approximating the solution of a PDE to the weighted sum of polynomials and then solving the system for the coefficients of these polynomials.

Rudolph (1990) used the ADI for simulation of electrochemical processes. Feldberg (1981) refined an exponentially expanding grid method, previously de-

scribed by Joslin and Pletcher (1974) for the digital simulation of electrochemical problems.

2.6 The Finite Element Method

2.6.1 Origin of the FEM

The finite element method was first conceptualised in the 1960's by engineers to solve problems of heat flow and stress analysis (Zienkiewicz and Cheung (1965)). From this mathematicians attempted to put a rigorous mathematical basis on it Clough (1960). In essence, finite element analysis developed as an adaption of the calculus of variations to suit data evaluation by computer. Good introductory books on this method include Becker (1981); Davies (1980); Lewis and Ward (1991) and Heubner and Thornton (1982).

2.6.2 Difference between FDM and FEM

Whereas the finite difference method gives a point-wise approximation, the need arose to introduce a tool for dealing with irregular geometries or unusual specification of boundary conditions. In the finite difference method the solution region is modelled as a set of points, but the finite element method it is a set of subregions or elements. The finite difference method gives a point-wise approximation whereas the finite element method gives a piecewise approximation.

2.6.3 Theory of FEM

In a continuum problem, the field variable (concentration, temperature etc.) will have an infinite number of values and therefore there are an infinite number of unknowns. Using the finite element method, the solution region is divided into a finite number of elements and therefore a finite number of unknowns. The

field variable is then expressed in terms of assumed approximate functions called interpolation functions. These functions are defined in terms of the field variables at specified points called nodes. Nodes usually lie on element boundaries although it is possible also to have internal nodes .

The nodal values of the field variables define the behaviour of the field completely within the element. In a finite element representation of the problem, the nodal variables become the new unknowns. Once these unknowns are found, the interpolation functions define the field variable throughout the assemblage of elements.

Since the finite element method was developed by mathematicians, scientists and engineers, various different approaches are taken to calculations. These include the direct approach, the variational approach, the weighted residuals approach and the energy balance approach. The ANSYS program uses the variational approach. Regardless of which approach is chosen, the same basic steps are involved in implementing the FEM. They are described below as follows:

2.6.4 Steps involved in implementing the FEM

The continuum is first discretised into sub-domains called elements. Nodes are assigned to each element and interpolation functions are chosen to represent the element behaviour. The interpolation function is usually a polynomial since these are easy to differentiate and integrate. The degree of the polynomial depends on the number assigned to each element and the continuity requirements. Next, matrices representing element properties are defined. The individual element matrices must be assembled together to produce the entire region which is then solved. Finally additional computation such as error estimation are made to complete the process.

Assume we have a domain Ω as in figure 2-2(a). The domain is divided into triangular elements as in figure 2-2(b). The vertices of each triangle are the nodes

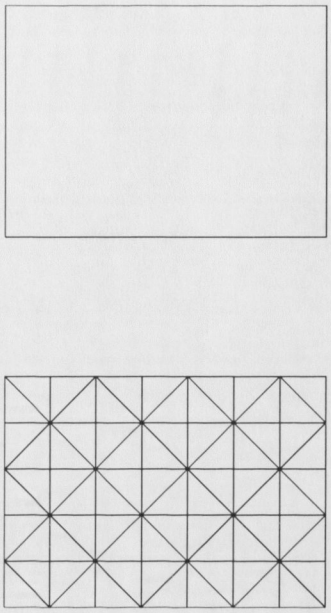

Figure 2-2: Domain Ω unmeshed (a); and meshed(b)

of the particular element p, labelled p_i, p_j and p_k respectively. The field variable

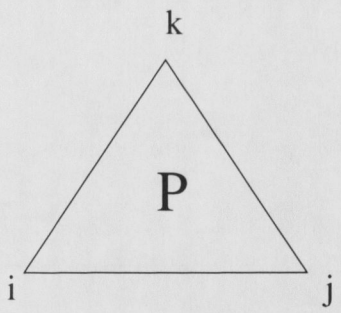

Figure 2-3: Arbitrary element P with nodes i,j,k

ϕ at each of these nodes is known. The field variable of the entire element is then a function of the field variables at each of the nodes

$$\phi_p = N_{pi}\phi_{pi} + N_{pj}\phi_{pj} + N_{pk}\phi_{pk} \tag{2.10}$$

The profile of the field variable for the entire domain is then given by

$$\phi_\Omega = \sum_{p=1}^{n} \phi_p \tag{2.11}$$

2.6.5 Solution of the diffusion equation using FEM

An example of the finite element method is described in Appendix C using the variational method since this is the approach adopted by both the ANSYS and DEQSOL programmes. However, such in-depth knowledge is not required and, in fact, the detail presented above is more than sufficient to use and understand the software.

2.7 Applications of FEM

In early work, Wilson and Nickell (1966) looked at application of FEM to heat conduction. An area of current topical interest in FEM is that of modelling orthopaedic implants (Prendergast (1997a)). Pan *et al.* (1995) have looked at using FEM for two dimensional diffusion - reaction equations. General topics on the use of FEM in diffusion studies are discussed by Ikeda (1983) and Ito (1992).

Chapter 3

Finite Element Modelling

3.1 Introduction

This chapter describes the preliminary work which was carried out using the finite element package ANSYS. We will illustrate the use of ANSYS for two aspects of transdermal drug diffusion. The first is the microscopic view of diffusion through the layers of the skin. The second model is a macroscopic model and we used this to examine diffusion at a more general level - from the applied patch into the skin. This technique of complementary macroscopic and microscopic modelling is commonly used for engineering problems which are solved using this software (Prendergast (1997b)). We will begin by introducing ANSYS and discussing its features. We then look at the system to be modelled, in this case the skin barrier, and discuss the complexities involved in modelling it. Finally we present some results and discuss the current limitations of the package.

3.2 ANSYS

ANSYS was developed by Swanson Analysis Systems Inc. (www.ansys.com - Canonsburg, PA, U.S.A.) and is used to solve numerically (using the finite ele-

ment method) problems in structural, thermal, electrical and fluid flow analyses. The capability of diffusion analysis is not explicitly specified within the ANSYS program but, as we have seen in chapter 1, the equations of heat conduction are exactly analogous to those of passive diffusion. Therefore this analogy can be exploited for our purposes to solve diffusion problems.

ANSYS is organised into three main stages: preprocessor, solution and post-processor. In the preprocessing stage data such as the geometry of materials and the type of element type (solid, shell *etc.*) are entered. The solution stage is where the analysis type is defined together with the loads and where the finite element solution is initiated. Finally the results obtained may be viewed in graphical and tabular form via the post-processor. Input is via menu commands and an example of the choice used is given in Appendix A.2.

3.3 The Skin

The skin is the largest organ in the human body, covering an average area of approximately 2m^2 and receiving one third of all the blood circulating in the body. The thickness of the skin varies depending on its location *e.g.* from 1.5 *mm* at the eyelids to 4.0 *mm* at the soles of the feet. A diagrammatic representation of the skin is shown in figure 3-1. Typically, the skin is described in terms of three regions. The uppermost region, that which is in contact with the external environment is called the *epidermis*. Beneath this lies the *dermis*. The hypodermis (technically not part of the skin) is situated directly below the skin and this contains the adipose tissue.

3.3.1 Composition and structure of the skin

The *epidermis* is a stratified structure consisting of five distinct layers as illustrated in figure 3-2. This highly resistive structure is the main barrier to sub-

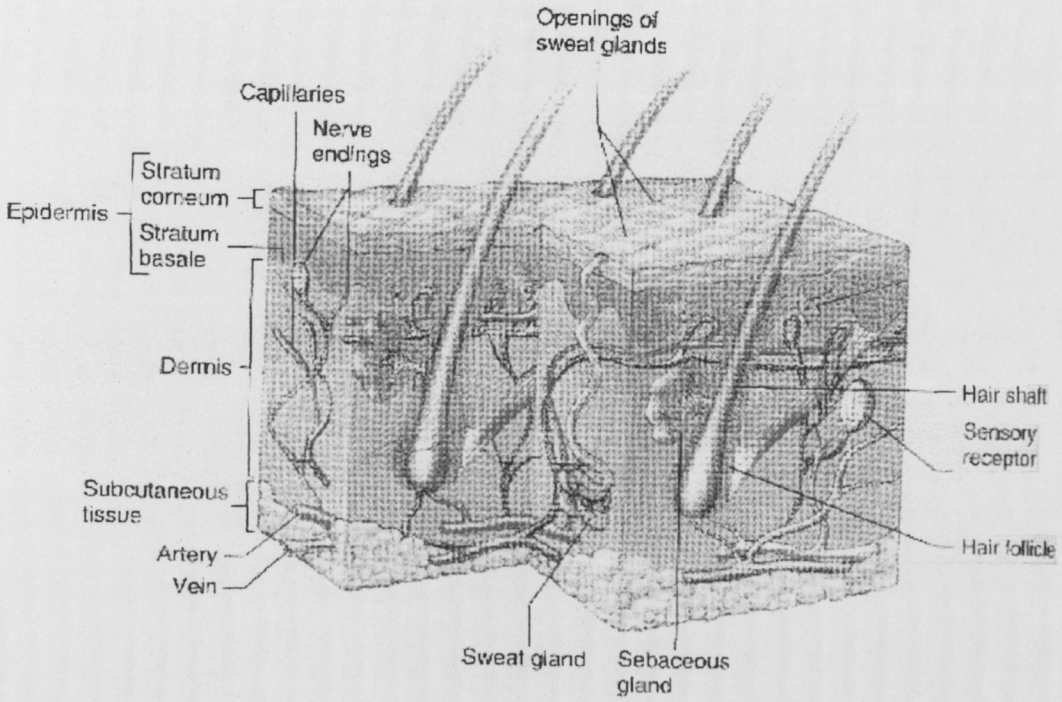

Figure 3-1: Cross section of human skin (taken from Solomon (1996))

stances entering and leaving the body via the skin. The outermost layer of the *epidermis* is called the *stratum corneum* and it plays a pivotal role in this barrier function (Walters (1996); Flynn (1992)). Consisting primarily of blocks of cytoplasmic protein matrices (called keratin) embedded in an extracellular lipid (Walters (1990)), this keratin gives the skin its protective function. The *stratum corneum* is on average 15-20 μm thick and accounts for three quarters of the overall depth of the epidermis. The structure of these layers has been well characterised by Honda *et al.* (1979).

Below this non-viable *stratum corneum* lies the viable epidermis. The layers in this section are *stratum lucidum*, *stratum granulosum*, *stratum spinosum* and *stratum basale*. These are known as the viable *epidermis* because having overcome the initial barrier of the *stratum corneum* substances are transported much more rapidly through the rest of the *epidermis*. The permeability of substances is much

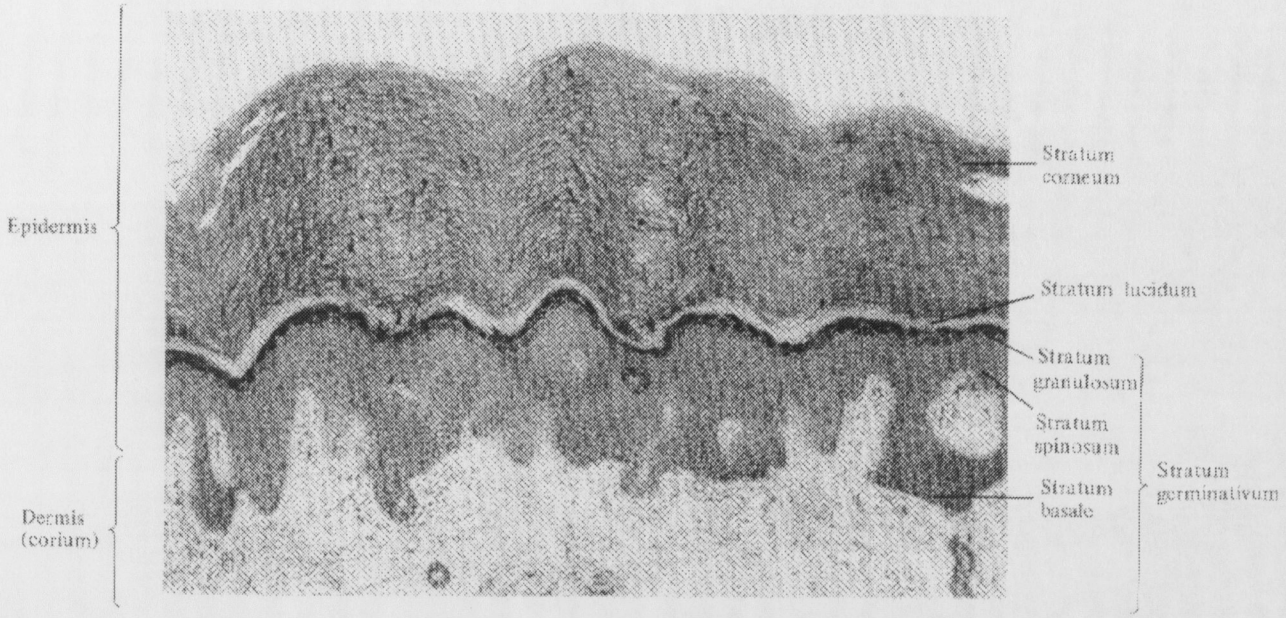

Figure 3-2: The epidermal layers of skin from the sole of the human foot (taken from Barrett (1986))

higher in the lower layers of the *epidermis* than in the *stratum corneum.* The lipids within these layers are neutral (as opposed to the polar lipids of the *stratum corneum*) and this leads to facile transport of lipophilic substances (Rothman (1954)). The *epidermis* is approximately 20 μm thick in total.

The *dermis* lies immediately below the *epidermis.* It is a thick fibrous tissue which forms the main bulk of the skin and is 20-30 times thicker than the *epidermis.* Below this again lies the subdermal layer where adipose cells are found. Both of these layers present a limited resistance to penetrating molecules (Brady (1991)).

3.3.2 Electrical Properties of Human Skin.

Since much of this work is concerned with electrically assisted drug delivery, it is pertinent to include a discussion on the electrical properties of the skin.

Complex impedance spectroscopy is generally used to determine the electrical properties of the skin (DeNuzzio and Berner (1990); Nolan *et al.* (1993)) and this technique has been used to show that the resistance of the *stratum corneum* decreases upon hydration (Clar *et al.* (1975)). Since the skin is a heterogeneous organ, its electrical properties vary throughout. The *stratum corneum* for example is an insulator. Yamamoto and Yamamoto (1976) have shown that by stripping successive layers of the *stratum corneum* , the resistivity of the skin decreases continuously to a constant value which agrees closely with the known value for the resistivity of deep tissues. They have represented the resistivity as an exponential equation:

$$\rho(x) = \rho_0 e^{-\alpha x} \tag{3.1}$$

where $\rho(x)$ is the resistivity at an arbitrary point x, ρ_0 is the resistivity of the outermost surface of the keratin layers, α is the attenuation coefficient and x is the distance between the deep tissues and the surface.

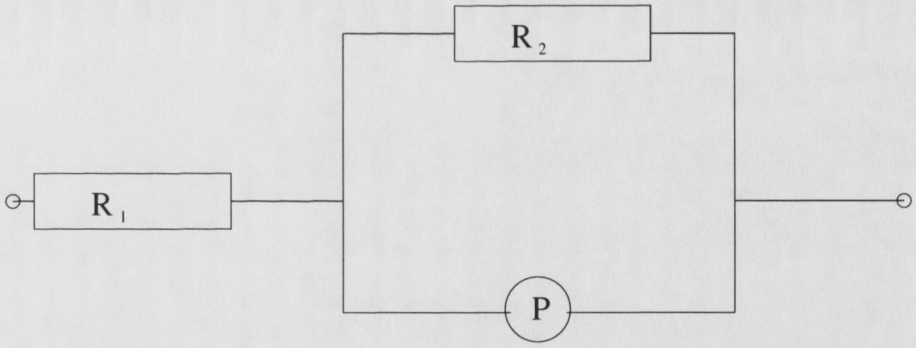

Figure 3-3: Equivalent circuit representing the resistance of the skin

The electrical characteristics of the skin may be represented by an equivalent electrical circuit as described by Traeger (1966). The circuit consists of a resistor R_1 in series with a resistor R_2 and a polarisation impedance P in parallel. This is show schematically in figure 3-3

The parallel resistivity R_2 is in the range $100 - 5000\text{k}\Omega\text{cm}$ and is a measure

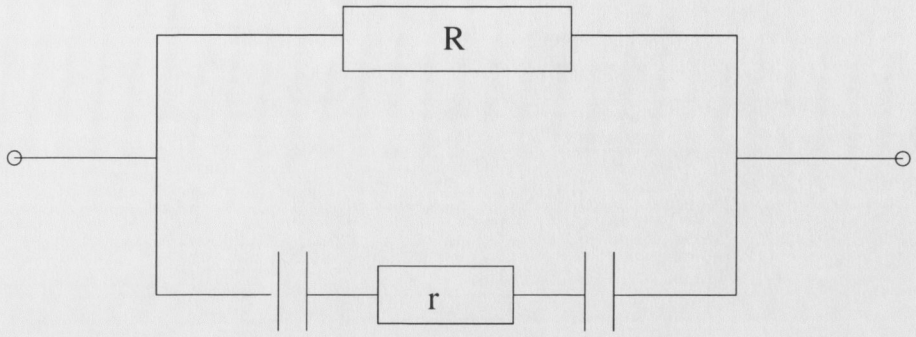

Figure 3-4: Equivalent circuit representing the resistance of the layers of the skin

of the steady state conduction through the *epidermis* and its appendages. Its reciprocal is analogous to the skin permeability - a measure of diffusion through the *stratum corneum.*

The small series resistivity, R_1, is the resistivity of the deeper tissue and has a value in the range 0.1-1 k Ωcm.

The polarisation impedance represents the fact that the current can oscillate between restraining membranes which hinder its steady passage. It is due to the fact that the cells are surrounded by a phospholipid membrane which restricts the current flow.

At zero frequency, the polarisation impedance tends to infinity and there is therefore d.c. through R_1 and R_2. At high frequency, the polarisation impedance falls to zero and the system is a purely resistive R_1. At intermediate frequencies the polarisation frequency is less than R_2 but greater than R_1, so that R_2 dominates.

Traeger (1966) has further represented the individual layers of the *stratum corneum* by the circuit shown in figure 3-4. The cell membranes are represented by the two capacitors, the intra-cellular resistance by r and the extracellular resistance by R.

It is useful to have these equivalent circuits especially when drawing com-

parisons with drug diffusion and heat conduction as will be evident later in this chapter.

3.3.3 Physical models of the skin

Human skin *in situ* cannot be used for testing the efficacy of a transdermal system. Ideally, skin taken from cadavers is used. However there are many problems associated with obtaining suitable samples since there are many variables including fat content and the anatomical site so it is impossible to repeatedly obtain equivalent samples. Cost is a further consideration. Therefore many scientists use skin taken from animals. Common among these are mice (Durrheim *et al.* (1980)) rabbits and rats (Rougier *et al.* (1987)), although it has been reported that snakeskin (Higuchi and Konishi (1987); Itoh *et al.* (1990)) or pig skin (Meyer *et al.* (1978)) have been used as alternatives. In terms of structure and diffusion rate, these animal models are good. The main difference between skin from different species is the thickness and density of the hair follicles.

In many cases, artificial membranes are used. In terms of mathematical modelling of the skin, Danielson (1973) has successfully reported the modelling the skin as an elastic membrane.

We have seen that the skin is a complex membrane and it is therefore intuitive to assume that percutaneous absorption should be an equally complex process. We will see in the next section how complex it actually is, but that by breaking it down into a sequence of small steps, it is possible to get a good understanding of the complete process.

3.4 Percutaneous Absorption

Percutaneous absorption is defined as the mass movement of substances from the surface of the skin to general circulation (Idson (1975)). This involves pene-

tration of the *stratum corneum*, the viable *epidermis* and the *dermis* and finally the removal of the penetrant and its metabolites from the dermis and into the circulatory system (Vickers and Wepierre (1980)).

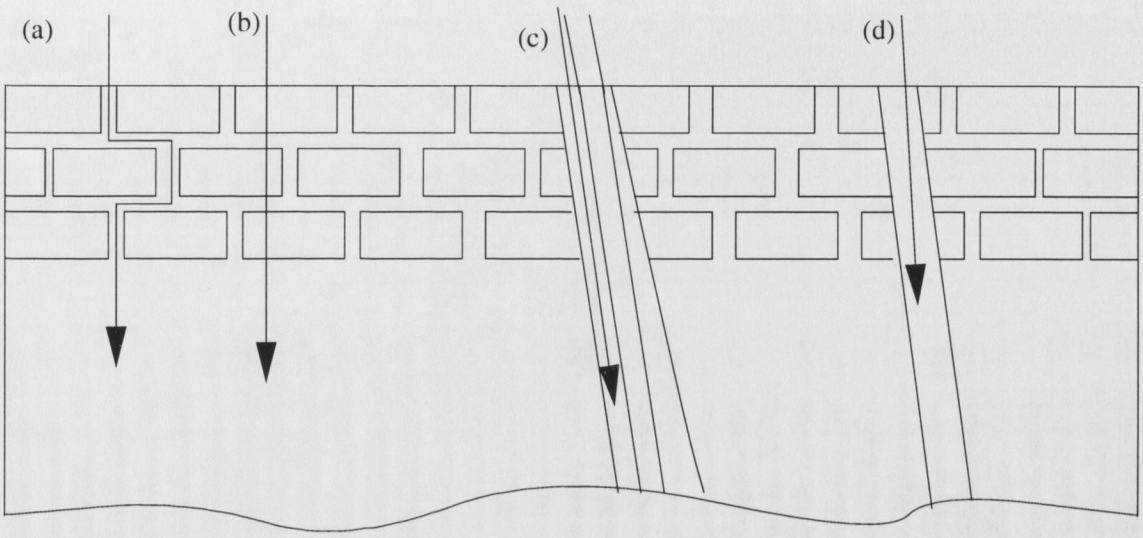

(a) intercellular transepidermal
(b) intracellular transepidermal
(c) through hair follicle
(d) via sweat duct

Figure 3-5: Schematic diagram showing possible routes of penetration of a substance into the skin, where (a) and (b) are transepidermal, and (c) and (d) are transappendageal.

There are two main routes of transport of a substance into the skin. These are transepidermal and transappendageal and are outlined in figure 3-5.

The transepidermal route involves moving through the *stratum corneum* in either of two ways. Drugs may migrate either though the material between the cells - inter-cellular- or may take the direct route through the cells (transcellular). These pathways are marked (a) and (b) in figure 3-5 respectively. Blank (1967) has shown that polar molecules diffuse principally through a polar pathway consisting of "bound water" within the hydrated *stratum corneum* while non-polar

molecules diffuse through the non-aqueous lipid matrix.

Bodde (1989) used transmission electron microscopy studies on Hg_2Cl_2 to show that initially, the inter-cellular pathway is the favoured migration route but that at long times the transcellular pathway will dominate.

The transappendageal route involves migration through the follicular regions, or through the sweat ducts. It has been shown that charged substances diffuse rapidly through the follicular canal and that this shunt route may be important. In particular, this pathway is favoured for large polar molecules

Depending on the nature of the absorbent, and the possibility of electrical enhancement, one particular path may dominate. There are conflicting views on this but it is agreed that no one path is singularly responsible for material transport.

For passive diffusion, Scheuplein (1967) claims that due to the higher diffusion coefficients of the follicles and sweat ducts compared with the *stratum corneum*, drugs are absorbed preferentially through the follicular regions. He concludes that initially, the main means of absorption is via the follicles . However, the ratio of the total fractional area of the follicular regions to the rest of the skin is a very small ($3 \times 10^{-5} : 1$) so as the time increases, the transepidermal path dominates. In general it only takes a short time (*circa* 300 seconds) Scheuplein (1967) for the transepidermal route to dominate. This pathway is therefore known as the path of bulk diffusion while the other is called the shunt route.

Wallace and Barnett (1978) used experimental data on permeation of methorexate to generate a computer model and elucidate the pertinent parameters such as diffusion coefficient and lag time. From this they concluded that there is more than one pathway for percutaneous absorption of the ester. An interesting review of this area which includes detailed discussions on the role of the various physico-chemical parameters is presented by Scheuplein and Blank (1971).

Of the four steps involved in percutaneous absorption, it has been shown that penetration of the *stratum corneum* is rate limiting (Parry *et al.* (1990)).

Many workers have been active in attempting to quantify this. Albery and Hadgraft (1979a) constructed a rotating diffusion cell in order to determine the rate constant for the transfer reaction across the interfaces on either side of the epidermal barrier. In a later paper Albery and Hadgraft (1979b) presented a theoretical description of percutaneous absorption including diffusion and depletion in the external phase, diffusion through the epidermis and the kinetics of transfer reactions at the interfaces. Following this, Albery and Hadgraft (1979c) did some *in vivo* experiments in order to determine the pathways of penetration for some esters.

They found that the route of penetration is through interstitial channels and not through the keratinized cells. Later Albery *et al.* (1983) looked at the percutaneous absorption of three different esters and made a mathematical model describing their findings.

Other mathematical models include that of Cooper (1976) who presented a model for estimating *in vivo* skin permeability coefficients and Michaels *et al.* (1975) also made a physical model of the the *stratum corneum* as a two-phase protein-lipid heterogeneous membrane. Albery and Hadgraft (1979b) used Michaels' model to explain that the low diffusion coefficients of substances through the lipid phase were due to the homogeneity of the structure. Another physical model is that of Rougire *et al.* (1983) who looked at percutaneous absorption from the viewpoint of the *stratum corneum* as a reservoir. They did quantitative experiments using an animal model and suggested verification of their results in humans.

There are many methods used to examine the pathways of permeation and permeation kinetics. These include application of dyes (Abramson and Gorin (1940)), spectroscopy (Reinl *et al.* (1995)), confocal microscopy (Cullander and Guy (1992)) and scanning electrochemical microscopy (Scott *et al.* (1992)).

3.5 Microscopic model

We now show how, given the resistances of various components in the skin, we have translated these into suitable parameters for ANSYS and obtained graphical solutions for the changes in concentration over time.

The average diffusion constants of a particular drug molecule through different parts of the skin are described by Scheuplein (1967). A less detailed version of his results is shown in the following table:

Appendage	Average Diffusion Constant	Typical diameter
Hair follicle	$2 \times 10^{-7} cm^2 sec^{-1}$	70 μm
Sweat duct	$2 \times 10^{-6} cm^2 sec^{-1}$	70 μm
Stratum corneum	$1 \times 10^{-10} cm^2 sec^{-1}$	13 μm
Hydrated Epidermis	$1 \times 10^{-6} cm^2 sec^{-1}$	110 μm

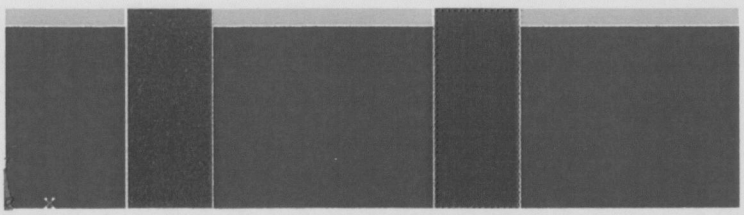

Figure 3-6: Graphical representation of the skin illustrating hair follicle (blue), sweat gland (green), *stratum corneum* (yellow) and *epidermis* (red)

Remembering the temperature/concentration analogy, ANSYS was set up to perform a thermal analysis. A cross section of the skin of the forearm was drawn schematically as in figure 3-6. (The method followed is contained in Appendix A.2.) The total dimensions of the model are 600 μm by 165 μm. Included in the representation are the following:

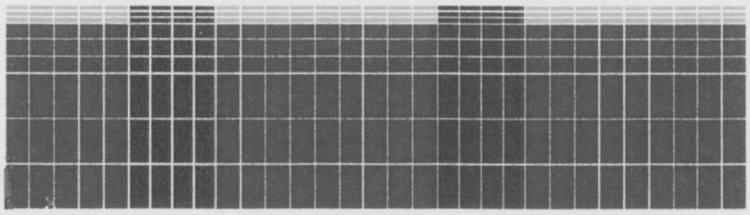

Figure 3-7: Meshed model of the skin showing individual simulated elements. This mesh was automated by ANSYS as the first step in finite element analysis.

- Hair Follicle

  This is coloured blue and has a width of 70 μm, corresponding to the nominal diameter of a hair follicle as in the table above.

- Sweat gland

  The sweat gland is represented by the green region in figure 3-6. Again, it has a nominal diameter of 70 μm.

- Epidermis

  The *epidermis* is represented by the yellow, and the red region in figure 3-6. The upper part of the *epidermis*, the *stratum corneum* has a depth of 15 μm and this is the yellow region. The rest of the *epidermis* is represented by the red region.

The different regions were distinguished only by their diffusion coefficients. The regions were then meshed into smaller elements as shown in figure 3-7. As is clear from the diagram, smaller elements were required for the smaller areas.

A normalised concentration of 1 was applied across the upper node of the *stratum corneum* as shown by the arrows in figure 3-8. The system was solved for various times commencing with 100 seconds and the results are shown in figure 3-10 and figure 3-11. In all cases the key code for the concentrations shown in figure 3-9 applies.

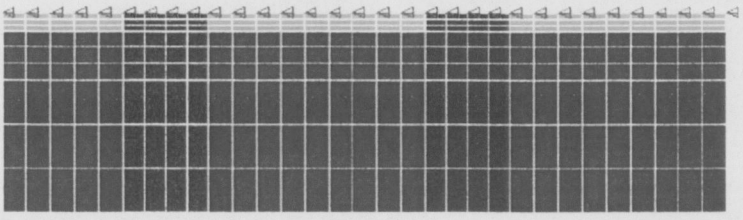

Figure 3-8: Meshed model of the skin where arrows show the nodes on which a temperature of 100° C (corresponding to a normalized concentration of 1) was applied

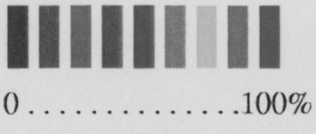

Figure 3-9: Colour coding for concentration plots

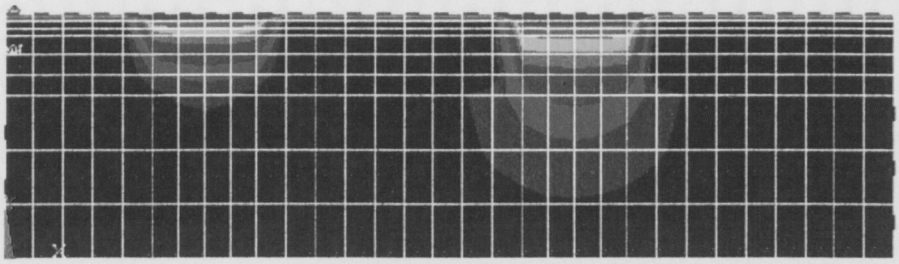

(a)

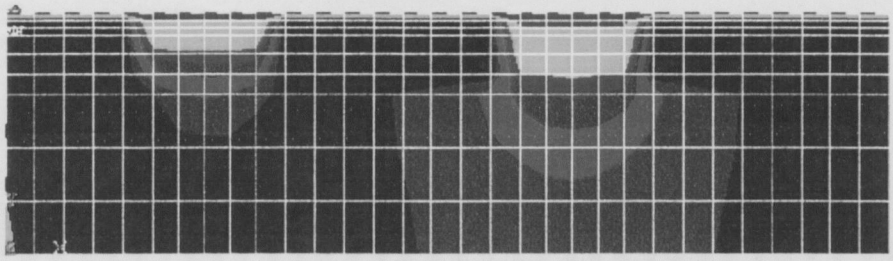

(b)

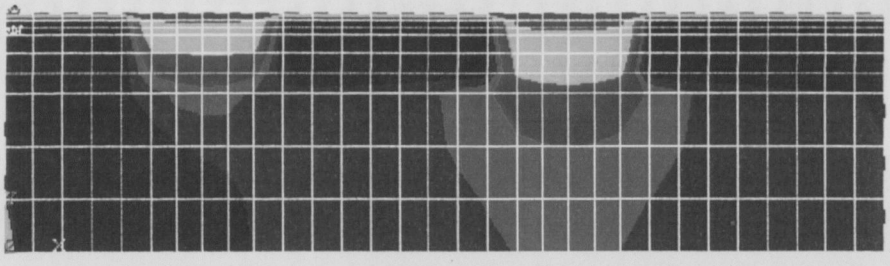

(c)

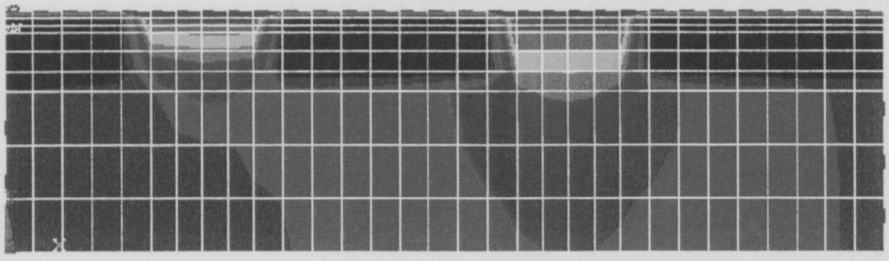

(d)

Figure 3-10: Diffusion pattern through shunts in the skin when a normalised concentration (=1) is applied across the surface at t= 100, 200, 300 and 500 seconds.

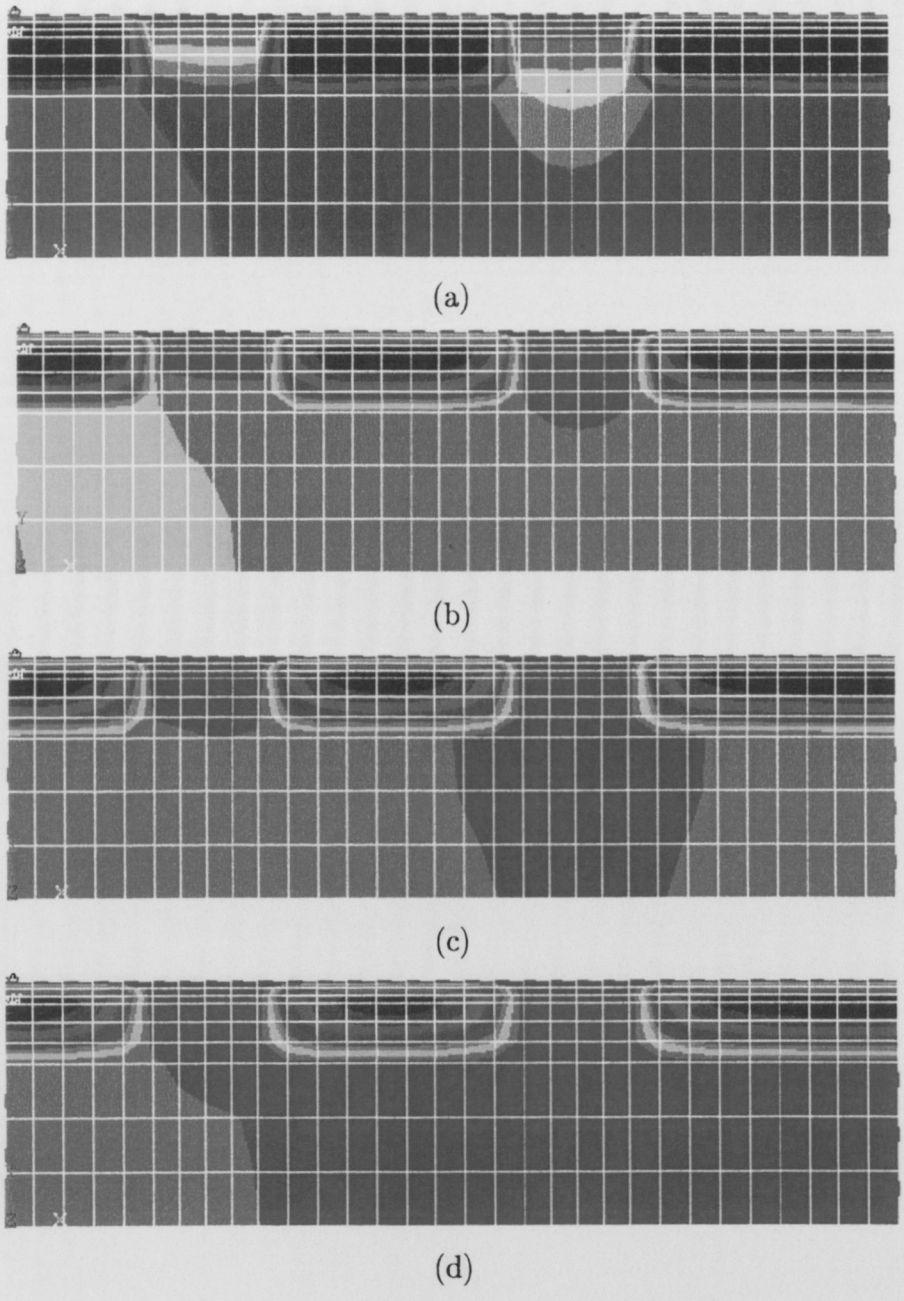

Figure 3-11: Diffusion pattern through shunts in the skin when a normalised concentration (=1) is applied across the surface at t= 0.1, 1 , 10, and 100 (x 10^4) seconds.

3.5.1 Discussion

After 100 seconds it can be seen in figure 3-10 that diffusion occurs fastest through the sweat gland. This is followed closely by diffusion through the hair follicle while there is virtually no transport through the unbroken *stratum corneum.*

The pattern continues in a similar manner at longer times, diffusion through the sweat gland becoming more extensive as time increases through 200 seconds. After 200 and more so after 300 seconds, the diffusion pattern has lost its symmetry since there is an overlap of the migratory region of the sweat gland and the hair follicle. In practice however, these two are not so close together and each would have its own distinct migratory pattern before they merge at a later time. However, due to the scale of the simulation system it would have been difficult to spread the shunts further apart, for, in order to reatin resolution, the number of cells would have to be increased beyond the capacity of the code. Separate diagrams of the individual follicles have shown that in the absence of one, the second pattern would remain symmetrical. The broadening is due to the absence of a sink at the bottom. At this point the model is no longer realistic.

As time continues, towards 0.1 x 10^4 seconds, we can see that while the drug concentration is as high as 50 % in the *epidermis*, the *stratum corneum* still contains some dark blue regions corresponding to there being virtually no drug present. The trend continues with the drug having been successfully transported into the bloodstream via the shunt routes at 1 x 10^4 seconds while it is not until after 10 - 100 (x 10^4) seconds that the *stratum corneum* also absorbs the drug.

3.5.2 Physical Interpretation and significance

The results obtained are in good agreement with intuition that the drug will migrate through the path of least resistance. They support the fact that initial absorption is transappendageal. What is shown in figure 3-10 and figure 3-11 is merely the result of a calculation by the finite element method using the values

for diffusion coefficient obtained in the literature and relating the initial concentration to the concentration after various time periods. The ANSYS program at present is not sufficiently sophisticated to deal with anything other than diffusion. For example, we have seen earlier that there are many physiological factors associated with drug migration into the skin. The ANSYS solution treats each component as having a fixed resistance even though it has been shown that the resistance of the skin decreases once the initial barrier has been broken. Another useful feature would be to monitor the time development of the profiles. Again, this facility is lacking in ANSYS. However, as this package becomes more widely used in the field of biomechanics the future should show some improvements and allow for greater versatility for work in this area which, as is evident at present, is limited.

3.6 Membrane

The previous section considered only the diffusion process in which it was assumed that the drug was applied directly onto the skin. We will now show how the work is performed when a control membrane is placed between the drug reservoir and the surface of the skin. The membrane is of the order of 1 *mm* thick (Bannon (1989)) but in the next model, figure 3-12, we have included a membrane of 0.3 *mm* thickness because the relative size of the rest of the model allows only this.

By varying the permeability (the diffusion constant) of the membrane therefore, it is possible to control the rate of drug transport into the skin. For example, a membrane of diffusion coefficient 1 x $10^{-6}m^2s^{-1}$ is compared with a membrane of diffusion coefficient 1 x $10^{-4}m^2s^{-1}$. The run time for both is set to 100 seconds.

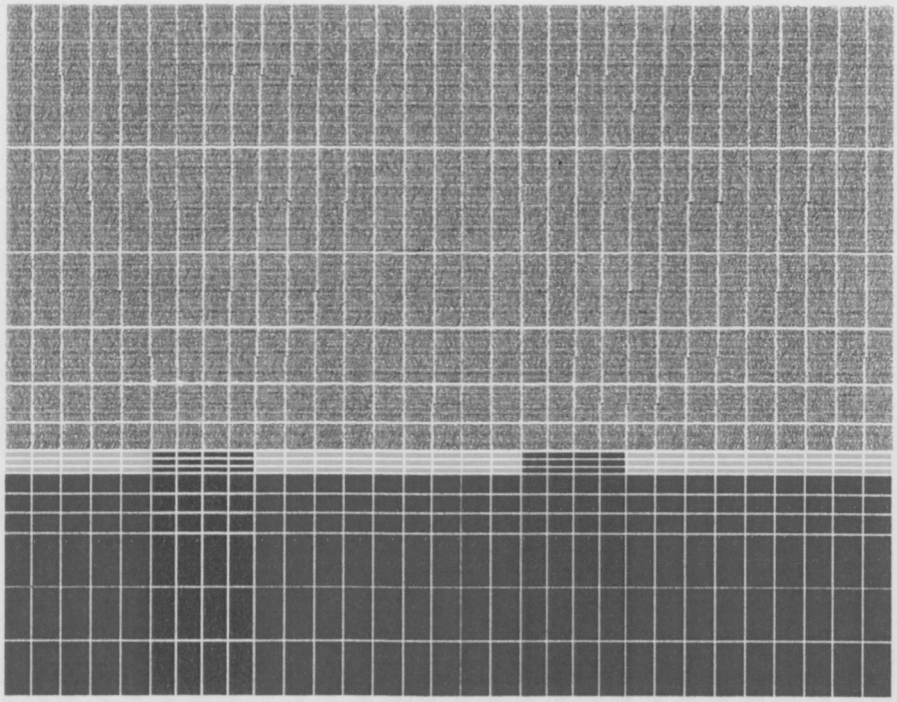

Figure 3-12: Representation of the skin system with the membrane of 0.3mm thickness included (grey region)

3.6.1 Discussion

Figure 3-13 is a comparison of the ratio of initial to final concentration for diffusion of the same drug through two membranes of different diffusion coefficients. One can easily see how the membrane with the higher diffusion constant allows faster penetration of the drug into the circulatory system. In reality, the membrane acts as a method of control. Depending on the desired delivery rate a membrane of suitable diffusion coefficient can be chosen. Again, due to the limitations of the software, we are unable to compare membrane controlled systems with for example matrix controlled systems. However, this should be possible in future studies as the system becomes more advanced.

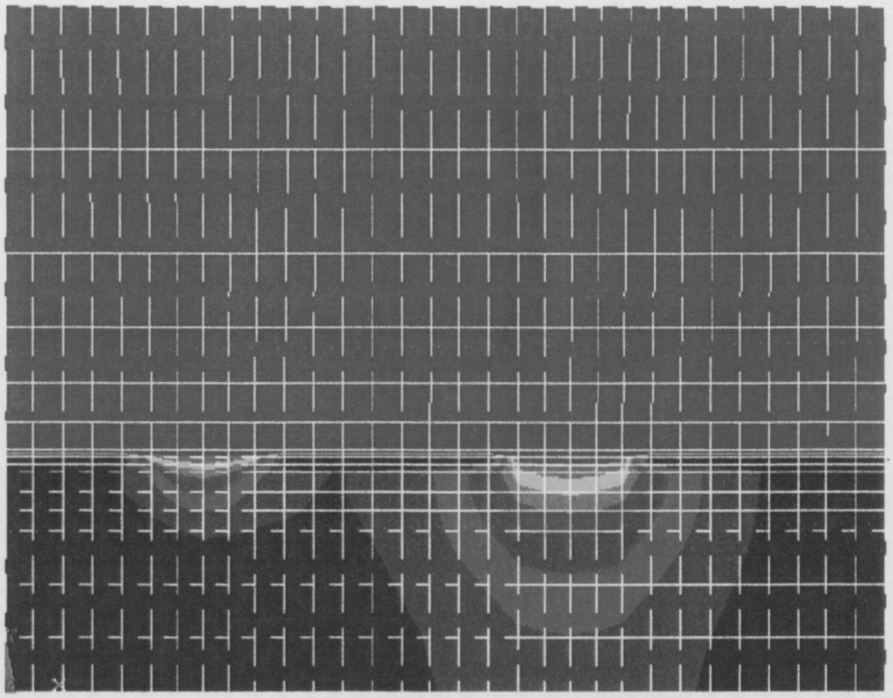

(a)

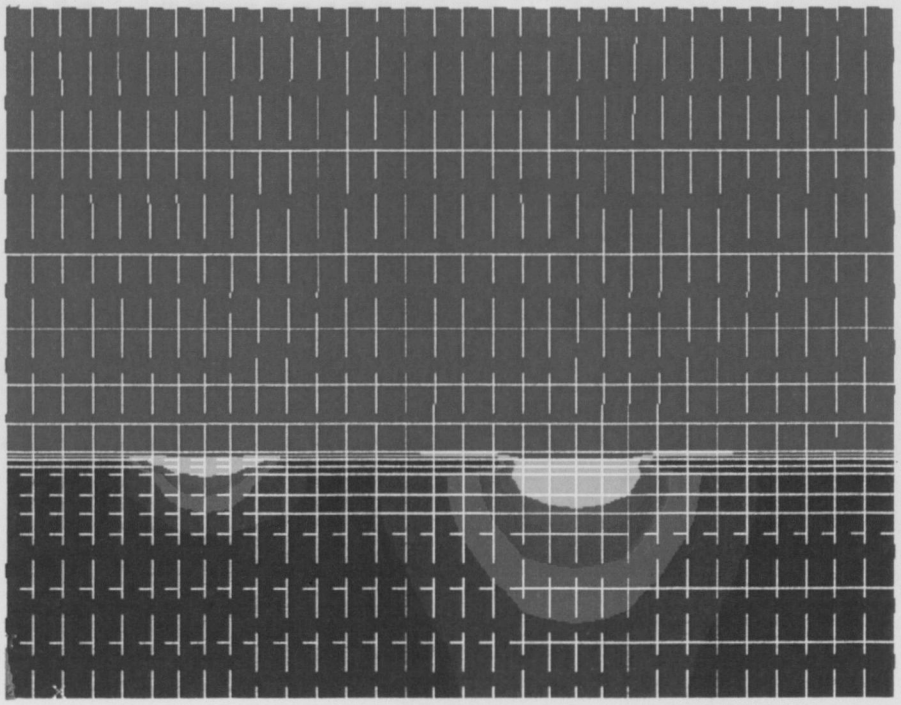

(b)

Figure 3-13: Diffusion through the shunts with membrane of high diffusion coefficient (a) and low diffusion coefficient (b)

3.7 Macro modelling

In this section we concentrate on a more macroscopic picture of drug diffusion from a transdermal patch and into the skin. As in the previous section the change in concentration of the drug over time is monitored.

3.7.1 The Model

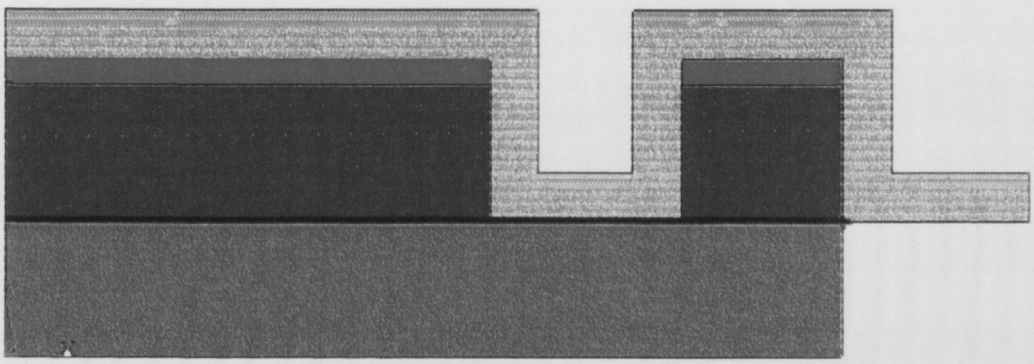

Figure 3-14: Diagrammatic representation of the different materials used to model the transdermal system. This is a cross-section of the system which must be rotated through 360° to generate the complete picture. The skin is represented by the orange material, the gel containing the drug is represented by the blue material. The control membrane is shown by the heavy black line and the electrodes are shown in red. The outer grey area is simply the housing for the patch and this is what would be seen by the user.

In the same manner as before, the temperature-diffusion analogy was used and a thermal analysis was carried out. A fully dimensioned plan of a working patch came in the form of an AUTOCAD drawing as shown above. The inner well containing the drug has a radius of 7 cm. The boundaries of the outer well are situated 10 cm and 12.5 cm from the centre. Thus, the volume of both wells is the same. The drawing was imported into ANSYS and suitably cut and edited. There are four distinct components to this system as shown in figure 3.14. Therefore four different materials were defined in ANSYS.

Material no.1, the skin was assigned a diffusion coefficient of 1 x $10^{-10}m^2s^{-1}$. The gel containing the drug – material no.2 – was assigned a diffusion constant of 1 x $10^{-11}m^2s^{-1}$. Gel is more viscous than water which is nominally assumed to have diffusion coefficient of 1 x $10^{-10}m^2s^{-1}$. Material no.3, the membrane was given a diffusion coefficient of 1 x $10^{-4}m^2s^{-1}$ and material no.4, the electrode was assigned a nominal diffusion coefficient of $1m^2s^{-1}$. These diffusion coefficients are standard values taken from Lide and Frederikse (1993) A temperature of 100 was applied along the active well. The system was run for a period of 10,000 and 20,000 seconds. The results for this macroscopic model are shown in Figure 3-15.

3.7.2 Discussion

As in the previous sections, the current limited capabilities of ANSYS mean that there are only a few basic observations to be discussed based on Figure 3-15. The outline of the patch can be seen by comparison with figure 3-14. It is clear that after 10,000 seconds, there has been drug flow from the well into the skin. After a longer time (20,000 seconds) this increase in concentration within the skin is more apparent.

Due to the limitations of the software, it is impossible to include effects such as increase in skin hydration, molecular characteristics of the drug Singh and Singh (1993) and other factors which affect the rate of transport.

Although the common units for diffusion coefficient are cm^2s^{-1}, the dimensions of these parameters and indeed all parameters are expressed in terms of SI units. This is to facilitate the finite element calculations and also the conversion from thermal to diffusion quantities.

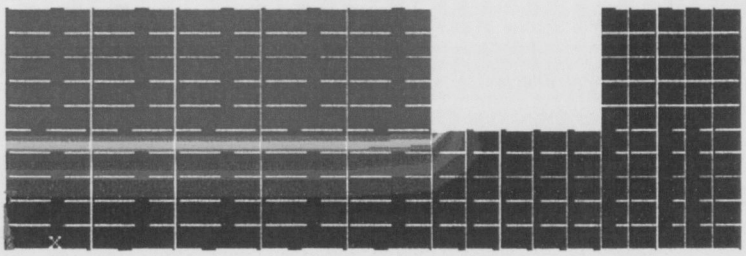

(a)

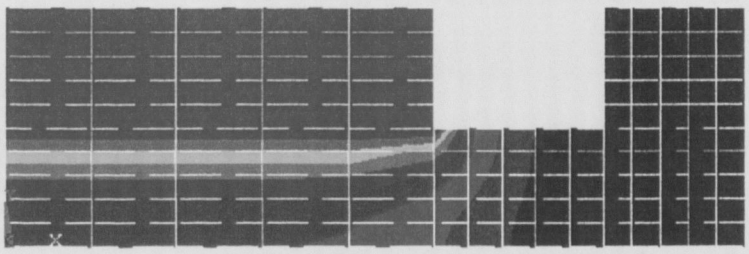

(b)

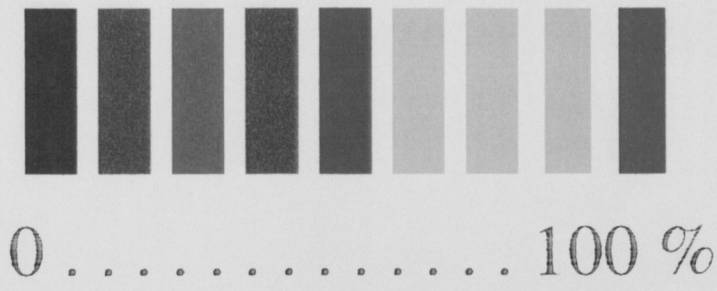

(c)

Figure 3-15: Diffusion through the skin at 10,000 and 20,000 seconds as modelled by ANSYS.

3.8 Iontophoresis

For the case of electrically assisted diffusion, we know that ions move under the influence of an electric field (Vincent (1976)). We expect there to be a high concentration of ions in regions of high electric field intensity and a low concentration of ions in regions with low field intensity Figure 3-16 is a plot

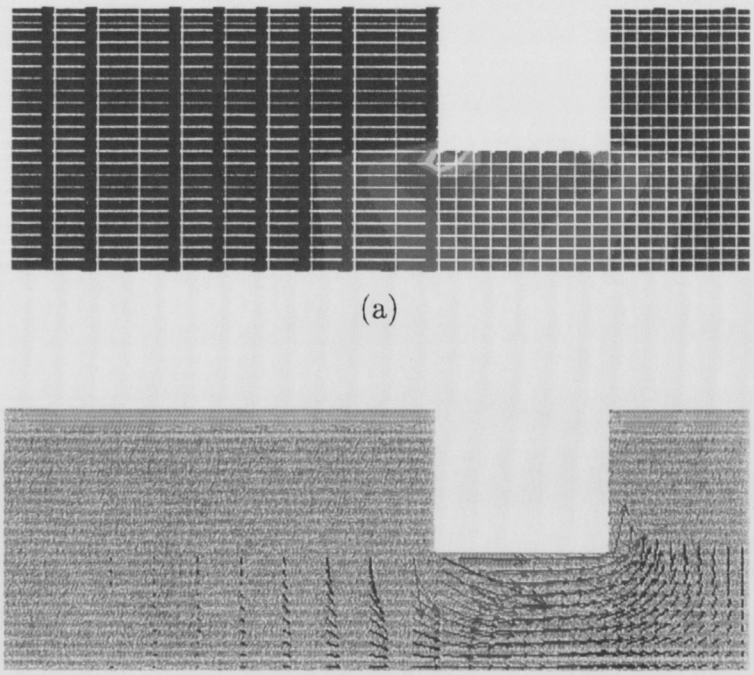

(a)

(b)

Figure 3-16: Graphical (a) and arrow (b) plot of electric field intensity which shows low electric field intensity (blue) to high field intensity (red)

of the electric field intensity for such a system as a contour plot and an arrow plot respectively. This plot was generated by ANSYS and it corresponds to the field intensity resulting from the application of the electric field described in the previous section. From this plot, it is reasonable to assume that drug will move more rapidly from the regions close to the interface of the patch and the skin That

is, the concentration of drug within the patch does not remain homogeneous.

Researchers at Elan Corporation plc (Foley (1997)) have done experimental work in an attempt to quantify this effect. It has not been possible, however, to simulate these conditions because as previously discussed ANSYS is not yet suitable to model such phenomena involving electrical fields.

3.8.1 Experimental

This section contains the results of work carried out by ELAN. A circular patch was cut into four areas as shown in figure 3-17. The areas were labelled A, B, C and D. The radii and areas of these regions are given in table 3.1. The aim was to have approximately the same area in each region (and thus the same amount of drug initially). This was coupled with the constraint that the cutting tools were of certain fixed diameters so it was not possible to meet the requirments exactly. Assuming that initially the drug concentration was homogeneous, the

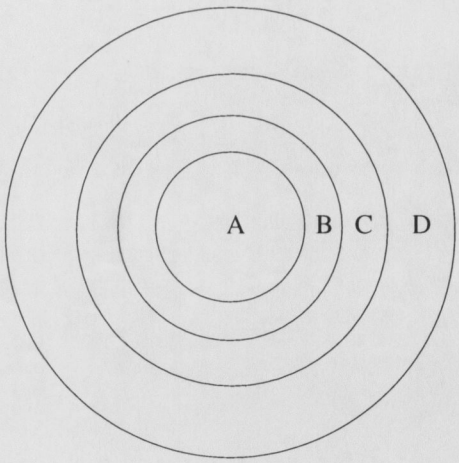

Figure 3-17: Transdermal patch divided into areas for separate analysis

total amount of drug present initially was proportional to the area. The drug was allowed to diffuse (iontophoretically) out of the patch and into a membrane The amount of drug present in each portion was measured after periods of 3 and

Item	A	B	C	D	Total
radius(mm)	5	7.5	10.49	14.9	14.9
area (mm^2)	79	98	169	354	700

Table 3.1: List of the radii and surface areas of the four regions of the patch

6 hours. These measurements are given in table 3.2. These amounts were then calculated as a percentage of the initial theoretical amount of drug present.

3.8.2 Discussion

Since these are the only results available from this study, it is difficult to draw definite conclusions. As is clear from the results, there is a lot of disparity and lack of agreement between the two sets of data (a) and (b). The error margins are quite large and the results must be regarded as requiring confirmation. However, the trend of more rapid concentration depletion from the outer edge of the patch is obvious even with these crude data. Therefore, this experimental data give an accurate, though not precise description of what was expected from the simulation results shown in figure 3-16.

3.8.3 ANSYS Simulation

We have seen that in order to include the effects of an electric current, we must include additional terms in the general diffusion equation (1.12). Where we have equated diffusion coefficient with thermal conductivity, it is clear from equation (1.13) that the electric field is equated with velocity.

However, from preliminary tests, we have seen that this is not a direct analogy. The velocity term arises from convection and is due to the motion of the medium containing the heat. This corresponds to the gel in the drug matrix.

As has been discussed earlier, the drug is released from the gel and the gel itself does not penetrate the skin. Therefore, this analogy cannot be expected to

Item	A	B	C	D	Total
initial amount(mg)	0.33	0.41	0.71	1.48	2.92
3hrs	.22	.27	.39	.66	
% of initial	66	65	55	45	
6hrs	.05	.03	.04	.06	
% of initial	15	7.3	5.7	4	

(a)

Item	A	B	C	D	Total
initial amount(mg)	0.33	0.42	0.71	1.50	2.96
3hrs	.17	.23	.27	.63	
% of initial	51	55	38	42	
6hrs	.05	.03	.03	.01	
% of initial	15	7.1	4.2	1.5	

(b)

Table 3.2: Amount of drug measured in each sector of the patch after the drug has diffused out after three and six hours. The results of two separate measurments (a) and (b) are given. (Note that the initial amount was not actually measured but in fact calculated from the amount of total drug present in the patch before it was sectioned.)

be valid

As a trial, an electrical analysis was carried out. The electric flux of each element was tabulated and then entered as the material property of conductivity in a subsequent thermal analysis.

Essentially, the equation solved by ANSYS via the finite element method became

$$\frac{\partial c}{\partial t} = (D + \beta)\frac{\partial^2 c}{\partial x^2} \tag{3.2}$$

This did not work since, by analogy with equation (1.18). β should be multiplied by the first derivative of c w.r.t. x and not the second derivative.

3.8.4 Conclusion

For a small range of cases we have seen that ANSYS is a good modelling tool for diffusion analysis. However, for complicated cases such as electrically assisted diffusion, the current limited capabilities of ANSYS mean that an alternative tool is necessary to model such processes. The results presented in this chapter are of limited use. They really serve to show how, with more versatility such software could be adapted and used as a modelling tool. What we have seen is that since the mathematics of the phenomena of heat transfer and matter transport are so closely related that the same tools can be used to represent both provided that there is some degree of flexibility within them. The aim of this work has been to investigate the usefulness of ANSYS as a modelling tool for the transdermal patch system. The work has clearly shown that more versatility of the software is a fundamental requirement if realistic systems are to be modelled.

Therefore, we adopted another approach to continue and extend our modelling. We started with the partial differential equations and solved them analytically. Where no analytical solution was available we used DEQSOL, the finite difference numerical solver package discussed in the chapter 2 and the results for

drug release from an inert matrix are given in the next chapter.

Chapter 4

Diffusion from an Inert Matrix

In this chapter we examine the migration of a drug, from a transdermal patch, into the skin. To this end we have developed a mathematical model. The model is based on diffusion from an inert matrix of finite size. It is assumed that there is a uniform concentration of drug present in the matrix, that the transport out of the matrix is governed by the diffusion equation and that this diffusion is planar. For simplicity it is also assumed that the skin is an infinite sink and that the flux on the other side of the matrix is zero - that is that the drug can only exit the matrix on one side. The pertinent differential equation for this model (equation (1.16)) has been solved and is derived in many textbooks (Jost (1960)). The purpose of this chapter is to extend the previous work to include the effect of an electric field applied across the matrix which will enhance or retard the passage of an ionized drug molecule into the membrane. The advantage of such electrically assisted transport is that it allows greater control over the rate of delivery. In addition, the system as programmed will allow a chemical reaction to take place within the matrix that will cause a further depletion in the drug concentration.

We will start by taking a brief look at the entire sequence of events that result in a transdermally administered drug being made available to the circulatory system. We will take a detailed look at the functions and features of a transdermal

delivery system. From here we will look at the phenomenon of iontophoresis. Finally, before discussing our particular model we will review the mathematical models in the literature.

4.1 Drug Delivery

The three aspects of drug delivery are drug input, pharmacokinetics and pharmodynamics. Drug input describes the rate and time course of systemic drug input. Pharmacokinetics is concerned with the uptake of the drug into the circulatory system and blood plasma levels. Pharmodynamics involves examining the interaction between the drugs and the cells in the body with the ultimate aim of maximising the therapeutic effects, minimising side effects and prevention of the development of tolerance to this therapeutic effect.

Of these three aspects, this work is only concerned with drug input. The pharmacokinetics are of some minor significance in that the aim of drug input is to ultimately detect blood plasma levels in order to confirm that the drug has indeed entered the body. In order to place this work in context, it is useful to have some knowledge of all three processes and a good review of this is presented by Mazer (1990).

4.1.1 Drug Input

We will see that it is possible to control the migration of a drug into the body either by choice of a delivery a matrix or by the use of a membrane as well as by other means. Our theories on matrix control are presented later in this chapter and those on membrane control are in chapter 5. We will therefore continue with a discussion on pharmacokinetics.

4.1.2 Pharmacokinetics

The purpose of pharmacokinetic modelling is to accurately predict blood plasma levels that will result from dermal penetration. A pioneer in this field was Hadgraft (1979) who looked at the epidermis in terms of its function as a reservoir and also at the metabolism that takes place therein (Hadgraft (1980)) An early model by Guy and Hadgraft (1982) described epidermal uptake via Michaelis-Menten kinetics with a a two-step model. Approximate solutions were found for long times where the concentration is considerably larger than the Michaelis-Menten constant and again at long times where the concentration is considerably smaller than the Michaelis-Menten constant. Later Guy and Hadgraft (1983) described another two step model for drug delivery from a vehicle into the skin, and then from the skin into the capillaries in order to derive approximate expressions for the total amount of a drug delivered into the circulatory system. These approximations were for long and short times, and can be used for comparison with experimental data once the various rate constants are known.

Physically-based pharmacokinetic models to predict plasma levels have been presented by Guy and Hadgraft (1984, 1985). Since then, several pharmacokinetic models have been proposed in the literature to describe the passive transdermal delivery of a variety of compounds for example, Selegine (Barrett *et al.* (1997a,b); Mahmood *et al.* (1994)). Most recently, Rohatagi *et al.* (1997) developed an integrated pharmacokinetic and metabolic model for Selegine and metabolites after transdermal administration. Other workers Riviere *et al.* (1992), Silcox *et al.* (1990) have looked at plasma levels developed using a flap of human *stratum corneum* applied to an animal model.

Having seen a brief picture of the developments in modelling the cycle of a drug from diffusion out of the patch to detection in the blood, we will now concentrate on the first aspect of this, drug input, and begin with some general considerations of transdermal drug delivery.

4.1.3 Transdermal drug delivery - General Considerations

An ideal transdermal delivery system provides a uniform zero-order delivery rate which is effective within a therapeutic window. It is effective for the administration of drugs with short half lives and it is non-invasive facilitating easy cessation by removal and therefore increased patient compliance (Corish and Corrigan (1990)). The main advantage of a transdermal delivery system over traditional routes is that it allows drug to enter the body at an approximately uniform rate over an extended period of time. There are many other advantages associated with this novel drug delivery technique. Since it goes directly into the bloodstream, the drug does not pass through the gastrointestinal tract where it can be partially degraded and it also avoids first-pass contact with liver where it could be partially metabolised (Ranade and Hollinger (1996)). It also avoids the risk and inconvenience of intravenous therapy.

The essential components of a transdermal device are a drug reservoir and a means to control the release of drug onto the surface of the skin. Older techniques used to control the release of a drug include covering it with a slow dissolving coating, formulating it in a suspension or emulsion, or complexing with ion exchange resins. More recent techniques which provide more control and are under current investigation include the encapsulation of a drug in a polymer for example a hydrogel (Conaghey *et al.* (1998a,b)), dissolution of the drug in a matrix (Scott and Hollenbeck (1991)) and the use of liquid crystals (Carr *et al.* (1997)) as novel delivery vehicles. We will concentrate on a simple membrane controlled system, that is where the release of drug to the skin is controlled by a membrane. A schematic representation of each of these types of devices is show in figure 4-1. A typical device, illustrated in figure 4-1(c) consists of an impermeable backing, a drug reservoir, a diffusion control membrane and an adhesive strip which ensures that the drug stays in contact with a particular chosen site on the skin. The rate of drug effusion to the skin depends on the diffusion coefficient of the drug

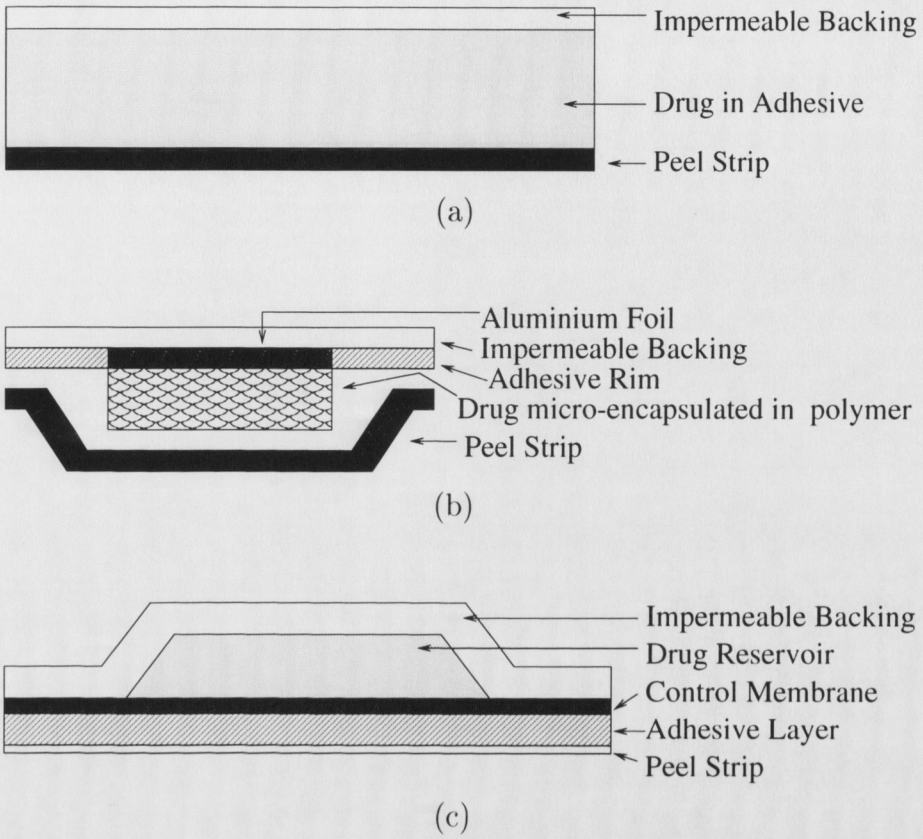

Figure 4-1: Schematic diagram of the various drug delivery systems, (a) adhesive control, (b) drug is microsealed in a polymer, (c) membrane control

through the membrane.

The particular design of the delivery device is very important to ensure zero order release. As we will see later in this chapter, the theoretical model of a matrix device was first described by Higuchi (1961). He found the release rate to be inversely proportional to time. The aim is to have a zero order rate of release. In order to achieve this Rhine *et al.* (1980) designed a hemispherical device with a hemispherical hole. Later Kuu and Yalkowsky (1985) described a rectangular device again with hemispherical holes. However, the fundamental problem with both of these devices is that they are difficult to manufacture on

a large scale. Mishra and Yalkowsky (1990) designed a device based on a much simpler geometry - a flat circular hole device - which has as its trade off the fact that it doesn't give exact zero order kinetics, but it is certainly a reasonable first attempt.

There are many physico-chemical and physiological factors governing the passage of a drug into the skin. A good discussion on these is presented in the review article by Singh and Singh (1993).

Some drugs such as nitro-glycerin pass through the skin naturally. Others may need a chemical penetration enhancer (Walters (1989)) or some form of thermal perturbation (Bodde *et al.* (1990)). It has been shown by Jenkinson and Walton (1974); Russo *et al.* (1980)and Shelly *et al.* (1950), that the application of an electric field as a means of driving drug into the skin can be an effective alternative. This phenomenon known as iontophoresis, is especially significant for transporting ionized drugs. We will now take a more detailed look at the area of iontophoresis.

4.2 Iontophoresis

Iontophoresis is a process which causes an increased permeation of ionized substances into or through a tissue by the application of an electric field (Tyle (1986)). This method was first suggested by Leduc (1900) at the beginning of the twentieth century as an alternative means of delivering medicine to the body. However despite the fact that knowledge of the technique has been gaining in momentum, its use is still not widespread (Singh and Maibach (1993)).

A typical iontphoretic device is show schematically in figure 4-2. It consists of an active well containing the drug and a passive well containing a buffer. Electrodes are attached to the wells and an electric potential is applied across them. This causes the drug to ionise and has the effect of driving the ions into the skin. Assuming that the drug ions are positive as shown in figure 4-2, a circuit is

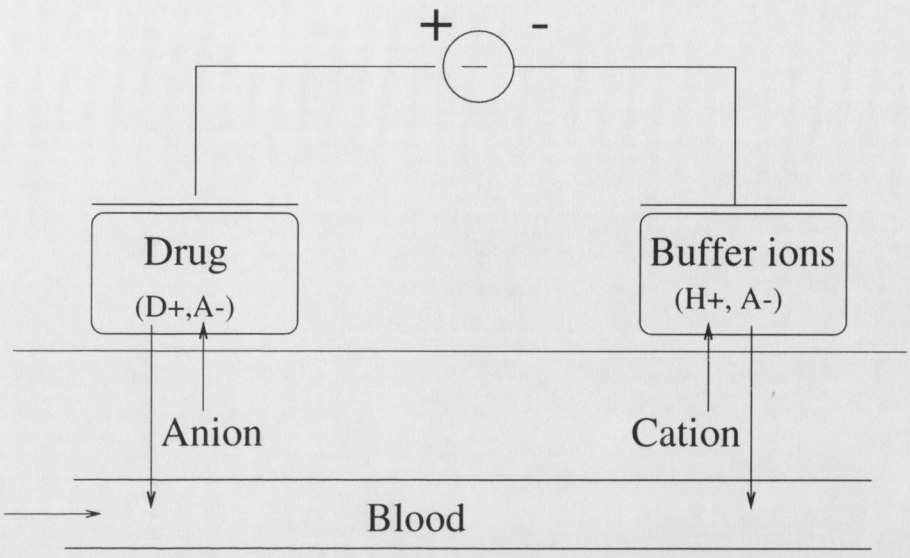

Figure 4-2: Schematic diagram of an iontphoretic device, adapted from a review by Burnette (1988)

set up whereby the positive drug ion (D^+) is driven into the bloodstream. Since the skin itself contains extracellular fluid with Na^+ as its primary cation and Cl^- as its primary anion, these ions are affected by the process. The sodium ion migrates towards the negative electrode and the chloride ion migrates towards the positive electrode. In addition the buffer ion (designated by A^- in the diagram) also migrates into the bloodstream.

As detailed in chapter 3, the transfollicular and transappendageal routes constitute the major pathways for penetration of ionized species and this penetration can be facilitated by the application of an electric field.

Foley and Corish (1992) have shown that the resistance of the skin decreases on the application of an electric current and used this fact to investigate the increased permeation of morphine hydrochloride into the skin. Vincent (1976) has discussed quantitatively the effect of applying an electric field to an ion and obtained expressions relating the magnitude of the force to the magnitude of the subsequent velocity. Many researchers have compared passive and iontophoretic

mechanisms *e.g.* Singh and Singh (1993). Masada *et al.* (1989) developed a theoretical equation relating flux enhancement to applied voltage and successfully applied their theory to a four-electrode system.

Burnette and Marrero (1986) compared iontophoretic and passive transport of thyrotropin across excised nude mouse skin and concluded that the motion of the charge and uncharged species was greater for in the presence of an electric current. Yoshida and Roberts (1995) used conductivity measurements to predict transport of various anions across excised skin.

As far as the mechanism and pathways through which iontophoresis takes place, Burnette and Ongpipattanakul (1987, 1988) have looked at the pore transport properties and they also characterised the permselective properties of excised skin during iontophoresis. There is therefore a great deal of interest and research in this technology.

However, despite the recent surge in research and knowledge of iontophoresis in the last two decades, further research is still required in order to maximize the advantages of this system

4.2.1 Mechanisms of flux enhancement

Iontophoresis enhances drug delivery by 3 mechanisms namely

- (i) the ion-electric field interaction provides an additional force which drives the ions into the skin
- (ii)the presence of a current increases skin permeability
- (iii) electro-osmosis produces bulk motion of solvent, carrying with it neutral species in solvent stream.

Pikal and Shah (1990) have examined the transport mechanisms in iontophoresis in particular looking at the effect of electrosomotic flow.

Praissman *et al.* (1973) reported that the phenomenon of electroosmosis occurs when a current is passed through a membrane separating two electrolytes. The momentum of ion flow produces bulk motion of the solvent and therefore increases the momentum of the neutral species. The role of electro-osmotic flow in transdermal iontophoresis is discussed by Pikal (1992). He suggests that the theory developed by Manning (1967) (who related electroosmosis to measurable quantities such as viscosity *etc.*) is reasonable in that it agrees closely with experiment. Pikal concludes that of the three mechanisms of flux enhancement by iontophoresis, electro-osmotic flow is the dominant flux enhancer for large ions. For smaller ions however, the ionic effect dominates. We have already discussed the first two mechanisms in chapter3. Of these three mechanisms, we will concentrate on the second one and models for this are presented in the next section. The increase in skin permeability was discussed in chapter 3 where we also presented a more general discussion on the function of the skin.

4.2.2 Models for iontophoresis

There are two models used to describe the ionic effect of iontophoretic transport of drugs across the skin. The first of these is the constant field approximation. By assuming a constant field field everywhere, the solution is applicable to ions of any valence. The steady state form of this approximation was derived by Goldman (1943) and the time dependent form was derived much later by Keister and Kasting (1986). Although this theory is the most mathematically tractable and useful for iontophoresis, it is important to be aware of a second model called the electro-neutrality model and described by Planck (1890). The main assumption of Planck's model is that all points within the membrane are electrically neutral on a microscopic scale. Planck obtained steady state solutions for a 1:1 electrolyte using this model and Schogl (1954) later extended this steady state model to include more complex electrolyte mixtures.

Norman (1975) examined the diffusional spread of iontophoretically injected ions and assumed a constant field approximation. His model was that of diffusion from an infinite source into an infinitely thick membrane. He remarked that the reason for using the constant field approximation was that the use the electroneutrality condition would require both the conductivity and the osmotic pressure to be significantly altered. This in turn would cause solvent movements which would interfere with the flux analysis.

However, Kasting and Keister (1988) later remarked that the constant field approximation is not suitable for thick membranes so the Norman (1975) analysis was deemed incorrect. They recently reviewed both of the models, showing the limits of usefulness of each. For our purposes we will consider very thin membranes and therefore the Goldman approximation is most useful. The Planck approximation is better when considering thicker membranes or when there are vastly different ion concentrations on either side of the membrane.

In all cases of iontophoretic models, the conclusions (in contrast with the solutions) have been simple: The skin is a very complex organ and there is more than one pathway through it. Additional considerations such as convective coupling between flows, the effect of fixed charges, the effect of more than one drug species, the variation in diffusivity and ion mobility upon the application of an electric field must also be taken into account in order to get a complete solution to the behaviour of a drug in the skin. It is very difficult to predict the behaviour of a drug which comes in contact with the skin. But in order to understand how the behaviour of the skin differs from the behaviour of an ideal membrane, one must first of all understand the behaviour of an ideal membrane.

This ends our theoretical description of iontophoresis. We will continue by reviewing the mathematical models that have so far been presented to describe drug release from a membrane and then present our extensions to these models.

4.3 Review of mathematical models

The subject of passive release of a drug from a bounded membrane has received considerable attention in the literature (Higuchi (1967)). The amount of solid material (Q) released from a planar system having a homogeneous matrix into a perfect sink has been derived by Higuchi (1961) as

$$Q = \sqrt{Dt(2C_0 - C_s)C_s} \tag{4.1}$$

where D is the diffusion coefficient, C_0 is the initial amount of drug per unit volume, C_s is the solubility of the drug in the medium and t is time.

In this case, there is clearly a linear relationship between Q and $t^{\frac{1}{2}}$. Therefore, for the system mentioned, a linear plot of Q versus $t^{\frac{1}{2}}$ should be a good indication of material transfer via this mechanism of diffusion.

However Schwartz *et al.* (1968) showed that the release of material from a matrix, if controlled by first order kinetics, could be described by a rate law such as

$$\frac{Q}{Q_0} = A\exp[kt] \tag{4.2}$$

where Q_0 is the amount of material present in the matrix initially, k is the first order rate constant and an A is arbitrary constant (which, for simplicity, we will set as 1). The above is a more constrained form of equation (4.1). It can be manipulated and rewritten as

$$log(Q) = kt - log(Q_0) \tag{4.3}$$

so that a plot of log(Q) against t should be linear. Examination of a matrix system demonstrated that both plots of Q against $t^{\frac{1}{2}}$ and $log(Q)$ against t can be essentially linear. Therefore further analysis was necessary in order to differentiate between the two possible mechanisms. This involved measuring the rate of

release or the permeability. Additional studies were conducted by Donbrow and Friedman (1975) confirm this, and suggest a standard procedure be applied to all data in order to fully exemplify the pertinent transport mechanism. This standard procedure consists of presenting plots of Q against $t^{\frac{1}{2}}$ and $log(Q)$ against t in addition to presenting a plot of $\frac{\partial Q}{\partial t}$ against $\frac{1}{Q}$. It can be easily shown that a linear plot of $\frac{\partial Q}{\partial t}$ against $\frac{1}{Q}$ will be a good indication of diffusion control whereas a non-linear plot suggests first order kinetic control. This is because a plot of Q against $t^{\frac{1}{2}}$ is essentially the same as a plot of $\frac{\partial Q}{\partial t}$ against $\frac{1}{Q}$ but the difference between diffusion control and kinetic control may not be apparent (due to size of error bars) when comparing a plot of $log(Q)$ against t with a plot of Q against $t^{\frac{1}{2}}$. The differences are in fact, an artefact of the fitting procedure.

4.4 More detailed models

For a planar system having a granular matrix, additional parameters including the tortousity factor of the capillary system, τ, and the porosity of matrix, ϵ, are included in the diffusion controlled model (Higuchi (1963)). This gives the more complex expression

$$Q = \sqrt{\frac{D\epsilon}{\tau}(2C_0 - \epsilon C_s)C_s t} \tag{4.4}$$

In a subsequent report Desai *et al.* (1965), showed that these factors are not independent. That is variation of one will automatically vary the others. This means that such a system is more difficult to model accurately than a system where all the parameters are independent of one another. In fact, all models to date assume that there is no correlation between any of the parameters and there is therefore a need for more sophisticated models in this area.

Higuchi (1960) also showed how a simple solution of the diffusion equation (given below - equation (4.5)), previously derived in many textbooks (*c.f.* Jost

(1960)), can be applied in order to quantify drug absorption from solutions.

$$\frac{\partial c}{\partial t} = D\frac{\partial^2 c}{\partial x^2} \tag{4.5}$$

Again given conditions of an infinite sink on one side of the solution matrix, he derived an expression for the concentration profile of the material within the matrix as a function of distance and time. This expression is then manipulated to obtain an expression for the quantity of material released as outlined in equation (4.6).

$$Q = hC_0[1 - \frac{8}{\pi}\sum_{n=0}^{\infty}\frac{1}{(2n+1)^2}\exp[\frac{-D(2n+1)^2\pi^2 t}{4h^2}] \tag{4.6}$$

where D and t are the diffusion coefficient and the time as defined before with the additions of h as the thickness of applied phase of drug solution and C_0 again being the initial concentration of the solute. It is clear that the solution phase has a finite thickness h. The relationship between Q and t is much more complex than the previous cases and makes the task of confirming this mechanism, a lot more difficult than the cases discussed in the previous section.

However, it can be shown (Higuchi (1962)) that, for semi-infinite diffusion, that is in the limit as h approaches infinity, the expression for Q is much more simple.

$$Q = 2C_0\left(\frac{Dt}{\pi}\right)^{\frac{1}{2}} \tag{4.7}$$

In figure 4-3 we have plotted Q against t from equations 4.6 and 4.7. This serves to clarify the assertion of Higuchi that for release of $< 60\%$, the simple expression for amount released from a semi-infinite matrix is a good approximation to the amount of of drug released from a matrix of finite thickness h.

Therefore for all the cases mentioned above, plots of Q against $\sqrt{t}$ will be essentially linear. In order to differentiate between diffusion obeying and not obeying Fick's law one should plot Q against C_0. A useful summary of models

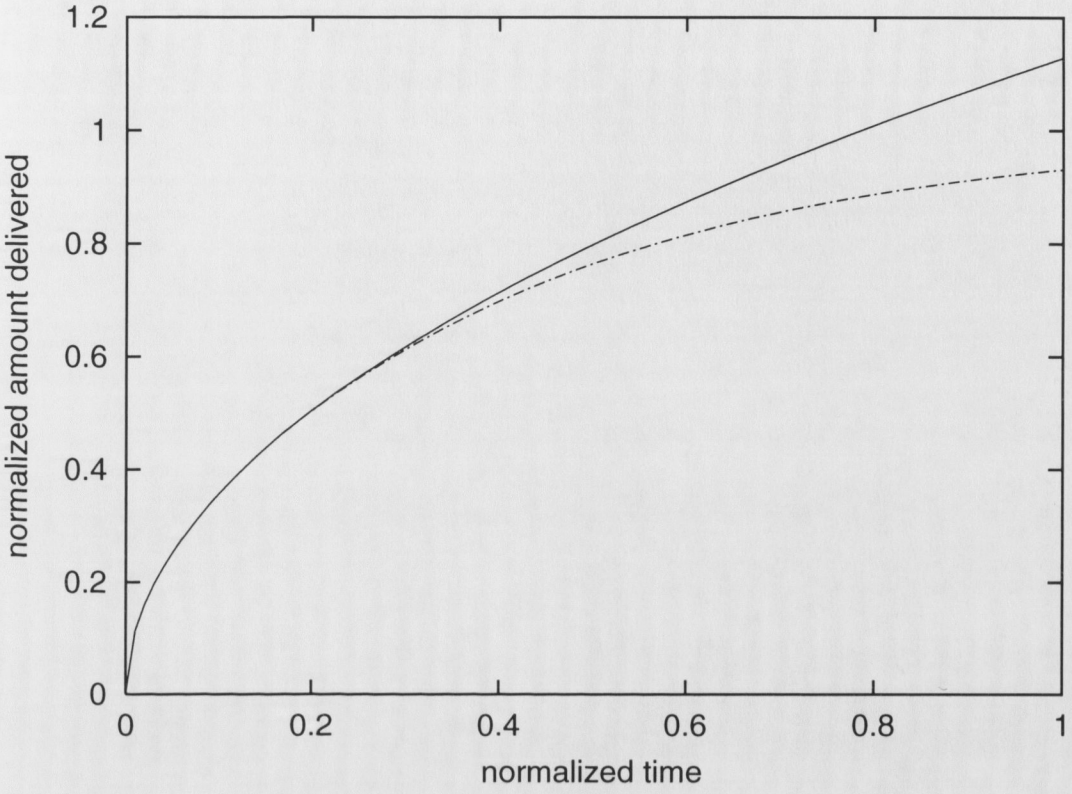

Figure 4-3: Comparison of diffusion from a semi-infinite source (equation (4.7)) with diffusion from a source of finite length (equation (4.6)) showing that the approximation is good up to 60%. The dashed line indicates the exact solution and the full line indicates the approximation.

discussed above is presented in a review paper by Higuchi (1967).

4.5 Extension of Models to include iontophoresis

We now show how we have extended the model based on Fick's law to include the effects of iontophoresis and first order chemical reaction within the matrix. We start by showing how the expressions for concentration, amount released and permeability for passive diffusion were derived. From here we use similar

techniques to derive the same quantities for transport via iontophoresis. The aim is to discuss these equations in as general terms as is possible so that it will be easy to transfer the knowledge to other applications of the diffusion equation.

4.6 General Description of the physical system and formulation of the boundary value problem

We represent the patch as a rectangular matrix of length L. We assume that there is a uniformly distributed concentration of drug in the patch initially and that diffusion is planar. The spatial region inside the patch is therefore defined as $0 \leq x \leq L$. The receptor for the drug is the skin and we assume that as soon as the drug reaches the surface of the skin it is transported into the lower layers. We will apply a uniform electric field E across the matrix only, and we will assume that the ionic mobility of the drug is μ. We will further allow the drug ions to undergo a chemical reaction with a first order rate constant k. Our initial condition is therefore that of a uniform concentration of drug c_0 in the matrix. The first boundary condition describes the skin as a uniform sink6 The only means of exit of the drug from the matrix will be into the skin and therefore the flux at the other extremity is zero. Thus we have the second boundary condition. The differential equation governing the transport and kinetics is

$$\frac{\partial c}{\partial t} = \frac{\partial^2 c}{\partial x^2} - \frac{\mu E L}{D}\frac{\partial c}{\partial x} - kc \tag{4.8}$$

This is presented in non-dimensional form by the use of the following normalised parameters

$$u = \frac{c}{c_0},\ \tau = \frac{Dt}{L^2},\ \chi = \frac{x}{L}\ \gamma = \frac{kL^2}{D},\ \beta = \frac{\mu E L}{D} = \frac{j_m}{j_D} \tag{4.9}$$

and is therefore transformed to a more manageable

$$\frac{\partial u}{\partial \tau} = \frac{\partial^2 u}{\partial \chi^2} - \beta \frac{\partial u}{\partial \chi} - \gamma u \tag{4.10}$$

where u represents a non dimensional penetrant concentration at any point in the membrane which is scaled with respect to the concentration c_0 at the donor solution/membrane interface. χ is the normalised distance variable scaled with respect to the total thickness L of the membrane. Hence we note that $0 < u < 1$ and $0 < \chi < 1$. Furthermore, γ, β represent a normalised diffusion/reaction and diffusion/migration parameter respectively. In fact the diffusion/reaction parameter γ is defined as the ratio of the flux due to the chemical reaction to the flux arising from the species diffusing through the matrix. In a similar way, the parameter, β defines the ratio of the migration flux to the diffusion flux and compares the magnitudes of the transport rate of penetrant through the matrix via migration and diffusion respectively. Consequently the ratio $\frac{\gamma}{\beta}$ compares the rate of penetrant species reaction at a site in the matrix to the rate of electro-migration of penetrant species within the matrix. The parameter β depends directly on both the electric field strength E within the matrix and on the ionic mobility μ of the penetrant species. It also depends on the matrix thickness and is inversely proportional to the diffusion coefficient D of the penetrant. In contrast the parameter γ is directly proportional to the first order rate constant for species removal within the matrix and is inversely proportional to the diffusion coefficient D. The expression presented in equation (4.10) should be compared with the the equation governing simple passive diffusion within the membrane which is well described by the time dependent Fick diffusion equation

$$\frac{\partial u}{\partial \tau} = \frac{\partial^2 u}{\partial \chi^2} \tag{4.11}$$

The problem is defined mathematically in terms of the following initial and boundary conditions:

$$u(\chi, 0) = 1, \quad \left(\frac{\partial u}{\partial \tau}\right)_{\chi=0} = 0, \quad u(1, \tau) = 0 \tag{4.12}$$

4.7 Solution of the Passive equation

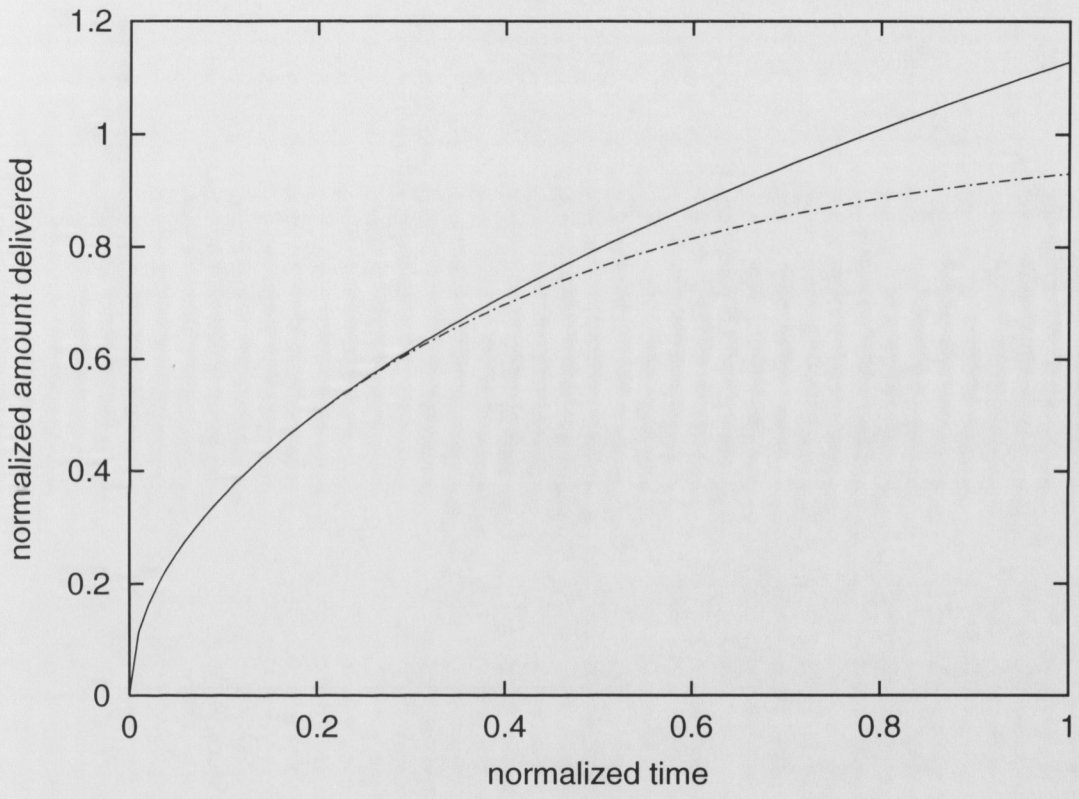

Figure 4-4: Concentration profile of diffusion from an inert matrix over time with values of τ starting at 0.01 (uppermost curve) and incrementing in ten steps of equal size 0.05 as far as 0.46

The passive equation is solved using the technique of separation of variables, a common method for solving differential equations which are dependent on more than one variable. We assume that the complete solution can be separated out into two components, one of which is dependent only on the spatial variable $X(\chi)$ and the other is only dependent on time $T(\tau)$. Both components are found and

the equation admits the following solution:

$$u(\chi,\tau) = \frac{4}{\pi}\sum_{n=0}^{\infty}\frac{(-1)^n}{2n+1}\cos\left(\frac{(2n+1)\pi\chi}{2}\right)\exp\left(-\frac{(2n+1)^2\pi^2 t}{4}\right) \tag{4.13}$$

Typical diffusant concentration profiles through the matrix obtained using equation (4.13) are presented in figure 4-4.

Initially the concentration profile shows a matrix full of drug with slight depletion at one end as the drug is carried into the skin. As time goes on, since this is not an infinite source, the drug concentration within the membrane decreases rapidly again with depletion occurring to a greater extent at the region closest to the skin until finally the membrane is devoid of drug completely.

An interesting way to look at this profile is as a surface plot of χ, τ and u (figure 4-5). Here we can see that initially there is a steep gradient in concentration change over time. However, the system rapidly settles down and there is a more or less uniform decrease in concentration across the matrix as time goes on. This is interesting because it is contrary to the arguments proposed by Higuchi in his theoretical description of drug release from a membrane, because he has assumed that the profile is more like a moving boundary, where the drug will be removed completely from the extremity at the infinite sink before there is any concentration change in the other extremity. This means that there is a sharp discontinuity in the profile as opposed to the situation pertaining to a drug present in solution where, except for the initial stages, the profile is smooth and continuous.

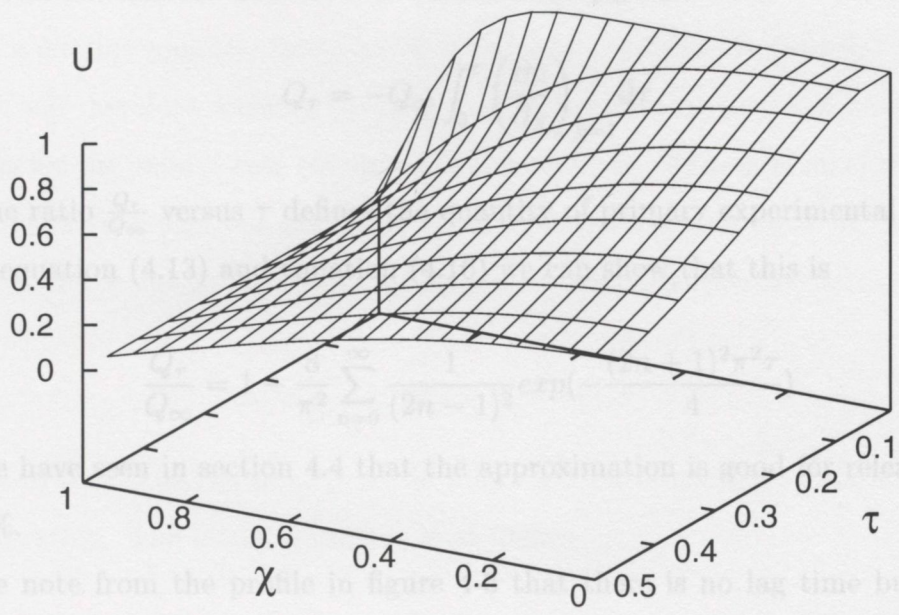

Figure 4-5: Surface plot of basic solution showing concentration profile over time with values of τ starting at 0.01 and incrementing in ten steps of equal size 0.05 as far as 0.46

4.8 Quantity delivered

In terms of the actual amount of drug delivered into the skin, this is obtained via the equation

$$Q_t = -DA \int_0^t \left(\frac{\partial c}{\partial x} \right)_{x=L} \mathrm{dt} \tag{4.14}$$

where A is the cross-sectional area of the plane. In terms of normalised parameters, this is

$$Q_\tau = -ALc_0 \int_0^\tau \left(\frac{\partial u}{\partial \chi} \right)_{\chi=1} \mathrm{d}\tau \tag{4.15}$$

The quantity ALc_0 denotes the total amount of diffusant contained initially in

the matrix and is the amount that would be released after an infinite amount of time Q_∞. It is clear that, in this case, $Q_\infty = 1$. However it is standard procedure to express the amount delivered as a fraction of Q_∞ and hence

$$Q_\tau = -Q_\infty \int_0^\tau \left(\frac{\partial u}{\partial \chi}\right)_{\chi=1} \mathrm{d}\tau \tag{4.16}$$

The ratio $\frac{Q_\tau}{Q_\infty}$ versus τ defines the quantity of primary experimental interest. From equation (4.13) and equation (4.16) we can show that this is

$$\frac{Q_\tau}{Q_\infty} = 1 - \frac{8}{\pi^2} \sum_{n=0}^{\infty} \frac{1}{(2n-1)^2} exp(-\frac{(2n+1)^2\pi^2\tau}{4}) \tag{4.17}$$

We have seen in section 4.4 that the approximation is good for release of up to 60%.

We note from the profile in figure 4-3 that there is no lag time but rather what is seen is a "burst effect" of drug released from the patch. It is useful to note that in reality there is some lag time and evidence of this can be seen in the work of Foley (1991) among others.

4.9 Electrically assisted diffusion with concurrent first order chemical reaction

Following from the results for concentration driven diffusion, the case of electrically assisted diffusion with concurrent first order chemical reaction is now considered. The objective is to determine once again, how the concentration changes over distance and time when a voltage is applied and when a chemical reaction involving the drug takes place. We will also look at the amount of substance released, the permeability and the lag time since these are the quantities of experimental significance. In terms of drug transport, this is associated with the phenomena of iontophoresis. However, as mentioned earlier, the general

case will be considered because then the governing differential equation may also be applied to another area of physical chemistry, namely, diffusion and migration and reaction in polymer-modified electrodes. For example, Yap *et al.* (1983) have solved a similar equation but related to polymer modified electrodes.

We will therefore consider the case with the same boundary and initial conditions as for the passive case (section 4.6) but with the addition of an electric field. The boundary conditions are those of zero flux at one extremity of the matrix and an infinite sink at the other. These are expressed mathematically as follows:

$$J_0 = \frac{\partial u}{\partial \chi_0} - \beta u_0 = 0, \quad u(1,\tau) = 0 \tag{4.18}$$

We recall that J is the flux, β is the migration parameter and u is normalized concentration. The initial condition is as before

$$u(\chi, 0) = 1 \tag{4.19}$$

Using the technique of separation of variables, the general solution of equation (4.10) is found to be

$$u(\chi,\tau) = \sum_{n=0}^{\infty} e^{a\chi}[C\cos(b\chi) + D\sin(b\chi))]exp(-\lambda^2 t) \tag{4.20}$$

This is solved with the conditions given above. The complete solution (detailed in Appendix D.1) is

$$u(\chi,\tau) = exp(\frac{\beta\chi}{2}) \sum_{n=0}^{\infty} B_n[\sin(b_n\chi)]exp(-\lambda^2 t) \tag{4.21}$$

where the coefficient of time in the exponential term, λ, contains functions of the migration and reaction parameters (β and γ) and is defined as

$$\lambda = b_n^2 + \frac{\beta^2}{4} - \gamma \tag{4.22}$$

The coefficients of the summation, B_n, are more complex

$$B_n = \frac{8b_n}{\beta^2 + 4b_n^2} \tag{4.23}$$

with b_n being a solution of the transcendental function

$$b_n = \frac{\beta}{2}\tan(b_n) \tag{4.24}$$

Interestingly, the coefficients B_n of the summation, contain functions of the migration parameter β only. Therefore, when considering diffusion and concurrent chemical reaction, the expression for the concentration profile is reasonably simple. Typical concentration profiles are given in figures 4-7 to 4-12 inclusive. These plots were generated by DEQSOL (the numerical finite difference package), because the analytical solution involves an aforementioned transcendental function which must be evaluated numerically. These are discussed in detail below.

4.10 Discussion

With some algebraic manipulation, we can show that when γ and β are set to zero that equation (4.21) reduces to equation (4.13) - the expression for the concentration with passive diffusion. This is shown explicitly in Appendix D.2. We will now look at the effect of the each of the migration and reaction parameters on the concentration profile. The figures presented in the following pages are surface plots showing how the normalised concentration u varies with distance χ and migration parameter β for the time periods $\tau = 0.01, 0.05, 0.1$ and 0.3. The reason for choosing these particular time periods is that they show an interesting range of change and they also correspond with the information contained in the profile for passive diffusion (figure 4-3) and are therefore useful for comparison.

Figure 4-6 is a development of the u, χ, γ surface as a function of time τ

and normalized migration parameter β. The first plot in the series shows the normalised concentration profile at $\tau = 0.01$ for typical positive values of the migration parameter β. The reaction parameter γ is zero. This early time profile indicates clearly that the drug is being repelled from the site of applied voltage and the magnitude of the repulsion is a *quasi* linear function of the magnitude of the applied voltage. However, since it is still a short time period, the effect of the voltage does not manifest itself to a great extent at the other extremity of the matrix. The concentration profile up to approximately 20% of the length of the matrix varies significantly with applied voltage but the profile beyond this limit is more or less independent of the voltage. The second plot in Figure 4-6 shows a similar surface plot but at a longer time period. Here we see a significant deviation from the passive profile as a function of the voltage. There is clearly a non-linear dependence of the concentration on the voltage. It is interesting to note that for $\beta = 5$, the force due to the voltage greatly outweighs the ability of the skin uptake and there is a concentration peak in the middle of the matrix. Even at $\beta = 1$, this peak prevails. There is therefore an optimal value of the voltage somewhere between $\beta = 0$ and $\beta = 1$ where the total force into the matrix is equal to the force out and there is no concentration build-up in the matrix. The third plot in figure 4-6 is the surface profile at longer times $\tau = 0.1$. This profile is very similar to that of $\tau = 0.05$, the difference being that the profile for large positive β is not as steep as the previous plot therefore indicating that much of the drug has exited the matrix. Finally we look at the profile for $\tau = 0.3$. In this case we see that the positive voltage had forced the drug through the matrix and for large β, the matrix is almost devoid of drug. This is in sharp contrast to the the profile where there is no field and $\beta = 0$. At this state the shape of the profile has not changed much from its appearance at the earlier time step. The overall concentration is reduced but there is still a large variation in the concentration at different positions.

Figure 4-7 contains the same information as figure 4-6 but now the reaction

parameter has been included and $\gamma = 1$. There is very little difference between these plots. The reason for this is that the layer thickness -X_K- defined as the distance the drug will travel before undergoing chemical reaction is given by $X_K = \frac{L}{\gamma}$. L denotes the layer thickness which is normalised so that $L = 1$. Therefore for $\gamma = 1$, the layer thickness is also unity so the drug will traverse the matrix before undergoing chemical reaction.

Figure 4-8 depicts the time evolution for $\gamma = 10$. In this case the layer thickness is $X_K = 3.2$ and so considerably more depletion is apparent compared with the case of no chemical reaction. In fact at later times, the drug has either exited the matrix completely or undergone reaction and the effect of the field is overshadowed by the extent of chemical reaction. The extreme case of $\gamma = 100$ is presented in figure 4-9. Here the ratio of migration to diffusion is in the range $.05 > \frac{\beta}{\gamma} > 0$. As would be expected, the effect of large reaction parameter is to cause considerable depletion of the drug before it has exited the matrix and even with the enhancement of an electric field, the high reaction rate dominates and it takes only a very short time ($\tau < 0.05$) before the matrix is completely devoid of drug.

Figure 4-10 shows more clearly the effect of the reaction parameter on the passage of drug. Here we see that in the absence of an electric field, the concentration of drug varies greatly across the matrix even for the small range of reaction parameters presented. As time goes on, the difference is even stronger as evident in the slope of the u, γ profile at $u = 0$. It is interesting to compare this with the profiles in Figure 4-11. Again the effect of the magnitude of the reaction parameter is clearly manifested in the profiles. The characteristic hump due to the push-start effect of the migration is also clearly evident. These profiles are very much different to those of figure 4-10 and they serve to show how the variation of one parameter has a large effect on the resultant concentration profile.

Figure 4-12 depicts the time evolution of the concentration profiles for negative

values of β. This means that the voltage is of opposite polarity to the ions in the matrix. Therefore, rather than being forced out of the matrix, the drug ions are attracted towards the voltage source. In fact, the physical importance of having this voltage is minimal. As is intuitive and as we have seen through the mathematics, this results in less drug being administered than is desired. It serves to retard rather than enhance the rate of delivery. However, if used in conjunction with a chemical enhancer or some other enhancer, this type of voltage may play a role in the fine tuning of the delivery rate.

Surprisingly though, this does not significantly inhibit the passage of the drug through the matrix and it is clear that the concentration profile is similar for the whole range of voltages in the latter half of the matrix, that is the part closest to the skin. However, there will be significant differences in the amount delivered for the different voltages at this time because, for high voltages, so much of the drug is attracted to the voltage source.

4.10.1 Quantity delivered

We shall now derive the expression for the total amount of drug exiting the matrix and discuss the effect of β and γ on this. We recall that the amount of drug delivered equation (4.16) is given by

$$Q_t = -Q_\infty \int_0^\tau \left[\frac{\partial u}{\partial \chi}\right]_{\chi=1} \mathrm{d}\tau \tag{4.25}$$

The first derivative of u w.r.t. χ from equation (4.21) was found. This derivative was then evaluated at $\chi = 1$ and integrated over time. The resulting equation showing the amount as a function of time is

$$\frac{Q_t}{Q_\infty} = -exp(\frac{\beta}{2}) \sum_{n=0}^{\infty} B_m[\frac{\beta}{2}\sin(b_m) + b_m \cos(b_m)] \exp(-\lambda^2 \tau) \tag{4.26}$$

$$\frac{Q_t}{Q_\infty} = -exp(\frac{\beta}{2}) \sum_{n=0}^{\infty} B_m[\beta \sin(b_m)] \exp(-\lambda^2 \tau) \tag{4.27}$$

where all the terms are defined as before. The expression for Q involves transcendental functions. The first few terms in the solution of this were evaluated numerically and are given in the Handbook of Mathematical Functions (Abramowitz and Stegun (1965)). This is not enough for an accurate solution. Therefore, in order to produce the results we have calculated the derivative using a central finite difference scheme and fitted this to a polynomial function. The polynomial was chosen as being of the form $Q = at^{\frac{1}{2}} + bt$ where the parameters a and b were fitted by least squares method. The reason for the particular choice of power law was that for the passive case, the amount is described by the function $at^{\frac{1}{2}}$ and for the case of electrical assisted delivery it has been noted Nolan (1996) from experimental data results that the profile takes on a linear shape at long values of τ. The plots shown in figure 4-13 are for various values of β with $\gamma = 0$. This corresponds to a physical case of iontophoresis with no reaction parameter. The plot of $\beta = 0$, or that of passive release, is also included for comparison. From these plots we can see that as the electric current is increased, the rate of release also increases. This is in agreement with what would be expected. It is also good to see that there is a good deal of similarity between this theoretical result and the experimental results produced by Foley (1991) which are depicted in figure 4-14.

4.11 Conclusions

In this chapter we have considered planar diffusion of a substance from an inert matrix and looked at the resulting concentration profiles in the presence of both electromigration and first order chemical reaction. We have applied this to the process of iontophoresis in an effort to understand more fully the mechanism of

this. However, there are limitations to the model which will result in differences between these theoretical predictions and experimental results. For example, we have considered planar diffusion and assumed that there is no spreading of the drug on the surface of the skin. Secondly, we have assumed that the skin is an infinite sink. As has been discussed in chapter 3 the *stratum corneum* is a barrier to foreign substances and will not transport the drug immediately into the lower layers of the skin. Neither have we been able to model the changes in permeability of the skin once the transport through the barrier begins. Further models of iontophoretic transport will need to take some of these modifications into account.

In terms of amount of drug delivered for the passive case, from a matrix controlled system, the dependence on time is $t^{\frac{1}{2}}$. An ideal delivery system will have a zero order dependence on time but we have seen at the beginning of this chapter that there have been some efforts in design of the patch made to attain this situation. Our model for iontophoretic transport cannot be reduced to a simple approximation as in the passive case. There is an obvious dependence on time and in order to control this, it may be advisable to apply a control membrane between the skin and the matrix. The analysis of this is the subject of the next chapter.

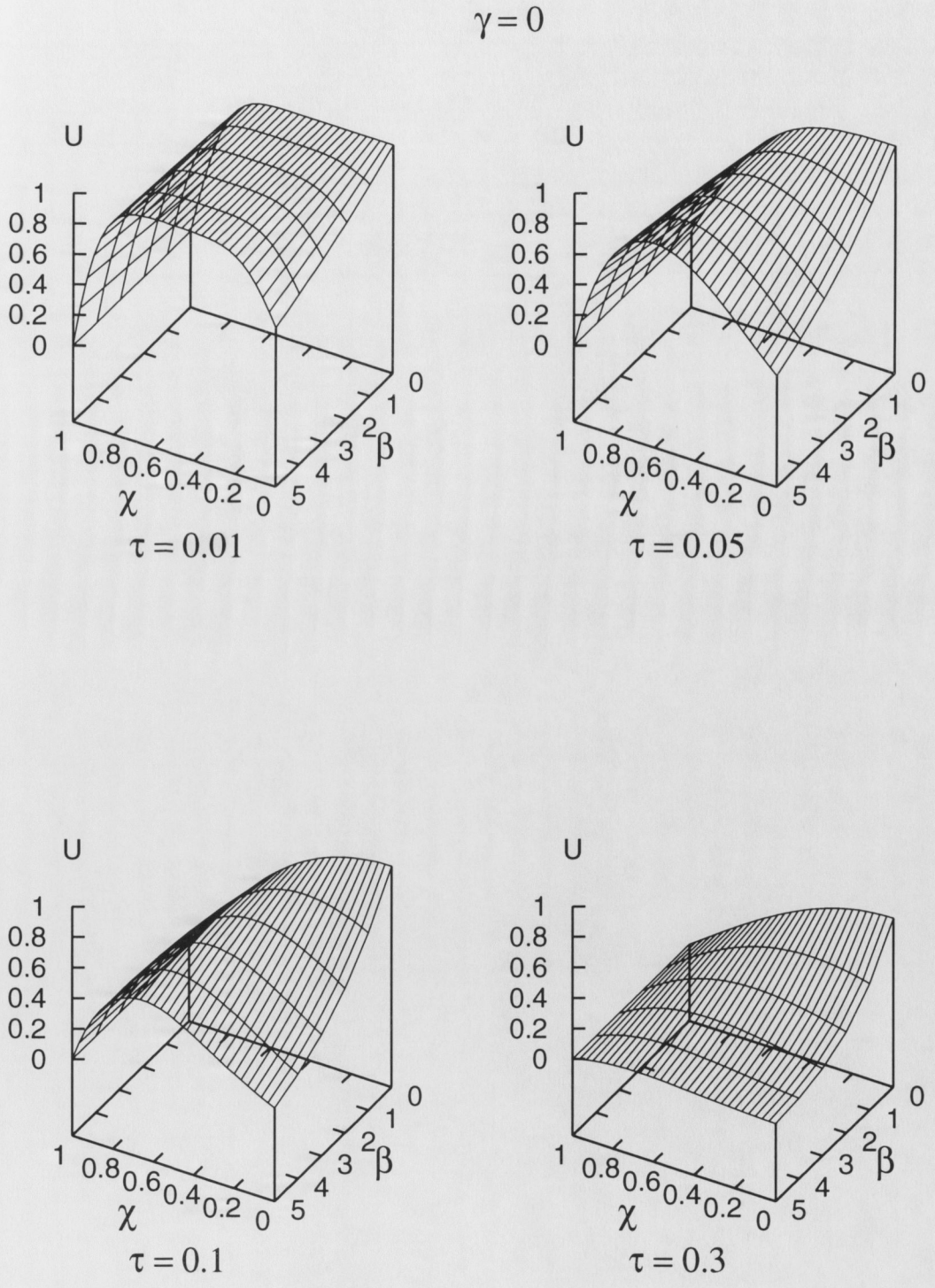

Figure 4-6: Surface plot of full solution of inert matrix showing time development of the concentration profile as a function of distance within the matrix and the migration parameter β. The migration parameters are positive indicating that the applied voltage is of the same charge as the ionized drug. The reaction parameter γ is zero.

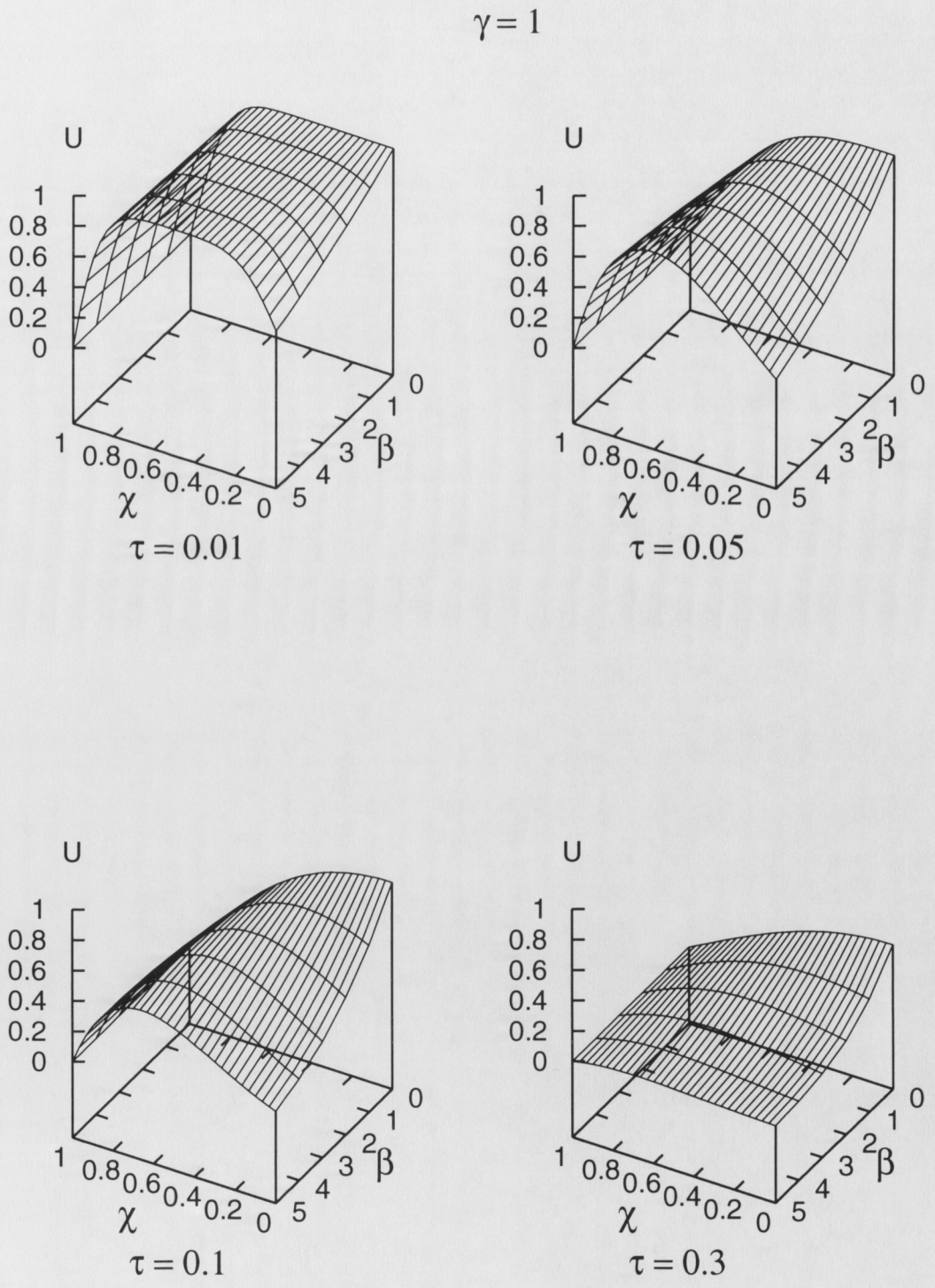

Figure 4-7: Surface plot of full solution of inert matrix showing time development of the concentration profile as a function of distance within the matrix and the migration parameter β. The migration parameters are positive indicating that the applied voltage is of the same charge as the ionized drug. The reaction parameter $\gamma = 1$.

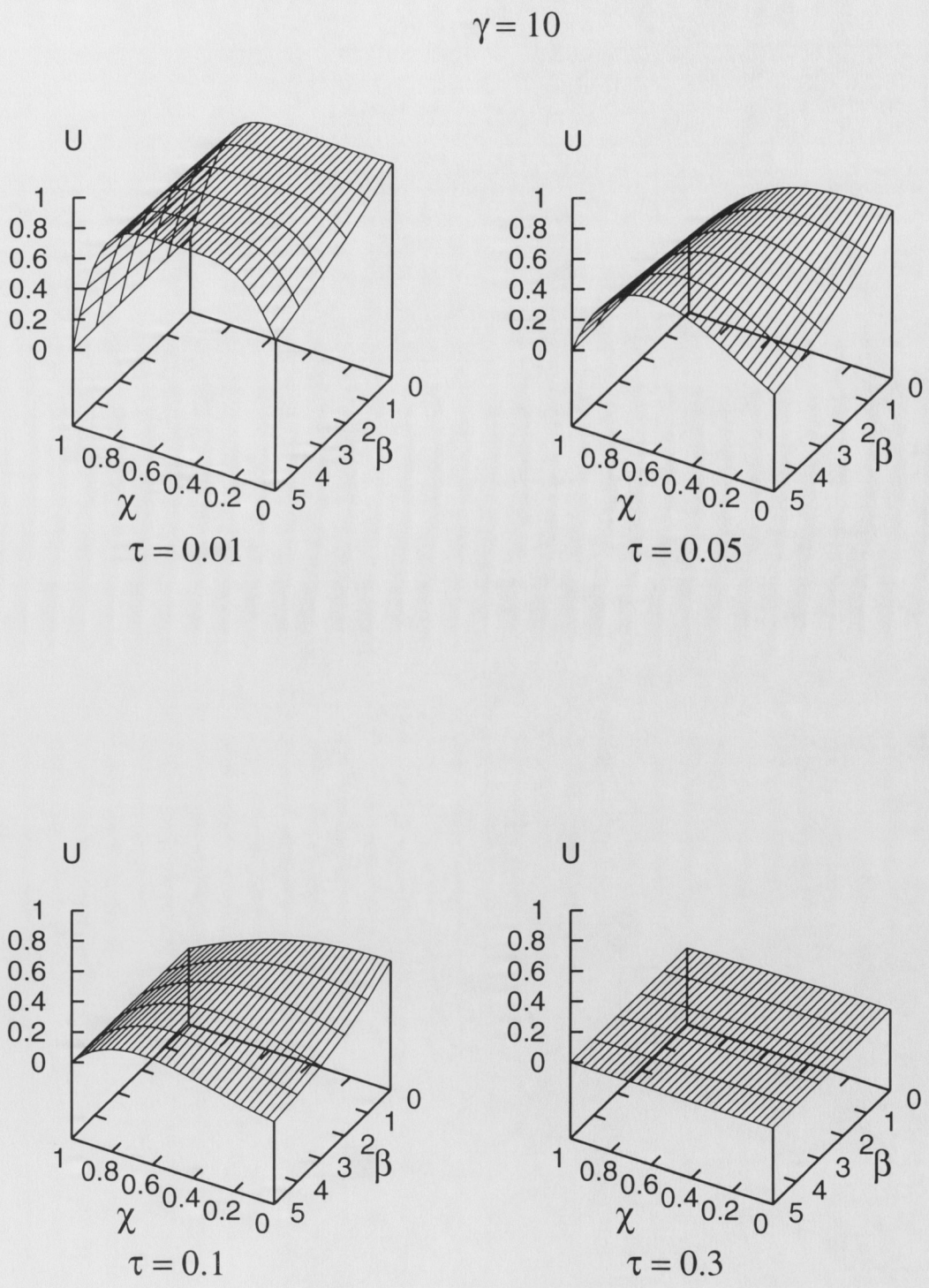

Figure 4-8: Surface plot of full solution of inert matrix showing time development of the concentration profile as a function of distance within the matrix and the migration parameter β. The migration parameters are positive indicating that the applied voltage is of the same charge as the ionized drug. The reaction parameter $\gamma = 10$.

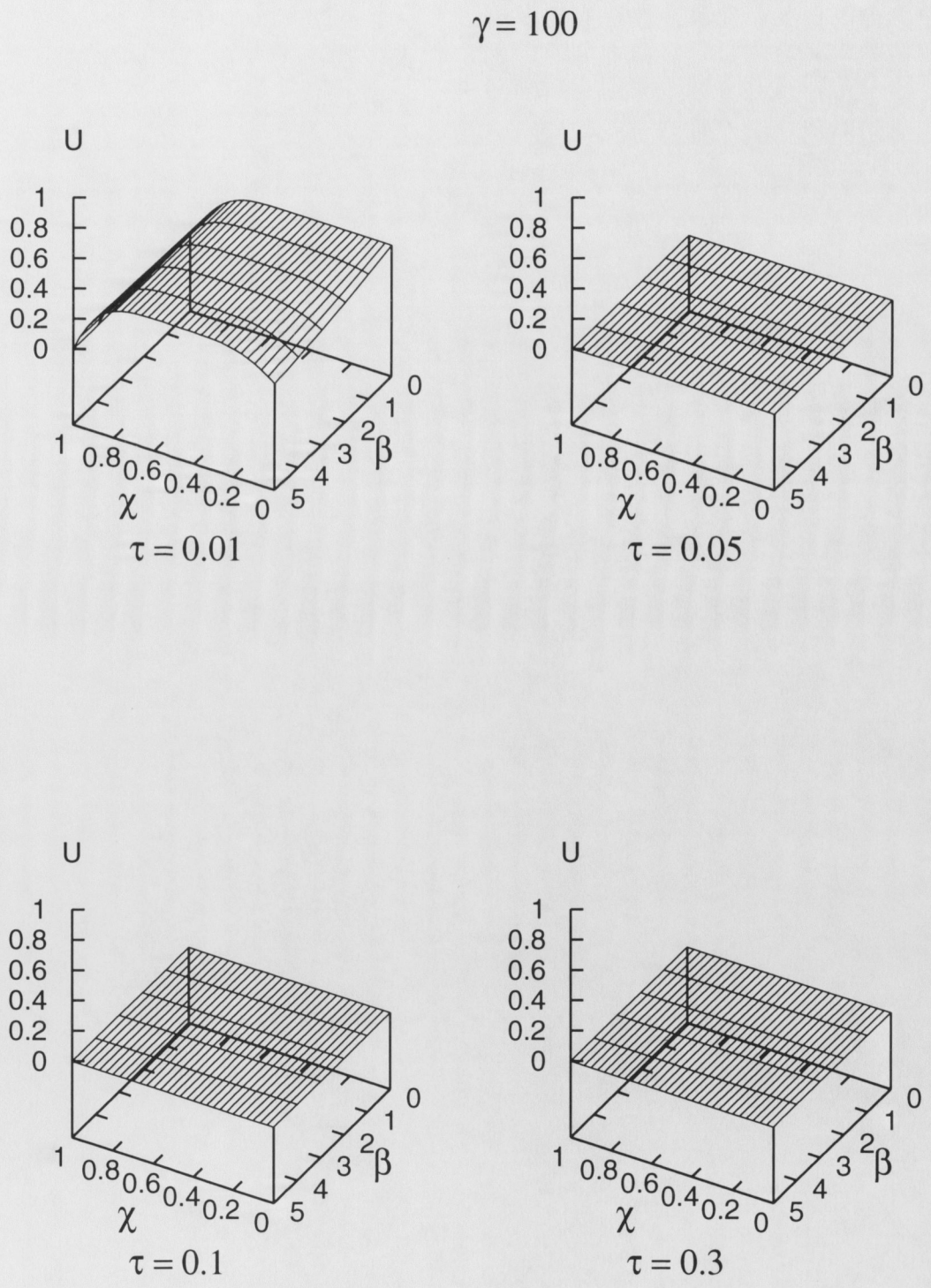

Figure 4-9: Surface plot of full solution of inert matrix showing concentration profile as a function of distance within the matrix and the migration parameter β. The migration parameters are positive indicating that the applied voltage is of the same charge as the ionized drug. The reaction parameter $\gamma = 100$.

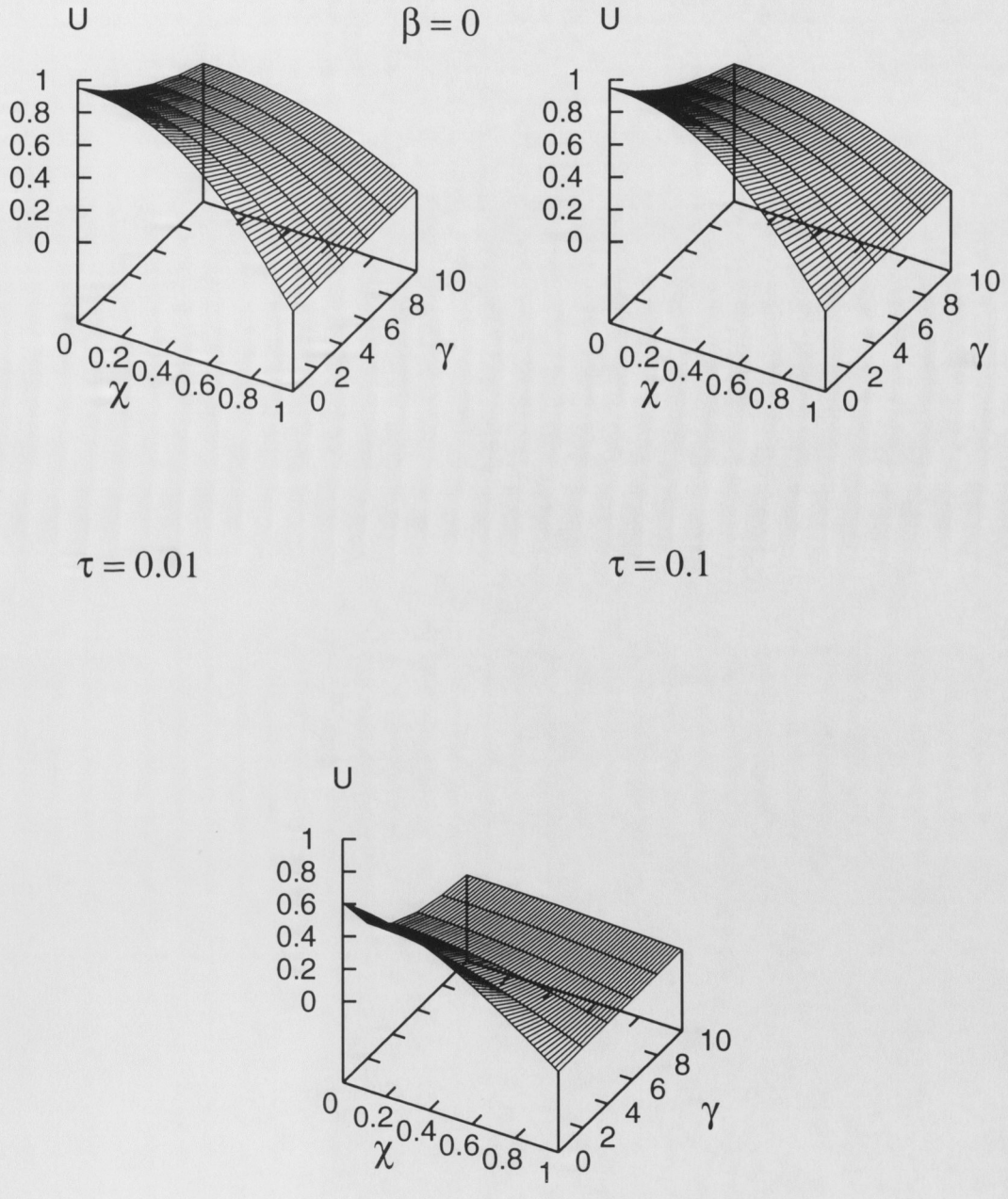

Figure 4-10: Surface plot of full solution of inert matrix showing concentration profile as a function of distance within the matrix and the reaction parameter γ. The reaction is causing a depletion in concentration within the matrix. There is no voltage present, $\beta = 0$

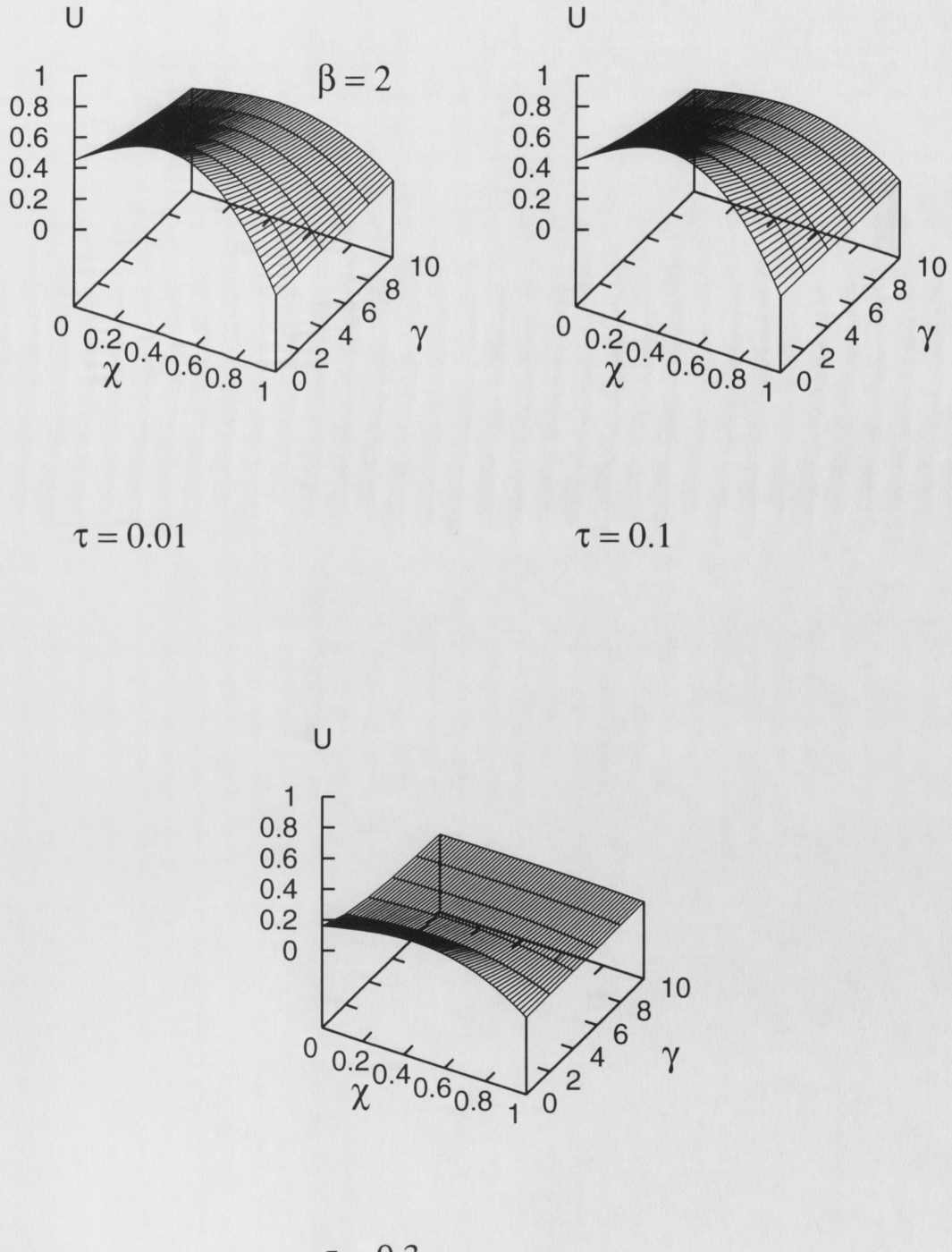

Figure 4-11: Surface plot of full solution of inert matrix showing concentration profile as a function of distance within the matrix and the reaction parameter γ. The reaction is causing a depletion in concentration within the matrix. The voltage is positive indication that it forces the drug out of the matrix.

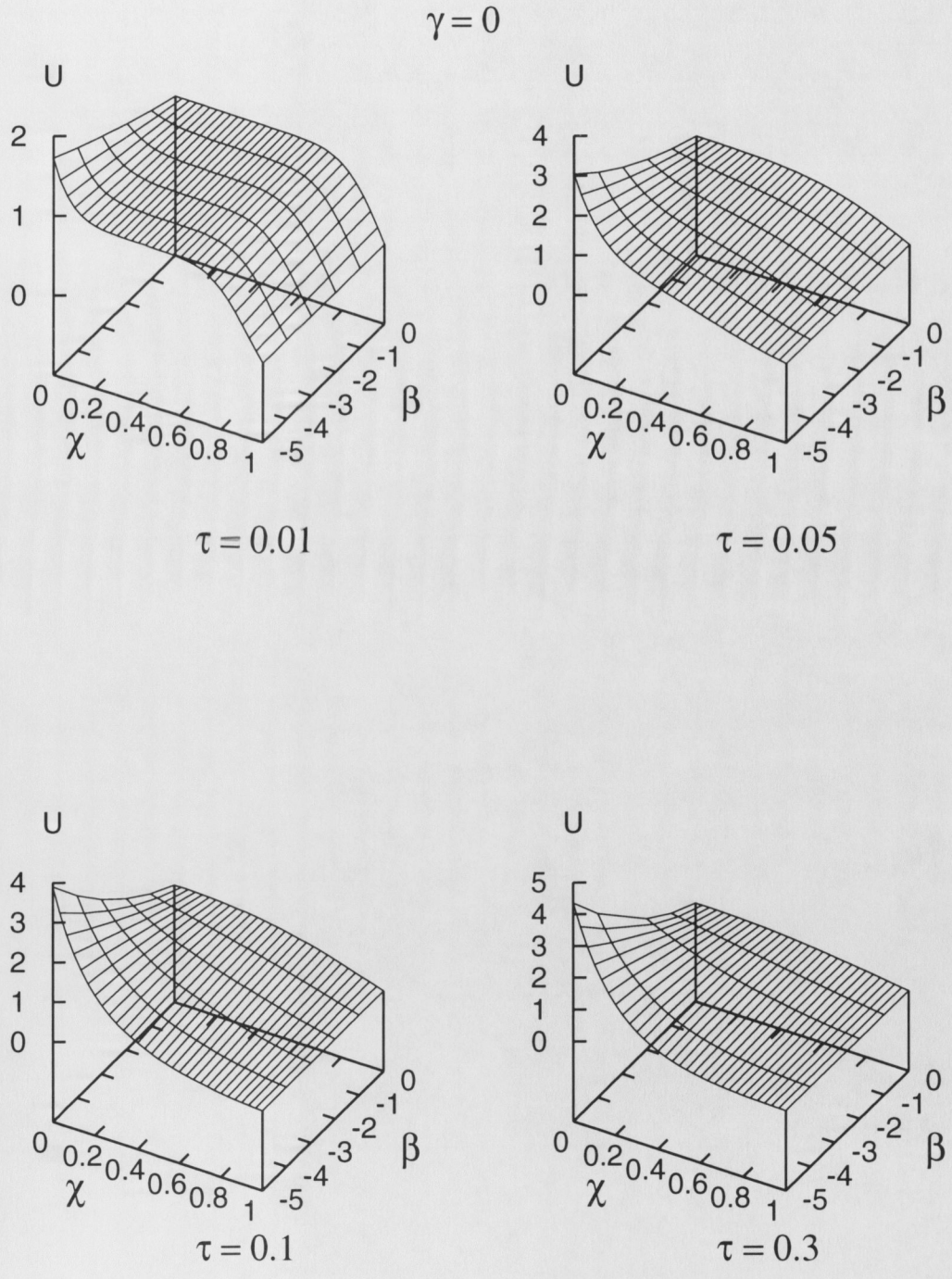

Figure 4-12: Surface plot of full solution of inert matrix showing concentration profile as a function of distance within the matrix and the migration parameter β. The migration parameters are negative indicating that the applied voltage is of the same charge as the ionized drug

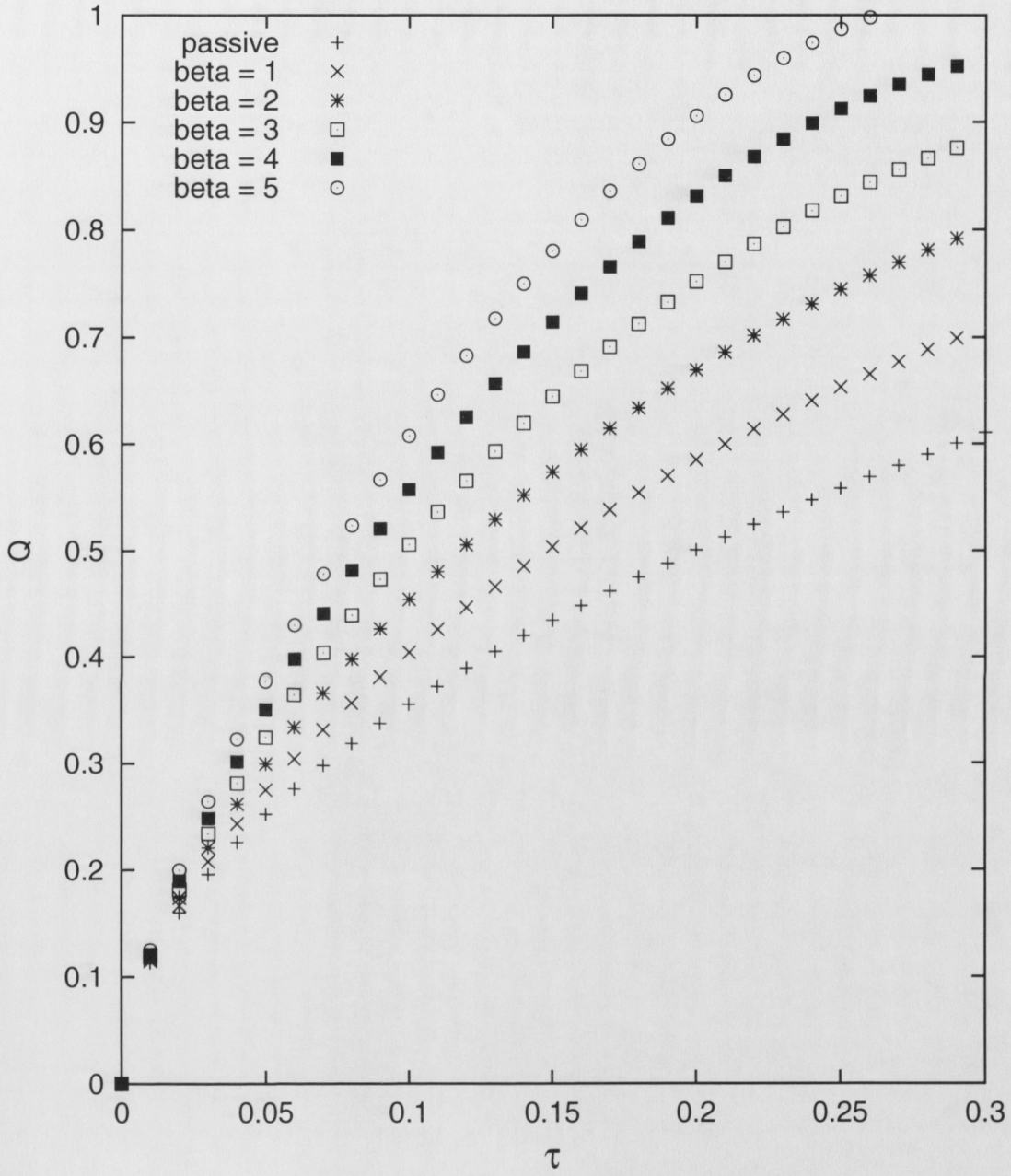

Figure 4-13: Theoretical plot of normalized amount of passive and electrically assisted drug release from an inert matrix (Q), against normalised time (τ) with the β parameter denoting the normalised magnitude of the electric current as 0,1,2,3,4,5

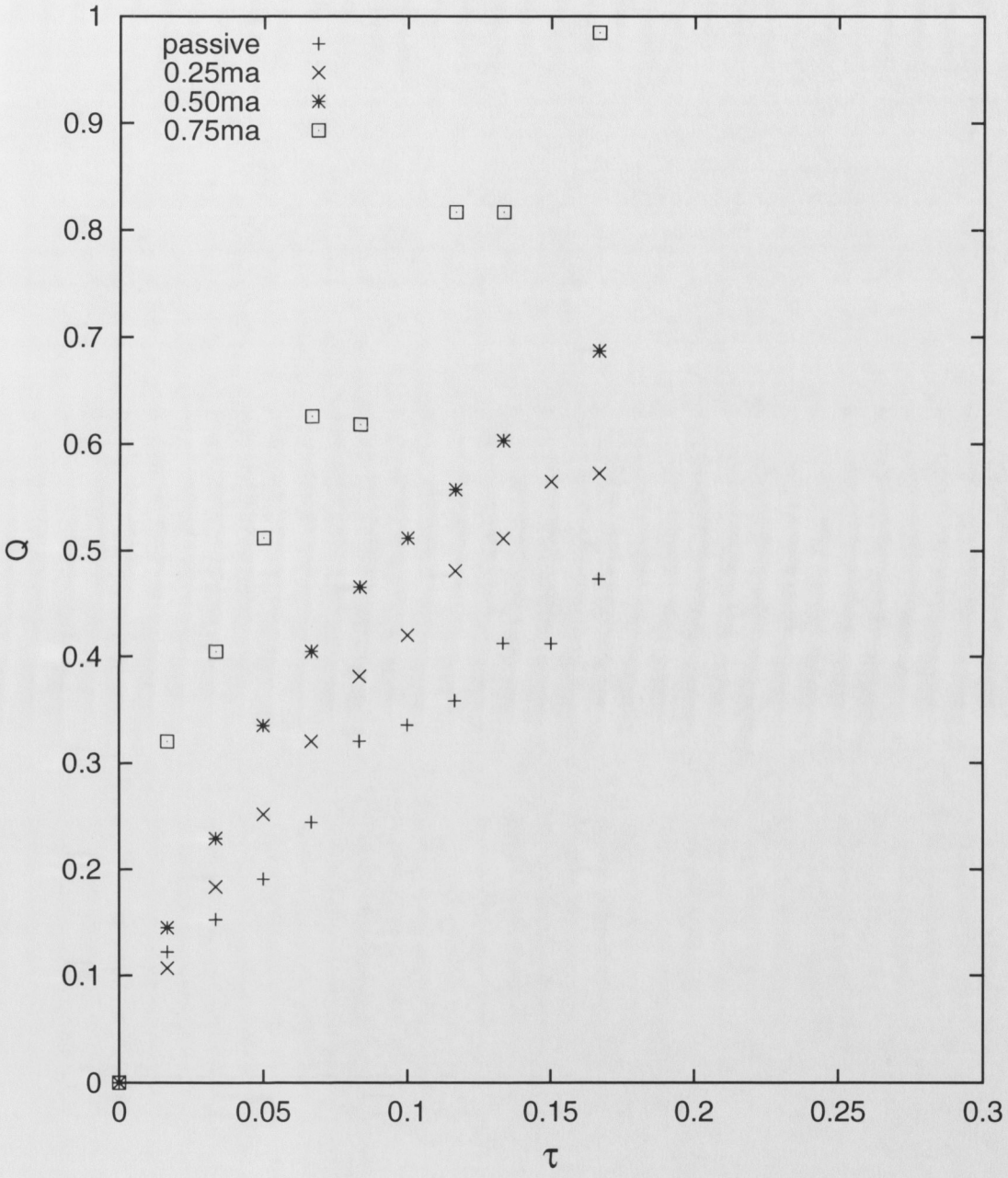

Figure 4-14: Experimental results of passive and electrically assisted delivery of morphine from hydrogels where $0.25ma$ represents a current of 0.25 milli-amps. (*This data is taken from the Ph. D. thesis of Foley (1991)*)

Chapter 5

Diffusion in a Finite Membrane

5.1 Introduction

The analysis of material transport in bounded membranes is a subject of much current interest. Time dependent passive diffusion of material through membranes and thin films has been the subject of mathematical modelling for many years and reference may be made to the classical monographs produced by Carlsaw and Jaeger (1977), Crank (1975), Barrer (1951) and Jost (1960) for a comprehensive survey of progress in this area.

The analysis of bounded diffusion processes in which the diffusing material is also subjected to applied electric fields and can undergo chemical reaction with sites located in the diffusion medium is considerably more complicated and for this reason has not received comparable attention to date.

Attention is focused on bounded diffusion/migration/reaction(DMR) problems because these processes describe the operation of systems of current technological importance such as electric field assisted iontophoretic drug delivery devices (Clemessy *et al.* (1991)), polymer modified electrode sensors (Andrieux and Saveant (1992), Evans (1990), Hilman (1987), Lyons (1994b), Lyons (1996)) and acid transport in a lead/acid cell (Nilson (1993)).

In this chapter we discuss the process of diffusion, reaction and migration through membranes of finite thickness L. Mathematical modelling of these systems involves the formation of a partial differential equation, a suitable initial condition and physically reasonable boundary conditions. The differential equation is then solved to obtain a closed form expression for the concentration profile of the diffusant as a function of distance and time. This expression may then be manipulated to obtain a closed form expression for the total quantity of material released from or entering into the membrane at any given time. The lag time τ_L of the penetrant species and the normalised permeability ρ may be obtained by algebraic manipulation of the expression for quantity released. The lag time is defined as the time required for attainment of the steady state diffusion conditions while the permeability is a measure of the steady state rate of material transport through the membrane material. Both of these quantities as well as the quantity diffusing may be readily determined via experiment. In particular, the lag time τ_L may be used to obtain an estimate of the diffusion coefficient D of the transported species via the expression $\tau_L = \frac{L^2}{6D}$ (Crank (1975)).

Aspects of material transport in membranes have been previously discussed in the literature. For instance, Ludloph *et al.* (1979), presented an analysis to calculate the lag time expected for bounded diffusion coupled with chemical reaction and sorption of diffusing species. They showed that the lag time for bounded passive diffusion coupled with reversible penetrant immobilisation within the membrane is given by $\tau_L = \frac{L^2}{6D}(1 + K)$ where K represents the equilibrium constant relating free and bound penetrant. Leypoldt and Gough (1980) and independently Manning (1980) examined the same system using finite Fourier transform methods. More recently Keister and Kasting (1986) modelled electric field enhanced active diffusion within a finite membrane by a separation of variables method, and derived an expression for the lag time. Chen and Rosenberger (1991) derived closed form solutions for the steady state permeability and lag time of a linear diffusion system with concurrent reaction using the Laplace transform

technique.

In this chapter we present an alternative analysis of bounded diffusion with concurrent chemical reaction and obtain closed form expressions for the concentration profile of the penetrant and the total quantity of diffusant exiting the membrane as a function of time. The effect of applied electric field and chemical rate constant on both the lag time and the permeability is also elucidated.

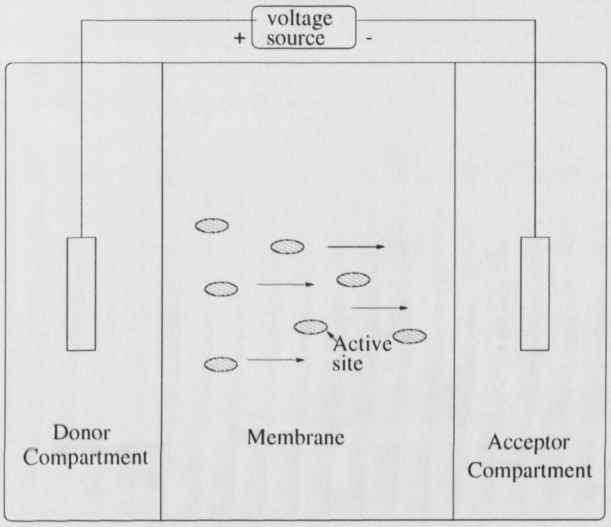

Figure 5-1: Schematic representation of free standing membrane of finite thickness L, containing immobilised active binding/reaction sites. The penetrant species passes through the membrane from a donor to a receptor compartment. A uniform electric field is present in the membrane which can facilitate transport of penetrant.

The mathematical model presented can be used to analyse the following experimental arrangement. We consider a thin homogeneous membrane of thickness L that separates two bulk volumes figure 5-1. We assume that the diffusion is planar. hence the spatial variable is defined over the range $0 \leq x \leq L$. The region $x \leq 0$ is designated as the donor compartment and the region $x \geq L$ is the receptor compartment. We also assume that the membrane is subjected to a constant uniform electric field. Furthermore the diffusing penetrant reacts within

the membrane according to a first order kinetic expression with a rate constant k. Initially, the membrane is devoid of penetrant. At time $t = 0$ the face of the membrane adjacent to the donor compartment is exposed to a concentration c_0 while the other face in contact with the receptor compartment is maintained at zero concentration. It is also assumed that the solutions on both sides of the membrane are well stirred, that the receiver solution acts as an infinite sink and that the donor solution serves as an infinite source.

The mathematical description of the problem involves a time dependent diffusion equation of the following type:

$$\frac{\partial u}{\partial \tau} = \frac{\partial^2 u}{\partial \chi^2} - \beta \frac{\partial u}{\partial \chi} + \gamma u \tag{5.1}$$

which is the same as equation (4.10). This expression is presented in non dimensional form. This is done via definition of the following normalised parameters as have been defined in the previous chapter :

$$u = \frac{c}{\kappa c_0}, \quad \tau = \frac{Dt}{L^2}, \quad \chi = \frac{x}{L}\gamma = \frac{kL^2}{D}, \quad \beta = \frac{\mu E L}{D} = \frac{j_m}{j_D} \tag{5.2}$$

where u represents a non-dimensional penetrant concentration at any point in the membrane which is scaled with respect to the concentration c_0 at the donor solution/membrane interface, and χ is the normalised distance variable scaled with respect to the total thickness L of the membrane. Hence we note that $0 < u < 1$ and $0 < \chi < 1$. The representations of γ and β have been previously described in section 4.6.

The expression presented in equation (5.1) should be compared with the the equation governing simple passive diffusion within the membrane which is well described by the time dependent Fick diffusion equation

$$\frac{\partial u}{\partial \tau} = \frac{\partial^2 u}{\partial \chi^2} \tag{5.3}$$

The problem is defined mathematically in terms of the following initial and boundary conditions:

$$u(\chi, 0) = 0, \quad u(0, \tau) = 1, \quad u(1, \tau) = 0 \tag{5.4}$$

The first condition is the initial condition. The second and third are boundary conditions and they describe an infinite source on one side and an inifinte sink on the other.

We shall initially present a solution of the simple passive diffusion problem governed by equation (5.3) and then outline how the more complex situation of diffusion coupled with concurrent electromigration and chemical reaction which is governed by the differential equation presented in equation (5.1) is tackled. In both cases we utilise the technique of Laplace Transformation which is the solution technique of choice when bounded diffusion problems are examined.

5.2 Passive diffusion in a finite membrane

We initially indicate the manner in which the Fick diffusion equation (5.3) is solved subject to the initial and boundary conditions presented in equation (5.4). The diffusion flux at the membrane receptor compartment interface corresponding to $\chi = 1$ is given by

$$j = -\frac{D\kappa c_0}{L}\left(\frac{\partial u}{\partial \chi}\right)_{\chi=1} \tag{5.5}$$

and the normalised diffusion flux is given by:

$$\Psi = -\frac{jL}{D\kappa c_0} = -\left(\frac{\partial u}{\partial \chi}\right)_{\chi=1} \tag{5.6}$$

We take Laplace transforms of equation (5.3) to obtain the following ordinary differential equation:

$$\frac{\partial^2 \bar{u}}{\partial \chi^2} - p\bar{u} = 0 \tag{5.7}$$

where p denotes the Laplace parameter and $\bar{u}$ represents the concentration of penetrant in Laplace space. Equation (5.7) is subject to the following transformed boundary conditions:

$$\bar{u}(0,p) = \frac{1}{p}, \qquad \bar{u}(1,p) = 0 \tag{5.8}$$

As outlined in appendix E.1, the solution of equation (5.7) is given by:

$$\bar{u}(\chi,p) = \frac{\cosh(\sqrt{p}\chi)}{p} - \frac{\sinh(\sqrt{p}\chi)}{p\tanh(\sqrt{p})} = \frac{\sinh(\sqrt{p}(1-\chi))}{p\sinh(\sqrt{p})} \tag{5.9}$$

We use the complex inversion theorem to obtain the inverse Laplace Transform and invert equation (5.9) to obtain the following expression for the normalised concentration profile:

$$u(\chi,\tau) = 1 - \chi - 2\sum_{n=1}^{\infty} \frac{\sin(n\pi\chi)}{n\pi} \exp(-n^2\pi^2\tau) \tag{5.10}$$

Typical diffusant concentration profiles through the membrane obtained using equation (5.10) are presented in figure 5-2.

We can use equation (5.6) and equation (5.10) to obtain the following expression for the diffusion flux at the membrane/receptor compartment interface:

$$\Psi(\tau) = -\left(\frac{\partial u}{\partial \chi}\right)_{\chi=1} = 1 + 2\sum_{n=1}^{\infty} \frac{\sin(n\pi\chi)}{n\pi} \exp(-n^2\pi^2\tau) \tag{5.11}$$

The total quantity $N(t)$ of penetrant passing through the membrane after time t is given by:

$$N(t) = A\int_0^t j(t)dt \tag{5.12}$$

where A is the membrane surface area. Since $dt = \frac{L^2}{D_s}d\tau$ then using equation (5.6) we can readily show that

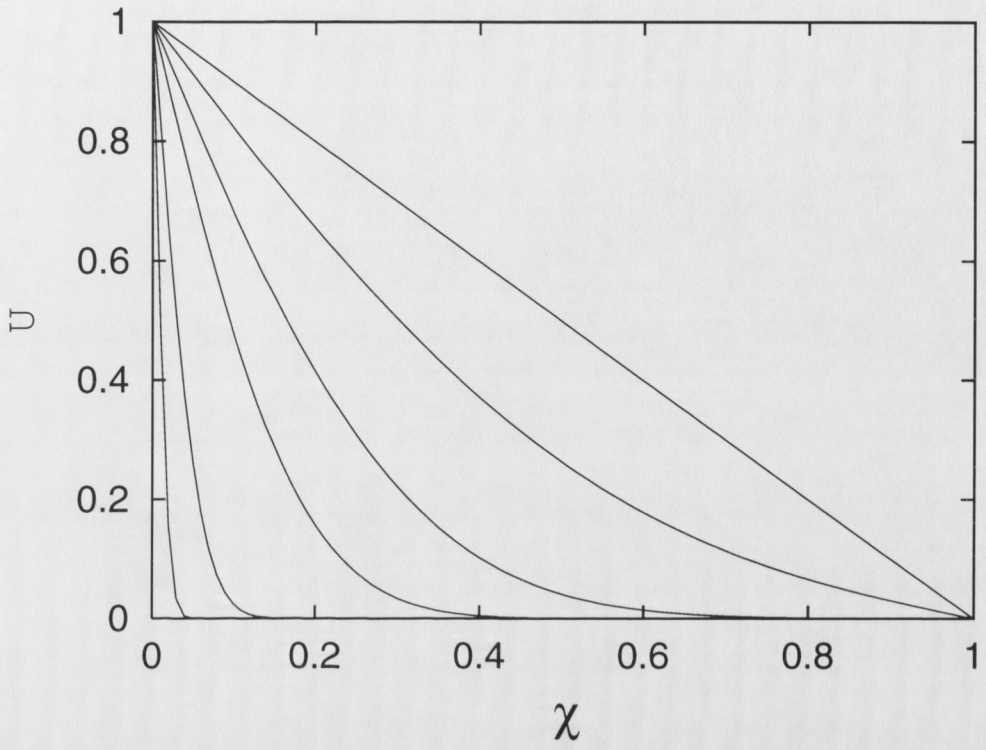

Figure 5-2: Typical concentration profiles computed using equation (5.10) for simple passive diffusion through a membrane of finite thickness. The concentration profiles are presented for normalised times (from left to right) of $\tau = 1\text{x}10^{-4}, 1\text{x}10^{-3}, 1\text{x}10^{-2}, 3\text{x}10^{-2}, 0.1$ and 0.6 respectively

$$N(\tau) = N_\infty \int_0^\tau \Psi(\tau) d\tau \tag{5.13}$$

where the total quantity of material released into the receptor compartment at very long times is given by $N_\infty = AL\kappa c_0$. The ratio $\frac{N(\tau)}{N_\infty}$ versus τ defines the quantity of primary experimental interest.

From equation (5.11) and equation (5.13) we can show that

$$Q(\tau) = \tau - \frac{1}{6} - 2\sum_{n=1}^{\infty} \frac{(-1)^n}{n^2\pi^2} \exp(-n^2\pi^2\tau) \tag{5.14}$$

and we can identify the normalised lag time as $t_L = \frac{1}{6}$. A typical release

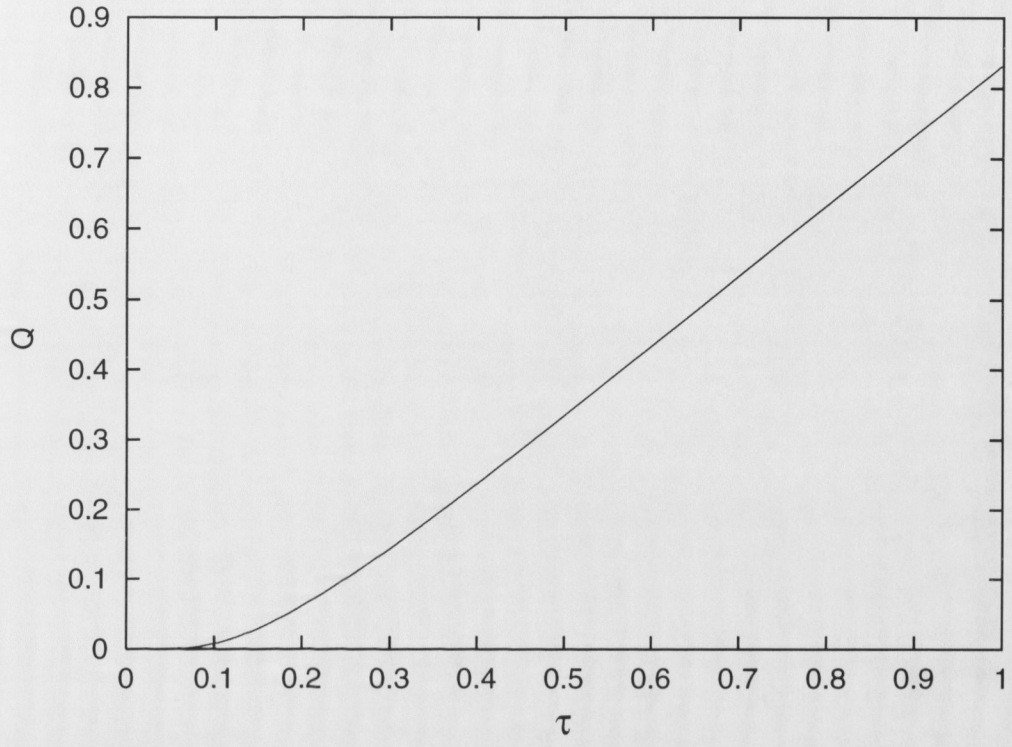

Figure 5-3: Variation in quantity of penetrant delivered to the receptor compartment as a function of normalised time. This curve was computed using equation (5.14)

profile is presented in figure 5-3.

We can obtain useful limiting expressions for the normalised release function $Q(\tau)$ in the limit of short and long times τ. We return to equation (5.9) and note that

$$\bar{u} = p^{-1}\text{cosech}\sqrt{p}\sinh(\sqrt{p}(1-\chi)) \tag{5.15}$$

Now short times correspond to $\tau \ll 1$ and $p \gg 1$. Under such conditions we note that $\text{cosech}(\sqrt{p}) \approx 2\exp(-\sqrt{p})$. Also $\frac{\partial \bar{u}}{\partial \chi}_{\chi=1} = -\sqrt{p}\ \text{cosech}\ \sqrt{p} \approx -2\sqrt{p}\exp(-\sqrt{p})$ and so the normalised release profile is given by

$$Q(\tau) = -L^{-1}\left[\int_0^{\tau}\left(\frac{\mathrm{d}\bar{u}}{\mathrm{d}\chi}\right)_{\chi=1} d\tau\right] = -L^{-1}\left[p^{-1}\left(\frac{\mathrm{d}\bar{u}}{\mathrm{d}\chi}\right)_{\chi=1} d\tau\right] \tag{5.16}$$

where L^{-1} represents the inverse Laplace Transformation operator and we have used the fact that integration with respect to time τ is equivalent to division by the Laplace parameter p. Hence the diffusant release profile at short times is obtained by inverting the expression:

$$Q(\tau) \approx 2L^{-1}\left[p^{\frac{-3}{2}} \exp(-\sqrt{p})\right] \tag{5.17}$$

We note (Churchill (1972))

$$L^{-1}\left[\frac{\exp[-\alpha\sqrt{p}]}{p^{\frac{-3}{2}}}\right] = 2\sqrt{\frac{\tau}{\pi}}\exp[-\frac{\alpha^2}{4\tau}] - \alpha\mathrm{erfc}[\frac{\alpha}{2\sqrt{\tau}}] = 2\sqrt{\tau}i\mathrm{erfc}[\frac{\alpha}{2\sqrt{\tau}}] \tag{5.18}$$

where $\alpha \geq 0$. If we set $\alpha = 1$ we obtain

$$Q(\tau) = 4\sqrt{\tau}i\mathrm{erfc}\left[\frac{1}{2\sqrt{\tau}}\right] \tag{5.19}$$

where we note that ierfc denotes the complementary error function integral which is defined as

$$i\mathrm{erfc(x)} = \frac{2}{\sqrt{\pi}}\int_{\mathrm{x}}^{\infty}(\theta - \mathrm{x})\exp[-\theta^2]\mathrm{d}\theta = \int_{\mathrm{x}}^{\infty}\mathrm{erfc}[\theta]\mathrm{d}\theta = \int_{\mathrm{x}}^{\infty}(1-\mathrm{erfc}[\theta])\mathrm{d}\theta \tag{5.20}$$

where θ is a dummy integration variable and erf(x) represents the well known error function. It can be shown Spanier and Oldham (1987) that the following asymptotic expansion is useful when the argument of the repeated integral of the complementary error function is large:

$$i^n\mathrm{erfc(x)} \approx \frac{2\exp[-\mathrm{x}^2]}{\sqrt{\pi}(2\mathrm{x})^{\mathrm{n}+1}} \sum_{\mathrm{j}=0}^{\infty} \frac{(-1)^{\mathrm{j}}(\mathrm{n}+2\mathrm{j})!}{\mathrm{n!j!}(2\mathrm{x})^{2\mathrm{j}}} \tag{5.21}$$

Specifically for $n = 1$ and setting $\eta = \frac{1}{2\sqrt{\tau}}$ we obtain for $\eta \gg 1$ (or $\tau \ll 1$)

$$i^n\mathrm{erfc}(\eta) \approx \frac{2\exp[-\eta^2]}{\sqrt{\pi}(2\eta)^2} \tag{5.22}$$

and so the expression for the release profile valid for short times is given by

$$Q(\tau) \approx 4\sqrt{\tau}\left[\frac{2\exp[-\frac{1}{4}\tau]}{\sqrt{\pi}(\frac{1}{\sqrt{\tau}})^2}\right] = \frac{8}{\sqrt{\pi}}\tau^{-\frac{3}{2}}\exp[-\frac{1}{4\tau}] \tag{5.23}$$

This expression is valid up to $\tau \approx 0.02$ (error 10%). For $\tau = 0.1$ there is a 50% error in using equation (5.23) to estimate the quantity of diffusant released from the membrane. The full expression must be used for τ values greater than 0.02.

Conversely for long times when $p \ll 1$ we use the fact that $\mathrm{cosech}\ \sqrt{p} \approx \frac{1}{\sqrt{p}} - \frac{\sqrt{p}}{6}$ to obtain $p^{-\frac{3}{2}}\ \mathrm{cosech}\ (\sqrt{p}) \approx \frac{1}{p^2} - \frac{1}{6p}$, and when the latter is substituted in equation (5.16) we obtain

$$Q(\tau) \approx \tau - \frac{1}{6} = \tau - \tau_L \tag{5.24}$$

This expression valid at long times is used experimentally to evaluate the lag time τ_L and hence the diffusion coefficient D_s of the penetrant through the membrane. Now the permeability in normalised form is defined as

$$\rho = \frac{LP}{\kappa D} = \left(\frac{\mathrm{d}Q}{\mathrm{d}\tau}\right)_{\tau\to\infty} \tag{5.25}$$

Hence from equation (5.24) we note that $\rho = 1$ as expected for a system exhibiting simple passive diffusion. Furthermore, the normalised lag time is

$$\tau_L = \frac{Dt_L}{L^2} = \frac{1}{6} \tag{5.26}$$

hence the lag time for passive diffusion through a membrane of thickness L is predicted to be $t_L = \frac{L^2}{6D}$ as is well known (Crank (1975)).

5.3 Electric field assisted diffusion with concurrent first order chemical reaction in a finite membrane

We now present a solution of equation (5.1) which describes electric field assisted diffusion with concurrent first order reaction kinetics in a finite membrane. Such a situation would typically correspond to iontophoretic transport of a charged drug species across a membrane barrier in which the drug can be metabolised via first order kinetics. The analysis could also be used to describe substrate transport and reaction within a free standing electronically conducting polymer membrane in which the diffusing substrate reacts with sites located on the polymer chains via first order kinetics.

We apply the Laplace transform to equation (5.1) to obtain:

$$\frac{\partial^2 \bar{u}}{\partial \chi^2} - \beta \frac{\partial \bar{u}}{\partial \chi} - (p + \gamma)\bar{u} = 0 \tag{5.27}$$

This ordinary differential equation with constant coefficients is solved using the Laplace Transformed boundary conditions presented in equation (5.8). The general solution to equation (5.27) is

$$\bar{u}(\chi, p) = \exp[\xi\chi]\left[A\cosh(\sqrt{\zeta + p}\chi) + B\sinh(\sqrt{\zeta + p}\chi)\right] \tag{5.28}$$

where we note that

$$\xi = \frac{\beta}{2}, \quad \zeta = \gamma + \xi^2 = \gamma + \frac{\beta^2}{4} \tag{5.29}$$

and A and B are constants of integration which are evaluated from the boundary conditions presented in equation (5.8). As outlined in appendix E.2 we can show readily that

$$\bar{u}(\chi, p) = \exp[\xi\chi]\left[\frac{\sinh(\sqrt{\zeta + p}(1-\chi)}{p\sinh\sqrt{\zeta + p}}\right] \tag{5.30}$$

When the diffusion is passive $\xi = 0$, and if there is no loss of penetrant via first order chemical reaction then $\zeta = 0$ and we note immediately that equation (5.30) reduces directly to equation (5.9) which we have previously examined. The Laplace transform presented in equation (5.30) may be inverted using the Heaviside expansion theorem or via the complex inversion formula (Spiegel (1965)). In appendix E.2 we use the former strategy to show that the normalised penetrant concentration profile within the membrane is given by

$$u(\chi, \tau) = u_s(\chi) - u_t(\chi, \tau) \tag{5.31}$$

where u_s represents the steady state component and u_t is the transient contribution to the concentration profile. The latter quantities are given by:

$$u_s(\chi) = \exp[\xi\chi]\left[\frac{\sinh(\sqrt{\zeta}(1-\chi)}{\sinh\sqrt{\zeta}}\right] = \exp[\frac{\beta}{2}\chi]\left[\frac{\sinh(\sqrt{\gamma + \frac{\beta^2}{4}}(1-\chi)}{\sinh\sqrt{\gamma + \frac{\beta^2}{4}}}\right] \tag{5.32}$$

and

$$u_t(\chi, \tau) = 2\exp[\frac{\beta}{2}\chi]\sum_{n=1}^{\infty}\frac{n\pi}{n^2\pi^2 + \gamma + \frac{\beta^2}{4}^2}\sin(n\pi\chi)\exp[-(n^2\pi^2 + \gamma + \frac{\beta^2}{4})\tau] \tag{5.33}$$

We can readily show that the expressions presented in equation (5.32) and equation (5.33) reduce to that outlined in equation (5.10) when the parameters β and γ are both zero and simple passive diffusion pertains. Normalised concen-

tration profiles for penetrant are presented in figure 5-4 - 5-11 for typical values of the migration parameter β and the reaction/diffusion parameter γ. These profiles are presented in a three dimensional format for ease of representation. For instance in figure 5-4 we show how the normalised concentration profile u varies with β at different values of normalised time τ ranging from $\tau = 0.01$ to steady state when the reaction/diffusion parameter γ is zero. In figure 5-5 concentration profiles are presented for various β and τ values but in this case $\gamma = 1$. The same computation is repeated in figure 5-6- 5-8 but in this case $\gamma = 10, 100$ and 1000 respectively. A further set of concentration profiles is presented in figure 5-9 - 5-11. In this case the effect of the sign and magnitude of the migration parameter on the shape of the (u, χ, γ) surface is explored. In figure 5-9 the effect of negative β on the value (u, χ, γ) surface is presented. Here the field opposes the migration of penetrant through the membrane. In figure 5-10 where $\beta = 0$ the time development of, and the effect of the reaction/diffusion parameter γ on the (u, χ, γ) surface is presented. In figure 5-11 the time variation of the (u, χ, γ) surface when $\beta = 10$ is presented. Here the field enhances penetrant transport through the membrane.

5.4 Discussion

In appendix E.3 we show that equation (5.1) may be integrated to obtain an analytical expression for the concentration profile of penetrant if a solution of the following form is assumed:

$$u(\chi, \tau) = \exp[\xi\chi] \exp[-\zeta\tau]\omega(\chi, \tau) \tag{5.34}$$

where $\omega(\chi, \tau)$ satisfies the simple Fick diffusion equation:

$$\frac{\partial\omega}{\partial\tau} = \frac{\partial^2\omega}{\partial\chi^2} \tag{5.35}$$

and also satisfies the following initial and boundary conditions:

$$\omega(\chi,0)=0, \quad \omega(0,\tau)=\exp[\zeta\tau], \quad \omega(1,\tau)=0 \tag{5.36}$$

where we define $\eta=\frac{\beta}{2}$. This alternative strategy can prove to be very useful when other types of bounded diffusion problems in membranes are considered.

As outlined in Appendix E.2 , we can show that the normalised release profile of penetrant from the membrane as a function of time is given by

$$Q(\tau)=\sqrt{\zeta}\exp[\xi]\mathrm{cosech}[\sqrt{\zeta}]\tau+2\exp[\xi]\sum_{\mathrm{n}=1}^{\infty}\frac{(-1)^{\mathrm{n}}\mathrm{n}^2\pi^2}{(\mathrm{n}^2\pi^2+\zeta)^2}(1-\exp[-(\mathrm{n}^2\pi^2+\zeta)\tau]) \tag{5.37}$$

We follow Leypoldt and Gough (1980) and note that the complex variable theory (specifically the method of contour integration) may be used to express the following infinite series in terms of a closed form expression involving the hyperbolic functions

$$\sum_{n=1}^{\infty}\frac{(-1)^n n^2\pi^2}{(n^2\pi^2+\zeta)^2}=-\frac{1}{4}\left(\mathrm{cosech}\sqrt{\zeta}\left(\coth\sqrt{\zeta}-\frac{1}{\sqrt{\zeta}}\right)\right) \tag{5.38}$$

and so the normalised release profile of penetrant becomes

$$Q(\tau)=\sqrt{\zeta}\exp[\xi]\mathrm{cosech}[\sqrt{\zeta}]\tau-\frac{1}{2}\exp[\xi]\left(\mathrm{cosech}\sqrt{\zeta}\left(\coth\sqrt{\zeta}-\frac{1}{\sqrt{\zeta}}\right)\right)(1-\exp[-(\mathrm{n}^2\pi^2+\zeta)\tau]) \tag{5.39}$$

In the limit of long time the last term on the right hand side of equation (5.39) reduces to zero and we obtain that

$$Q(\tau\to\infty)=\sqrt{\zeta}\exp[\xi]\mathrm{cosech}[\sqrt{\zeta}]\tau-\frac{1}{2}\exp[\xi]\left(\mathrm{cosech}\sqrt{\zeta}\left(\coth\sqrt{\zeta}-\frac{1}{\sqrt{\zeta}}\right)\right) \tag{5.40}$$

The normalised permeability may immediately be evaluated from the latter expression and is given by

$$\rho = \left(\frac{\mathrm{d}Q}{\mathrm{d}\tau}\right)_{\tau\to\infty} = \sqrt{\zeta}\exp[\xi]\mathrm{cosech}[\sqrt{\zeta}] \tag{5.41}$$

We also note that equation (5.40) can be written in the form

$$Q(\tau \to \infty) = \rho(\zeta,\xi)\tau - \rho(\zeta,\xi)\tau_L(\zeta) \tag{5.42}$$

and so the normalised lag time for electric field assisted diffusion with concurrent first order chemical reaction is given by

$$\tau_L(\zeta) = -\frac{1}{2\sqrt{\zeta}}\left(\coth\sqrt{\zeta} - \frac{1}{\sqrt{\zeta}}\right) = -\frac{1}{2\sqrt{\zeta}}\mathrm{L}(\sqrt{\zeta}) \tag{5.43}$$

where L(x) is the well known Langevin function which is given by

$$L(x) = \coth(\mathrm{x}) - \frac{1}{\mathrm{x}} \tag{5.44}$$

Equation (5.43) may also be written in another way

$$\tau_L(\zeta) = -\frac{1}{6}\left(\frac{3}{\sqrt{\zeta}}L(\sqrt{\zeta})\right) = \tau_L(\zeta)\left(\frac{3}{\sqrt{\zeta}}L(\sqrt{\zeta})\right) \tag{5.45}$$

where $\tau_L(0)$ denotes the normalised lag time for passive diffusion. Equation (5.41) and Equation (5.45) may be used to examine the way in which the permeability and the lag time vary with the diffusion/migration parameter β and the diffusion/reaction parameter γ. When the η parameter is very small we note that $\coth\sqrt{\zeta} \approx \frac{1}{\zeta}(1+\frac{\zeta}{3})$and $\frac{3}{\zeta}L(\sqrt{\zeta}) \approx 1$ and we obtain that $\tau_L(\zeta) \approx \tau_L(0)$ as one would expect. Also since $\mathrm{cosech}\ \sqrt{\zeta} \approx \frac{1}{\zeta}$ and $\exp(\xi) \approx 1+\xi$, for small values for ξ and ζ, then from equation (5.41) we note that the normalised permeability ρ reduces to $\rho \approx 1+\xi \approx 1$ as indeed it should.

For the specific case of active diffusion or iontophoresis corresponding to $\gamma = 0$ the pertinent expressions for the permeability and lag time are given by

$$\rho(\beta) = \frac{\beta}{2}\exp[\frac{\beta}{2}]\text{cosech}[\frac{\beta}{2}] = \frac{1}{1-\exp -\beta} = \frac{\mathrm{j_E}}{\mathrm{j_P}}$$
$$\tau_L(0)\Big(\frac{6}{\beta}L(\frac{\beta}{2})\Big) = \tau_L(0)\frac{6}{\beta}\Big(\coth[\frac{\beta}{2}] - \frac{2}{\beta}\Big) \tag{5.46}$$

The first expression in equation (5.46) provides and analytical expression for the degree of current or flux enhancement at the membrane receptor interface due to iontophoresis under steady state conditions. The second expression is equation (5.46) indicates how the normalised lag time varies with migration parameter β. The expressions provided in equation (5.46) are represented graphically in figures 5-12 - 5-14. In figure 5-12 the current enhancement factor is plotted as a function of the migration parameter β. The same function is displayed in semi-logarithmic format in figure 5-13. Now $\beta = \frac{\mu EL}{D} = \frac{zF\nabla V}{RT}$ where ∇V denotes the applied potential difference across the membrane and z is the valence of the diffusing species. Hence from figure 5-12 we note that the enhancement ratio or the ratio of steady state flux with applied voltage to the steady state passive flux is an asymmetric function of applied voltage ∇V. For large positive values of β the enhancement factor is a linear function of β. For negative values of β, when the applied voltage inhibits the flow of charged species through the membrane, the enhancement factor is a rapidly decreasing function of β (figure 5-13). Typically for $\beta = -10, \rho = -4.54$ x 10^{-4} or $j_E = -4.54$ x $10^{-4} j_P$. The species flow is therefore strongly inhibited. As noted from figure 5-14 the ratio $\frac{\tau_L(\beta)}{\tau_L(0)}$ is a symmetric function of the β parameter. The lag time for active diffusion relative to that observed for passive diffusion is reduced with increasing positive values of β. However due to symmetry of the function $\frac{\tau_L(\beta)}{\tau_L(0)}$, the lag time is also reduced for increasingly negative values of the β parameter. This observation has also been noted by Keister and Kasting (1986) and while it may seem at first unusual, it can be explained by the fact that the steady state flow is much lower and therefore

it takes less time to attain this steady state. It is interesting to note that Chen and Rosenberger (1991) have determined that the symmetry exhibited by the lag time expression arises mathematically from the symmetry with respect to the exchange of the co-ordinate variables exhibited by the corresponding Green's function for the general diffusive/convective boundary value problem.

The results presented in equation (5.46) derived from the more general expressions presented in equation (5.41) and equation (5.45) are in exact agreement with those previously published by Keister and Kasting (1986) who examined iontophoretic drug transport through a finite membrane and solved the diffusion/migration equation via the separation of variables technique.

For the specific case of passive diffusion couples with concurrent first order chemical reaction corresponding to the situation of $\beta = 0$, the normalised permeability and lag time are given by the following expressions:

$$\begin{aligned} \rho(\gamma) &= \sqrt{\gamma}\,\mathrm{cosech}\sqrt{\gamma} \\ \tau_L(\gamma) &= \frac{1}{2\sqrt{\gamma}}\left\{\coth\sqrt{\gamma} - \frac{1}{\sqrt{\gamma}}\right\} \\ &= \frac{\tau_L(0)}{\sqrt{\gamma}}\left\{3\left(\coth\sqrt{\gamma} - \frac{1}{\sqrt{\gamma}}\right)\right\} \end{aligned} \tag{5.47}$$

When γ is small then noting that $\mathrm{cosech}\,\sqrt{\gamma} \approx \frac{1}{\sqrt{\gamma}}$ and $\coth\sqrt{\gamma} \approx \frac{1}{\sqrt{\gamma}} + \frac{\sqrt{\gamma}}{3}$, we can readily show that $\rho(\gamma) \to 1$ and $\tau_L(\gamma) \to \tau_L(0)$. Conversely when γ is large then $\mathrm{cosech}\,\sqrt{\gamma} \approx 2\exp(-\sqrt{\gamma})$ and $\coth\sqrt{\gamma} \approx 1 + 2\exp(-\sqrt{\gamma})$ and therefore

$$\begin{aligned} \tau_L(\gamma) &\approx \frac{3\tau_L(0)}{\sqrt{\gamma}}\left\{1 - \frac{1}{\sqrt{\gamma}} + 2exp\left(-\sqrt{\gamma}\right)\right\} \\ &\approx \frac{3\tau_L(0)}{\sqrt{\gamma}}\left\{1 - \frac{1}{\sqrt{\gamma}}\right\} \end{aligned} \tag{5.48}$$

Hence we expect that the normalised permeability and the lag time decrease

rapidly with increasing values of γ when γ is large. This contention is supported by the computations presented in figure 5-15 and figure 5-16. We note from figure 5-15 that if a semi-logarithmic scale is used, the normalised permeability exhibits only a small decrease with increasing γ up to a value close to 0.5. It then decreases quite rapidly with increasing reaction/diffusion parameter. A similar behaviour is observed for the normalised lag time.

The general situation corresponding to finite values of β and γ is described by equation (5.41) and equation (5.45). In figure 5-17 we indicate the manner in which the normalised permeability ρ varies with the migration parameter β for various values of the reaction/diffusion parameter γ. When the reaction/diffusion parameter is small then ρ varies linearly with β. Hence we observe a marked enhancement in the steady state flux with increasing value of the electric field. When γ becomes significant the ρ versus β behaviour changes. We note from figure 5-17 that ρ still increases with increasing β but when γ is significant the strictly linear increase is not observed for all values of β. Indeed for β values in the range 0.01 to 1, ρ can be less than unity if γ is finite. Hence if the electric field is small and the concurrent chemical reaction is operative then the steady state flux of penetrant can be less that that observed for simple passive diffusion in the absence of electric fields and chemical reaction. Penetrant flux enhancement is only observed for β values greater that 1, and indeed the operation of a chemical reaction within the membrane reduces the enhancing effect of the electric field on the transport rate of penetrant species. This statement can be seen more easily in figure 5-18 where we show the variation of ρ with γ for different β values. We see from this that ρ decreases smoothly with increasing γ for all values of β examined, but the dis-enhancing effect of γ on ρ is not as marked for β values.

The variation of lag time with β and γ given by equation (5.45) is illustrated in figure 5-19 and figure 5-20. Here the computational datum is the ratio of the normalised lag time for finite β and γ to that expected for simple passive diffusion. In figure 5-19 we indicate how the latter quantity varies with migration parameter

β for given values of the reaction /diffusion parameter γ. The lag time decreases significantly with increasing β for all values of γ examined, although the rate of decrease is not as marked when γ is large. furthermore, any effect that γ has on the lag time ratio is not resolvable for β values greater than 70. In figure 5-20 we indicate the manner in which the lag time ratio varies with γ for various β values. Again the lag time ratio decreases with increasing γ for small to intermediate β values but when β becomes significant (> 20) very little variation in lag time ration with γ is observed.

5.5 Concluding Comments

In the initial sections of this chapter we examined passive diffusion through a membrane of finite thickness and derived (via Laplace Transform analysis of the time dependent Fick diffusion equation) analytical solutions for the concentration profile of penetrant through the membrane as a function of time and for the amount of penetrant released into a receptor compartment as a function of time. The lag time and penetrant permeability can be derived from the latter expression.

In the second part of the chapter we have shown that the technique of Laplace Transformation provides a useful protocol for the solution of material transport problems in finite membranes in which diffusion , migration and concurrent first order chemical kinetics are considered. The variation of the substrate permeability and lag time with both reaction/diffusion parameter and migration/diffusion parameter is computed via analytical solution of the diffusion /reaction/migration equation to obtain closed form expressions. These expressions are used to compute dimensionless working curves for the steady state permeabilities and the lag times that can be compared with experimental data.

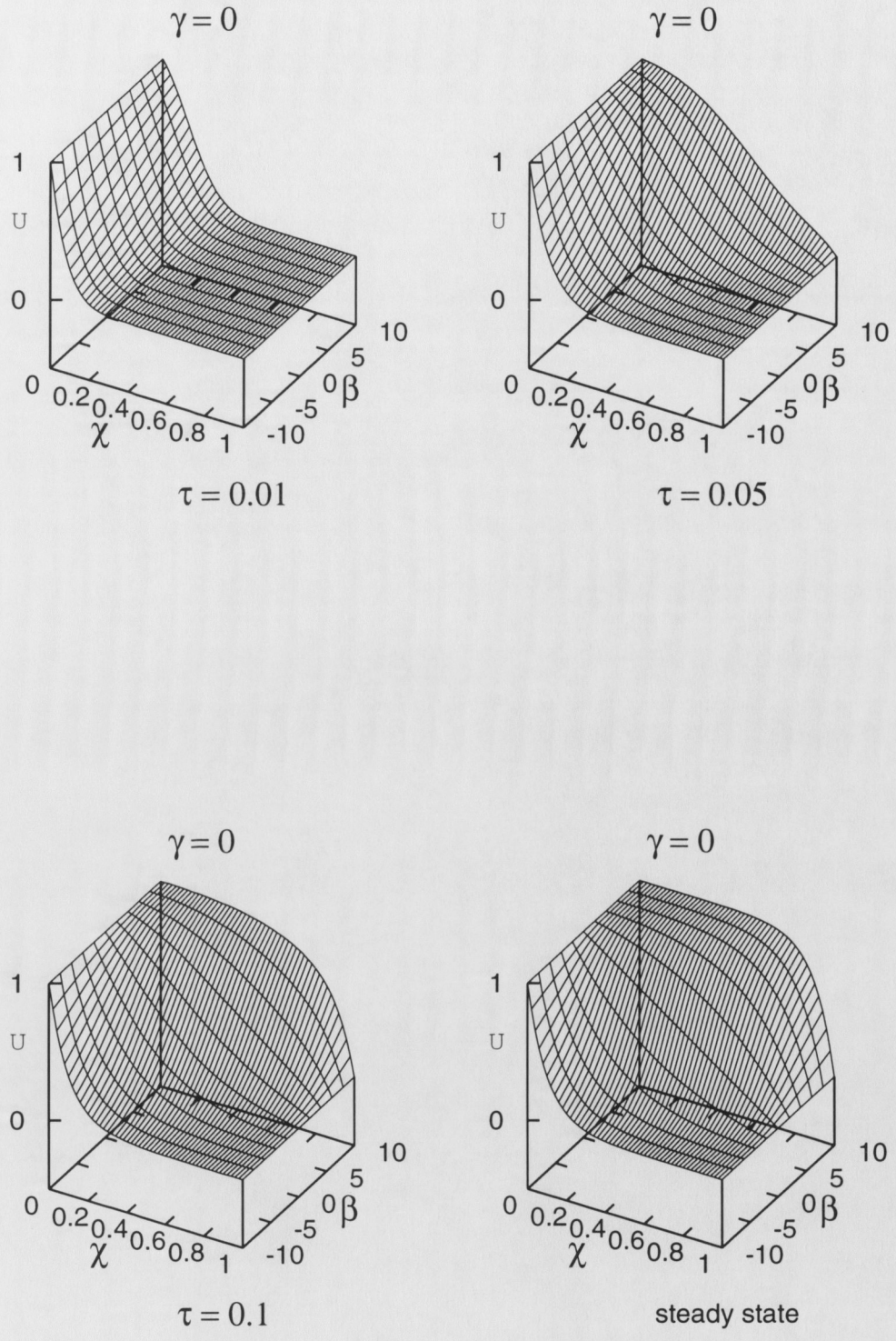

Figure 5-4: Development of the (u, χ, β) surface as a function of both normalised time and reaction/diffusion parameter γ

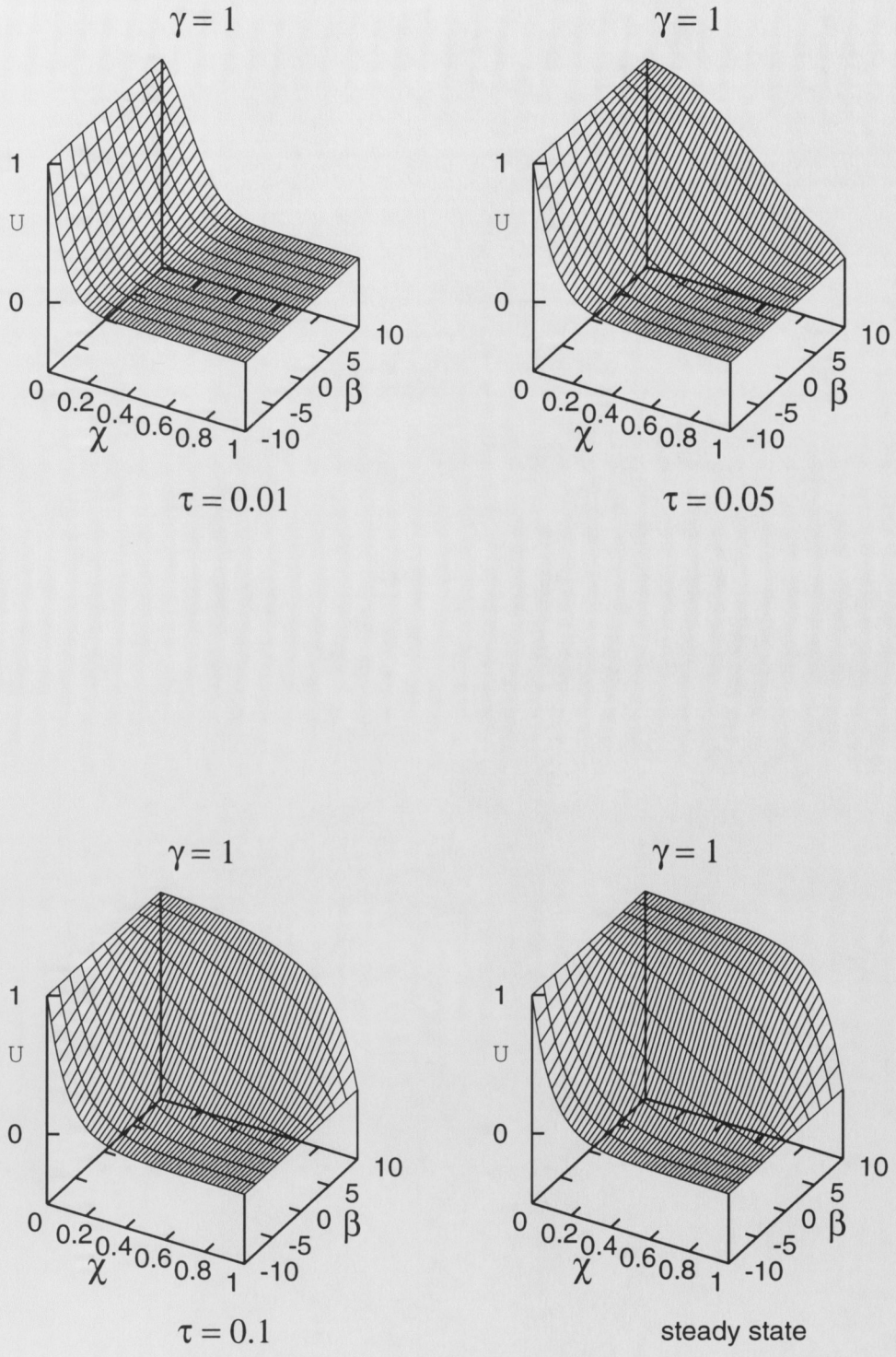

Figure 5-5: Development of the (u, χ, β) surface as a function of both normalised time and reaction/diffusion parameter γ

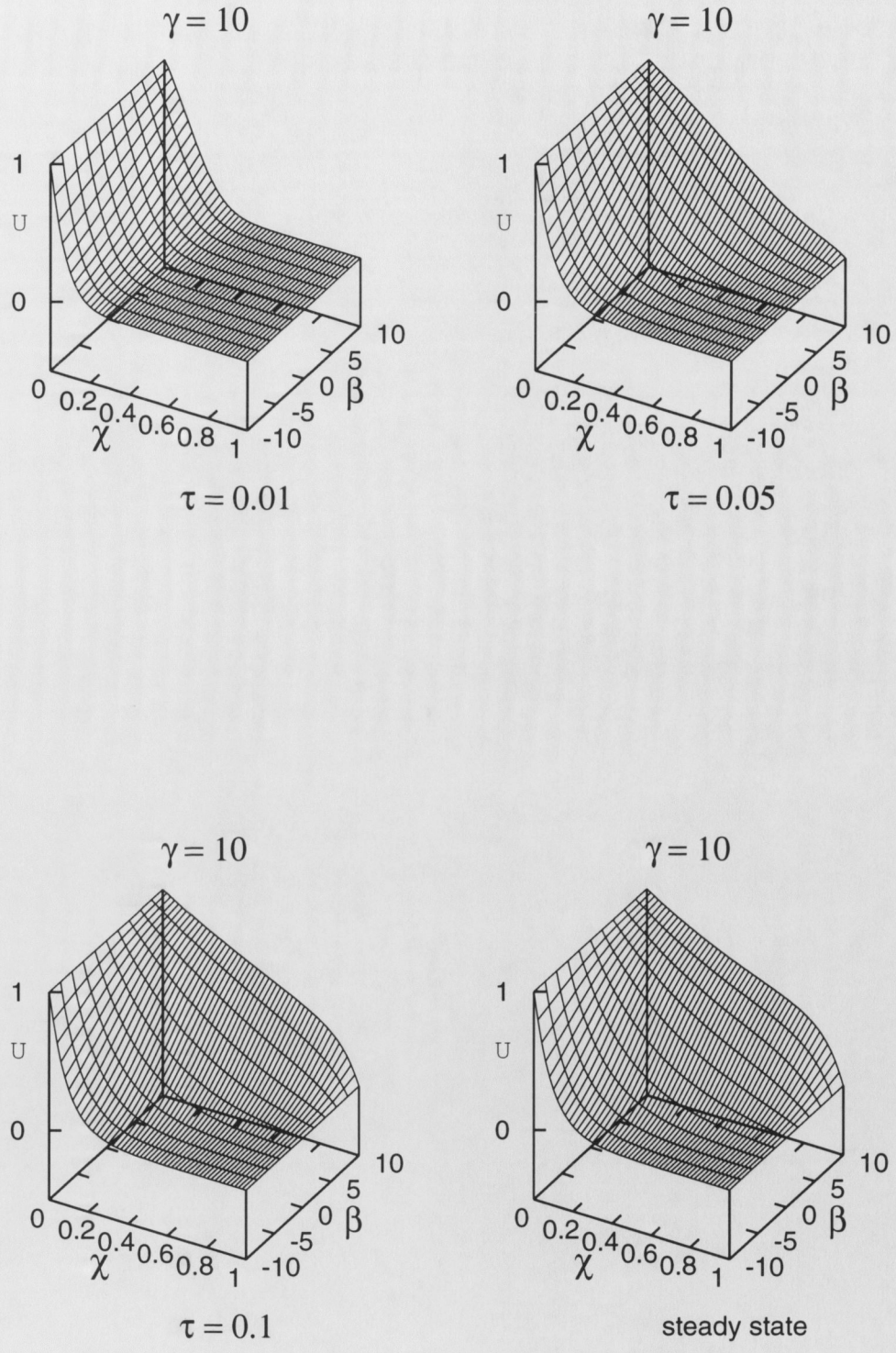

Figure 5-6: Development of the (u, χ, β) surface as a function of both normalised time and reaction/diffusion parameter γ

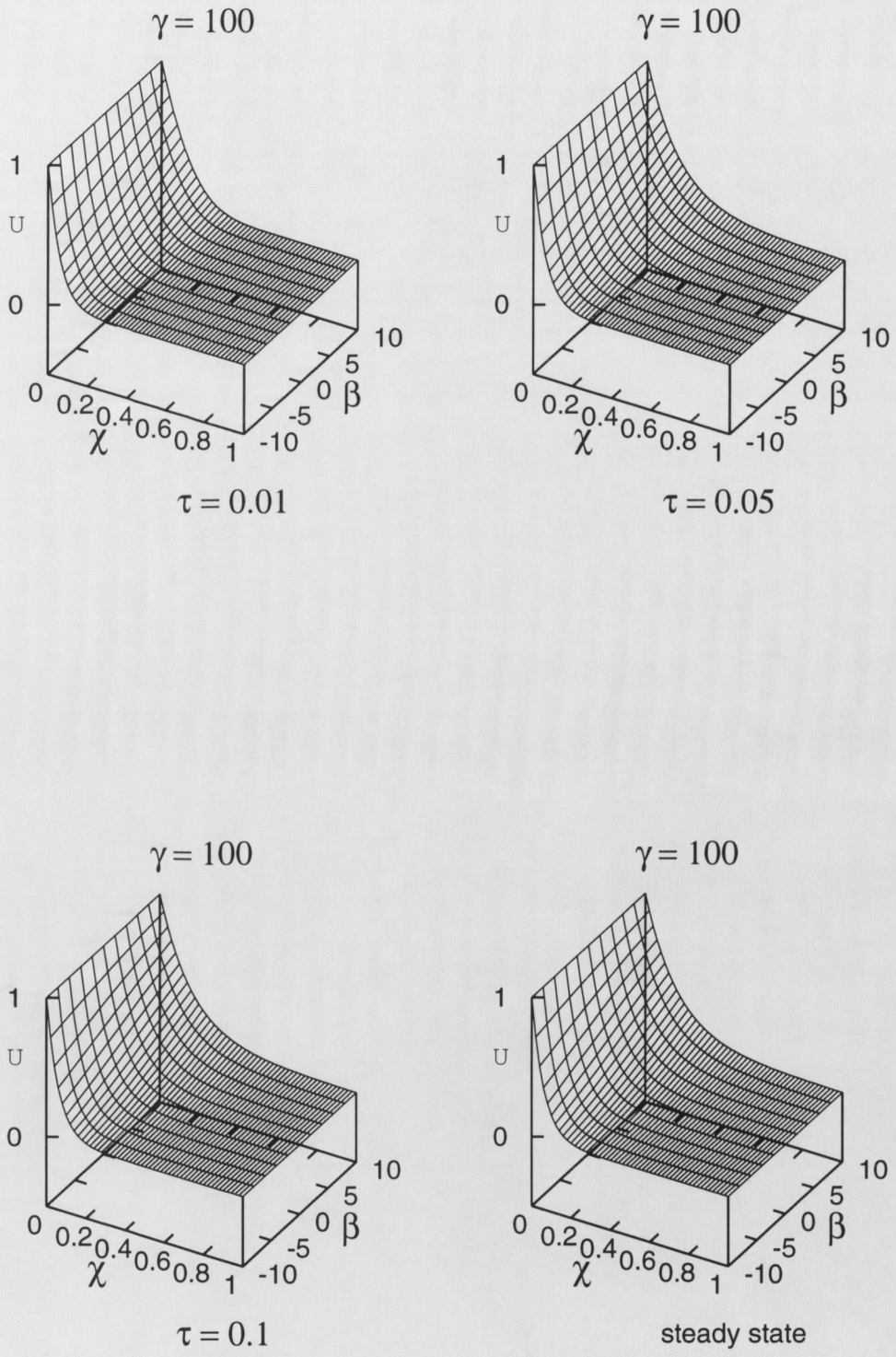

Figure 5-7: Development of the (u, χ, β) surface as a function of both normalised time and reaction/diffusion parameter γ

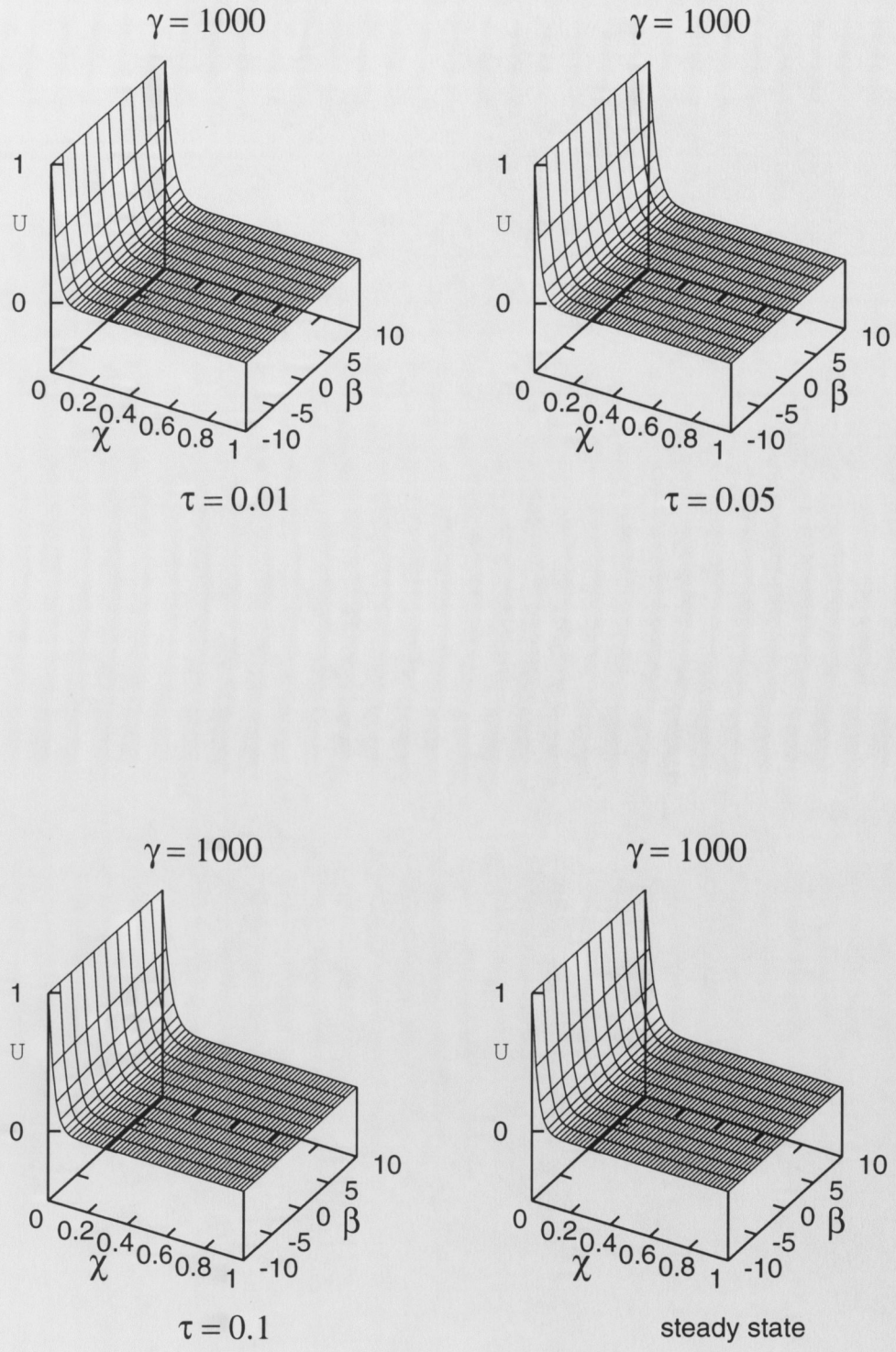

Figure 5-8: Development of the (u, χ, β) surface as a function of both normalised time and reaction/diffusion parameter γ

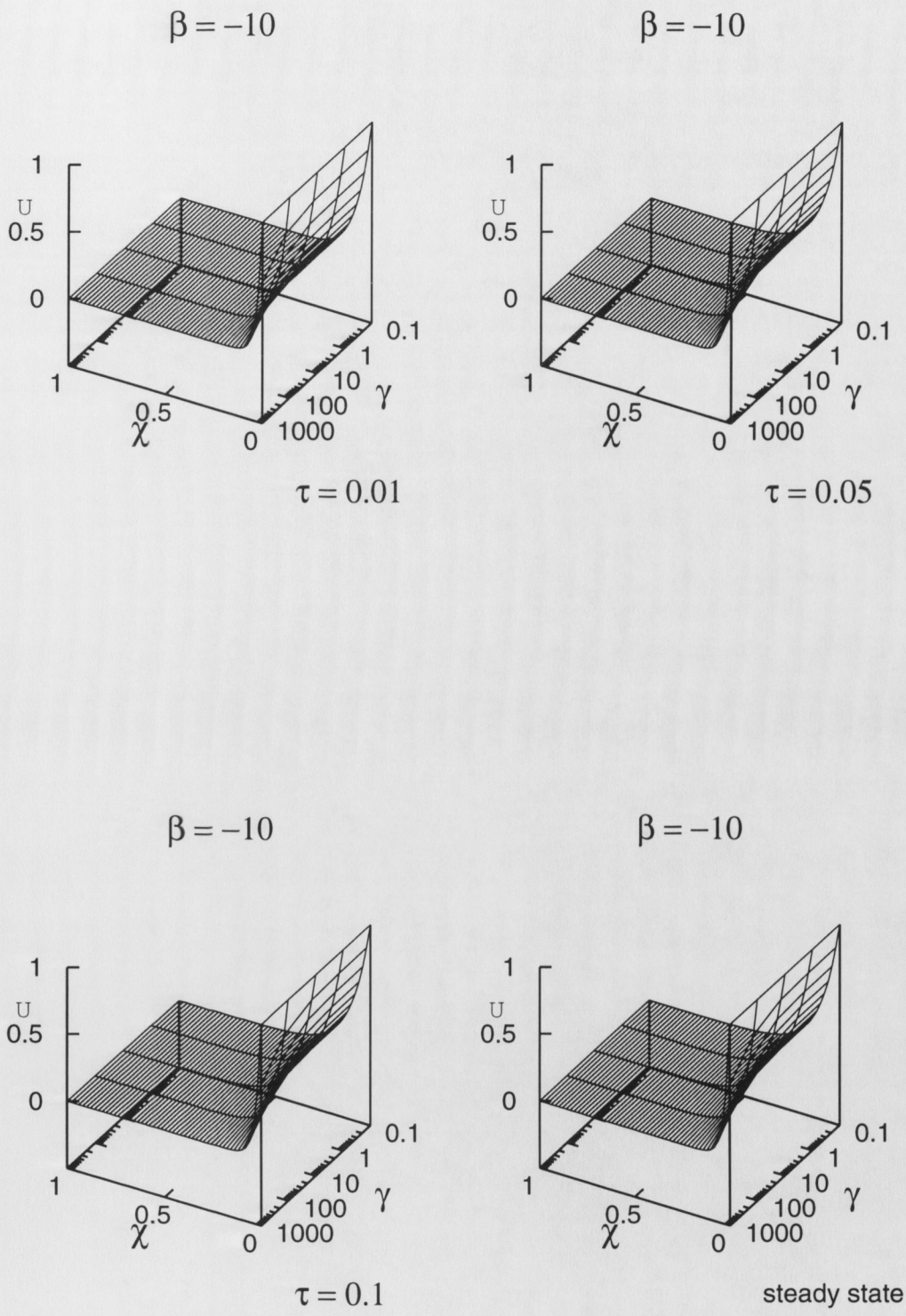

Figure 5-9: Development of the (u, χ, β) surface as a function of both normalised time and migration parameter β

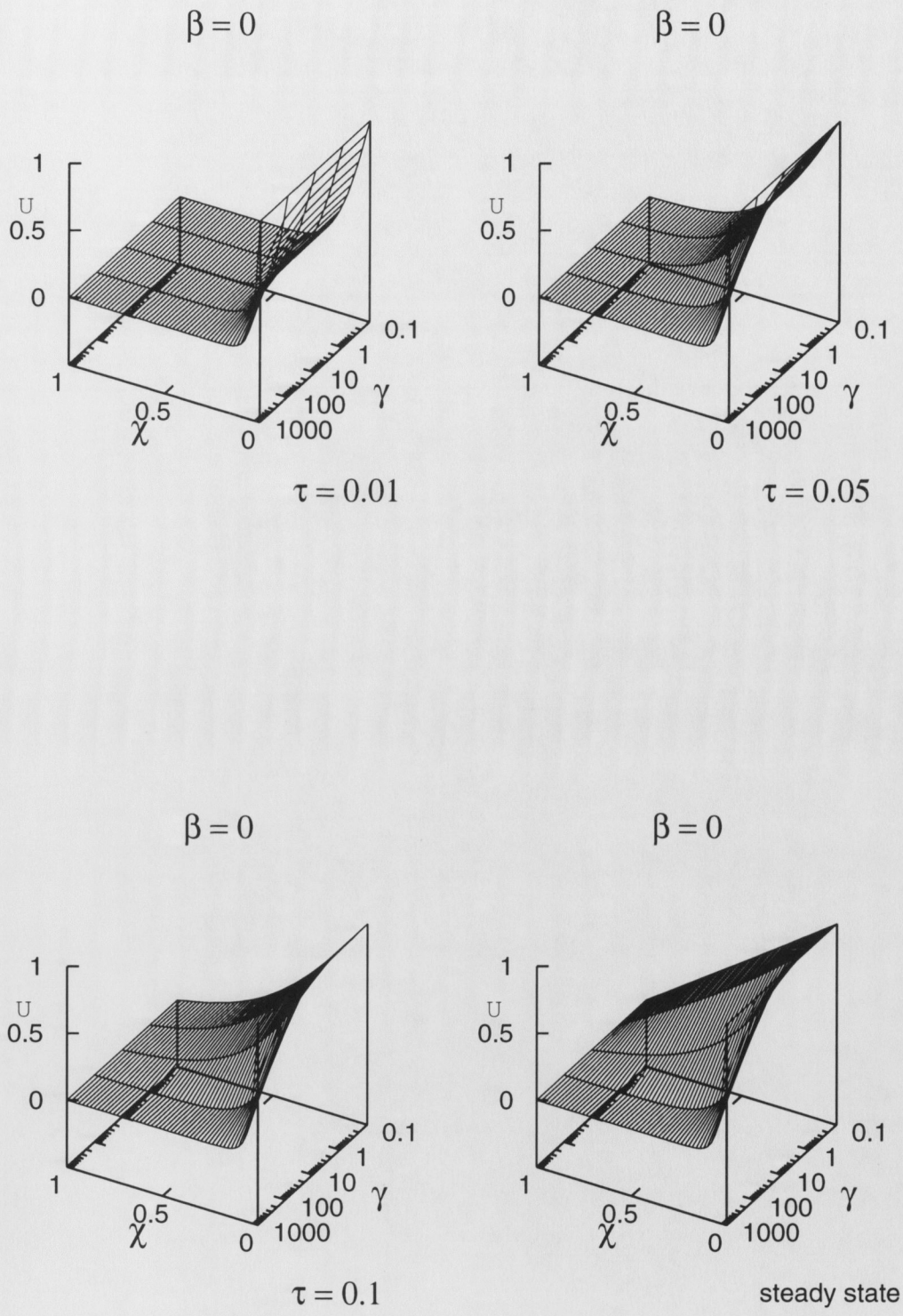

Figure 5-10: Development of the (u, χ, β) surface as a function of both normalised time and migration parameter β

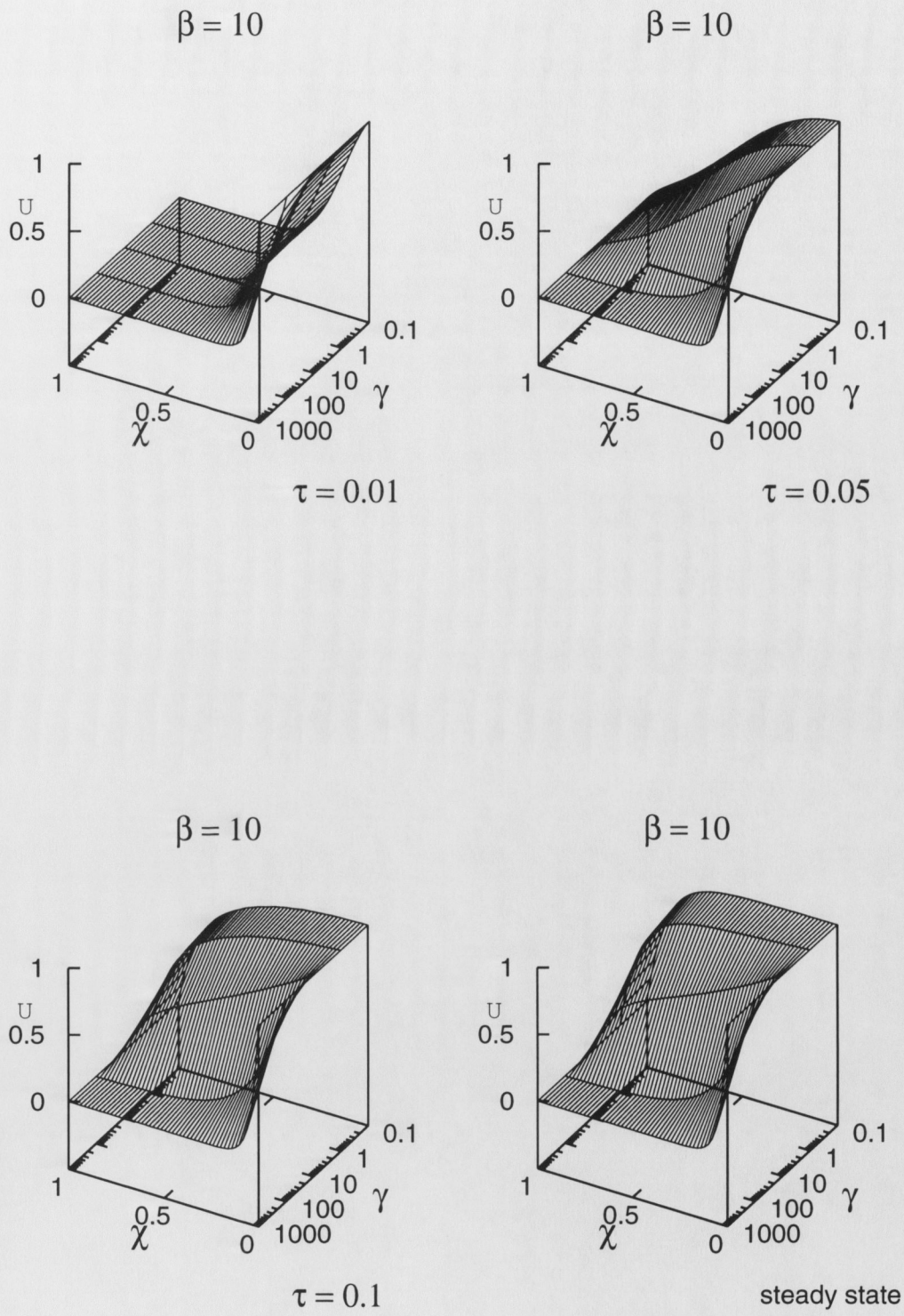

Figure 5-11: Development of the (u, χ, β) surface as a function of both normalised time and migration parameter β

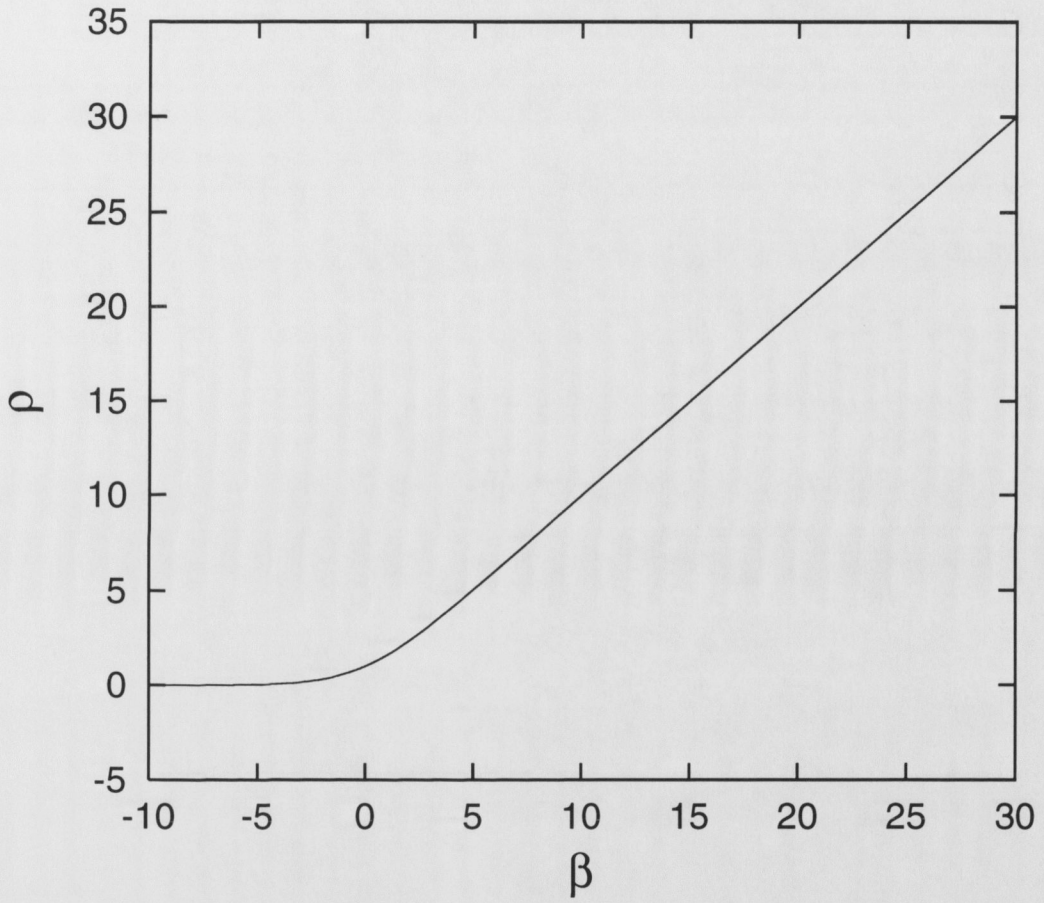

Figure 5-12: Variation of the flux enhancement parameter ρ with migration parameter β

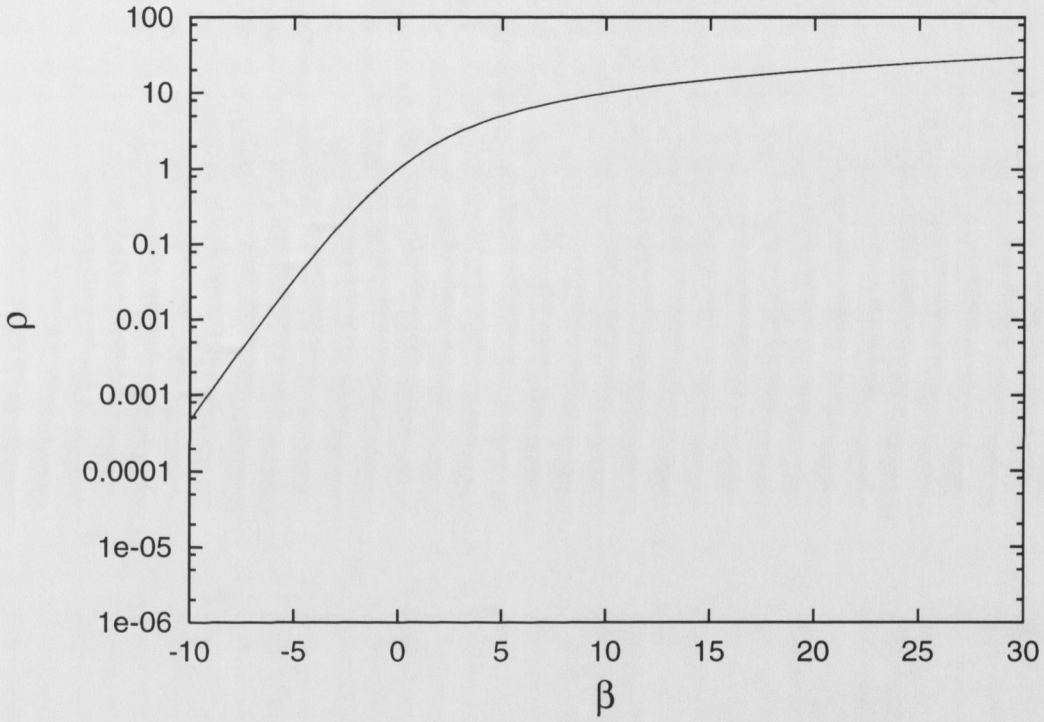

Figure 5-13: Semi-logarithmic presentation of variation of the flux enhancement parameter ρ with migration parameter β

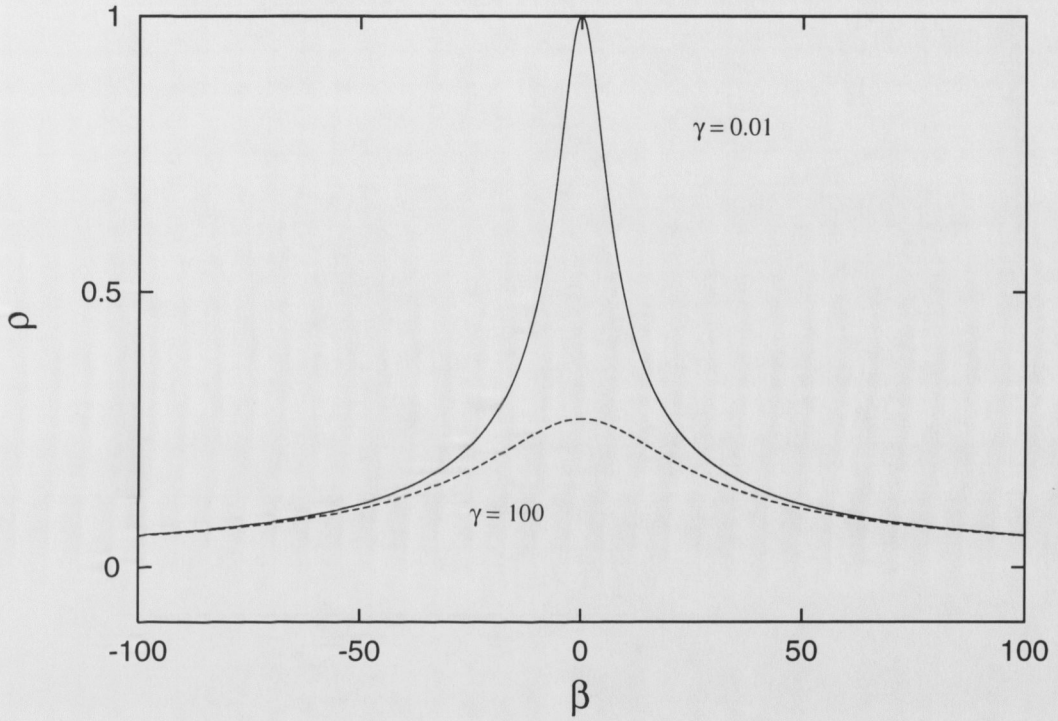

Figure 5-14: Variation of the ratio of the penetrant lag time in the presence of a field $\tau_L(\beta)$ with that due to simple passive diffusion $\tau_L(0)$ with the migration parameter β. Note that the lag time ratio function exhibits symmetry with respect to the migration parameter. This symmetry is maintained regardless of the value of the reaction/diffusion parameter adopted.

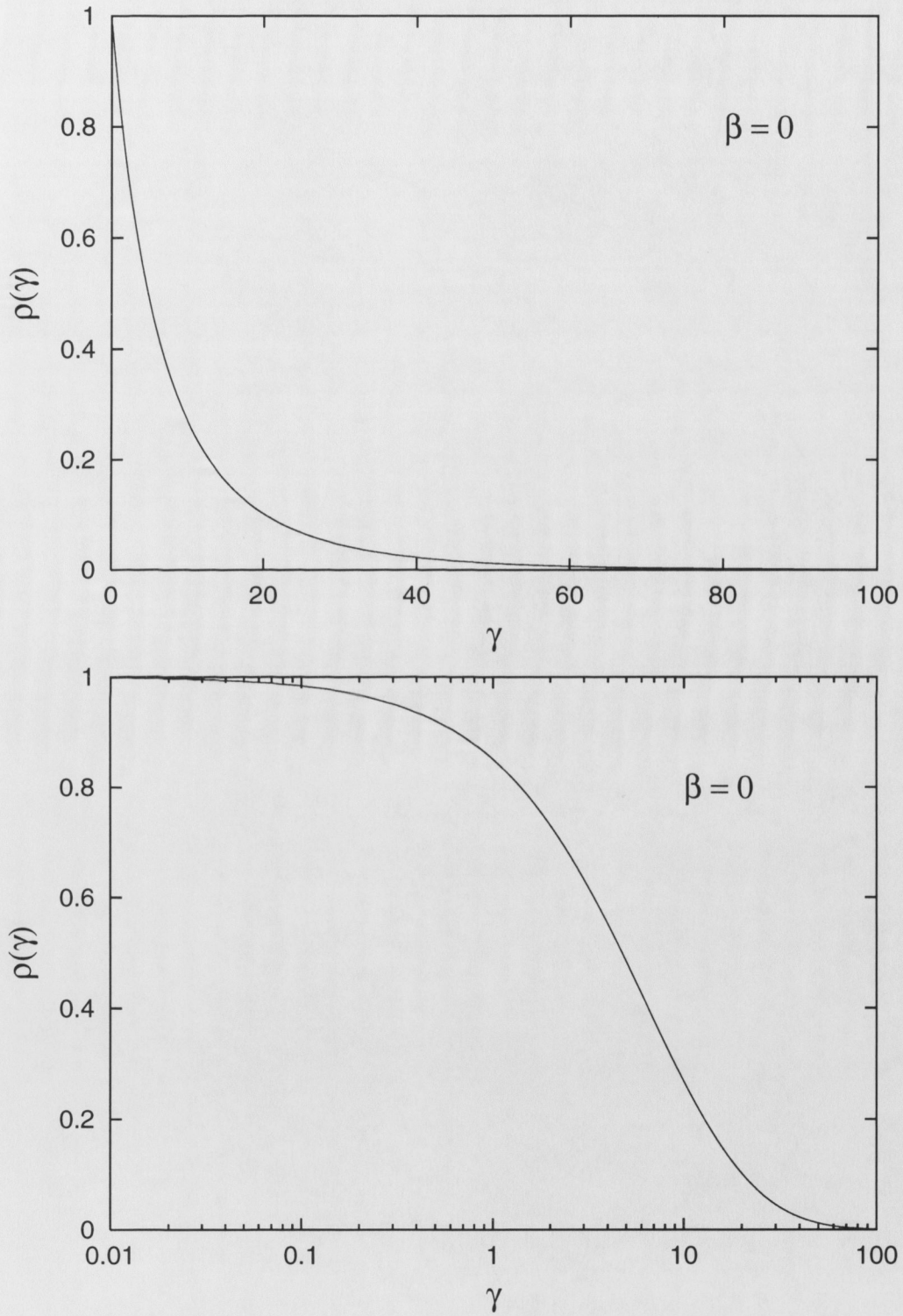

Figure 5-15: Variation of flux enhancement factor ρ with reaction/diffusion parameter γ.The data is generated from equation (5.48) and $\beta = 0$ is assumed. The data is presented in both linear and semi-logarithmic form for clarity.

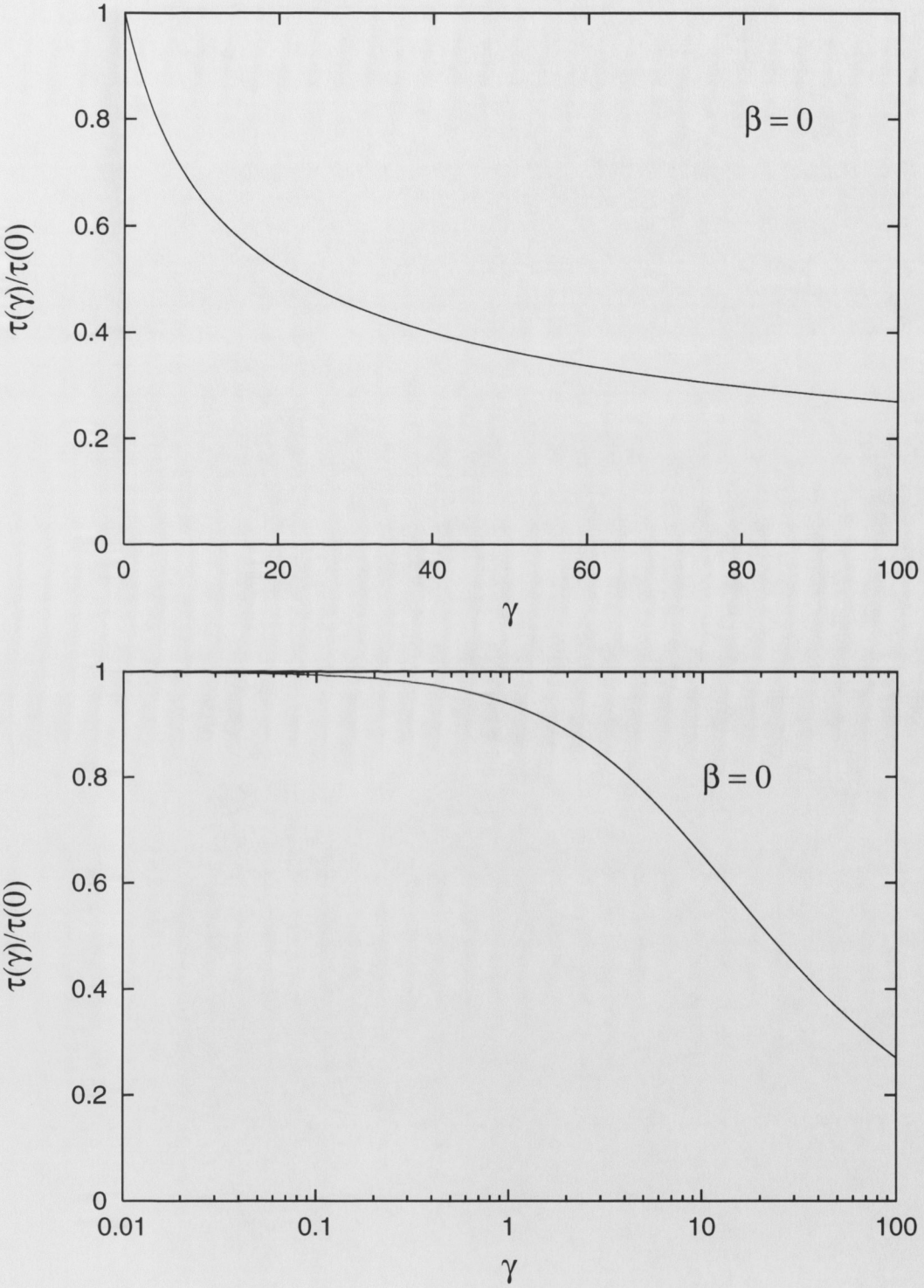

Figure 5-16: Variation of normalised lag time with reaction/diffusion parameter γ. The data is generated from equation (5.48) and $\beta = 0$ is assumed. The data is presented in both linear and semi-logarithmic form for clarity.

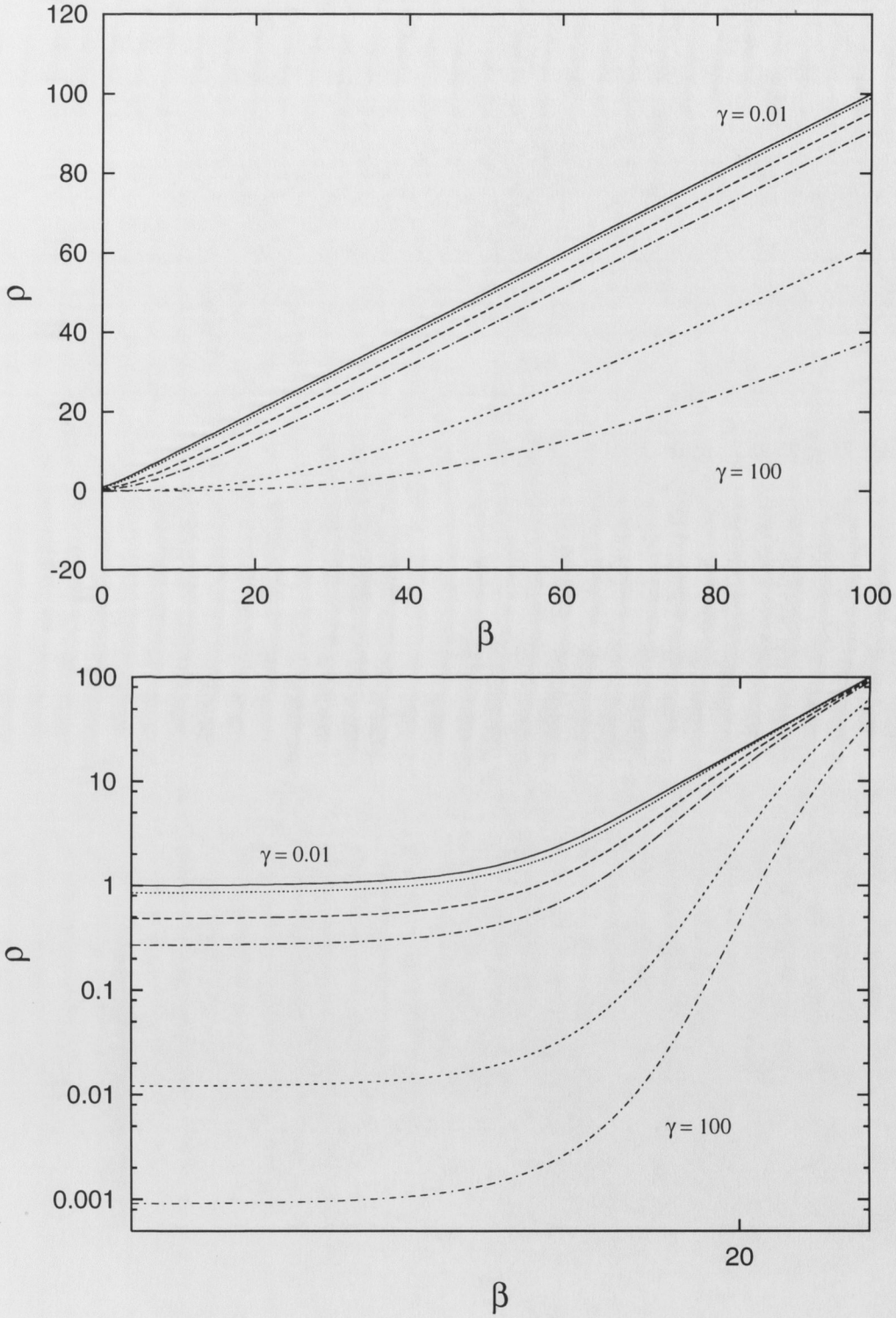

Figure 5-17: Variation of flux enhancement parameter ρ with migration parameter β for various fixed values of the reaction/diffusion parameter γ. The curves were computed using equation (5.41) for various γ values in the range 0.01 to 100. The data is presented in both linear and semi-logarithmic form for clarity.

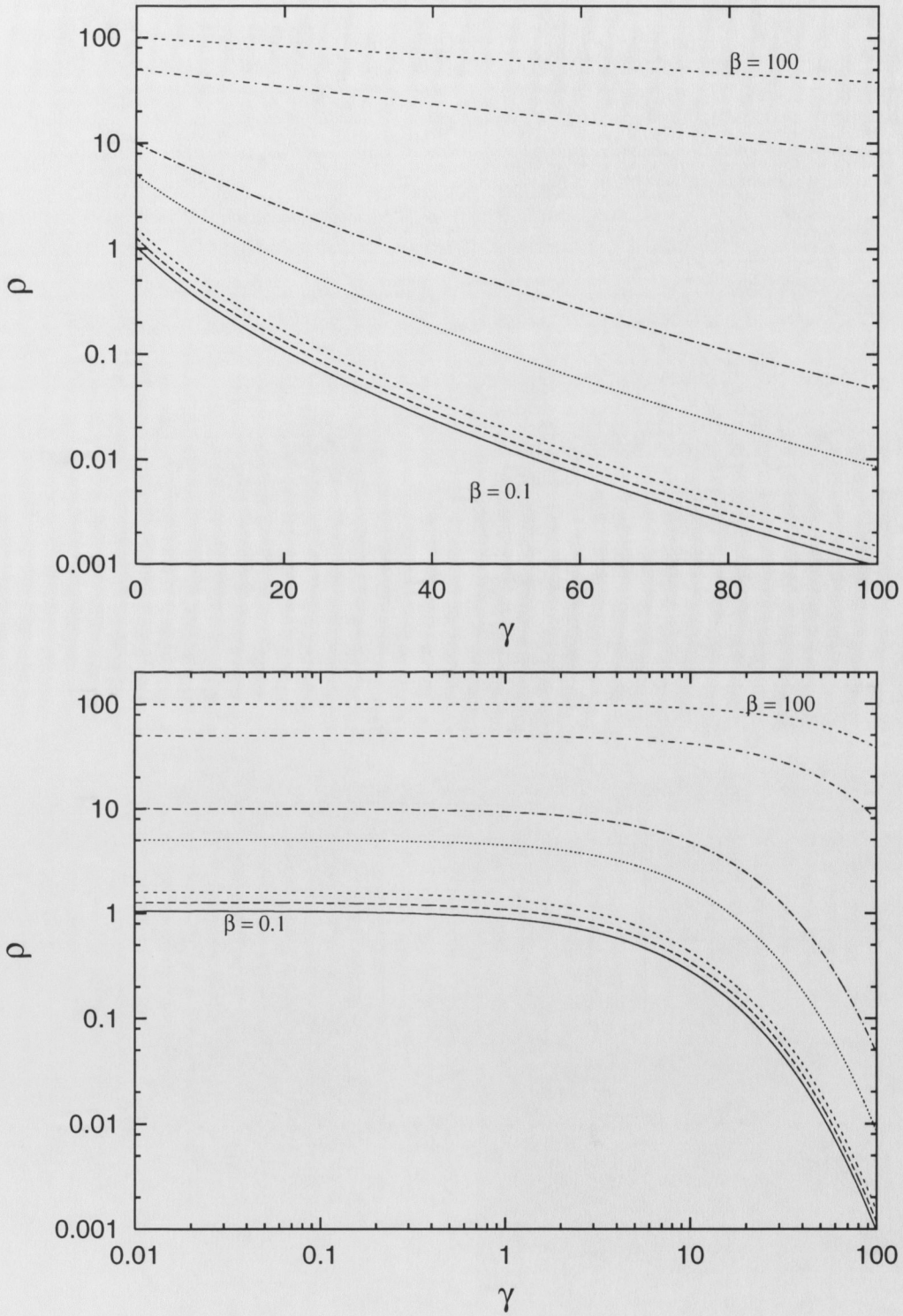

Figure 5-18: Variation of flux enhancement parameter ρ with reaction/diffusion parameter γ for various fixed values of the migration parameter β. The curves were computed using equation (5.41) for various β values in the range 0.01 to 100. The data is presented in both linear and semi-logarithmic form for clarity.

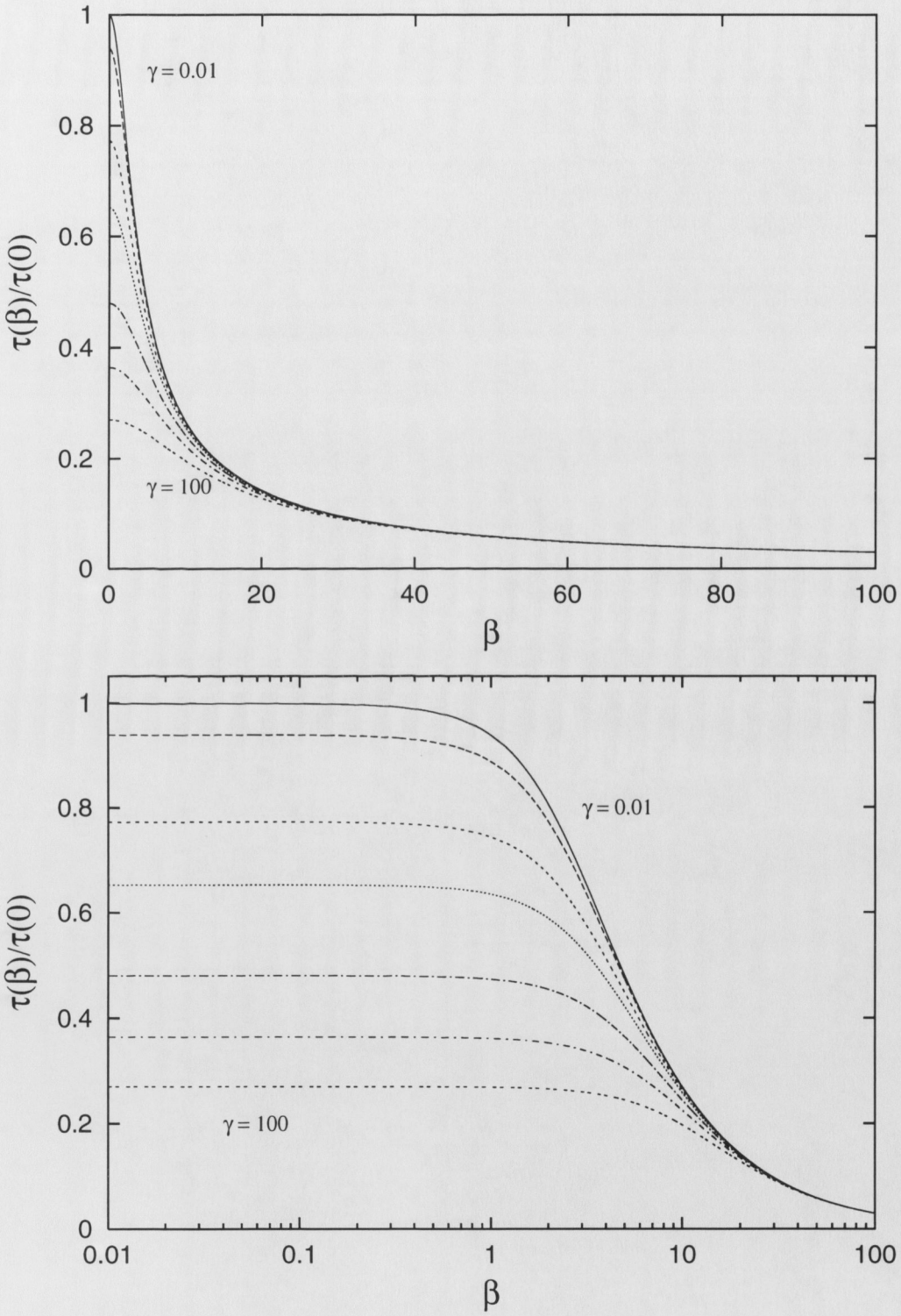

Figure 5-19: Variation of normalised lag time with migration parameter β. The curves were computed using equation (5.41) for various γ values in the range 0.01 to 100. The data is presented in both linear and semi-logarithmic form for clarity.

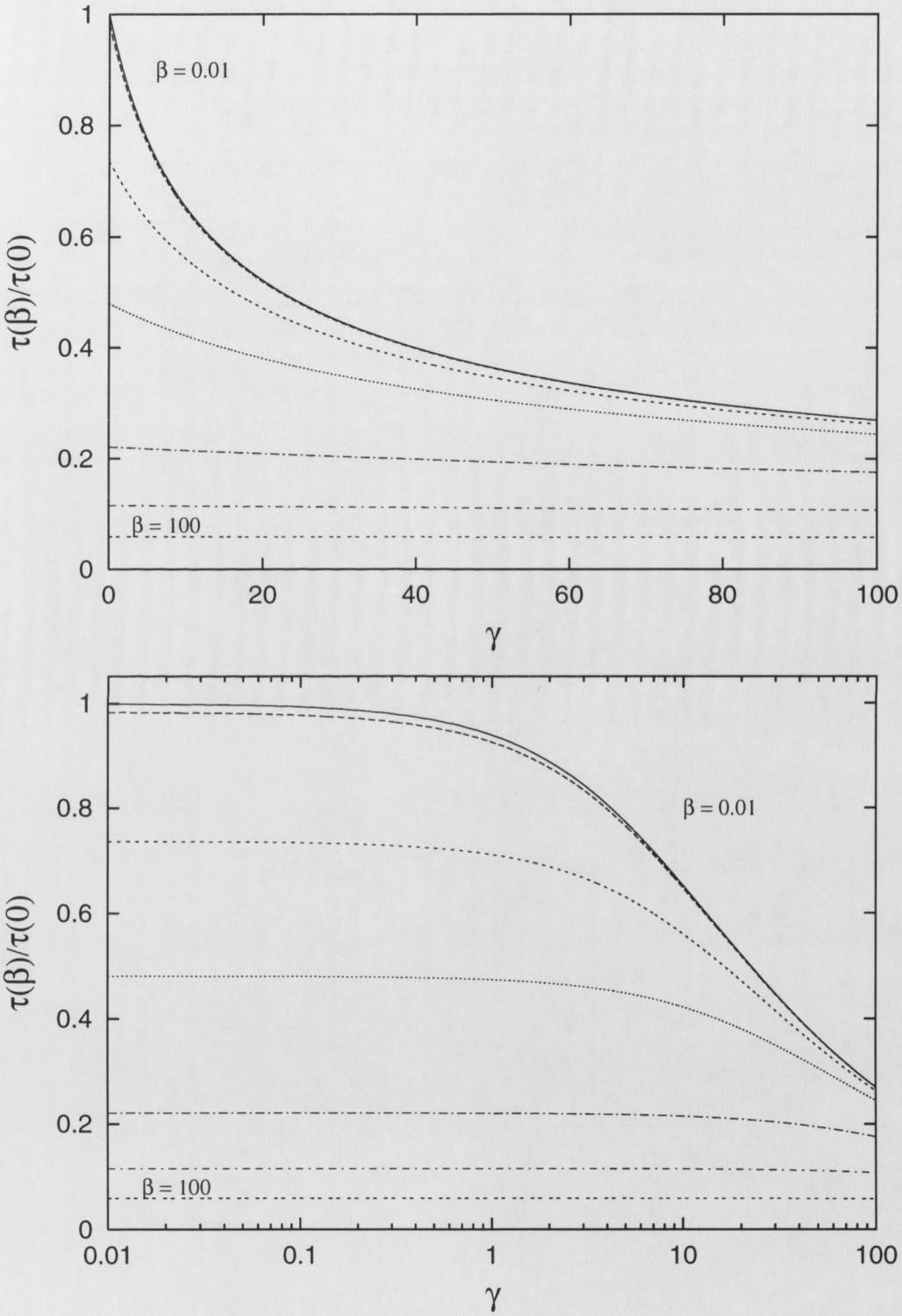

Figure 5-20: Variation of normalised lag time with reaction/diffusion parameter γ. The curves were computed using equation (5.45) for various β values in the range 0.01 to 100 The data is generated from equation (5.48) and $\beta = 0$ is assumed. The data is presented in both linear and semi-logarithmic form for clarity.

Chapter 6

Diffusion, Migration and Reaction in Conducting Polymer Modified Electrodes

6.1 Introduction

Electroactive polymer films have received considerable attention in the literature recently because of their wide range of possible applications. These include electrocatalysis, molecular electronics and chemical and biosensor technology. A thin film of an electroactive polymer deposited on the surface of a support electrode constitutes a chemically modified electrode. This deliberate immoblization of a chemical microstructure on a host electrode surface (to perform a specific task) is usually performed via a process of electropolymerization. The electropolymerization is carried out by immersing an inert conductive support electrode into a solution containing an electroactive monomer. The monomer is then deposited onto the inert conductive support surface to form a three-dimensional conductive microstructure. The particular application of electrocatalysis is of interest to us and useful summaries of work to date in this area are provided by Hilman (1987),

Lyons (1990, 1994a,b), Evans (1990), Wring and Hart (1992) and Murray (1992).

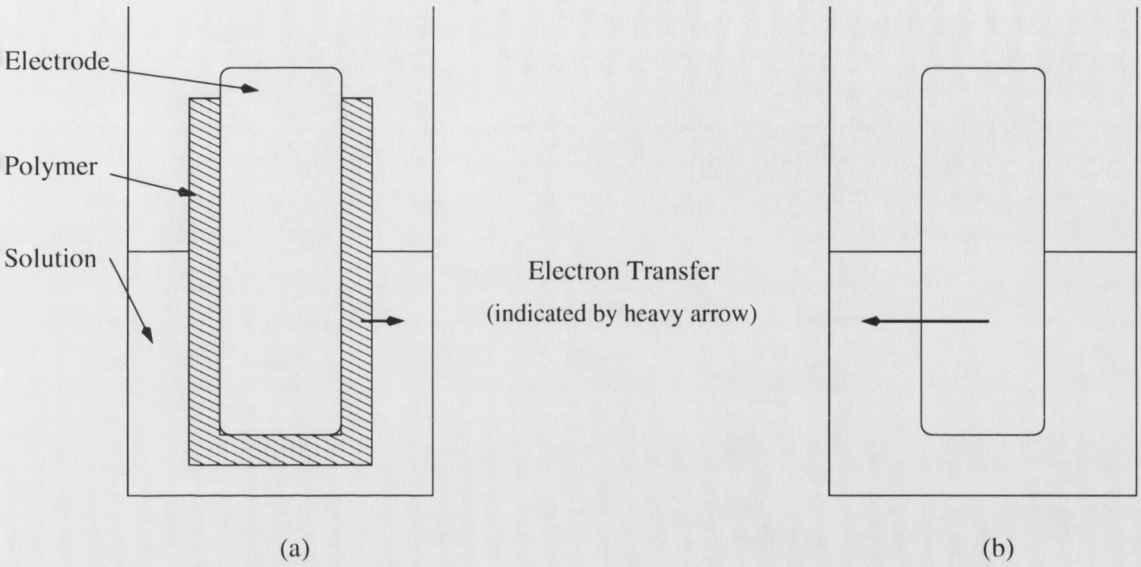

Figure 6-1: Schematic diagram outlining the difference between mediated electron transfer (a) and conventional electron transfer (b). In figure (a) the electron transfer takes place between the polymer film and the redox species in solution as opposed to conventional electron transfer (b) where there is direct transfer between the Fermi level of the metal and the redox species in solution.

Electrocatalysis of electrode reactions involves direct participation of the polymer material. Conventional electron transfer as (discussed in monographs on electrode kinetics) describes the direct electron transfer between the Fermi level of the metal and the redox species in solution. This is in contrast to heterogeneous mediated electrocatalysis where the electron transfer is mediated by the species in the film. One advantage of this is that the coated electrode adopts the characteristics of the deposited microstructure and the overpotential of the coated electrode is often considerably less than the overpotential of the uncoated electrode, therefore facilitating the process of charge transfer. In fact the support electrode pays a passive role in the electron transfer process, its sole function being a connector for electron flow in the electric circuit.

However, the main advantage of a surface modification is that an electrode

may be suitably modified to perform a specific task. By choosing an appropriate coating, one can exercise complete control over the redox reaction. In order to exploit this to its full potential, a thorough understanding of fundamental principles of the way in which the deposited layer mediates the oxidation or reduction process is necessary. Although the physical process is quite complex, we can develop a simple mathematical model to describe it. This involves generating a suitable differential equation to describe the coupled diffusion migration and reaction. Given a suitable initial condition and physically reasonable boundary conditions, this equation is solved. Where an analytical solution is possible, it is possible to obtain the current response. However, the chemical reaction term is described by the complex Michaelis Menten kinetics and this results in a non-linear differential equation which can only be solved numerically. The purpose of this work is to solve and analyse these equations but we begin with a brief historical and mathematical background.

6.2 Classification of Polymer modified Electrodes

The first chemically modified electrode system was developed as a two dimensional structure. The chemical microstructure was very thin, usually only one monolayer and they are the called *monolayer modified electrodes.* These simple structures are easy to model mathematically but are of limited utility because a three-dimensional dispersion of active sites is not attained.

A further development was that of a three dimensional chemical microstructure, the so-called *polymer modified electrode.* In this system the active species has a dual function, namely to shuttle electrons and to provide good electrocatalytic activity. Their operational characteristics are described by Andrieux *et al.* (1978) and Albery and Hillman (1984).

The dual function of the active species can be restrictive so a further improvement on this came in the form of a polymer based integrated system known as

a *microheterogeneous system.* In this integrated system the functions of charge transfer to the catalytic site and catalytic activity are performed by different components within the layer. This means that both functions can be performed in parallel and there is no competition or restriction. The theory of these microheterogeneous systems has been established by Lyons *et al.* (1989a,b); Lyons and Bartlett (1991); Lyons *et al.* (1992, 1994). Their are a number of advantages of these systems. Firstly, they are easy to fabricate. Secondly, the functions are distinct and separate. Thirdly, the three-dimensional dispersion gives a high concentration of sites thereby providing excellent catalytic advantages. Fourthly, the microscopic particles can act as catalytic sites for multi electron transfer reactions and finally the polymer matrix stabilises the whole system.

6.3 Heterogeneous Mediated Catalysis - General Considerations

The process of heterogeneous catalysis is a basic two step process. We will outline this as follows:

$$\begin{aligned} A + ne^- &\rightarrow B \\ S + B &\rightarrow P + A \end{aligned} \tag{6.1}$$

The first step requires charge injection to convert the precatalyst (A) to its catalytically active form (B). The second step involves the reaction of the activated catalyst (B) with the substrate (S) to give the product (P) and to regenerate the precatalyst. This is therefore a cyclic process and the regenerated precatalyst from step two is used to repeat step one.

The first step is characterised in terms of the rate constant k'_E, the symmetry factor α and the standard potential $E^0(A - B)$. The second step has a second

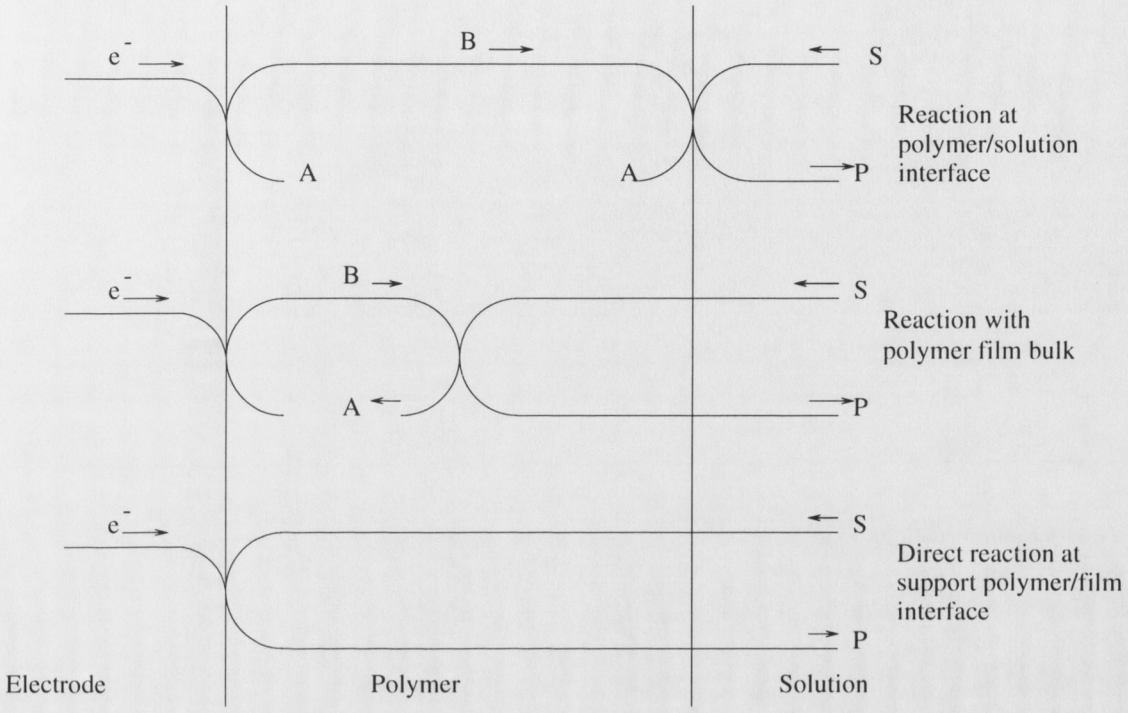

Figure 6-2: Schematic representation of mediated electrocatalysis at a conducting polymer electrode material

order rate constant of k. It is usual that the rate of transfer for both steps is very fast and that $k'_E >> k$. In this case the electron transfer will take place at a potential close to that of the couple $A - B$. This is what we mean by mediated electrocatalysis.

The kinetics are determined by the rate of reaction between the activated catalyst (B) and the substrate (S) - the rate constant k, and the rate of diffusion of the substrate from the bulk solution to the interface with rate constant k_D. Therefore we must also consider concentration polarization.

The above model adequately describes two-dimensional systems. A description of a three dimensional system requires additional considerations such as the rate of charge propagation through the matrix and the permeability of the membrane. The kinetics of heterogeneous mediated catalysis involves a combination

of the following steps

First there is charge injection at electrode-polymer interface. This is generally kinetically facile. The next step is conversion of the precatalyst to the catalytically active species This is potential gradient driven. Following this there is charge propagation in the polymer layer, a concentration gradient driven process described by the diffusion coefficient D_E. Finally the substrate and catalytically active species react with rate constant k in the "reaction zone". The "reaction zone" is in the polymer layer and depending on whether the relative rate of substrate to electron transfer, may be situated closer to the electrolyte or the electrode interface.

We will now take a look at the interaction between sites and substrates in the polymer film. The substrate binds to sites in the polymer to form a complex. This complex subsequently decomposes into products. The steady state current response exhibits biphasic behaviour with respect to the concentration. That is, in the limit of low concentration, the reaction exhibits first order kinetics whereas for high concentrations, zero order kinetics pertain (Lyons (1994b)). This is characteristic of a Michaelis-Menten process, which has been well established in enzyme kinetics.

The coating of a metal oxide with an electronically conducting polymer to facilitate the oxidation of catechol, ascorbate or glucose have been studied in our laboratory. None of these systems contain redox enzymes and yet they exhibit Michaelis Menten behaviour. This serves as adequate justification that our postulation of Michaelis Menten behaviour is correct.

Chemical reaction and substrate diffusion are not the only processes which had to be considered when modelling the amperometric response of conductive polymer sensors. As noted in the recent work of Doblhofer and Vorotyntsev (1994), quite significant potential gradients can exist within the thin films. One cannot assume that the gradients are uniform and since many organic substances (e.g. ascorbic acid) are ionized when they penetrate the polymer, it is reason-

able to assume that the substrate will migrate as well as diffuse in the polymer layer. Therefore we will consider the problem of reaction/diffusion/migration of a substrate through a thin polymer film.

6.4 Description of the Boundary Value Problem

For the purposes of mathematical modelling, we consider a thin electronically conductive film deposited on the surface of an inert support electrode to form a chemically modified electrode. We assume that the layer is of uniform thickness L. We further assume that the mediator sites are uniformly dispersed throughout the bulk of the layer and that the polymer film is electronically conducting so that charge percolation from site to site throughout the polymer layer is not rate determining. We also, for the sake of simplicity, neglect concentration polarization effects of the substrate in solution.

The following reaction sequence is postulated:

$$S + B \rightleftharpoons [SB]^{+} \rightarrow P + A \tag{6.2}$$

This reaction sequence is the well known Michaelis-Menten tight binding mechanism, and K_m and k_c denote the Michaelis constant and the catalytic rate constant respectively.

The differential equation quantifying the transport and kinetics with in the polymer film may be written as

$$\frac{\partial s}{\partial t} = -D\frac{\partial^2 s}{\partial x^2} - \frac{k_c c_\Sigma s}{K_M + s} \tag{6.3}$$

where s is the substrate concentration, t is time , x is distance D is the diffusion coefficient of the substrate in the layer and c_Σ denotes the total catalyst concentration in the film.

Although the expression presented in equation (6.3) adequately describes the

substrate reaction kinetics mediated via immoblized polymer sites, the inherent non-linearity of the Michaelis-Menten reaction term makes a full analytical solution of the differential equation difficult, especially when electromigration effects are also considered. Consequently, we shall consider a more simple reaction rate term in which the substrate reaction kinetics are pseudo first order. This is a good approximation for the low concentration limit (Lyons (1994b)). Hence the reaction rate term is given by $ks = \frac{k_c c_\Sigma s}{K_M + s}$.

We assume that the transport processes of diffusion and migration obey the Nernst -Planck equation and so the electromigration term is given by the quantity

$$\frac{zFD_sE}{RT}\frac{\partial s}{\partial x} = \mu_s E \frac{\partial s}{\partial x} \tag{6.4}$$

where z denotes the valence of the charged substance, E denotes the electric filed within the polymer film μ_s denotes the mobility of the substrate within the polymer and s represents the concentration of substrate in the layer.

The pertinent reaction diffusion migration equation describing the substrate transport and kinetics within the polymer film is therefore given by

$$\frac{\partial s}{\partial t} = -D\frac{\partial^2 s}{\partial x^2} - \frac{zFED_s}{RT}\frac{\partial s}{\partial x} - ks \tag{6.5}$$

This equation must be solved subject to the following boundary conditions: when $x = 0$, $\frac{\partial s}{\partial x} = 0$ and when $x = L$, $s = \kappa s^\infty$ where κ denotes the partition coefficient of the substrate and s^∞ denotes the bulk concentration of the substrate in solution. The first boundary condition implies that the substrate reacts on the polymer sites and not on the support electrode surface, whereas the second boundary condition implies that concentration polarisation of the substrate in the solution can be neglected.

As with previous chapters, the diffusion/reaction/migration equation is recast into dimensionless form. The following normalised parameters are introduced

$$u = \frac{s}{\kappa s^{\infty}} \quad \chi = \frac{x}{L} \quad \gamma = \frac{kL^2}{D_s} \quad \beta = \frac{zFE_0DL}{D_sRT} \tag{6.6}$$

and equation (6.5) becomes

$$\frac{\partial u}{\partial \tau} = \frac{\partial^2 u}{\partial \chi^2} - \beta \frac{\partial u}{\partial \chi} - \gamma u \tag{6.7}$$

The normalised boundary conditions are

$$\left(\frac{\partial u}{\partial \chi}\right)_{\chi=0} = 0, \quad u(1,\tau) = 1, \quad \textit{and} \quad u(\chi,0) = 0. \tag{6.8}$$

Before presenting the solution to this boundary value problem, we will briefly discuss the normalised steady-state current response.

6.4.1 Current Response

The rate at which ions can be discharged at electrodes is quantified by the current density j, the electric current per unit area. The current density is simply a measure of the charge flux and is obtained from the differential equation describing the transfer process. The flux j is given by

$$j = \frac{i}{nFA} = \int_0^L ks(x,t)\mathrm{d}x = \frac{D_s\kappa s^{\infty}}{L}\gamma \int_0^1 u(\chi,\tau)\mathrm{d}\chi \tag{6.9}$$

Hence the normalized current response y is then given by

$$y = \frac{iL}{nFAD_s\kappa s^{\infty}} = \gamma \int_0^1 u(\chi,\tau)\mathrm{d}\chi \tag{6.10}$$

Therefore in order to determine the steady-state current response y we must firstly integrate the differential equation equation (6.7) subject to the boundary conditions outlined in equation (6.8).

At steady state and for a simple case of diffusion and reaction, as in equation

(6.11) below, the normalised current response may be very much simplified.

$$\frac{\partial u}{\partial \tau} = \frac{\partial^2 u}{\partial \chi^2} - \gamma u \tag{6.11}$$

Since the time derivative is zero, the integral of u times γ over the width of the membrane is given by the derivative of u with respect to normalized distance χ as shown below:

$$\gamma \int_0^1 u(\chi, \tau) \mathrm{d}\chi = \left(\frac{\partial u}{\partial \chi} \right)_{\chi=1} \tag{6.12}$$

It is then natural to assume that for the more complicated case of diffusion migration and reaction, by similar arguments, the steady state normalised current response would be given by

$$\gamma \int_0^1 u(\chi, \tau) \mathrm{d}\chi = \left(\frac{\partial u}{\partial \chi} \right)_{\chi=1} - \beta u_{\chi=1} \tag{6.13}$$

However, it is important to be aware of the nature of the electric field which causes the migration. As detailed by Doblhofer and Vorotyntsev (1994), the electric field is not uniform within the membrane and its effects are really only noticeable at the metal/polymer interface. Therefore, since there is a negligible field at the polymer/electrolyte interface (i.e. where $\chi = 1$) we will assume that in this case, although we include the migration term in calculating the concentration profile, it is more reasonable to omit it in estimating the current response. Hence the steady state current response for diffusion /migration /reaction is given by equation (6.12).

6.5 Solution of the Differential Equation

Equation (6.7) was solved using the technique of separation of variables. We first of all separate the solution into a steady state term (which is dependent only on

χ) and a transient term which is dependent on both χ and τ. The steady state solution is obtained by forcing the boundary conditions to be valid for the steady state solution. The initial condition is then imposed on the transient component and this solution is obtained by separation of variables or Laplace Transforms. In Appendix F.1 we show how the solution was obtained. It is given as follows:

$$u(\chi, \tau) = u_{ss} + u_{tr} \tag{6.14}$$

where u_{ss} is the steady state solution and u_{tr} is the time dependent portion. The steady state solution is given by

$$u_{ss} = \exp(a(\chi - 1)) \left(\frac{a \sinh(b\chi) - b \cosh(b\chi)}{a \sinh(b) - b \cosh(b)} \right) \tag{6.15}$$

where $a = \frac{\beta}{2}$ and $b = \left(\frac{\beta^2}{4} + \gamma\right)^{\frac{1}{2}}$. The transient portion is defined as

$$u_{tr} = \exp(a(\chi - 1)) \sum_{n=1}^{\infty} D_n \sin(b_n(1 - \chi)) \exp(-\lambda^2 \tau) \tag{6.16}$$

In this case the coefficient of time in the exponential term, λ, is defined as $\lambda = \left(\frac{\beta^2}{4} + \gamma - b_n\right)^{\frac{1}{2}}$, D_n is a rather complicated

$$D_n = \frac{2}{b^2 + b_n^2} \left[\left(R b_n \cos(b_n) - b \sin(b_n) \right) \sinh(b) \right. \tag{6.17}$$

$$\left. + \left(b_n cos(b_n) - R b \sin(b_n) \right) \cosh(b) - b_n \right] \tag{6.18}$$

where

$$R = \frac{a \cosh b - b \sinh b}{b \cosh b - a \sinh b} \tag{6.19}$$

and b_n are the solutions of the transcendental equation

$$b_n = a \tan(b_n) \tag{6.20}$$

6.6 Results

We will begin by discussing the steady state results. The steady state concentration profile is given by equation (6.15). It can be seen from this equation that the profile is dependent on both the migration factor β and the reaction parameter γ. In the following section we discuss plots of the concentration profile as a function of both of these parameters. Let us first look at the sign convention of β and γ. β is the migration parameter and it can enhance or retard the motion of the ions depending on whether it is positive or negative. From the mathematics above, we have chosen negative β to be when the electric field is opposite in polarity to the ions and therefore this enhances the motion of them since they are attracted towards the electrode where the field is strongest (*c.f.* Doblhofer and Vorotyntsev (1994)). Therefore positive β is when the field is of the same polarity as the ions and they are therefore repelled away from it. This is show schematically in figure 6-3.

The reaction parameter γ is only ever positive. Since the differential equation has been defined using the term $-\gamma u$, the effect of the reaction parameter is to reduce the amount of substrate present in the film. As γ increases, the rate of substrate depletion decreases since, as mentioned earlier, we have assumed a first order chemical reaction with rate constant γ. A negative value for γ has no physical meaning. In mathematical terms this would correspond to an increase in concentration of the substrate over time but there is no generation of the substrate within the film - all of it enters from the redox solution and therefore we will only look at the physical case of positive γ.

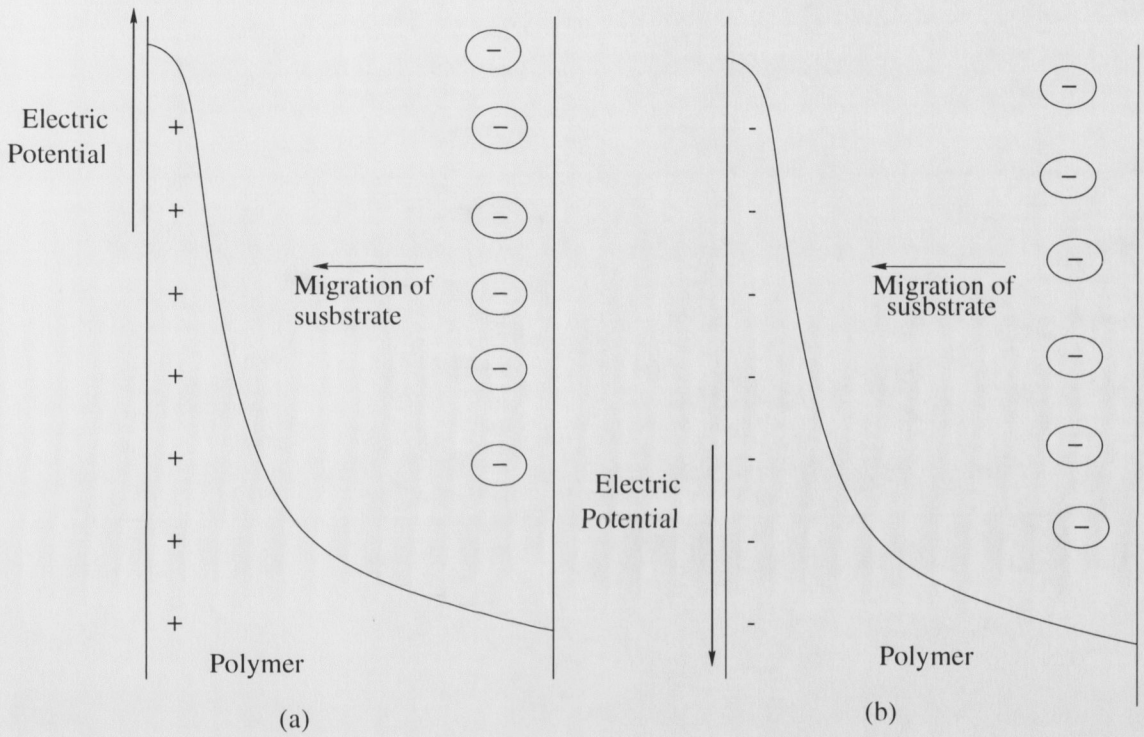

Figure 6-3: Pictorial representation of the enhancement (a) and retardation (b) of ions in a polymer due to the effect of the field. The substrate (shown as negative ions) moves from left to right across the polymer film. If the field is opposite in polarity to the substrate, the migration is enhanced and this corresponds to a negative β parameter. Conversely if the field is the same polarity as the substrate, the migration is retarded and this corresponds to positive β.

6.6.1 Steady State Concentration Profiles

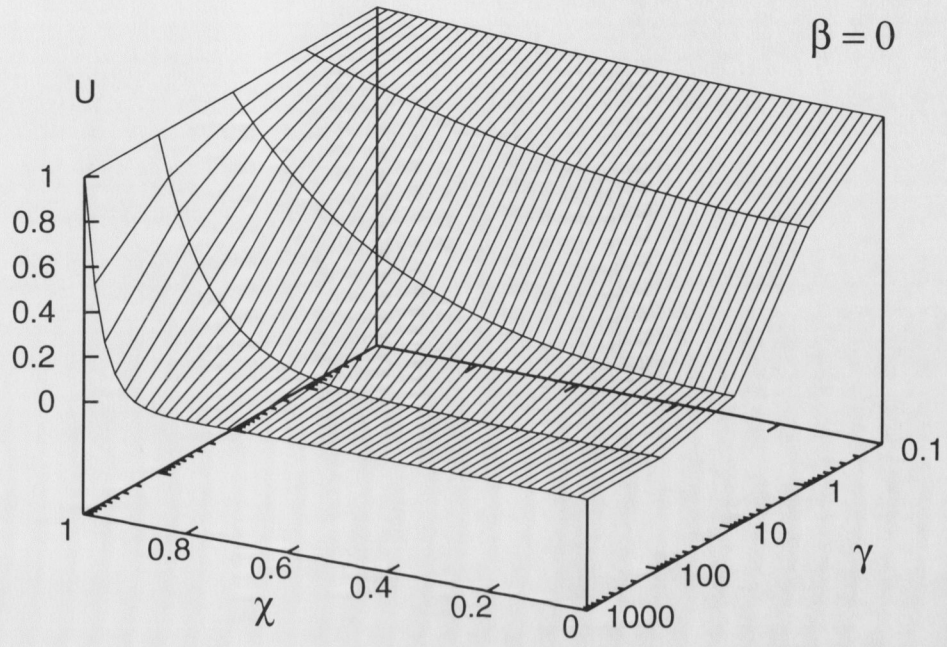

Figure 6-4: Variation of normalised substrate concentration u with normalised distance χ for mediated catalysis at a conducting polymer electrode. The β migration parameter is zero.

Figure 6-4- 6-6 are steady state surface plots of the variation in normalised substrate concentration across the membrane as a function of the reaction parameter γ for fixed values of the migration parameter β. The purpose of these plots is to demonstrate the effect of positive and negative β relative to γ. We will first of all discuss the effect of γ. Basically as the reaction parameter increases, the concentration within the polymer matrix decreases. The migration parameter is zero in figure 6-4. It has a value of $\beta = -10$ in figure 6-5 and $\beta = 10$ in figure 6-6. It is interesting to note that the the difference in the concentration profile

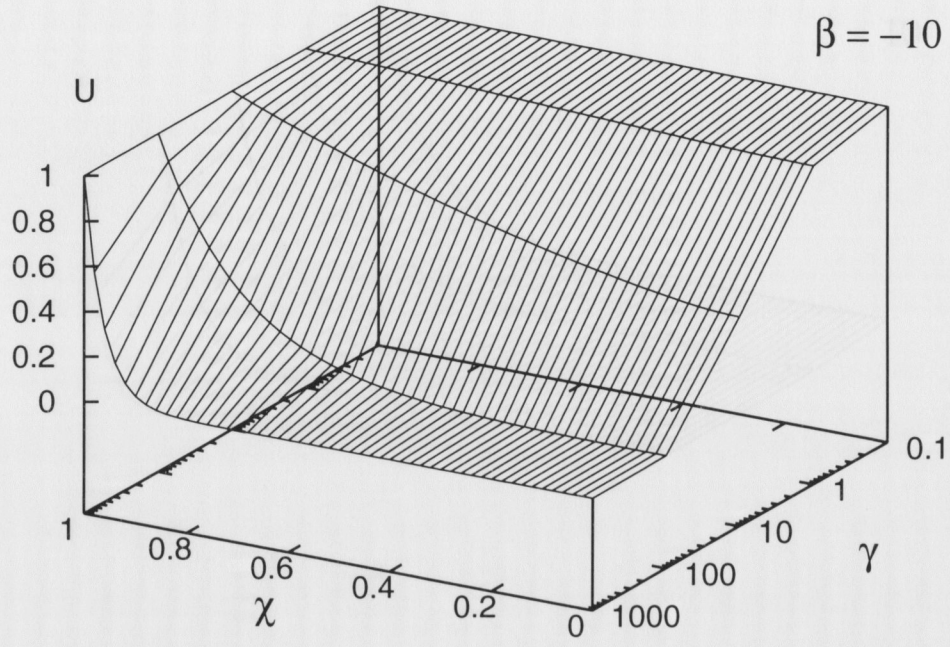

Figure 6-5: Variation of normalised substrate concentration u with normalised distance χ for mediated catalysis at a conducting polymer electrode. The β migration parameter is -10.

for positive values of β is much greater than that for negative values of β, relative to $\beta = 0$.

It should be noted that contrary to the convention presented in earlier chapters, but in agreement with literature convention, positive β corresponds to retardation of migration - meaning that the electric field is opposite in polarity to the ions and they are therefore attracted away from the reaction interface. Conversely, negative β corresponds to enhancement of migration where the field speeds up the process of migration across the film.

In figure 6-7 the steady state concentration profile corresponding to a fixed γ value of 0.1 are presented. Hence the magnitude of the chemical reaction

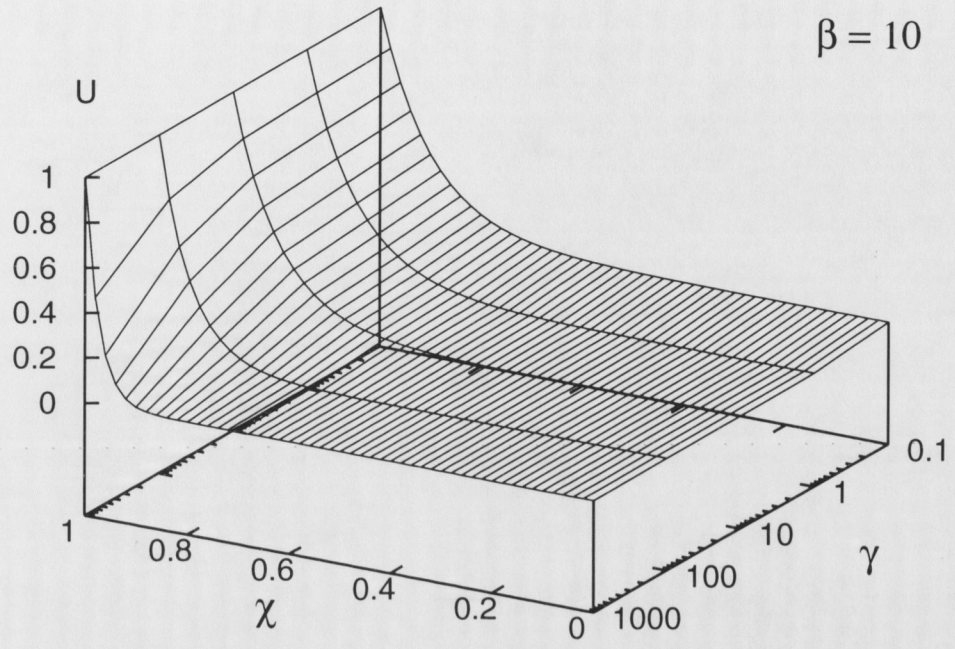

Figure 6-6: Variation of normalised substrate concentration u with normalised distance χ for mediated catalysis at a conducting polymer electrode. The β migration parameter is 10.

flux is one tenth that of the substrate diffusion flux. The concentration profiles corresponding to migration parameter values in the range $-10 \leq \beta \leq 10$ are presented. This corresponds to the range $-100 \leq \frac{\beta}{\gamma} \leq 100$. If we focus initially on the $\beta = 0$ case, we see that there is very little depletion of the substrate throughout the bulk of the polymer film. Now we recall that when γ is small the substrate reaction flux is slower than the substrate diffusion flux and we expect a rapid permeation of substrate throughout the entire layer followed by a small amount of chemical reaction which occurs throughout the entire film. Indeed we recall that $\sqrt{\gamma} = \frac{L}{X_k}$ where L denotes the layer thickness and X_k represents a characteristic reaction layer thickness which is defined as the distance

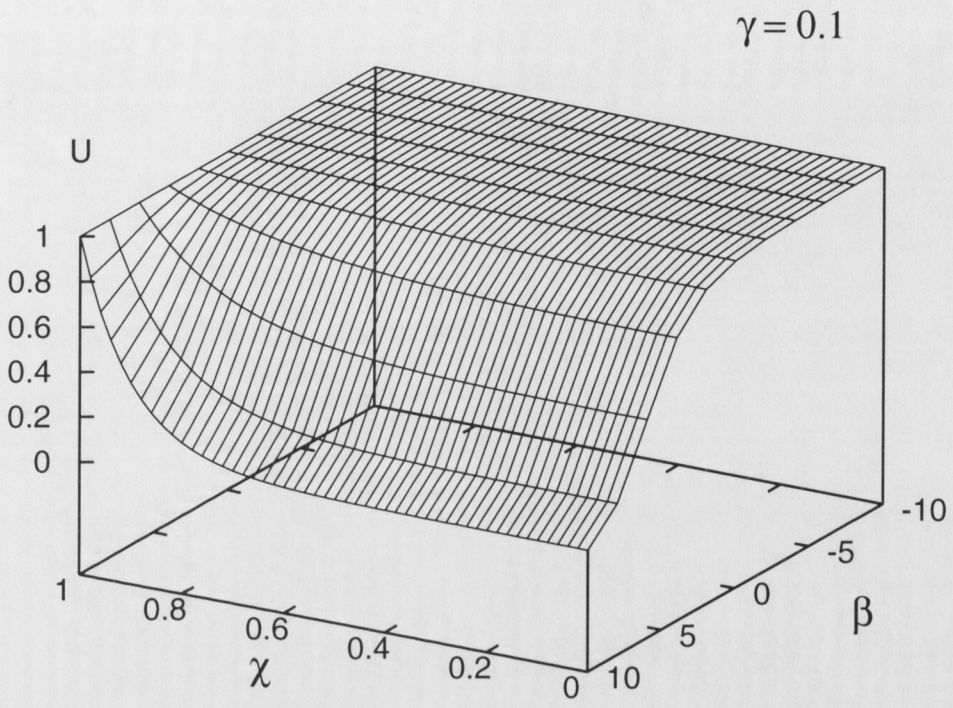

Figure 6-7: Variation of normalised substrate concentration u with normalised distance χ for mediated catalysis at a conducting polymer electrode. The reaction parameter $\gamma = 0.1$ and the migration parameter is in the range $-10 \leq \beta \leq 10$.

the substrate travels in the layer before it undergoes chemical reaction with the polymer sites. Hence for $\gamma = 0.1$, $\sqrt{\gamma} = \frac{L}{X_k} = 0.32$. The reaction layer thickness is considerably larger than the physical dimension of the layer. This is attributed to the rapid diffusion and slow rate of chemical reaction. For optimum transport, the reaction layer thickness should tend to infinity, requiring that the substrate should travel infinitely far before depletion by chemical reaction. When the migration parameter is finite and negative, the substrate concentration profiles indicate a large amount of substrate migration due to the fact that the field accelerates the transport of the charged substrate. On the other hand, when the migration parameter is finite and positive the electric field retards substrate transport and

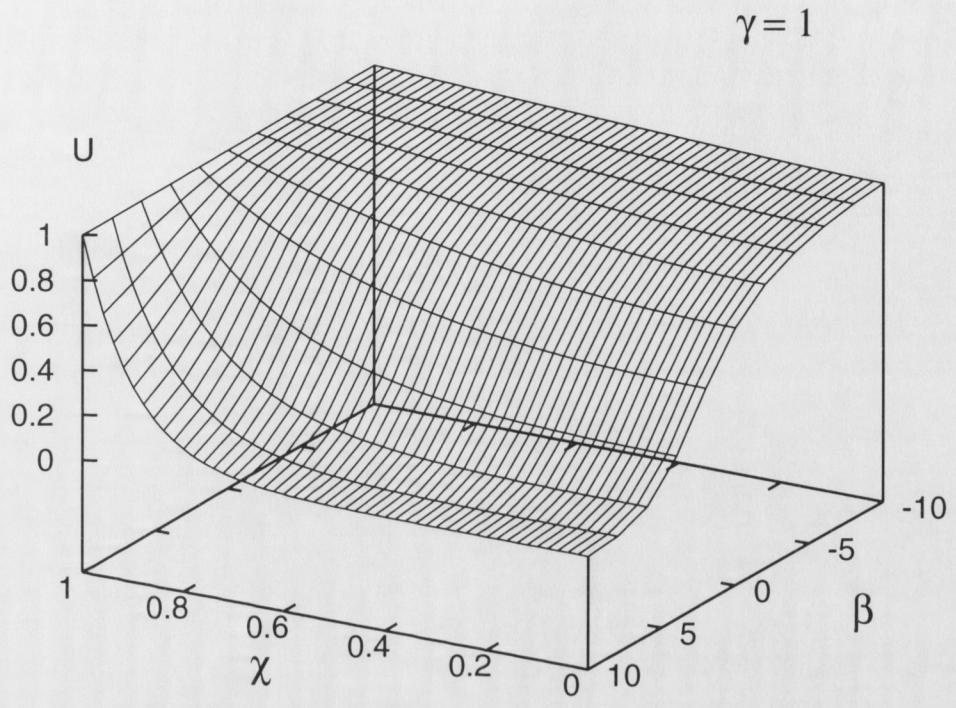

Figure 6-8: Variation of normalised substrate concentration u with normalised distance χ for mediated catalysis at a conducting polymer electrode. The reaction parameter $\gamma = 1.0$ and the migration parameter is in the range $-10 \leq \beta \leq 10$.

there is a very low concentration of substrate in the film relative to the simple reaction/diffusion case.

In figure 6-8 the corresponding situation for $\gamma = 1$ is presented. Here $L = X_k$ and the reaction layer thickness extends over the entire physical dimension of the polymer film. The concentration profile computed in the absence of electric field indicates a steady depletion of substrate through the layer. The concentration profiles computed for negative β values are relatively full again indicating the effect of the field in attracting the substrate into the film. However, the profiles observed for positive β values indicate that much less substrate has penetrated the film than in the absence of a field. When $\beta = 10$, virtually all of the substrate

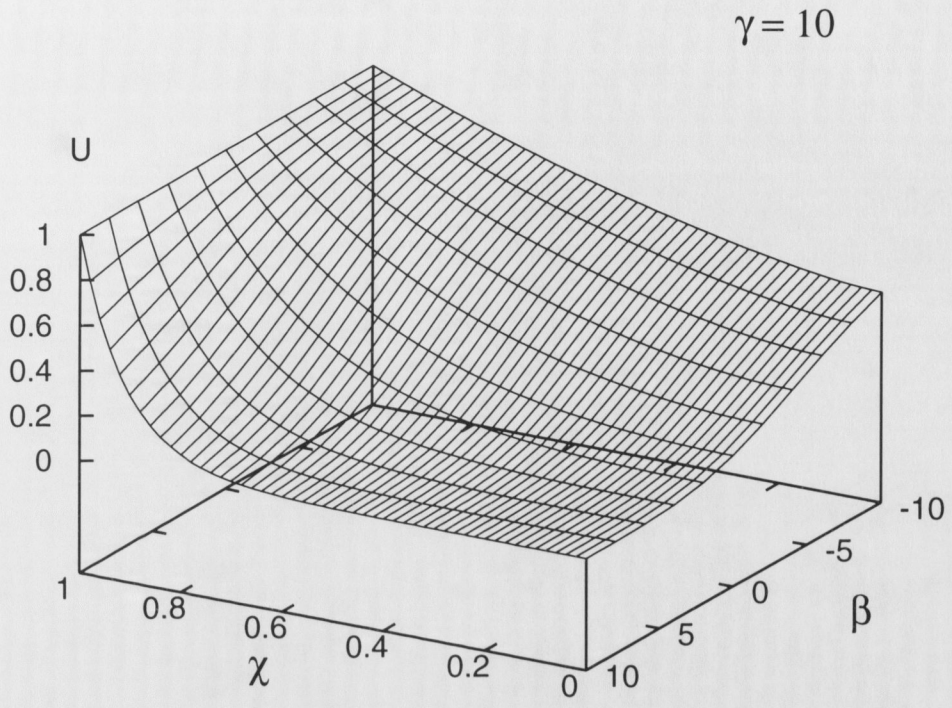

Figure 6-9: Variation of normalised substrate concentration u with normalised distance χ for mediated catalysis at a conducting polymer electrode. The reaction parameter $\gamma = 10.0$ and the migration parameter is in the range $-10 \leq \beta \leq 10$.

that has entered the film has undergone reaction at normalised distance values less than 0.5.

The situation pertaining for $\gamma = 10$ is presented in figure 6-9. Here $\frac{L}{X_k} = 3.2$ and so in the absence of electromigration effects we expect that the facility of the reaction kinetics between substrate and polymer site will be such that much of the substrate will undergo reaction before it has had a chance to diffuse far into the layer. If the applied electric field serves to inhibit substrate transport, then we note that again, any substrate entering the film is rapidly depleted. For the case of enhanced electric field, since the reaction term is larger, less substrate is present in the film because it has been depleted at a greater rate than for smaller

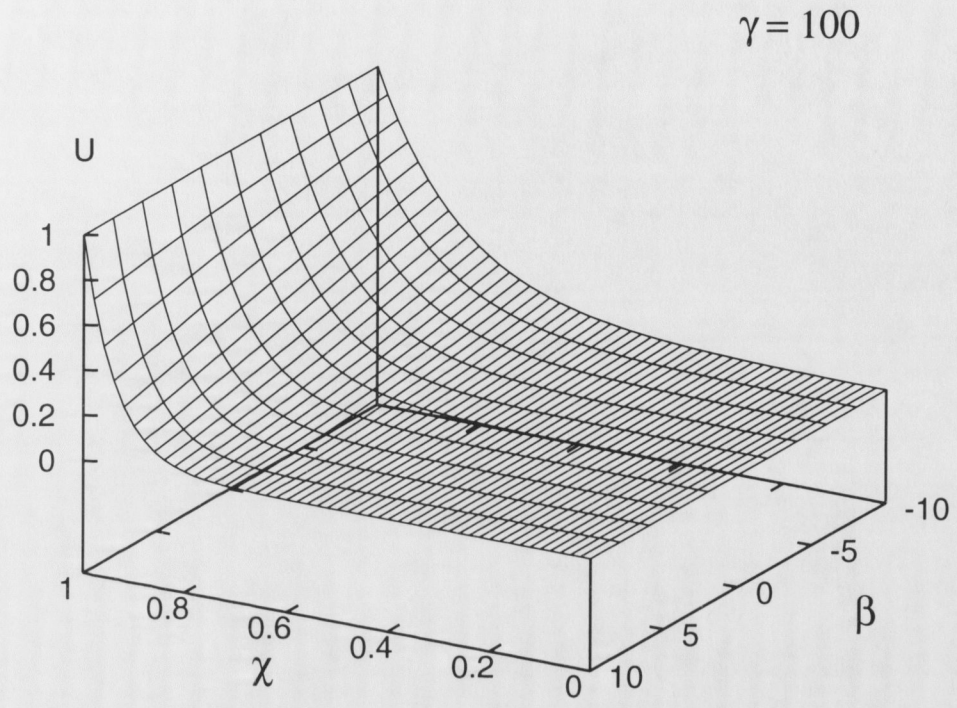

Figure 6-10: Variation of normalised substrate concentration u with normalised distance χ for mediated catalysis at a conducting polymer electrode. The reaction parameter $\gamma = 100.0$ and the migration parameter is in the range $-10 \leq \beta \leq 10$.

values of γ.

The situation pertaining for large γ values is presented in figure 6-10. Here $\frac{L}{X_k} = 10$ and the rate of chemical reaction is considerably faster than that of diffusion, Hence much of the substrate is consumed in a first-order reaction near the polymer/solution interface. The magnitude and sign of the migration parameter β have only a small effect on the shape of the concentration profile.

It is instructive to use equation (6.15) to evaluate u_0, the normalized concentration of substrate present in the steady state at the support electrode/polymer interface. The results of such a calculation are presented in figure 6-11 where u_0 is plotted as a function of the migration parameter β for four values of the

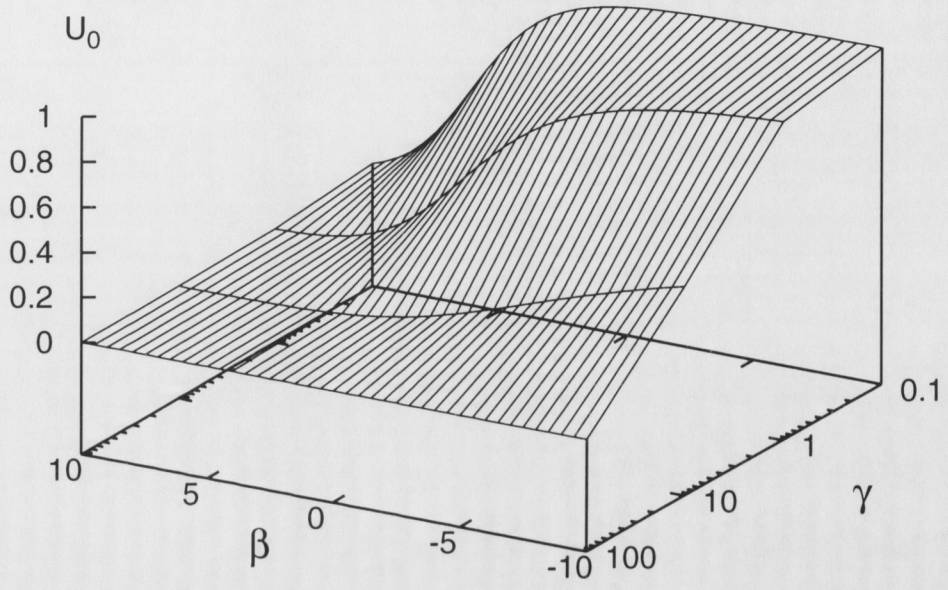

Figure 6-11: Variation of normalised substrate concentration at the support electrode/polymer interface as a function of migration parameter β for different values of the reaction/diffusion parameter γ.

reaction/diffusion parameter γ. When γ is small, the rate of chemical reaction is much slower that the rate of substrate diffusion. Hence u_0 remains close to unity for β values between -10 and zero. However, u_0 subsequently drops rapidly to values near zero when there is a positive ($\beta > 0$, retarding) electromigrative contribution to the substrate transport and kinetics.

This observation implies that when the local electric field in the film serves to retard the rate of migration of substrate to the reaction interface, this is the dominant force. Indeed, even a small degree of retardation - when β is positive but still close to zero - manifests as a large reduction in substrate concentration at the interface relative to that when there is no field. This is especially evident

for $\gamma > 0.1$.

6.6.2 Transient Solution

We have seen that the transient solution is given by equation (6.14) where the specific terms are detailed in equation (6.15)-(6.20). The difficulty with this lies in the fact that equation (6.20) is a transcendental function. The numerical roots of this function are given by Abramowitz and Stegun (1965) for certain values of β but even with these only the first ten terms in the sum are calculated. In this case, there was insufficient convergence. Another way to obtain the roots is graphically but this is long and complex. The graphical roots are only approximations as-well so another approximate method is to solve the entire differential equation via the finite difference method as discussed in chapter 2.

The following plots are results obtained using DEQSOL the software package which solves differential equations via the finite difference method. In terms of measuring accuracy, we did a benchmark test by solving the steady state form with DEQSOL and comparing this with the analytical solution described in equation (6.15). The results matched to an accuracy of $> 99\%$.

6.6.3 Transient Concentration Profiles

In figure 6-12 and 6-13 the time development of the concentration profiles corresponding to a fixed γ value of 0.1 are presented. The analytical steady state profile has been presented in figure 6-7 and it is clear that this matches the profile obtained numerically as depicted in figure 6-13. At short times ($\tau = 0.01$) the concentration profile is essentially uniform across the range of β values shown. As time increases to $\tau = 0.03$ the effect of the enhanced migration parameter given by negative β manifests itself. There is a higher concentration of substrate at the incoming side of the polymer matrix but the concentration at the polymer/electrode interface is still zero for all β. As the time is increased further

to $\tau = 0.05$, the concentration at the polymer/electrode interface is observed to be noticeably larger for finite negative β and again as time is further increased, the profile takes a different shape with the substrate moving quickly through the matrix for enhanced migration and more slowly (even resembling the initial state) for finite positive β (retarded migration). As we proceed even further along the time scale the difference between the profiles is more pronounced. It is interesting to note that at steady state the concentration for finite negative β is approximately unity whereas for the finite positive β, the profile has not progressed much beyond what was observed initially.

Figure 6-14 and 6-15 show the time development of the surface across the range of β values $-10 > \beta > 10$. As we have noted for the previous case, the steady state solution obtained in this manner matches that presented via the analytical solution in figure 6-8. The same arguments apply for these plots as for the previous case where $\gamma = 0.1$. However despite the fact that the reaction layer thickness is ten times that of the previous case, there is very little to differentiate between the plots and the real differences manifest only as we approach steady state conditions. At steady state the difference between the profiles for $\gamma = 0.1$ and $\gamma = 1$ is apparent in that for the larger reaction layer thickness, there is significantly more concentration depletion throughout the polymer.

The most significant observation in the profiles for $\gamma = 10$ (figure 6-16 and 6-17)is that it now takes a much longer time for the substrate to diffuse to the polymer/electrode interface. Even at steady state conditions, the concentration of enhanced field substrate is approximately 50% of what it was for the case of $\gamma = 1$. There is very little change in the profile for retarded field migration (positive γ). The reason for this is that if there is negligible substrate present in the first instance, the effect of concentration depletion through large γ results in negligible substrate at the end and there is therefore no appreciable difference in the profile as γ is increased.

Finally then the profiles at the extreme case of $\gamma = 100$ are presented in figure

6-18 and 6-19. Here the rate of chemical reaction is considerably faster than that of diffusion. Hence any substrate entering the film is consumed in a first order reaction near the polymer/electrode interface. The magnitude and sign of the migration parameter have no significant effect on the shape of the concentration profile.

Figure 6-20 -6-25 are time development surface plots of the variation in concentration across the membrane as a function of the migration parameter γ. We have chosen to look a two extreme cases of finite positive β and finite negative β with the third case of $\beta = 0$ for comparison. For $\beta = 0$ there is very little change in the plot over the first four time snap-shots. The difference between the profiles of $\gamma = 0.1$ and $\gamma = 100$ is very small. For this reason we have included an additional $\gamma = 1000$. The difference in each of the reaction terms is very much apparent as we approach steady state. Here the concentration at the polymer/electrode interface sweeps from unity for $\gamma = 0.1$ when the reaction parameter has little effect, to zero for $\gamma = 1000$ when the effect of the reaction parameter overshadows all other phenomena. When $\beta = -10$ the migration parameter enhances movement into the matrix and there is a clear distinction between the shape of the plots at each different time shot. For small γ the migration enhancement dominates and the substrate rapidly moves into the film with relatively little depletion. In contrast, for large γ ($= 1000$) the migration enhancement has no effect and the profile remains as it was for no field enhancement i.e. $\beta - 0$. Again at steady state there is a contrast between the profile for positive and negative γ. This contrast is so stark that there is not a smooth transition between the various profiles but it must be remembered that this is a logarithmic scale so such effects are magnified greatly. Again, as seen in previous plots for the case of $\beta = 10$ and retardation of the substrate the increase in γ and time have little effect on the profile which remains as zero throughout the majority of the film.

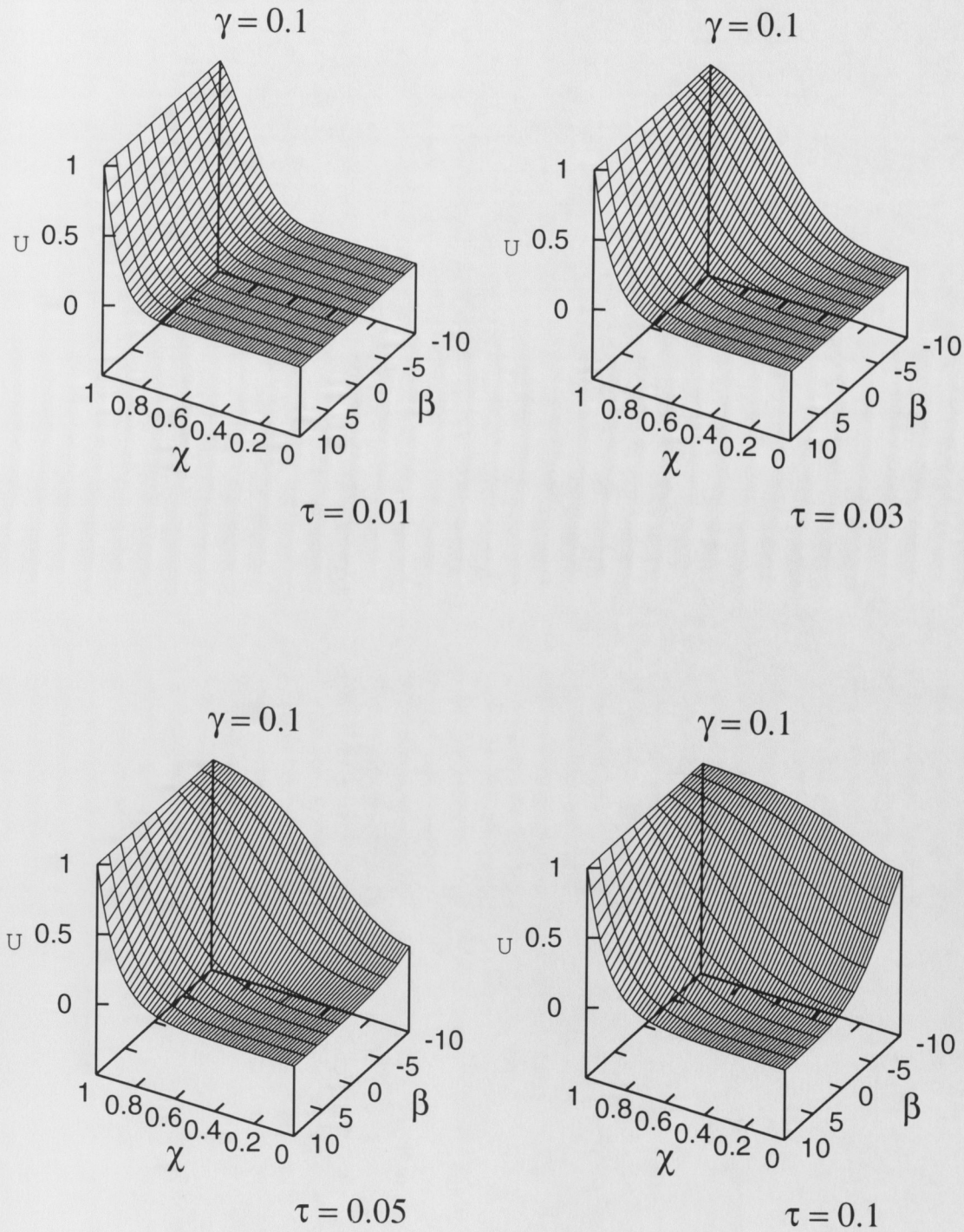

Figure 6-12: Development of the u, χ, γ surface as a function of both normalised time τ and migration parameter β.

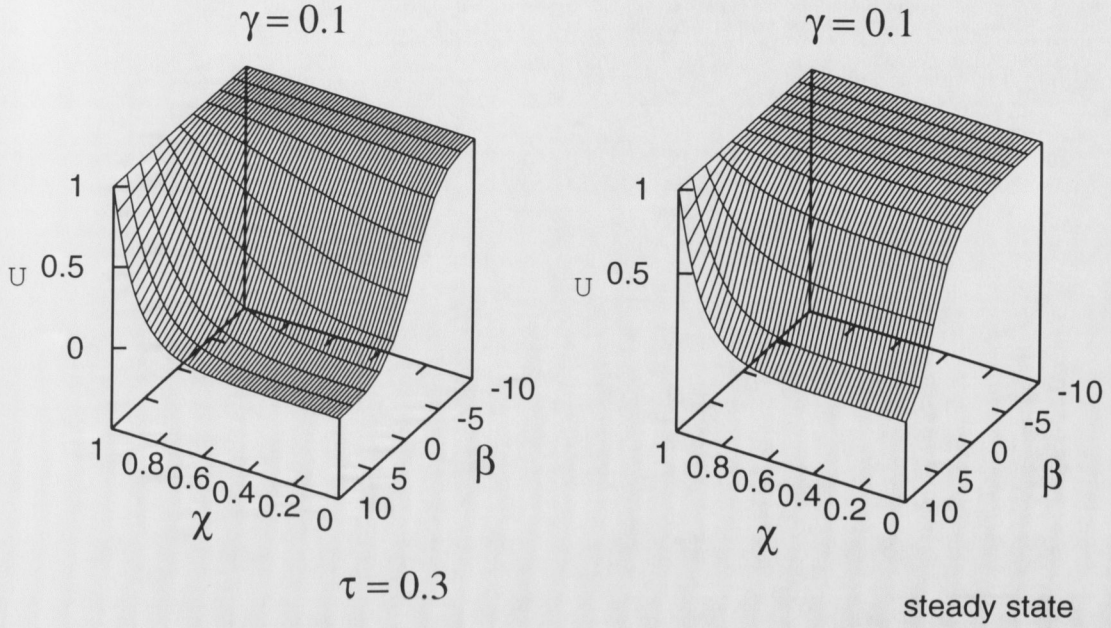

Figure 6-13: Development of the u, χ, γ surface as a function of both normalised time τ and migration parameter β.

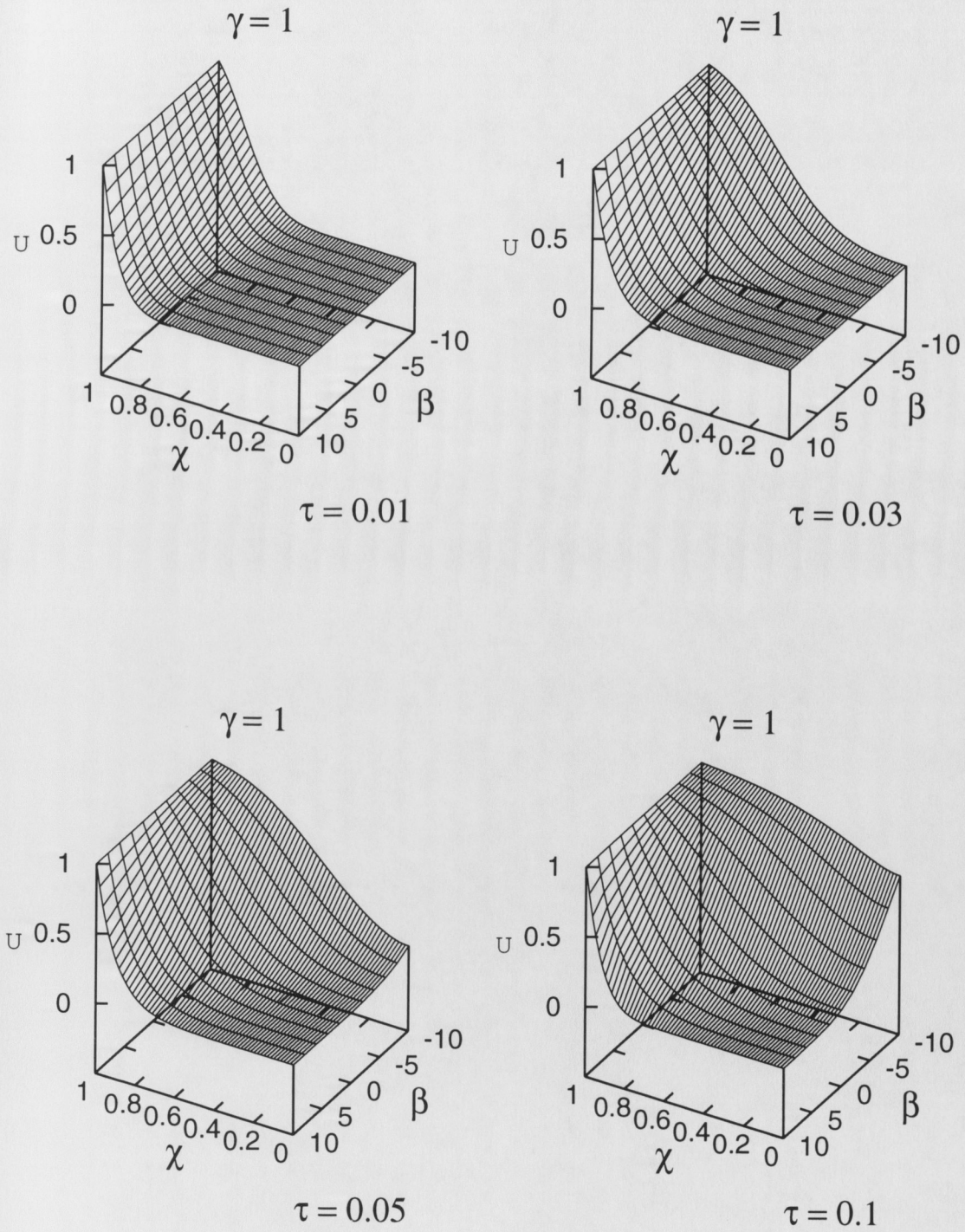

Figure 6-14: Development of the u, χ, γ surface as a function of both normalised time τ and migration parameter β.

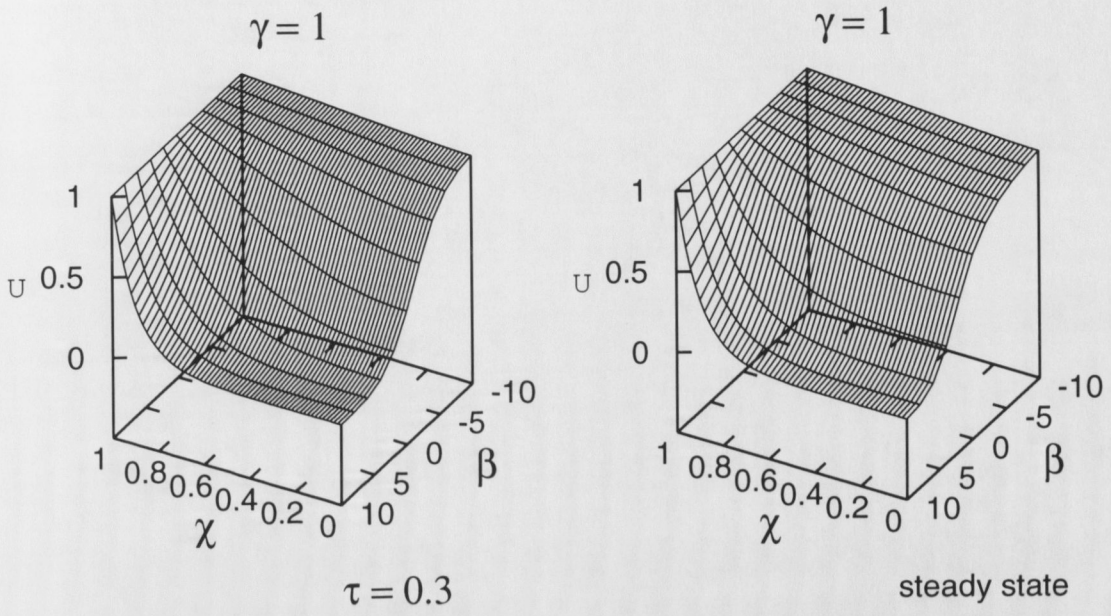

Figure 6-15: Development of the u, χ, γ surface as a function of both normalised time τ and migration parameter β.

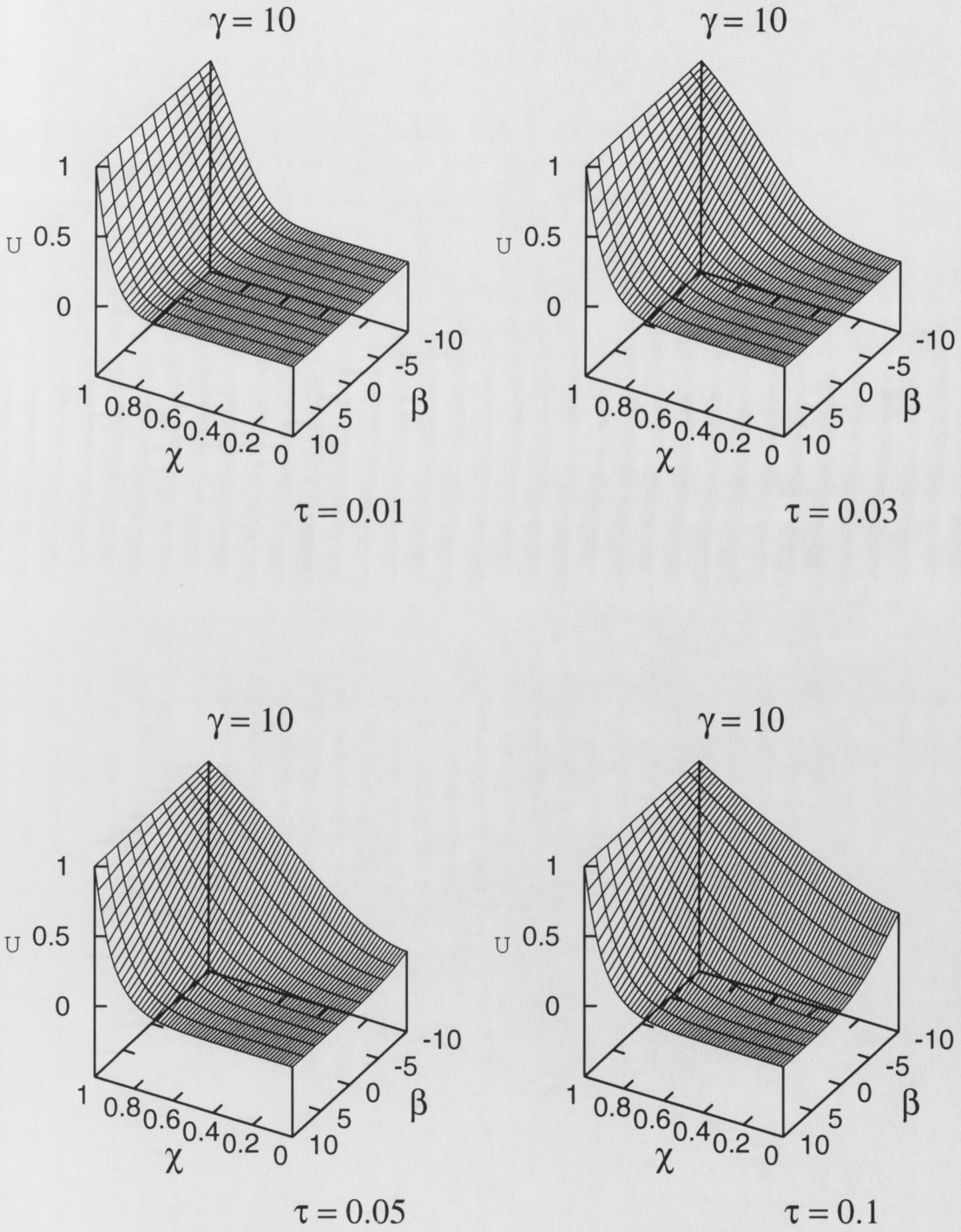

Figure 6-16: Development of the u, χ, γ surface as a function of both normalised time τ and migration parameter β.

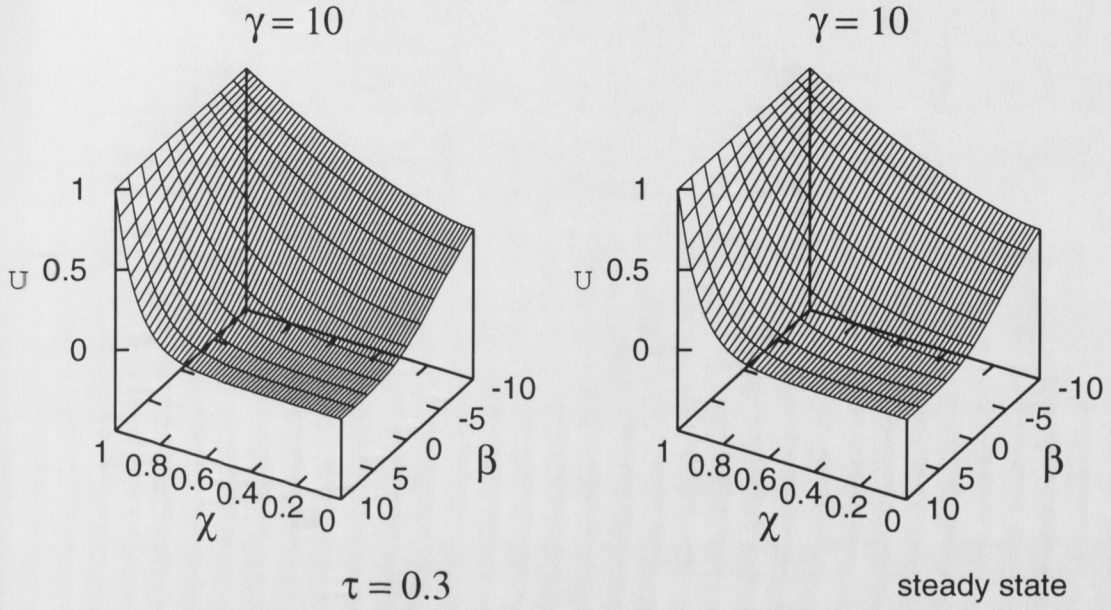

Figure 6-17: Development of the u, χ, γ surface as a function of both normalised time τ and migration parameter β.

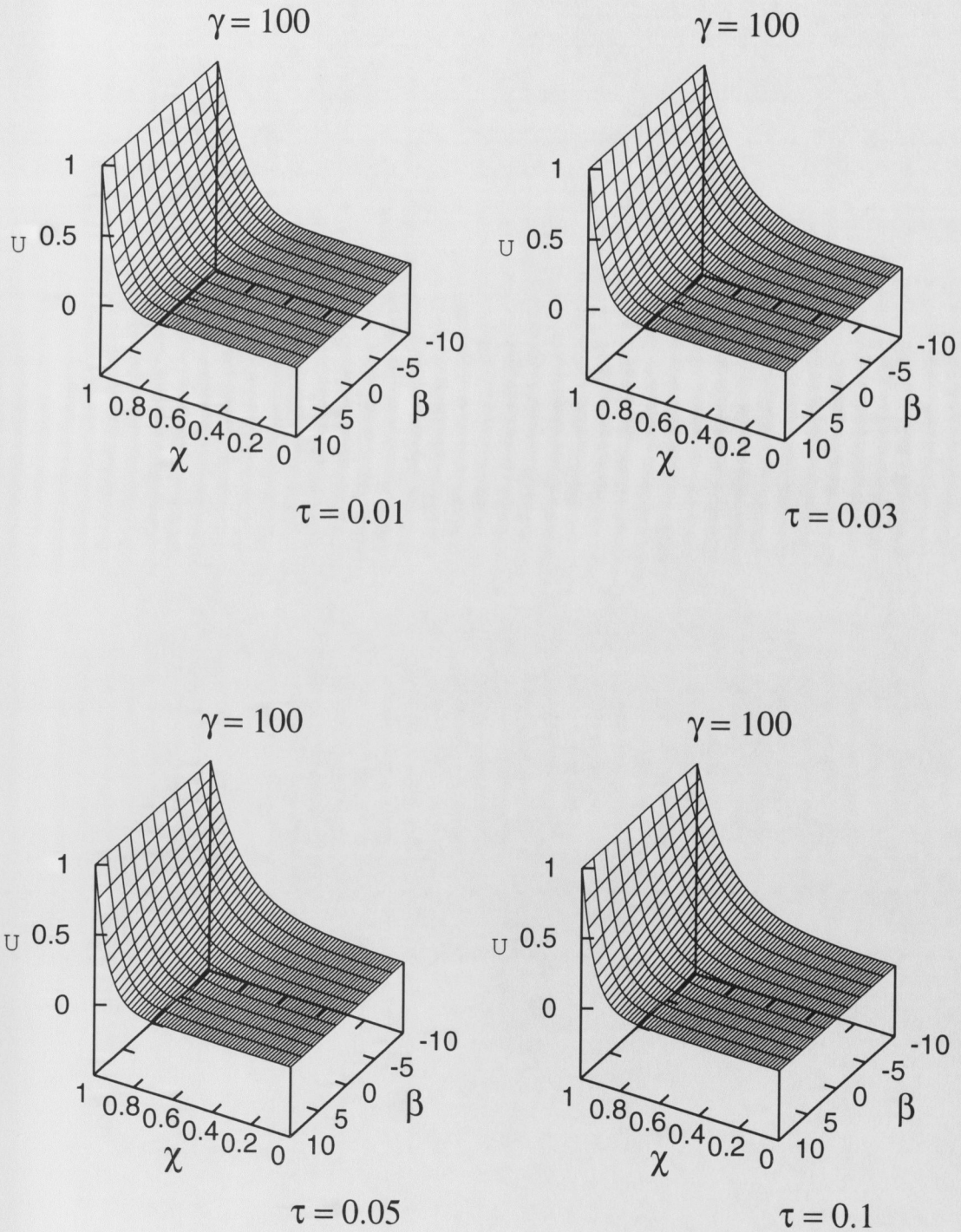

Figure 6-18: Development of the u, χ, γ surface as a function of both normalised time τ and migration parameter β.

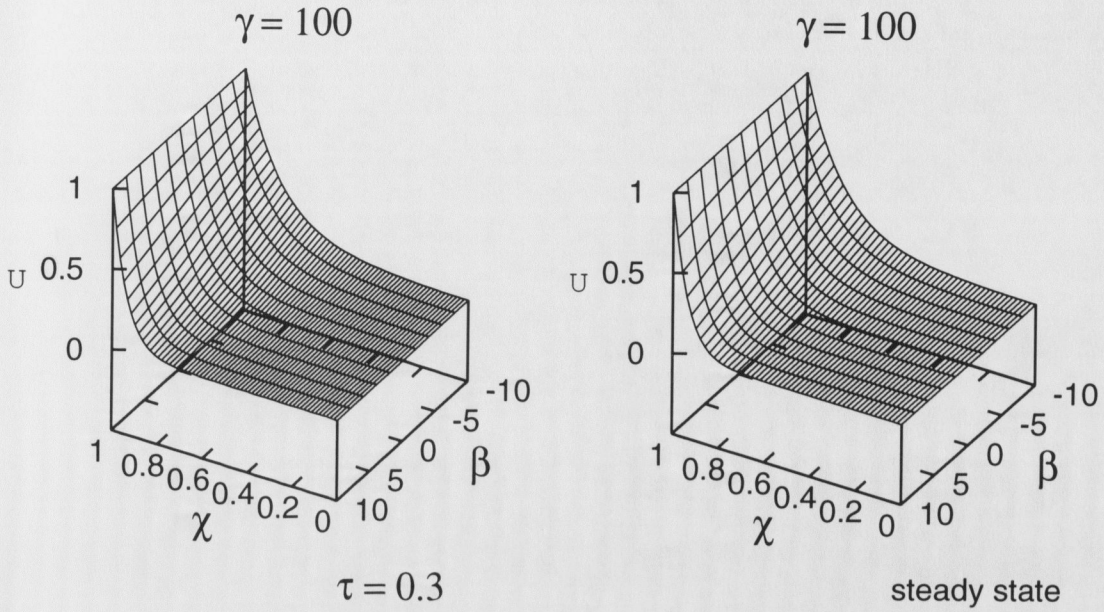

Figure 6-19: Development of the u, χ, γ surface as a function of both normalised time τ and migration parameter β.

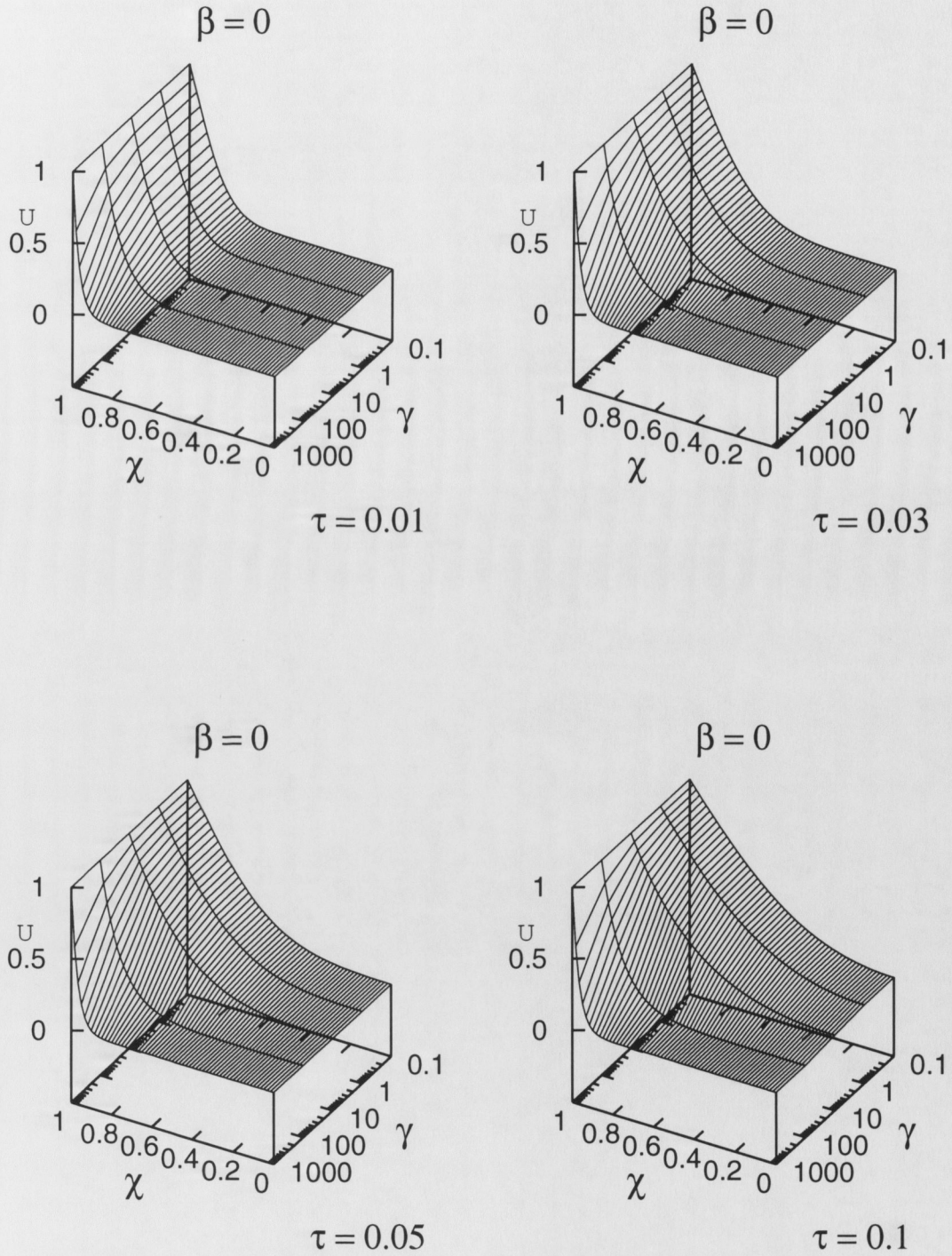

Figure 6-20: Development of the u, χ, γ surface as a function of both normalised time τ and reaction/diffusion parameter γ. The γ parameter is presented in logarithmic form.

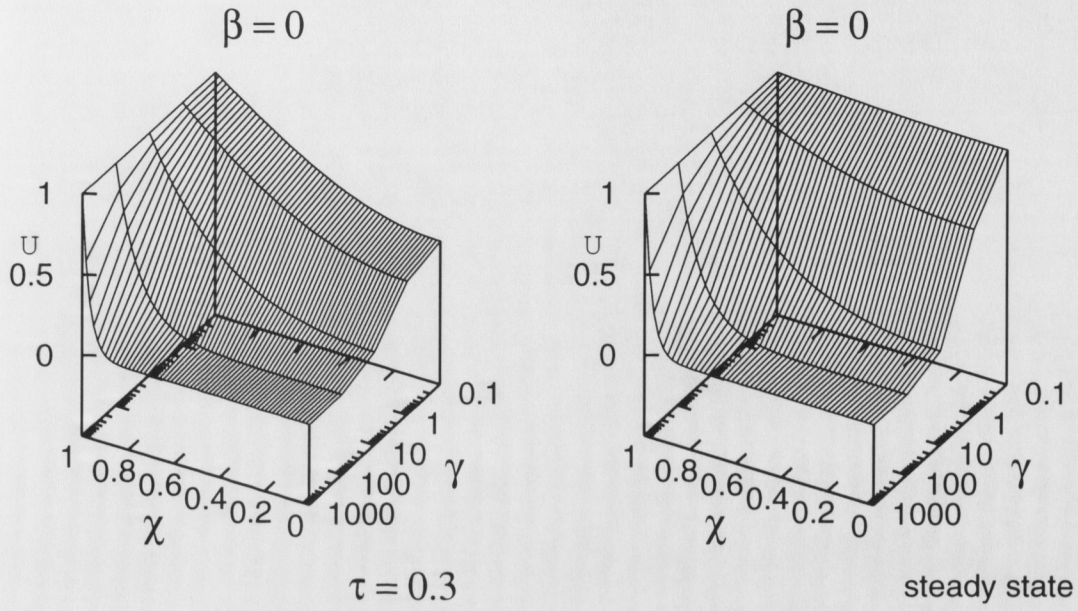

Figure 6-21: Development of the u, χ, γ surface as a function of both normalised time τ and reaction/diffusion parameter γ. The γ parameter is presented in logarithmic form.

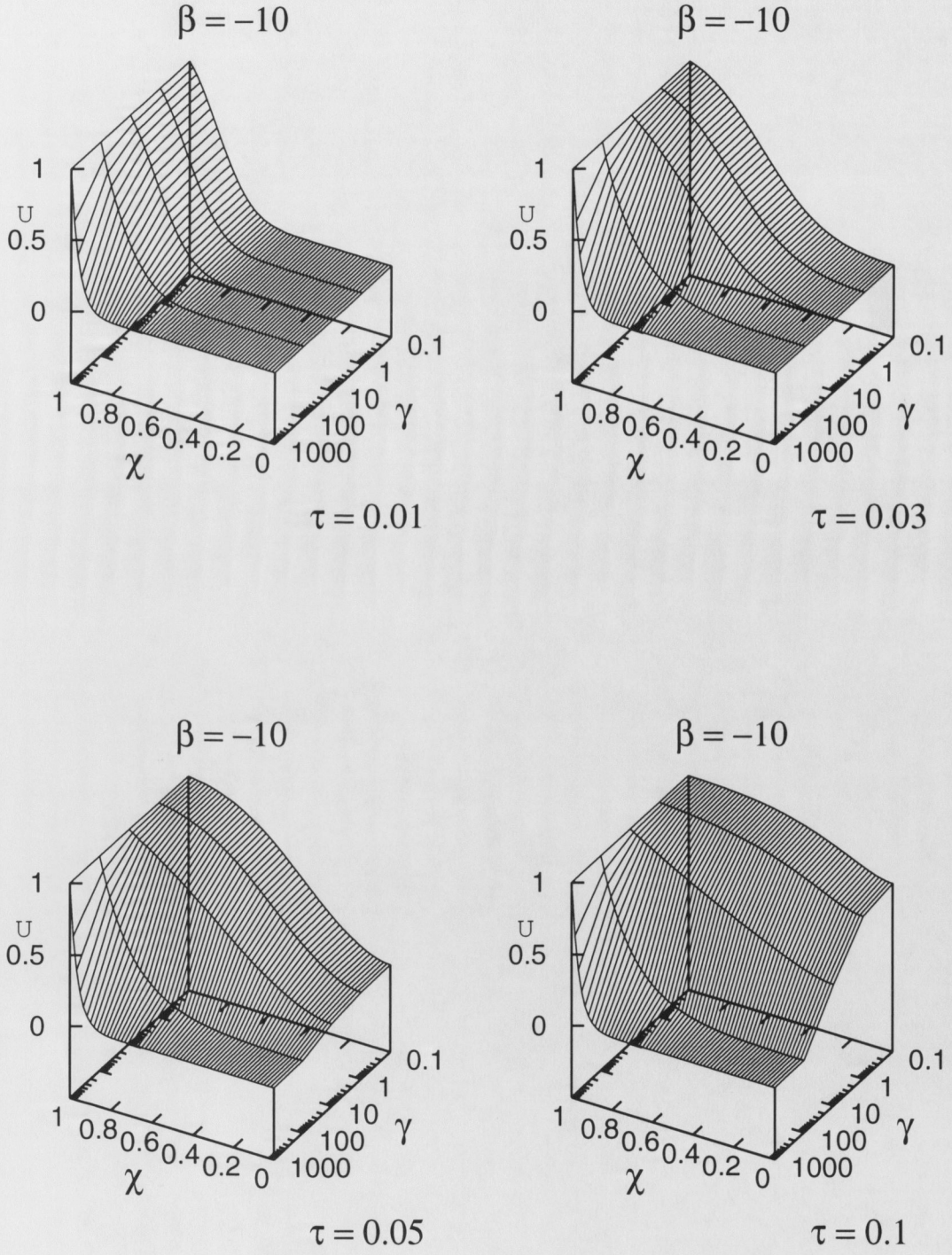

Figure 6-22: Development of the u, χ, γ surface as a function of both normalised time τ and reaction/diffusion parameter γ. The γ parameter is presented in logarithmic form.

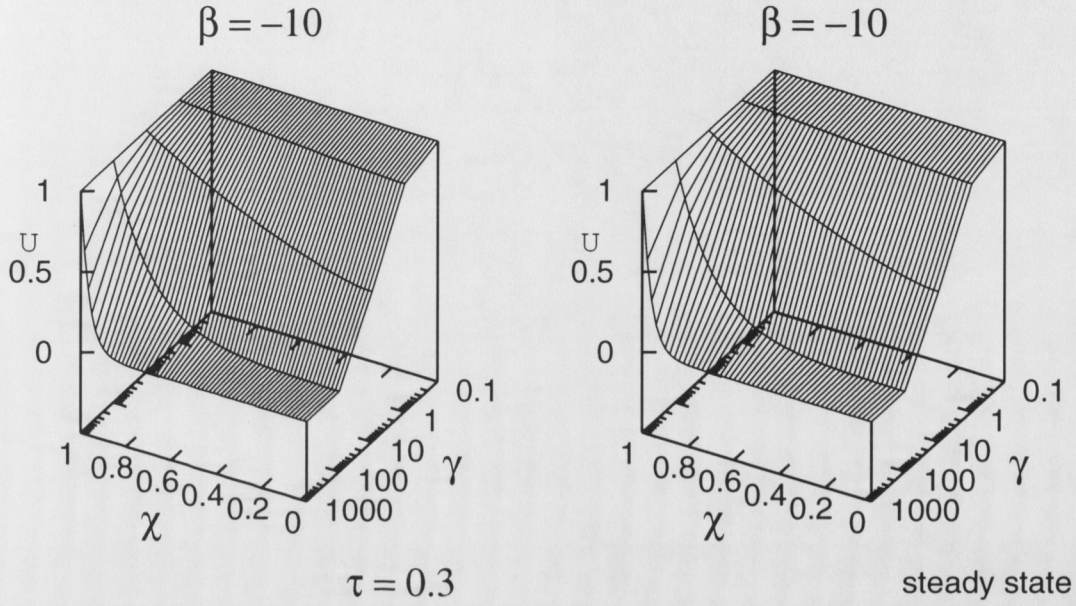

Figure 6-23: Development of the u, χ, γ surface as a function of both normalised time τ and reaction/diffusion parameter γ. The γ parameter is presented in logarithmic form.

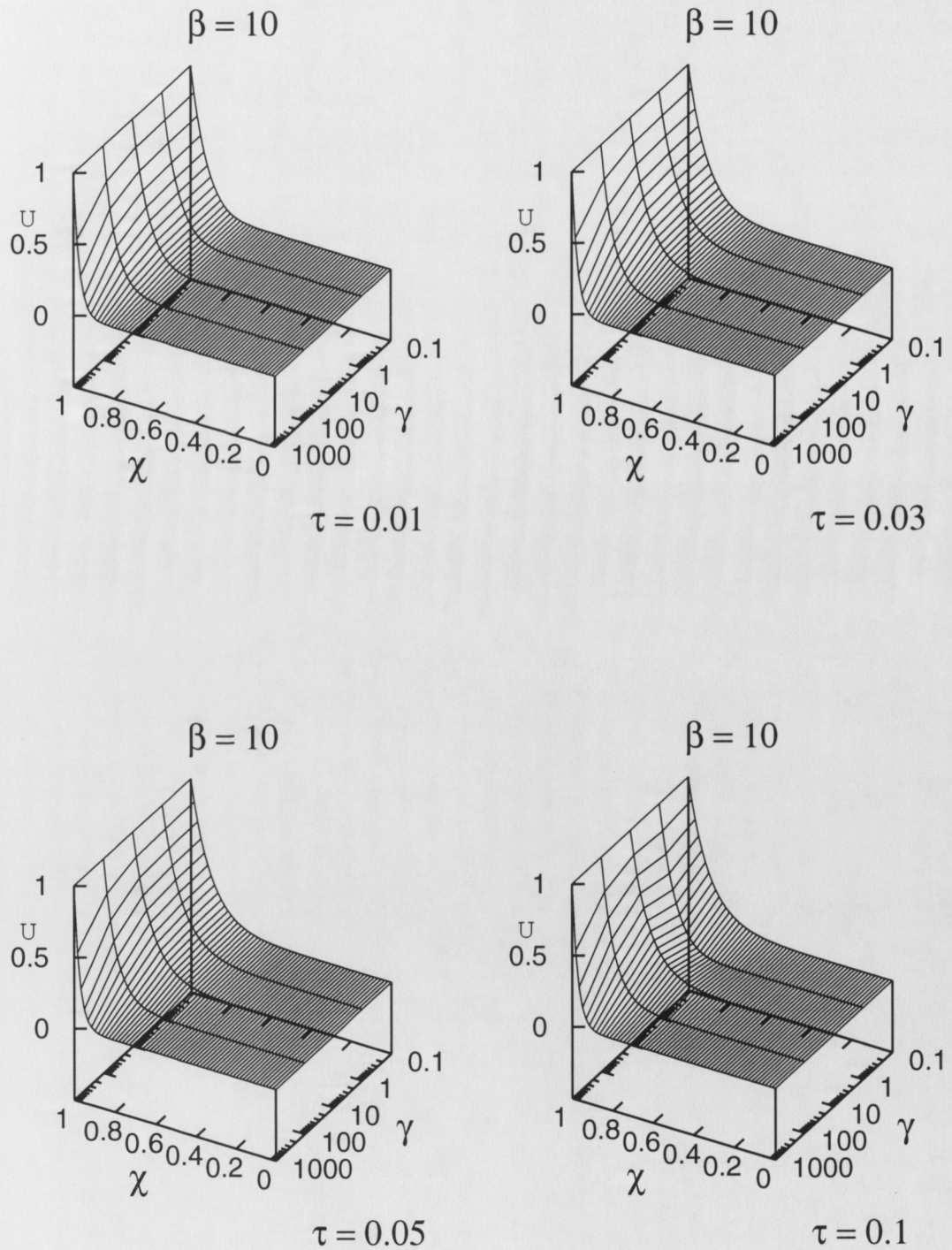

Figure 6-24: Development of the u, χ, γ surface as a function of both normalised time τ and reaction/diffusion parameter γ. The γ parameter is presented in logarithmic form.

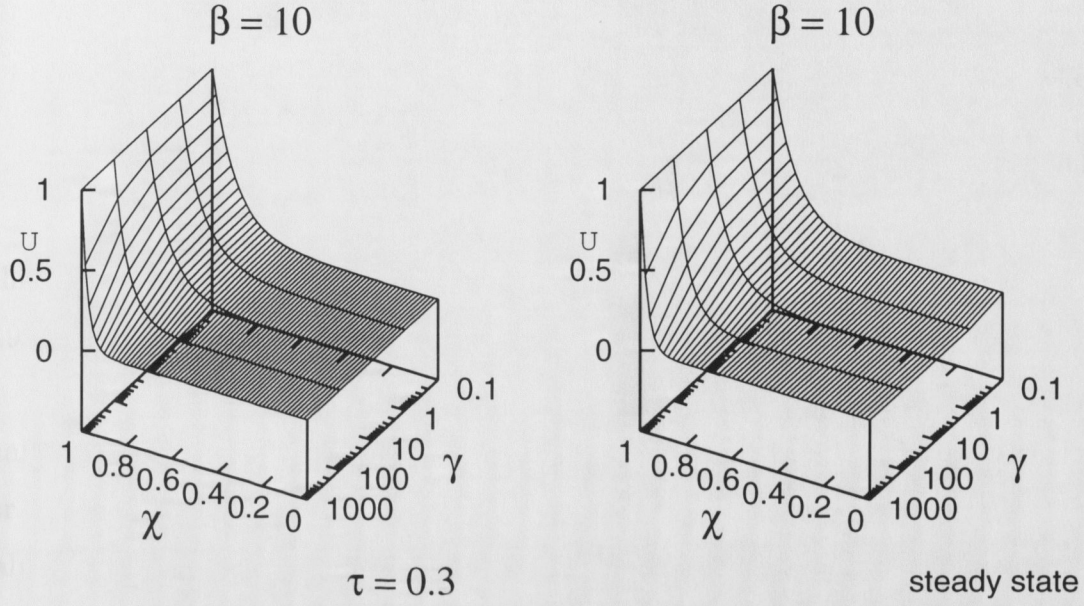

Figure 6-25: Development of the u, χ, γ surface as a function of both normalised time τ and reaction/diffusion parameter γ. The γ parameter is presented in logarithmic form.

6.6.4 Current Response

The normalised steady state current response is given by

$$y_{ss} = \frac{\gamma \tanh \sqrt{\gamma + \frac{\beta^2}{4}}}{\sqrt{\gamma + \frac{\beta^2}{4}} - \frac{\beta}{2} \tanh \sqrt{\gamma + \frac{\beta^2}{4}}} \tag{6.21}$$

We note that when $\beta = 0$, this reduces to

$$y_{ss} = \sqrt{\gamma} \tanh \sqrt{\gamma} \tag{6.22}$$

which is in agreement with an expression previously derived by Lyons *et al.* (1996).

We illustrate equation (6.21) in figure 6-26 where we present a plot of normalised current response y_{ss} as an explicit function of the migration parameter β for various values of the reaction/diffusion parameter γ. We note that for a given value of γ the normalised current increases with increasing value of the migration parameter β. In figure 6-27 we present a log/log plot of normalised current as a function of reaction/diffusion parameter β. The shape of the plot changes as the value of the migration parameter varies from large negative values to large positive values. for instance, for $\beta = 0$, the plot of log y_{ss} versus log γ exhibits a clear "dog-leg" form with the slope changing from unity to 0.5 with increasing γ value. This behaviour can be readily understood as follows. for instance , when $\beta = 0$ we note that equation (6.22) predicts that when γ is small, $tanh\sqrt{\gamma} \approx \sqrt{\gamma}$ and so $y \approx \gamma$ and so the log/log plot should exhibit a slope of unity. On the other hand, when γ is large we note that $tanh\sqrt{\gamma} \approx 1$ and $y_{ss} \approx \sqrt{\gamma}$ and the slope of the double logarithm plot should be 0.5. This is indeed as observed in figure 6-27. The situation is more complicated when the migration parameter is finite. For instance, if we assume that the reaction/diffusion parameter is large and that $\gamma >> \frac{\beta^2}{4}$ or $\sqrt{\gamma} = \frac{L}{X_k} >> \frac{\beta}{2}$ then we can assume that $\tanh \sqrt{\gamma} + \frac{\beta^2}{4} \approx \tanh \sqrt{\beta}$ and so the current response presented in equation (6.22) reduces to

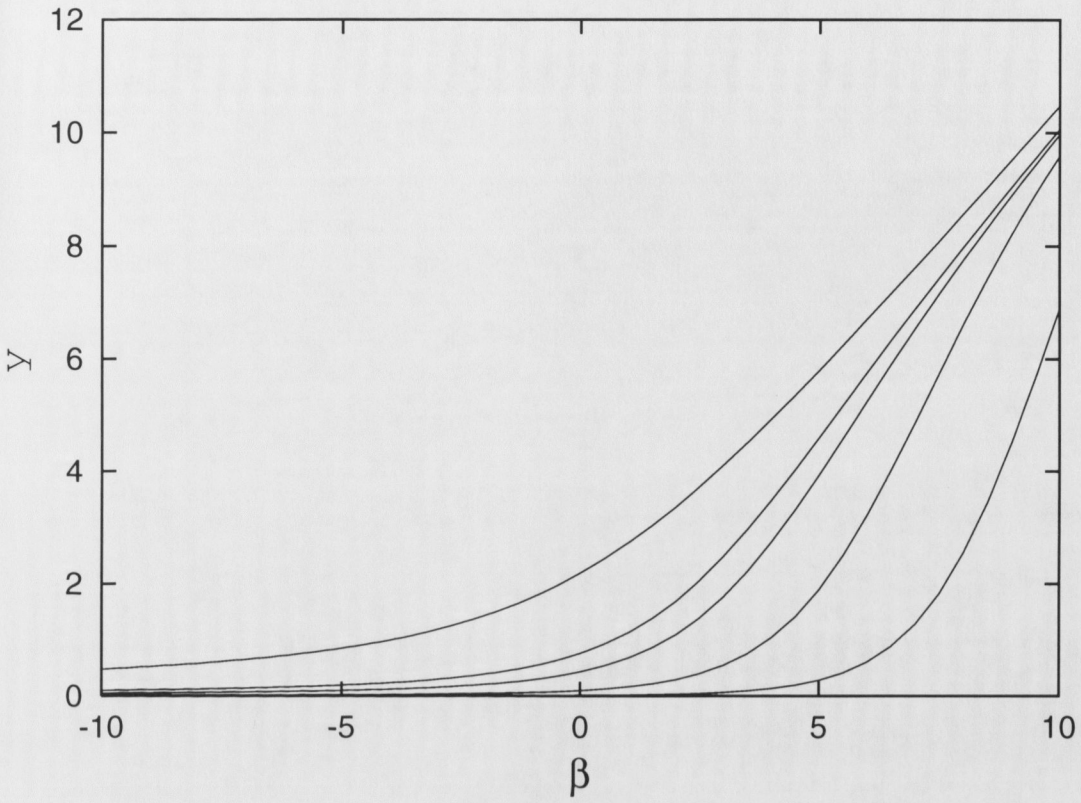

Figure 6-26: Variation of normalised steady state current response with migration parameter β. Data are presented for the region of small and large γ values. The γ values are $\gamma = 0.01, 0.1, 0.5, 1, 5$ from top to bottom.

$$y_{ss} \approx \frac{2\gamma\sqrt{\gamma}}{2\gamma + \beta \tanh\sqrt{\gamma}} \tag{6.23}$$

Now since $\sqrt{\gamma}$ is large we can assume that $\tanh\sqrt{\gamma} \approx 1$ and so equation (6.23) reduces to

$$y_{ss} \approx \frac{2\gamma}{2\sqrt{\gamma} + \beta} = \frac{\sqrt{\gamma}}{1 + \frac{\beta}{2\sqrt{\gamma}}} \longrightarrow \sqrt{\gamma}\left(\frac{\gamma\text{large}}{\beta\text{small}}\right) \tag{6.24}$$

Hence when $\sqrt{\gamma}$ is large we note from equation (6.23) that the normalised current response would increase with $\sqrt{\gamma}$ but that the rate of increase is moderated by the electric filed dependent factor $\left(1 + \frac{\beta}{2\sqrt{\gamma}}\right)^{-1}$.

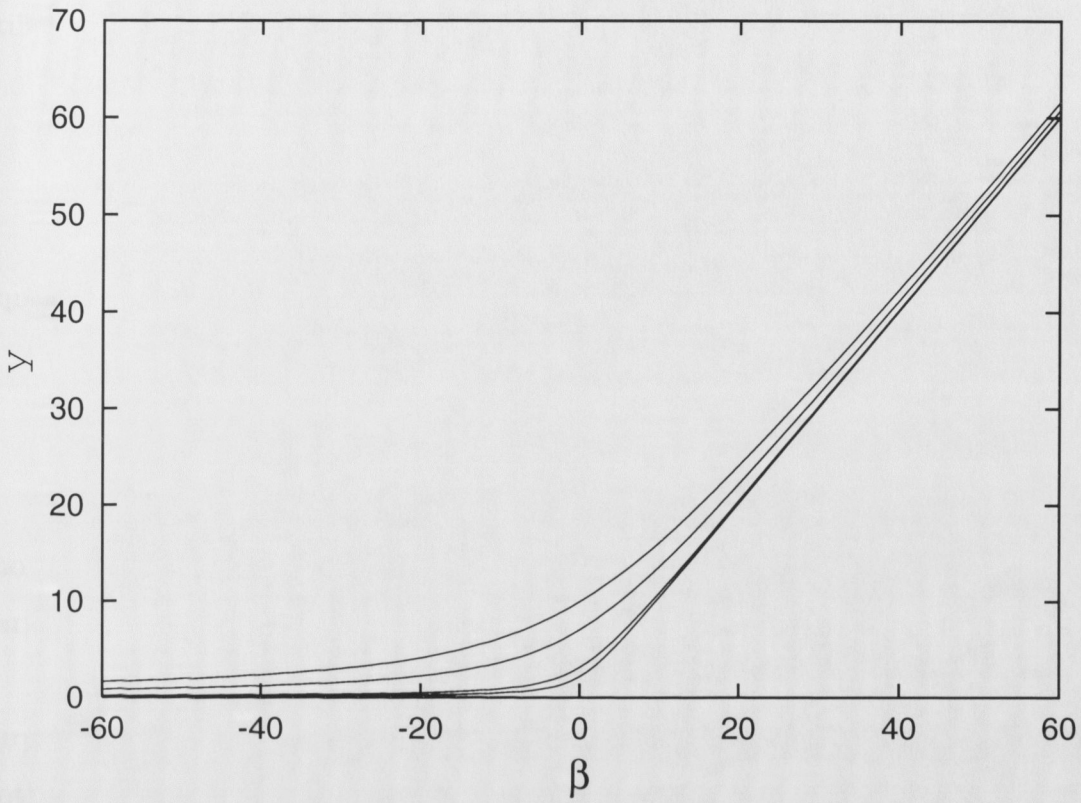

Figure 6-27: Double logarithmic plot illustrating the variation of normalised current with reaction/diffusion parameter γ for a wide range of β values. $\gamma = 5, 10, 50, 100$ from top to bottom.

In contrast, when $\sqrt{\gamma} << \frac{\beta}{2}$ we can assume that $\sqrt{\gamma + \frac{\beta^2}{4}} \approx \frac{\beta}{2}$ and so the current response reduces to

$$y_{ss} \approx \frac{2\frac{\gamma}{\beta}\tanh\frac{\beta}{2}}{1+\tanh\frac{\beta}{2}} \tag{6.25}$$

In this case the hyperbolic functions involve the migration parameter alone. Now if the migration parameter is very large and the diffusion /reaction parameter is small, then $\tanh\frac{\beta}{2} \approx 1$ and equation (6.25) reduces to

$$y_{ss} \approx 2\beta^{-1}\gamma \tag{6.26}$$

If the migration parameter is small but the diffusion.reaction parameter is still smaller, then we can write $\tanh \frac{\beta}{2} \approx \frac{\beta}{2}$ and equation (6.25) reduces to

$$y_{ss} \approx \left(1 + \frac{\beta}{2}\right)^{-1} \gamma \tag{6.27}$$

Specifically for the range $-1 < \frac{\beta}{2} < 1$ we note that $\left(1 + \frac{\beta}{2}\right)^{-1} \approx 1 - \frac{\beta}{2}$ and so equation (6.27) simplifies further to

$$y_{ss} \approx \left(1 - \frac{\beta}{2}\right) \gamma \longrightarrow \gamma(\beta \to 0) \tag{6.28}$$

Hence for small values of γ we predict that the normalised current response y should vary linearly with the reaction/diffusion parameter γ, but the rate of this variation will depend on the field-dependent factor $\left(1 + \frac{\beta}{2}\right)^{-1}$.

When the latter limiting forms of equation (6.22) are considered it is not surprising that the simple dog-leg behaviour exhibited by the $\beta = 0$ situation is not observed for finite no-zero β values. The slope of unity is observed over most of the range of γ values examined when β is negative. However when β si positive the unity slope region in the double logarithmic plot is observed only over a more restricted range of γ values. When β is large and positive, very little variation of normalised current y with reaction/diffusion parameter γ is observed.

We can obtain a further insight into the transport and kinetics by comparing selected critical values of the flux reaction parameter $\frac{\beta}{\gamma} = \frac{j_M}{j_R}$ with selected values of the reaction/diffusion parameter $\gamma = \frac{j_R}{j_D}$. This exercise results in the construction of a schematic case diagram which is presented in figure 6-28. For all values of $\frac{\beta}{\gamma}$ and when γ is large, the reaction is diffusion controlled. In the upper right hand quadrant the reaction flux will be much larger than the reaction flux and both will be much larger than the flux due to substrate diffusion. In the lower right hand quadrant the reaction flux will be much larger than the electromigration flux, which is in turn much larger than the diffusion flux. both

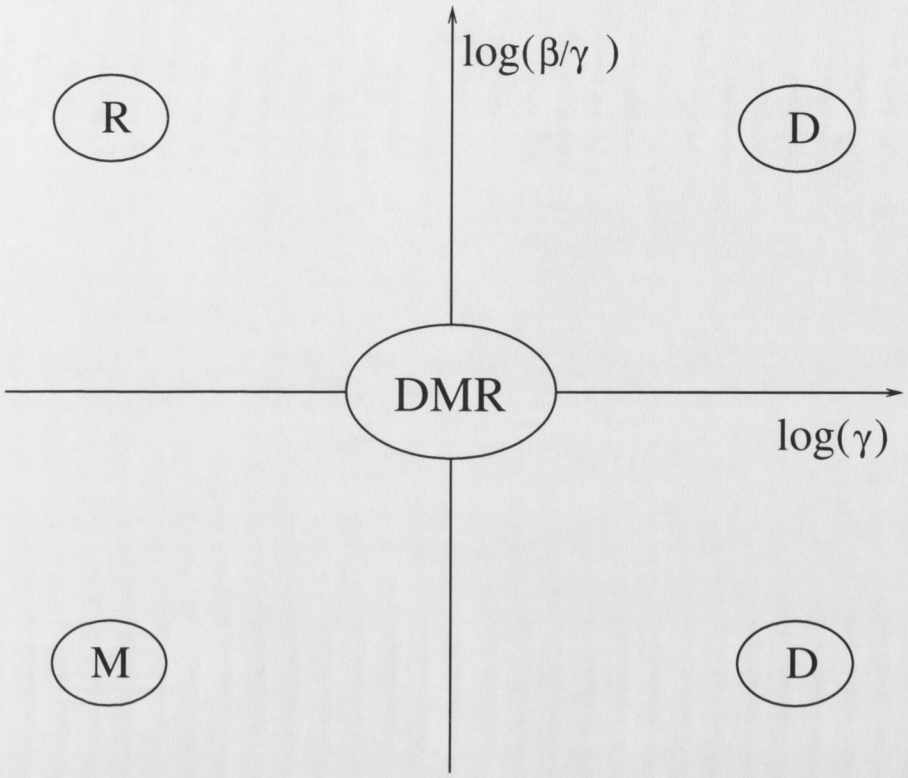

Figure 6-28: Schematic case diagram illustrating the possible rate-determining steps as a function of the parameters $\frac{\beta}{\gamma}$ and γ

of these situations are designated case D. in contrast in the upper left hand quadrant when $\frac{\beta}{\gamma}$ is large and when γ is small the net reaction rate or current will be controlled by a slow rate determining chemical reaction. this is designated R. In this quadrant the electromigration flux is greatest. In the lower left-hand quadrant when $\frac{\beta}{\gamma}$ is small and when γ is small, the net current will be governed by the electromigration flux. This is case M. Here the flux due to substrate diffusion will be largest. In the region close to the origin of the coordinate system, the general DMR applies where $\frac{\beta}{\gamma} = \gamma = 1$. In this region the current will be equally determined by each of the underlying processes.

As discussed earlier, the transient current response is given by

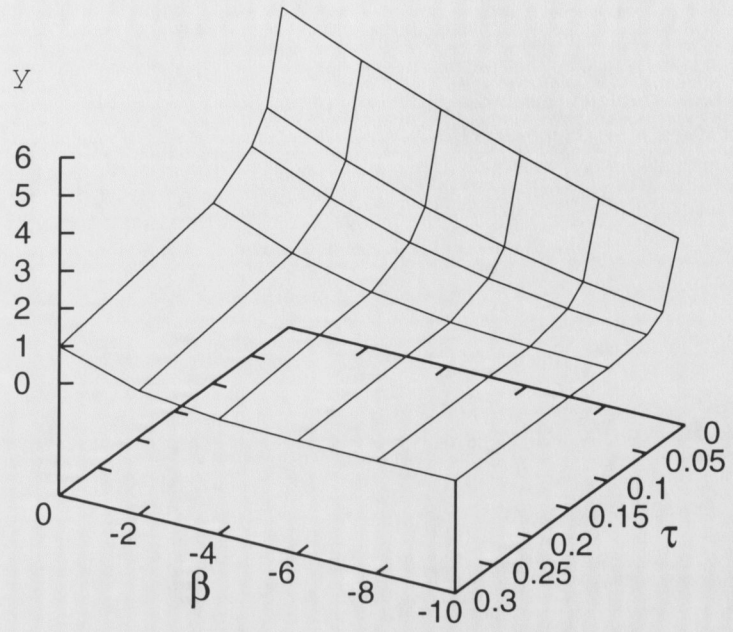

Figure 6-29: Transient current plot illustrating how the current response varies as a function of time for different negative values of β. The variation with time is best seen with negative β (*c.f.* figure 6-26 where there is a large variation in current response for positive β). The reaction parameter $\gamma = 0$.

$$y = \left(\frac{\partial u}{\partial \chi}\right)_{\chi=1} \tag{6.29}$$

The derivative of equation (6.14) was evaluated at $\chi = 1$. It comes out as

$$y_{tr} = y_{ss} - \sum_{n=0}^{\infty} b_n D_n \exp(-\lambda^2 \tau) \tag{6.30}$$

All the terms have been defined earlier in the chapter. Unfortunately the appearance of a transcendental function in the form of b_n makes evaluation difficult.

In figure 6-29 we show how the current response changes over time.

6.6.5 Concluding Comments

The effect of substrate electromigration within an electrodeposited elcectroactive polymer thin film sensor on the shape of both the substrate concentration profiles and the amperometric current response has been elucidated via the analytical solution of the governing reaction/diffusion migration differential equation for the steady state case and numerical finite difference method for the time dependent case. The electromigration effect has been quantified in terms of a parameter β which depends on the magnitude of the electric field strength to the diffusion flux. The effect of the internal electric field will be most apparent when the reaction/diffusion parameter γ is small (the γ parameter reflecting the ratio of the chemical reaction flux to the diffusion flux). Hence the electromigration will be relatively unimportant when the rate of chemical reaction is large compared with the rate of substrate diffusion. Under such circumstances the mediated reaction takes place in a reaction layer at the polymer/solution interface, which is of molecular dimension.

This analysis is also restricted in scope in that we only consider the situation where the reaction kinetics are first order in substrate concentration. Consequently the analysis will only be valid for situations where the substrate concentration in the film will be less than the Michaelis constant K_M. Under such conditions we expect that the layer will be unsaturated, i.e. not all polymer active sites will be occupied by the substrate. This work will be performed in this laboratory in the future.

Chapter 7

Concluding Remarks

The work contained in this thesis describes mathematical modelling of two physico-chemical phenomena, namely transdermal drug delivery and charge transfer in polymer modified electrodes. We have used both numerical and analytical techniques for the purpose of modelling.

Initially we looked at the finite element method and the associated software package ANSYS. We examined diffusion of a drug from an external patch into the skin and then further diffusion of the drug through the layers of the skin. Although this analysis gave good insight, we also saw the limitations of the package and concluded that it was not yet versatile or sophisticated enough to cope with our systems.

We then looked at analytical methods for solving the equations of diffusion. These are discussed in chapter 5. While analytical methods are undoubtedly superior to numerical methods, we can be faced with tedious mathematics. For the purpose of comparison with experiment, it is necessary to find a simpler approximation by deciding which of the parameters may be eliminated. This is a possibility for future work in the area. Chapters 4 and 6 describe how the diffusion equation was solved numerically, using the finite element package DEQSOL. Both of these analysis have helped to give a clearer insight into the physico-chemical

phenomena they describe.

In all cases we have developed partial differential equations to describe the processes of diffusion. The solution of these equations describes the concentration as a function of distance, time and the reaction and migration parameters. In order to concur with experiment, time-lag and transient kinetic studies have been carried out, or in some cases, the concentration expression has been manipulated in order to obtain an expression for amount of material which has passed through a particular region as a function of time.

Our models are that of bulk diffusion through the system. The systems have been examined on a macroscopic level. In order to obtain further insight into both systems, it might be useful to carry out a microscopic diffusion analysis where diffusion is described in terms of Brownian motion and a random walk.

The two software packages used for numerical simulations have distinct characteristics and differences. The finite difference package DEQSOL is ideal for the beginner. It is user-friendly and good for solving systems with simple geometries. For more systems with more complicated geometries however, the finite element method is better and ANSYS is useful in this regard. However, this package is not as user-friendly and the beginner may obtain strange results if he has not clearly defined all the parameters of the problem.

The availability of resources changes over the three to four years of Ph.D. research. During the course of this work, a new supercomputer was purchased and is used jointly by Trinity College and Queen's University, Belfast. The arrival of this computer has created more opportunities to advance work in modelling and simulation. For example, a joint project between Hitachi and Pharmaceutics Department was developed with the aim of simulating drug dissolution in the human stomach. The applications of computers in chemical modelling are boundless. This research still forms part of the *foundation* of physico-chemical modelling.

Appendix A

Numerical input files

In this appendix we will present a typical DEQSOL input file followed by a detailed line-by-line explanation on the meaning of each part of the code. We will then show how an ANSYS model is created. Since the ANSYS program is menu driven, the exact file is not presented.

A.1 DEQSOL sample input file

The following is a DEQSOL input file which was used in the solution of one of the equations discussed in the thesis.

```
1  PROG E2;
2  METHOD FDM;
3  DOMAIN X=[0:1];
4  TIME T=[0:.05];
5  TSTEP DLT=[0(.0001).05];
6  MESH X=[0:1:300];
7  REGION R=(1),
   L=(0),
   WHOLE=(*);
8  VAR U,W;
9  BCOND U = 0.0 AT L,
   U = 0 AT R,
   W:=U;
10 ICOND U=1 AT WHOLE,
   W:=U;
11 COUNT NT;
12 SCHEME;
13 ITER NT UNTIL NT GE 500;
14 SOLVE W OF
   (W-U)/DLT= (1/2*(DXX(U)+DXX(W))
   BY 'GAUSS' WITH EPS(1.0D-15);
15 U=W;
16 END ITER;
17 WRITE X TO FILE13;
   WRITE W TO FILE13;
18 END SCHEME;
19 END;
```

1. The program is defined and given the name E2.
2. The method of analysis is the finite difference method (FDM)
3. The domain is defined on the x as between 0 and 1.
4. The time range is from 0 to .05 in this analysis.
5. The time is divided into 500 sub steps of .0001 seconds.
6. The mesh region between 0 and 1 is divided into 300 sub-steps.
7. The region is assigned the name R(right) and L(left) for each of its boundaries. The full area is called "Whole".
8. The variables are defined as U and W.
9. The boundary conditions are defined as $u = 0$ at the left boundary, $u = 0$ at the right and the same boundary conditions apply to W as apply to U.
10. The initial condition is defined as $U = 1$ everywhere. Again, this is also true for W.
11. The name of the counter which will count the number of repetitions of the computation is called NT
12. The solving scheme is initialised.
13. The loop will run 500 times.
14. The equation to be solved is entered here in its Crank-Nicholson format.
15. The value of U is renewed.
16. The iteration is completed.
17. The results are written to file 10.

18. The scheme is ended.

19. The program is complete.

A.2 ANSYS procedure

PREFERENCES
structural thermal or electromagnetic
PREPROCESSOR
Define Element Type (Plane55)
Define Real Constants
Define Material Properties (therm. conductivity, density, heat cap.)
Create model using key points lines and areas
Mesh Model
SOLUTION
Define Analysis Type (transient)
Loads
Apply initial conditions
Set time and timestep
Solve
GENERAL POSTPROCESSOR
Plot Results (nodal soln, temperature)

Appendix B

Analytical methods used to solve Partial Differential Equations

B.1 Separation of Variables

In the case of diffusion, the solution – the value of concentration at a particular point and a particular time – is given by $u(\chi, \tau)$. Using the separation of variables technique u is separated into two functions $X(\chi)$ and $T(\tau)$. It is assumed that the variables are separable. The solution of the diffusion equation is given by

$$u = X(\chi)T(\tau) \tag{B.1}$$

where X is a function of χ only and T is a function only of τ. Equation B.1 then becomes

$$XT' = TX'' \tag{B.2}$$

This may then be rearranged (the variables separated) to give

$$\frac{X''}{X} = \frac{T'}{T} = -\lambda^2 \tag{B.3}$$

where $-\lambda^2$ is an arbitrary constant.

We therefore have two ordinary differential equations

$$\frac{X''}{X} = -\lambda^2 \tag{B.4}$$

and

$$\frac{T'}{T} = -\lambda^2 \tag{B.5}$$

These are solved to give

$$X = A\sin(\lambda\chi) + B\cos(\lambda\chi) \tag{B.6}$$

and

$$T = e^{-\lambda^2\tau} \tag{B.7}$$

The two separate solutions are then reunited to give

$$u = e^{-\lambda^2\tau}[A\sin(\lambda\chi) + B\cos(\lambda\chi)] \tag{B.8}$$

This is the general solution, and the constants A, B and λ are determined by satisfying the particular initial and boundary conditions. We will apply this to the following boundary conditions:

$$u(0,\tau) = 0, \quad u(1,\tau) = 0 \tag{B.9}$$

Inserting the first condition:

$$u(0,\tau) = 0 = e^{-\lambda^2\tau}[B] \tag{B.10}$$

From this we see that $B = 0$.

$$u(1,\tau) = 0 = e^{-\lambda^2\tau}[A\sin(\lambda)] \tag{B.11}$$

Therefore $\lambda = n\pi$. The initial condition gives a value for A:

$$u(\chi,0) = 1 = A\sin(n\pi\chi). \tag{B.12}$$

Checking for orthogonality this is

$$\int_0^1 A_n \sin(n\pi\chi)\sin(m\pi\chi)\mathrm{d}\chi = 2\delta_{\mathrm{nm}} \tag{B.13}$$

$$\delta_{nm} = \begin{cases} 1 & \text{if} \quad m = n \\ 0 & \text{if} \quad m \neq n \end{cases} \tag{B.14}$$

Therefore A is given by

$$A_n = \frac{4}{n\pi} \tag{B.15}$$

where n is odd. The particular solution is therefore:

$$u = \frac{4}{\pi}\sum_{n=0}^{\infty}\frac{1}{2n+1}e^{-(2n+1)^2\pi^2\tau}\sin((2n+1)\pi\chi). \tag{B.16}$$

This, as we recall, is a well known solution to the diffusion equation and it describes the passive form of planar diffusion of a substrate from a matrix. In the next section, we will show how this same equation is solved using the method of Laplace transforms.

B.2 Laplace Transforms

Laplace Transforms are a powerful technique in solving differential equations which are dependent on both space and time. The methodology has been discussed at length in a number of textbooks (Spiegel (1965) Kreyzig (1993)). Application of the Laplace transform to a differential equation results in the removal of the time variable and an ordinary differential equation which is purely space dependent remains. The solution of this equation is then easier to obtain. The solution to the differential equation of interest is obtained by finding the inverse Laplace transform of the solution of the purely space dependent equation.

The inverse Laplace transform of a function is then found either via a variety of special techniques (Spiegel (1965)), through tables (McCollum (1965))

or more generally via the Complex Inversion formula. The choice of inversion depends on the complexity of the transform.

If the Laplace transform of a function $f(t)$ is $f(p)$, where p is the Laplace parameter then

$$f(p) = \int_0^\infty e^{pt} f(t) \mathrm{d}t \tag{B.17}$$

B.2.1 Laplace form of the diffusion equation

The diffusion equation is given by

$$\frac{\partial u}{\partial \tau} = \frac{\partial^2 u}{\partial \chi^2} \tag{B.18}$$

From equation (B.17) we can see that

$$L(f') = pL(f) - f(0). \tag{B.19}$$

Therefore the reduced diffusion equation (equation (B.18)) is transformed as

follows:

$$p\bar{u} - 1 = \frac{\partial^2 \bar{u}}{\partial \chi^2} \tag{B.20}$$

This equation admits the following general solution

$$\bar{u} = \frac{1}{p} + A\cosh(p^{1/2}\chi) + B(\sinh p^{1/2}\chi) \tag{B.21}$$

where A and B are constants determined by the boundary conditions. Since the differential equation was transformed, the boundary conditions must also undergo a Laplace transform. So, since

$$u(0,\tau) = 0, \qquad \Rightarrow \bar{u_0} = 0 \tag{B.22}$$

$$u(1,\tau) = 0, \qquad \Rightarrow \bar{u_1} = 0 \tag{B.23}$$

$$u(\chi,0) = 1, \qquad \Rightarrow \bar{u}_{p=0} = \frac{1}{p} \tag{B.24}$$

Then,

$$U(0,\tau) = 0 = \frac{1}{p} + A \tag{B.25}$$

So

$$A = -\frac{1}{p} \tag{B.26}$$

and

$$U(1,\tau) = 0, \quad \Rightarrow \frac{1}{p} - \frac{1}{p}\cosh(p^{1/2}) + B\sinh(p^{1/2}) \tag{B.27}$$

Therefore,

$$B = \frac{\cosh(p^{1/2})}{p\sinh(p^{1/2})} - \frac{1}{p\sinh(p^{1/2})} \tag{B.28}$$

The solution then becomes

$$\bar{u} = \frac{1}{p} - \frac{\cosh(p^{1/2}x)}{p} + \frac{\cosh(p^{1/2})\sinh(p^{1/2}x)}{p\sinh(p^{1/2})} - \frac{\sinh(p^{1/2}x)}{p\sinh(p^{1/2})}. \tag{B.29}$$

B.2.2 Evaluation of the inverse Laplace Transform

The concentration is then obtained by evaluating the sum of the inverse Laplace transforms. That is

$$u(\chi,\tau) = L^{-}1[\frac{1}{p}] - L^{-}1[\frac{\cosh(p^{1/2}}{p})] + L^{-}1[\frac{\cosh(p^{1/2})\sinh(p^{1/2}x)}{p\sinh(p^{1/2})}] - L^{-}1[\frac{\sinh(p^{1/2}x)}{p\sinh(p^{1/2})}] \tag{B.30}$$

These can all be found in tables (McCollum (1965)) but for more complex terms, the complex inversion formula must be used.

B.3 The Complex Inversion Formula

The Complex inversion formula as detailed in Spiegel (1965) is as follows: If

$$f(p) = Lf(t),$$

then

$$L^{-1}f(p)$$

is given by

$$F(t) = \frac{1}{2\pi i}\int_{\gamma-i\infty}^{\gamma+i\infty} e^{pt}f(p)\mathrm{d}s$$

The integral is evaluated using the Bromwich contour: $\frac{1}{2\pi i}\int^C e^{st}f(p)\mathrm{d}p$ where C is the contour line shown in figure B-1. If we represent the arc by Γ, it follows

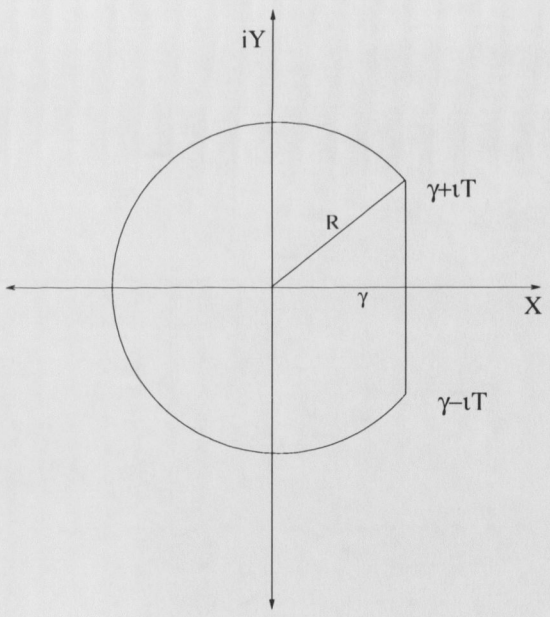

Figure B-1: Bromwich Contour represented by a circle cut off by the line $X = \gamma$

that since $T^2 = R^2 - \gamma^2$,

$$F(t) = \lim_{R\to\infty}\frac{1}{2\pi i}\int_{\gamma-iT}^{\gamma+iT} e^{pt}f(p)\mathrm{d}p$$

$$F(t) = \lim_{R\to\infty}[\frac{1}{2\pi i}\int_{\gamma-i\infty}^{\gamma+i\infty} e^{pt}f(p)\mathrm{d}p - \frac{1}{2\pi i}\int_{\gamma-i\infty}^{\gamma+i\infty} e^{pt}f(p)\mathrm{d}p]$$

If we choose γ such that the only singularities of $f(p)$ are poles all of which lie to the left of the line $s = \gamma$ for some real constant γ, and the integral around Γ approaches zero as $R \to \infty$, then by the residue theorem we can write

$$F(t) = \sum_{n=0}^{\infty} \text{ residues of } e^{pt}f(p) \text{ at the poles of } f(p). \tag{B.31}$$

B.3.1 Implementation of the Complex Inversion Formula

We now evaluate the individual inverse Laplace Transforms as outlined in section B.3.

$L^{-1}[\frac{1}{p}]$

The root of the denominator is $p = 0$ so the pole of the contour is at $p = 0$. The residue at pole $p = 0$ is

$$\lim_{p\to 0}(p-0)\frac{1}{p}e^{(pt)} = 1 \tag{B.32}$$

$L^{-1}[\frac{\cosh p^{1/2}}{p}]$:

Again, for this transform the pole is at $p = 0$. The residue at pole $p = 0$ is therefore

$$\lim_{p\to 0}(p-0)\frac{\cosh(p^{1/2})}{p}e^{pt} = 1. \tag{B.33}$$

$L^{-1}[\frac{\cosh p^{1/2}\sinh p^{1/2}x}{p\sinh(p^{1/2})}]$:

Here the poles are at $p = 0$ and $p = -n^2\pi^2$ (since $\sinh(p^{1/2}) = 0$) We now find the residues of

$$\frac{\cosh(p^{1/2})\sinh(p^{1/2}x)}{p\sinh(p^{1/2})}e^{pt}$$

at the poles. The residue at pole $p = 0$ is

$$\lim_{p\to 0}(p-0)\frac{\cosh(p^{1/2})\sinh(p^{1/2}x)}{p\sinh(p^{1/2})}e^{pt}. \tag{B.34}$$

Using L'hopital's rule, it turns out that the limit is $= 0$. The residue at pole $p = -n^2\pi^2$ is

$$\lim_{p\to -n^2\pi^2}(p+n^2\pi^2)\frac{\cosh p^{1/2}\sinh(p^{1/2}x)}{p\sinh(p^{1/2})}e^{pt}. \tag{B.35}$$

Again L'hopital's rule is required to evaluate the limit which is

$$-\sum_{n=0}^{\infty}\frac{2}{n\pi}\sin(n\pi x)e^{-n^2\pi^2 t}. \tag{B.36}$$

And the sum of the residues is

$$-\sum_{n=0}^{\infty}\frac{2}{n\pi}\sin n\pi x e^{-n^2\pi^2 t}. \tag{B.37}$$

Therefore

$$L^{-1}[\frac{\cosh p^{1/2}\sinh p^{1/2}x}{p\sinh p^{1/2}}] = -\sum_{n=0}^{\infty}\frac{2}{n\pi}\sin n\pi x e^{-n^2\pi^2 t}. \tag{B.38}$$

The inverse Laplace transform of $\frac{\sinh(p^{1/2}x)}{p\sinh(p^{1/2})}$ is evaluated in a similar manner. Again the poles are at $p = 0$ and $p = -n^2\pi^2$.

The residue at pole $p = 0$ is

$$\lim_{p\to 0}(p-0)\frac{\sinh(p^{1/2}x)}{p\sinh(p^{1/2})}e^{pt}. \tag{B.39}$$

This limit is evaluated as $= 0$.

The residue at pole $p = -n^2\pi^2$ is

$$\lim_{p \to -n^2\pi^2} (p + n^2\pi^2) \frac{\sinh(p^{1/2}x)}{p \sinh(p^{1/2})} e^{pt}. \tag{B.40}$$

Using L'hopital's rule this becomes

$$\sum_{n=0}^{\infty} -(-1)^n \frac{2}{n\pi} \sin(n\pi x) e^{-n^2\pi^2 t}.$$

And the sum of the residues is

$$\sum_{n=0}^{\infty} -(-1)^n \frac{2}{n\pi} \sin(n\pi x) e(-n^2\pi^2 t). \tag{B.41}$$

Therefore,

$$L^{-}1[\frac{\sinh p^{1/2}\chi}{p \sinh p^{1/2}}] = \sum_{n=0}^{\infty} -(-1)^n \frac{2}{n\pi} \sin(n\pi\chi) e^{-n^2\pi^2 t}. \tag{B.42}$$

The concentration profile is therefore given by

$$u(\chi, \tau) = \frac{2}{\pi}[\sin(n\pi\chi) e^{-(n)^2\pi^2 t} + (-1)^n \sin(n\pi x) e^{-n^2\pi^2 t}] \tag{B.43}$$

More concisely this is

$$u(\chi, \tau) = \frac{4}{\pi} \sum_{n=0}^{\infty} \frac{1}{2n+1} \sin\Big[(2n+1)\pi\chi\Big] e^{-(2n+1)^2\pi^2 t}. \tag{B.44}$$

B.4 Fourier Transforms

The final analytical method of solving a partial differential equation to be discussed here is the method of Fourier Transforms. Complete discussion on Fourier transforms are available in a variety of textbooks (Spiegel (1965); Kreyzig (1993)). We will first of all show how a function is expanded into a Fourier Series and then how the Fourier transforms arise.

B.4.1 Theory

If a function $F(x)$ is continuous, periodic and bounded, then for every point of continuity, we have

$$F(x) = \frac{a_0}{2} + \sum_{n=0}^{\infty} \left[a_n \cos(\frac{n\pi x}{l}) + b_n \sin(\frac{n\pi x}{l}) \right]. \tag{B.45}$$

This is called the Fourier Series of $F(x)$.

The finite Fourier *sine* transform of $F(x)$ in the range $0 < x < l$ is

$$f_s(n) = \int_0^l F(x) \sin(\frac{n\pi x}{l}) \mathrm{d}x. \tag{B.46}$$

where n is an integer. $F(x)$ is called the inverse finite Fourier *sine* transform of $f_s(n)$.

Similarly the finite Fourier *cosine* transform is

$$f_c(n) = \int_0^l F(x) \cos(\frac{n\pi x}{l}) \mathrm{d}x \tag{B.47}$$

Therefore, if $F(x) = u$, then

$$f_s(u) = \int_0^l u \sin(\frac{n\pi x}{l}) \mathrm{d}x \tag{B.48}$$

if $F(x) = \frac{\partial u}{\partial x}$, then

$$f_s\left(\frac{\partial u}{\partial x}\right) = \int_0^l \frac{\partial u}{\partial x} \sin(\frac{n\pi x}{l})\mathrm{d}x \tag{B.49}$$

which upon integrating by parts becomes

$$f_s\left(\frac{\partial u}{\partial x}\right) = u \sin(\frac{n\pi x}{l}) - \frac{n\pi}{l} \int_0^l u \cos(\frac{n\pi x}{l})\mathrm{d}x \tag{B.50}$$

which simplifies to

$$f_s\left(\frac{\partial u}{\partial x}\right) = -\frac{n\pi}{l} f_c(u). \tag{B.51}$$

Proceeding to evaluate $F(x) = \frac{\partial^2 u}{\partial x^2}$

$$f_s\left(\frac{\partial^2 u}{\partial x^2}\right) = -\frac{n\pi}{l} f_c\left(\frac{\partial u}{\partial x}\right) \tag{B.52}$$

$$f_s\left(\frac{\partial^2 u}{\partial x^2}\right) = \frac{n^2\pi^2}{l^2} f_s(u) + \frac{n\pi}{l}.[u(0,t) - u(l,t)\cos n\pi] \tag{B.53}$$

In a similar fashion, it can be shown that

$$f_c\left(\frac{\partial u}{\partial x}\right) = \frac{n\pi}{l} f_s(u) - [u(0,t) - u(l,t)\cos n\pi] \tag{B.54}$$

and

$$f_c\left(\frac{\partial^2 u}{\partial x^2}\right) = -\frac{n^2\pi^2}{l^2} f_s(u) + \frac{n\pi}{l}[u_x(0,t) - u_x(l,t)\cos n\pi] \tag{B.55}$$

where u_x denotes the partial derivative of u with respect to x.

Therefore, if one has boundary conditions of flux (u_x), the Fourier *cosine* transform is used to solve the differential equation whereas boundary conditions in terms of concentration dictate the use of the Fourier *sine* transform.

B.4.2 Fourier transforms applied to the diffusion equation

We recall that the problem is to solve the equation

$$\frac{\partial u}{\partial \tau} = \frac{\partial^2 u}{\partial \chi^2} \tag{B.56}$$

subject to the following initial and boundary conditions:

$u(\chi, 0) = 1 \qquad u(0, \tau) = 0 \qquad u(1, \tau) = 0$

Since we have boundary conditions involving the species concentration alone, the Fourier *sine* transform is chosen.

Equation B.56 then becomes

$$\int_0^1 \frac{\partial u}{\partial \tau} \sin(n\pi\chi) = \int_0^1 \frac{\partial^2 u}{\partial \chi^2} \sin(n\pi\chi) \tag{B.57}$$

Let

$$v = F_s(u) = \int_0^1 u \sin(n\pi\chi) \tag{B.58}$$

$$\Rightarrow \frac{\mathrm{d}v}{\mathrm{d}\tau} = -n^2\pi^2 v + n\pi(u_0 - u_1 cos(n\pi)) \tag{B.59}$$

Since $u_0 = 0$ and $u_1 = 1$, equation B.59 becomes

$$\Rightarrow \frac{\mathrm{d}v}{\mathrm{d}\tau} = -n^2\pi^2 v \tag{B.60}$$

The solution to this equation is

$$v = Ce^{-n^2\pi^2\tau} \tag{B.61}$$

.

A value for C is obtained by transforming the initial condition and inserting into equation B.61

$u(x,0) = 1, \quad \Rightarrow F_s(u_0) = \frac{1}{n\pi}[(-1)^n - 1]$ and $v(n,0) = \frac{1}{n\pi}[-1^n - 1]$

$$C = \frac{1}{n\pi}[(-1)^n - 1] \tag{B.62}$$

$$C = \frac{2^{2n+1}}{n\pi}. \tag{B.63}$$

Therefore

$$v = \frac{2^{2n+1}}{n\pi} e^{-n^2\pi^2\tau}. \tag{B.64}$$

The inverse Fourier Series of $v(= u)$ is then

$$u = 2\sum_{n=0}^{\infty} v \sin(n\pi\chi) \tag{B.65}$$

$$u = \frac{4}{\pi}\sum_{n=0}^{\infty} \frac{1}{2n+1} e^{-(2n+1)^2\pi^2\tau} \sin((2n+1)\pi\chi). \tag{B.66}$$

Appendix C

Finite Element Method

C.1 Example of implementation of the Finite Element Method

Consider the diffusion equation:

$$\frac{\partial c}{\partial t} = D\frac{\partial^2 c}{\partial x^2} \tag{C.1}$$

As with previous examples we begin by redefining the diffusion equation in non- dimensional terms. Equation (C.1) becomes

$$\frac{\partial u}{\partial \tau} = \frac{\partial^2 u}{\partial \chi^2} \tag{C.2}$$

We will further simplify things by taking $\frac{\partial u}{\partial \tau}$ to be a constant. By this we look at steady state diffusion or diffusion after a long time has elapsed. The constant $\frac{\partial u}{\partial \tau}$ is given the value F say. Then equation (C.2) becomes

$$\frac{\partial u}{\partial \tau} = F \tag{C.3}$$

In solving by variational approach this is equivalent to finding a value for u,

that minimises the functional

$$\int_0^1 [\frac{1}{2}\left(\frac{\partial u}{\partial \chi}\right)^2 - Fu]\mathrm{d}\chi$$

The finite element procedure is executed as follows: The membrane will

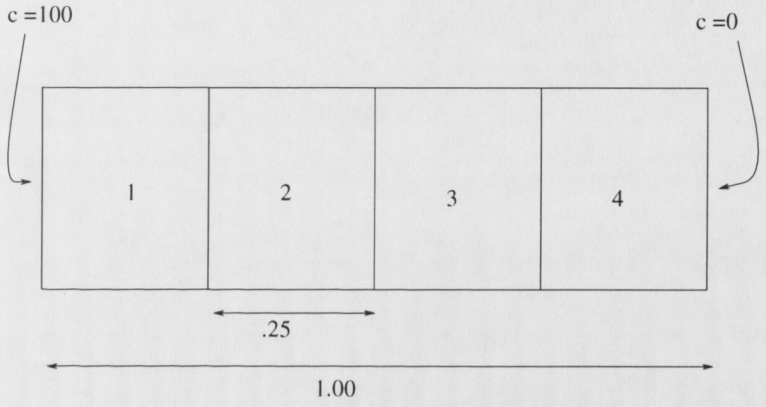

Figure C-1: Schematic diagram of the membrane meshed with four elements

be divided into four elements of equal length as shown in figure C-1. Since the membrane is 1 unit long this corresponds to elements of 0.25 units length and the functional becomes

$$\int_0^{.25} [\frac{1}{2}\left(\frac{\partial u}{\partial \chi}\right)^2 - Fu]\mathrm{d}\chi$$

for each element.

We will select linear interpolation functions to describe the concentration variation so that for each element the concentration at each node is described by

$$u_n = \alpha_1 + \alpha_2 \chi_n \tag{C.4}$$

where $n = 1, 2, 3, 4, 5$.

The concentration in a particular element is then given by

$$u = N_i u_i + N_{i+1} u_{i+1} \tag{C.5}$$

where i is the number of the element and c_i is the concentration at the i^{th} node. Therefore the concentration in the first element is given by

$$u = N_1 u_1 + N_2 u_2 \tag{C.6}$$

It can be shown that

$$N_1 = \frac{\chi_{i+1} - \chi}{\chi_{i+1} - \chi_i} \quad N_2 = \frac{\chi - \chi_i}{\chi_{i+1} - \chi_i} \tag{C.7}$$

Since $\chi_{i+1} - \chi_i = L = \frac{1}{.25}$, it follows that

$$N_1 = \frac{1 - \chi}{L} \quad N_2 = \frac{\chi}{L} \tag{C.8}$$

It is customary to write this in matrix form as

$$u = \begin{bmatrix} \mathrm{N}_1 & N_2 \end{bmatrix} \begin{bmatrix} u_1 \\ u_2 \end{bmatrix} \tag{C.9}$$

More concisely this is

$$u = [N][U] \tag{C.10}$$

$$\frac{\partial u}{\partial \chi} = \frac{-1}{.25} u_1 + \frac{1}{.25} u_2 \tag{C.11}$$

In matrix form this becomes

$$\frac{\partial u}{\partial \chi} = \begin{bmatrix} 1/L & 1/L \end{bmatrix} \begin{bmatrix} u_1 \\ u_2 \end{bmatrix} \tag{C.12}$$

or again more concisely

$$\frac{\partial u}{\partial \chi} = [B][U] \tag{C.13}$$

The functional is then rewritten as

$$\int_0^{.25} \frac{1}{2}[B]^T[U]^T[B][U] - [F][N][U]\mathrm{d}\chi \tag{C.14}$$

Minimising with respect to [U], this becomes

$$\int_0^{.25} \frac{1}{2}[B]^T[B][U] - [F][N]\mathrm{d}\chi = 0 \tag{C.15}$$

or

$$\int_0^{.25} \frac{1}{2}\begin{bmatrix} -1/L \\ 1/L \end{bmatrix}\begin{bmatrix} 1/L & 1/L \end{bmatrix}[U] - [F]\begin{bmatrix} 1 - x/L \\ x/L \end{bmatrix}\mathrm{d}\chi = 0 \tag{C.16}$$

Upon performing the integration this becomes

$$\begin{bmatrix} 1/L & -1/L \\ -1/L & 1/L \end{bmatrix}_0^L [U] = [F]\begin{bmatrix} L/2 \\ L/2 \end{bmatrix}_0^L \tag{C.17}$$

A similar expression is obtained for each of the other nodes and the entire solution is assembled to give the following:

$$1/L\begin{bmatrix} 1 & -1 & 0 & 0 & 0 \\ -1 & 2 & -1 & 0 & 0 \\ 0 & -1 & 2 & -1 & 0 \\ 0 & 0 & -1 & 2 & -1 \\ 0 & 0 & 0 & -1 & 1 \end{bmatrix}\begin{bmatrix} u_1 \\ u_2 \\ u_3 \\ u_4 \\ u_5 \end{bmatrix} = L\begin{bmatrix} F_1 \\ F_2 \\ F_3 \\ F_4 \\ F_5 \end{bmatrix} \tag{C.18}$$

This is simplified to give

$$\begin{bmatrix} 1 & -1 & 0 & 0 & 0 \\ -1 & 2 & -1 & 0 & 0 \\ 0 & -1 & 2 & -1 & 0 \\ 0 & 0 & -1 & 2 & -1 \\ 0 & 0 & 0 & -1 & 1 \end{bmatrix} \begin{bmatrix} u_1 \\ u_2 \\ u_3 \\ u_4 \\ u_5 \end{bmatrix} = L^2 \begin{bmatrix} F_1 \\ F_2 \\ F_3 \\ F_4 \\ F_5 \end{bmatrix} \tag{C.19}$$

Inserting the correct figures, ($L = 0.25$ and $F_n = 200$) together with the boundary conditions ($u_1 = 100$ and $u_5 = 0$), the matrices may be solved and the following results are produced:

$u_2 = 93.75$

$u_3 = 75$

$u_4 = 43.75$

Mathematically, the direct approach is easier to work out. Galerkin's method of weighted residuals Heubner and Thornton (1982) is also used for this type of problem and examples of these may be found in many FEA textbooks (Becker (1981); Davies (1980); Lewis and Ward (1991)).

Appendix D

Inert Matrix

In this section we will show how the expression for the transient concentration profile in chapter 4 was obtained from the pertinent diffusion equation. The method used was separation of variables and the solution is detailed as follows:

D.1 Transient Profile

Given the equation

$$\frac{\partial u}{\partial \tau} = \frac{\partial^2 u}{\partial \chi^2} - \beta \frac{\partial u}{\partial \chi} - \gamma u \tag{D.1}$$

with boundary conditions

$$J_0 = \frac{\partial u}{\partial \chi_0} - \beta u_0 = 0, \quad u(1, \tau) = 0 \tag{D.2}$$

and the initial condition

$$u(\chi, 0) = 1 \tag{D.3}$$

We may rewrite the above as

$$\frac{\partial u}{\partial \tau} = \frac{\partial^2 u}{\partial \chi^2} + 2a\frac{\partial u}{\partial \chi} + (a^2 - b^2)u \tag{D.4}$$

where

$$a = \frac{\beta}{2} \qquad \text{and} \qquad b^2 = a^2 - \gamma \tag{D.5}$$

We apply separation of variables to get

$$u = X(\chi)T(\tau) \tag{D.6}$$

Therefore

$$XT' = X''T - 2aX'T - (a^2 - b^2)XT \tag{D.7}$$

and

$$\frac{T'}{T} = \frac{X''}{X} - \beta\frac{X'}{X} - \gamma = \text{constant} = -\lambda^2 \tag{D.8}$$

The time dependent portion has the following solution:

$$T(\tau) = A\, exp(-\lambda^2\tau) \tag{D.9}$$

The X-dependent portion is solved as follows:

$$X'' - \beta X' - (\gamma - \lambda^2)X = 0 \tag{D.10}$$

We note that equation (D.10) is a second order linear differential equation with constant coefficients, and consequently in may be integrated using standard methods. We assume a solution of the following form:

$$X = A'e^{d\chi} \tag{D.11}$$

where d must be determined. Substituting the latter expression and its derivatives into equation (D.10) we obtain the following characteristic equation

$$\alpha^2 - \beta\alpha - (\gamma - \lambda^2) = 0 \tag{D.12}$$

This quadratic equation has two distinct roots given by

$$\alpha = \frac{\beta}{2} + (\frac{\beta^2}{4} + (\gamma - \lambda^2))^{\frac{1}{2}} \tag{D.13}$$

and

$$\alpha = \frac{\beta}{2} - (\frac{\beta^2}{4} + (\gamma - \lambda^2))^{\frac{1}{2}} \tag{D.14}$$

The general solution is then

$$X = e^{a\chi}[A\cos(b_2\chi) + B\sin(b_2\chi)] \tag{D.15}$$

The complete transient solution is therefore

$$u_{tr} = \sum_{n=0}^{\infty} e^{a\chi}[C\cos(b_2\chi) + D\sin(b_2\chi)]exp(-\lambda^2\tau) \tag{D.16}$$

We will now apply the boundary and initial conditions in order to obtain particular values for the arbitrary constants. To make the calculations easier, the boundary conditions will be transformed according to $\chi \to 1 - \chi$. Therefore,

$$J_0 = \frac{\partial u}{\partial \chi_0} - \beta u_0 = 0 \quad \to \quad J_1 = \frac{\partial u}{\partial \chi_1} - \beta u_1 = 0 \tag{D.17}$$

and

$$u(1,\tau) = 0 \quad \to \quad u(0,\tau) = 0 \tag{D.18}$$

The first boundary condition is applied

$$u_{tr}(0,\tau) = 0 \quad \Rightarrow C = 0 \tag{D.19}$$

The second boundary condition is applied

$$J_1 = \frac{\partial u}{\partial \chi_1} - \beta u_1 = 0 \tag{D.20}$$

$$\frac{\partial u}{\partial \chi} = ae^{-a\chi}[B\sin(b_2\chi)] + be^{-a\chi}[B\cos(b_2\chi)]exp(-\lambda^2\tau) \tag{D.21}$$

$$\frac{\partial u}{\partial \chi}_{\chi=1} - \beta u_{\chi=1} = [aB\sin(b_2) + bB\cos(b_2) - 2aB\sin(b_2)]e^{-a}exp(-\lambda^2\tau) = 0 \tag{D.22}$$

$$b\cos(b_2) - a\sin(b_2) = 0 \tag{D.23}$$

B is given by the transcendental function

$$b = a\tan b \tag{D.24}$$

We apply the initial condition

$$u(\chi, 0) = 1 \tag{D.25}$$

and get

$$u(\chi, 0) = 1 = e^{-a\chi}[B\sin(b_2\chi)] \tag{D.26}$$

Therefore

$$e^{a\chi} = [B_n\sin(b_n\chi)] \tag{D.27}$$

We multiply by $\sin(b_m\chi)$ and apply orthogonality to get a value for B_n.

$$2\sum_{m=0}^{\infty} e^{a\chi}\sin(b_m\chi) = 2\sum_{m=0}^{\infty} B_n \sin(b_n\chi)\sin(b_m\chi) \tag{D.28}$$

$$2\sum_{m=0}^{\infty} e^{a\chi}\sin(b_m\chi) = B_n \tag{D.29}$$

Replacing the summation by integration, this is

$$B_n = 2\int_0^1 e^{a\chi}\sin(b_m\chi)\mathrm{d}\chi \tag{D.30}$$

We note that $e^{ib_m\chi} = \cos(b_m\chi)+i\sin(b_m\chi)$. Therefore the integration is simplified by taking the imaginary part of $e^{ib_m\chi}$ as follows:

$$B_n = 2\int_0^1 e^{a\chi}e^{ib_m\chi}\mathrm{d}\chi \tag{D.31}$$

We perform the integration and multiply above and below by the complex conjugate of $a + ib$ in order to remove the unwanted complex numbers.

$$B_n = \frac{2}{a^2+b_m^2}e^{a\chi}[(a-ib_m)(\cos(b_m\chi)+i\sin(b_m\chi)] \tag{D.32}$$

Considering the imaginary part only:

$$B_n = \frac{2e^{a\chi}}{a^2+b_m^2}[a\sin(b_m\chi) - b_m\cos(b_m\chi)]_0^1 \tag{D.33}$$

$$B_n = \frac{8}{4a^2+4b_m^2}[e^a a\sin(b_m) - e^a b_m\cos(b_m) + b_m] \tag{D.34}$$

Remembering that

$$b = a\tan b \quad \Rightarrow \quad b_m\cos b_m = a\sin b_m \tag{D.35}$$

Therefore

$$B_n = \frac{8b_n}{\beta^2 + 4b_n^2} \tag{D.36}$$

$$u(\chi, \tau) = exp(\frac{\beta\chi}{2}) \sum_{n=0}^{\infty} B_n \sin(b_n\chi) exp(-\lambda^2 t) \tag{D.37}$$

D.2 Reduction to passive diffusion

Given the transient equation:

$$u(\chi, \tau) = exp(\frac{\beta\chi}{2}) \sum_{n=0}^{\infty} B_n \sin(b_n\chi) exp(-\lambda^2 t) \tag{D.38}$$

We set $\beta = \gamma = 0$. Therefore $a = b = 0$. The expression for the concentration profile then becomes:

$$u(\chi, \tau) = \sum_{n=0}^{\infty} \frac{8b_n}{4b_n^2} \sin(b_n\chi) exp(-\lambda^2 t) \tag{D.39}$$

Simplifying this, we get

$$u(\chi, \tau) = \sum_{n=0}^{\infty} \frac{2}{b_n} \sin(b_n\chi) exp(-\lambda^2 t) \tag{D.40}$$

Then, since

$$b_n \cos b_n = a \sin b_n = 0 \quad \Rightarrow \quad \cos b_n = 0 \tag{D.41}$$

$$b_n = \sum_{n=0}^{\infty} \frac{(2n+1)\pi}{2} \tag{D.42}$$

Therefore the expression for the concentration profile becomes:

$$u(\chi, \tau) = \sum_{n=0}^{\infty} \frac{4}{(2n+1)\pi} \sin(\frac{(2n+1)\pi\chi}{2}) \exp(-(\frac{(2n+1)\pi}{2})^2\tau) \tag{D.43}$$

When we re appy the transformation $\chi \to 1 - \chi$, this becomes

$$u(\chi,\tau) = \sum_{n=0}^{\infty} \frac{4(-1)^n}{(2n+1)\pi} \cos(\frac{(2n+1)\pi\chi}{2}) \exp(-(\frac{(2n+1)\pi}{2})^2\tau) \qquad \text{(D.44)}$$

which is exactly that obtained for the passive case equation (4.13).

Appendix E

Finite Membrane

E.1 steady state amount

The general solution to equation (5.7) is given by

$$\bar{u}(\chi, p) = A\sinh[\sqrt{p}\chi] + B\cosh[\sqrt{p}\chi] \tag{E.1}$$

Note that we choose hyperbolic functions since the diffusion space is finite and lies in the range $(0, 1)$. When $\chi = 0, \bar{u} = \frac{1}{p}$ and so $B = \frac{1}{p}$. Also when $\chi = 1, \bar{u} = 0$ and so $A = \frac{1}{p\tanh\sqrt{p}}$. Hence substitution of these quantities into equation (5.7) immediately produces

$$\begin{aligned}\bar{u} = \frac{1}{p}\cosh(\sqrt{p}\chi) &= \frac{\cosh(\sqrt{p})\sinh(\sqrt{p}\chi)}{p\sinh(\sqrt{p})} \\ = \frac{1}{p}\frac{\sinh(\sqrt{p})\cosh(\sqrt{p}\chi) - \cosh(\sqrt{p})\sinh(\sqrt{p}\chi)}{\sinh(\sqrt{p})} \\ &= \frac{1}{p}\frac{\sinh(\sqrt{p(1-\chi)}}{\sinh(\sqrt{p})}\end{aligned} \tag{E.2}$$

which results in equation (5.9) in chapter 5.

We now use the complex inversion formula to invert equation (5.9). We recall

that if $\bar{y}(p)$ represents the Laplace transform of a function $y(\tau)$, then according to the complex inversion formula we can state that:

$$y(\tau) = \frac{1}{2\pi i}\int_{c-i\infty}^{c+i\infty} \exp(p\tau)\bar{y}(p)dp = \frac{1}{2\pi i}\oint \exp(p\tau)\bar{y}(p)dp \tag{E.3}$$

where the integration in equation (E.3) is to be performed along the line $p = c$ in the complex plane where $p = x + iy$. The real number c is chosen such that $p = c$ lies to the right of all the singularities, but is otherwise assumed to be arbitrary. In practice however, the integral is evaluated by considering the contour integral presented on the *rhs* of equation (E.3) which is evaluated using the so-called Bromwich contour. The contour integral is then evaluated using the residue theorem which states that for any analytic function $F(z)$:

$$\oint F(z)dz = 2\pi i \sum_n Res[F(z)]_{z-z_n} \tag{E.4}$$

where the residues are computed at the poles of the function $F(z)$. Hence, from equation (E.3) we note that

$$y(\tau) = \sum_n Res[\exp(p\tau)\bar{y}(p)] + p = p_n \tag{E.5}$$

From the theory of complex variables we can show that the residue of a function $F(z)$ at a simple pole $z = a$ is given by

$$Res[F(z)]_{z-z_n} = Lim_{z\to a}[(z-a)F(z)] \tag{E.6}$$

Hence in order to invert equation (5.9), we need to evaluate $Res\left[\frac{\sinh(\sqrt{p\chi'}}{p\sinh(\sqrt{p})}\right]$ at the poles.

Note that we have set $\chi' = 1-\chi$. Now the poles are obtained from $p\sinh\sqrt{p} = 0$. Hence there is a simple pole at $p = 0$ (this will ultimately produce the steady state contribution to the concentration profile) and there are infinitely many poles given by the solution of the equation $\sinh\sqrt{p_n} = 0$ and so $p_n = -n^2\pi^2$ with

$n = 1, 2, 3...$.

These will ultimately produce the transient contribution to the concentration profile. Hence we note that

$$u(\chi,\tau) = Res\left[\frac{\sqrt{p\chi'}}{p\sinh\sqrt{p}}\right]_{p=0} + Res\left[\frac{\sqrt{p\chi'}}{p\sinh\sqrt{p}}\right]_{p=p_n}$$

$$= Lim_{p\to 0}(p-0)\left[\exp(p\tau)\frac{\sinh\sqrt{p\chi'}}{p\sinh\sqrt{p}}\right] + Lim_{p\to p_n}(p-p_n)\left[\exp(p\tau)\frac{\sinh\sqrt{p\chi'}}{p\sinh\sqrt{p}}\right] \quad \text{(E.7)}$$

The following Taylor series expansion of the hyperbolic terms are useful

$$\frac{\sinh\sqrt{p\chi'}}{\sinh\sqrt{p}} = \frac{\sqrt{p\chi'} + \frac{\sqrt{p\chi'}^3}{3!} + ...}{\sqrt{p} + \frac{\sqrt{p}^3}{3!} + ...} = \frac{\chi' + \frac{p\chi'}{3!} + ...}{1 + \frac{p}{3!} + ...} \quad \text{(E.8)}$$

Using this expansion we note that the first residue in equation (E.7) is given by

$$Res\left[\frac{\sinh\sqrt{p\chi'}}{\sinh\sqrt{p}}_{p=0}\right] = \lim_{p\to 0}\left[\exp(p\tau)\left(\frac{\chi' + \frac{p\chi'}{3!} + ...}{1 + \frac{p}{3!} + ...}\right)\right] \quad \text{(E.9)}$$

The second residue can be evaluated as follows. It is established that is $F(z)$ can be expressed as $F(z) = \frac{f(z)}{g(z)}$ where the functions f and g are analytic at $p = P_n$ and $g(p_n) = 0$ while $g'(p_n) \neq 0$ and $f(p_n) \neq 0$, then $Res[F(z)]_{p=p_n} = \sum_{n=1}^{\infty} \frac{f(p_n)}{g'(p_n)} \exp[p_n\tau]$.Consequently from equation (E.7) we set $f(p_n) = \frac{\sinh\sqrt{p\chi'}}{p_n}$ and $g(p_n) = \sinh\sqrt{P_n}$. Noting that $p_n = -n^2\pi^2$, then $g'(n) = \frac{1}{2n\pi i}\cosh[n\pi i] = \frac{\cos[n\pi]}{2n\pi i} = \frac{-1^n}{2n\pi i} \neq 0$. Also $f(p_n) = \frac{\sinh[\sqrt{-n^2\pi^2\chi'}]}{-n^2\pi^2} = \frac{\sinh[in\pi\chi']}{-n^2\pi^2} = \frac{i\sin[n\pi\chi']}{-n^2\pi^2}$. Hence we can show that

$$Res\left[\frac{\sinh\sqrt{p\chi'}}{\sinh\sqrt{p}}_{p=0}\right]\frac{2}{\pi}\sum_{n=1}^{\infty}\frac{-1^n}{n}\sin[n\pi\chi']\exp(n^2\pi^2\tau) \quad \text{(E.10)}$$

and the concentration profile is given by

$$u(\chi,\tau) = 1 - \chi - 2\sum n = 1^{\infty} \frac{1}{n\pi} \sin[n\pi\chi'] \tag{E.11}$$

which is equation (5.10) in the text. In arriving at equation (E.11) we have noted that $\sin[n\pi\chi'] = \sin[n\pi(1-\chi)] = -(-1)^n \sin[n\pi\chi]$. Note that the transient contribution to the concentration profile subtracts from the steady state profile as it should. We not indicate the manner in which equation (5.14) is obtained. Using equation (5.11) and equation (5.13) we obtain

$$Q(\tau) = \int_0^{\tau} \left[1 + 2\sum n = 1^{\infty} (-1)^n exp(-n^2\pi^2\tau)\right] d\tau \tag{E.12}$$

This expression simplifies to

$$Q(\tau) = \tau + 2\sum n = 1^{\infty} \frac{(-1)^n}{n^2\pi^2} - 2\sum n = 1^{\infty} \frac{(-1)^n}{n^2\pi^2} exp(-n^2\pi^2\tau) \tag{E.13}$$

We recall that $\frac{pi^2}{12} = -\sum n = 1^{\infty} \frac{(-1)^n}{n^2}$. Hence, using the latter identity we note that equation (E.13) reduces to equation (5.14) as desired.

E.2 transient amount

In this appendix we indicate how equation (5.30) was derived. We begin with equation (5.28) and evaluate the constants A and B. When $\chi = 1, \bar{u} = 0$ and so from equation (5.28) we note that

$$A = -B \tanh[\sqrt{\zeta + p}] \tag{E.14}$$

Also when $\chi = 0, \bar{u} = \frac{1}{p}$ and so

$$A = \frac{1}{p} \tag{E.15}$$

From equation (E.14) and refb2 we get

$$B = \frac{1}{\tanh[\sqrt{\zeta + p}]} \tag{E.16}$$

Hence the normalised concentration profile in Laplace space is given by

$$\begin{aligned} \bar{u}(\chi, p) &= \exp[\xi\chi]\left[\frac{\cosh\sqrt{\zeta+p}\chi}{p} - \frac{\sinh\sqrt{\zeta+p}\chi}{p\tanh\sqrt{\zeta+p}}\right] \\ &= \exp[\xi\chi]\left[\frac{\cosh\sqrt{\zeta+p}\chi}{\sinh}\sqrt{\zeta+p} - \sinh\sqrt{\zeta+p}\chi\cosh\sqrt{\zeta+p}p\sinh\sqrt{\zeta+p}\right] \\ &= \exp[\xi\chi]\left[\frac{\sqrt{\zeta+p}(1-\chi)}{p\sinh\sqrt{\zeta+p}}\right] \end{aligned} \tag{E.17}$$

which is equation (5.30) .

We now indicate how equation (E.17) may be inverted using the Heaviside expansion theorem. We firstly set $\phi^2 = p + \zeta$ and hence $\frac{\sqrt{\zeta+p}(1-\chi)}{p\sinh\sqrt{\zeta+p}} = \frac{\phi(1-\chi)}{p\sinh\phi}$.Now the Heaviside expansion theorem states that if we can express a Laplace Transform as $\bar{y}(p) = \frac{f(p)}{g(p)}$ and if we can set $g(p) = (p-\alpha_1)(p-\alpha_2)(p-\alpha_3).....(p-\alpha_n)$ where $\alpha_k, k = 1, 2, 3....$ are constants, then the inverse Laplace transform is given by

$$y(\tau) = \sum_{k-1}^{n} \frac{f(\alpha_k)}{g'(\alpha_k)}\exp(\alpha_k\tau) \tag{E.18}$$

We need to evaluate the zeroes of $p\sinh\phi = 0$. Clearly $p = 0$ is a zero and the others are given by $sinh\phi_n = -i\sin[i\phi_n] = 0$. Hence $\sin[i\phi_n] = 0$ or $\phi_n = in\pi, n = 1, 2, 3....$ Now $p_n = \phi_n^2 - \zeta = -n^2\pi^2 - \zeta$. Thus we have our roots. We can readily show that $\frac{\mathrm{d}p\sinh\phi}{\mathrm{d}p} = \sinh\phi + p\cosh\phi\frac{\mathrm{d}\phi}{\mathrm{d}p}$. Since $\phi = \sqrt{p+\zeta}$, then $\frac{\mathrm{d}\phi}{\mathrm{d}p} = \frac{1}{2\sqrt{p+\zeta}} = \frac{1}{2\phi}$. Hence $\frac{\mathrm{d}p\sinh\phi}{\mathrm{d}p}_{p=p_n} = \sinh\phi_n + p_n\cosh\phi_n\frac{1}{2\phi_n}$. We can obtain an expression for the concentration profile by considering each root in turn, $p = 0$ and $p = p_n$ and using the Heaviside expansion formula presented in equation

(E.18).

The term for $p = 0$ gives the steady state concentration profile. Here $\phi = \sqrt{\zeta}$ and so

$$u_s(\chi) = \exp[\xi\chi]\left[\frac{\sqrt{\zeta}(1-\chi)}{\sinh\sqrt{\zeta}}\right] \tag{E.19}$$

which is equation (5.32). The transient contribution to the concentration profile is given by

$$u_t(\chi,\tau) = \exp[\xi\chi]\sum_{n=1}^{\infty}\frac{\sqrt{\zeta+p_n}(1-\chi)}{\sinh\sqrt{\zeta+p_n}+\frac{p_n}{2\ sqrt\zeta+p_n\cosh\sqrt{\zeta+p_n}}}\exp(p_n\tau) \tag{E.20}$$

where $p_n = -n^2\pi^2-\zeta = -n^2\pi^2-\gamma-\frac{\beta^2}{4}$. We can readily show that $\sinh\sqrt{\zeta+p_n} = \sinh[in\pi] = i\sin[n\pi] = 0$. Also $\frac{p_n}{2\ sqrt\zeta+p_n} = \frac{-n^2\pi^2-\zeta}{2in\pi}$ and we note that $\cosh\sqrt{\zeta+p_n} = \cosh[in\pi] = \cos[n\pi](-1)^n$. We finally note that $\sinh\sqrt{\zeta+p_n}(1-\chi) = i\sin[n\pi(1-\chi)] = -i(-1)^n\sin[n\pi\chi]$. If we substitute the latter identities into equation (E.20) we obtain

$$u_t(\chi,\tau) = -2\exp[\xi\chi]\sum_{n=1}^{\infty}\frac{n\pi\sin[n\ pi\chi]}{n^2\pi^2+\zeta}\exp(-(n^2\pi^2+\zeta)\tau) \tag{E.21}$$

We now indicate how equation (5.37) is derived. The normalised release profile is given by

$$Q(\tau) = -\int_{\infty}^{\tau}\left(\frac{\partial u}{\partial\chi}\right)_{\chi=1}d\tau \tag{E.22}$$

We differentiate equation (E.19) and set $\chi = 1$ to obtain

$$\left(\frac{\partial u_s}{\partial\chi}\right)_{\chi=1} = -\exp[\xi]cosech\sqrt{\zeta} \tag{E.23}$$

Similarly from equation (E.21) we can show that

$$\left(\frac{\partial u_t}{\partial \chi}\right)_{\chi=1} = 2\exp[\xi]\sum_{n=1}^{\infty}\frac{(-1)^n n^2\pi^2}{n^2\pi^2+\zeta}\exp[-(n^2\pi^2+\zeta)\tau] \tag{E.24}$$

Hence using equation (E.22) we obtain

$$\begin{aligned} Q(\tau) = -\int_{\infty}^{\tau}\sqrt{\zeta}\exp[\xi]cosech\sqrt{\zeta}d\tau + 2\exp[\xi]\sum_{n=1}^{\infty}\frac{(-1)^n n^2\pi^2}{n^2\pi^2+\zeta}\exp[-(n^2\pi^2+\zeta)\tau]d\tau \\ = 2\exp[\xi]\sum_{n=1}^{\infty}\frac{(-1)^n n^2\pi^2}{n^2\pi^2+\zeta} + \sqrt{\zeta}\exp[\xi]cosech\sqrt{\zeta}\tau \\ -2\exp[\xi]\sum_{n=1}^{\infty}\frac{(-1)^n n^2\pi^2}{n^2\pi^2+\zeta}\exp[-(n^2\pi^2+\zeta)\tau] \end{aligned} \tag{E.25}$$

which is equation (5.37).

E.3 alternative method

In this appendix we discuss the use of the substitution presented i equation (5.34) of the paper as an alternative way of solving the RDM boundary value problem. We begin with equation (5.34)

$$u(\chi,\tau) = \exp[\xi\chi]\exp[-\zeta\tau]\omega(\chi,\tau) \tag{E.26}$$

and propose that ω obeys the simple Fick diffusion equation:

$$\frac{\partial\omega}{\partial\tau} = \frac{\partial^2\omega}{\partial\chi^2} \tag{E.27}$$

now the initial and boundary conditions for the u function are $u(\chi,0)=0, \quad u(0,\tau)=1, \quad u(1,\tau)=0$. Utilising these conditions and substituting into equation (E.26) immediately yields that ω satisfies the following initial and boundary conditions:

$$\omega(\chi,0)=0, \quad \omega(0,\tau)=\exp[\zeta\tau], \quad \omega(1,\tau)=0 \tag{E.28}$$

We now take Laplace Transforms of equation (E.27) to obtain

$$\frac{\partial^2\bar{\omega}}{\partial\chi^2}-p\bar{\omega}=0 \tag{E.29}$$

and the boundary conditions transform as

$$\bar{\omega}(0,p)=\frac{1}{p-\zeta} \quad \bar{\omega}(1,p)=0 \tag{E.30}$$

The solution to equation (E.29) has the form

$$\bar{\omega}=A\cosh[\sqrt{p\chi}]+B\sinh[\sqrt{p\chi}] \tag{E.31}$$

Now when $\chi=1,\bar{\omega}=0$ and so $A=-B\tanh\sqrt{p}$. Also when $\chi=0,\bar{\omega}=\frac{1}{p-\zeta}$ and so $A=\frac{1}{p-\zeta}$. Hence $B=\frac{1}{(p-\zeta)\tanh\sqrt{p}}$. Substituting this result into equation (E.31) yields

$$\begin{aligned}\bar{\omega}&=\frac{\cosh[\sqrt{p\chi}]}{p-\zeta}-\frac{\sinh[\sqrt{p\chi}]}{(p-\zeta)\tanh\sqrt{p}}\\ &=\frac{\cosh[\sqrt{p\chi}]\sinh[\sqrt{p}]-\sinh[\sqrt{p\chi}]\cosh[\sqrt{p}}{(p-\zeta)\sinh\sqrt{p}}\\ &\qquad\frac{\sinh\sqrt{p(1-\chi)}}{(p-\zeta)\sinh\sqrt{p}}\end{aligned} \tag{E.32}$$

which must be inverted. This can be done using tables of inverse Laplace transforms to obtain:

$$\omega(\chi,\tau)=\frac{\sinh\sqrt{\zeta(1-\chi)}}{\sinh\sqrt{\zeta}}\exp[\zeta\tau]+2\sum_{n=1}^{\infty}\frac{(-1)^n n\pi}{n^2\pi^2+\zeta}\sin[n\pi(1-\chi)]\exp[-n^2\pi^2\tau] \tag{E.33}$$

Substituting into equation (E.26) affords

$$u(\chi,\tau) = \frac{\sinh\sqrt{\zeta(1-\chi)}}{\sinh\sqrt{\zeta}}\exp[\zeta\tau]+2\exp[\eta\chi]\sum_{n=1}^{\infty}\frac{(-1)^n n\pi}{n^2\pi^2+\zeta}\sin[n\pi(1-\chi)]\exp[-(n^2\pi^2+\zeta)\tau] \tag{E.34}$$

which is equivalent to equation (5.32) and 5.33.

Appendix F

Polymer Modified Electrode

As in the two previous cases, we assume that the solution consists of a steady state term u_{ss} and a transient term u_{tr}.

The strategy for obtaining the concentration profile is set out as follows:

- Assume that the solution can be split up into a steady state term u_{ss} and a transient term u_{tr}.

$$u(\chi, \tau) = u_{ss} + u_{tr}$$

- Obtain a general solution for u_{ss}.
- Impose the boundary conditions on u_{ss} and obtain values for the arbitrary constants in the general solution.
- Solve the transient solution by separation of variables to get a general transient solution containing two arbitrary constants.
- Impose the condition that since u_{ss} satisfies the boundary conditions, $u_{tr} = 0$ at the boundaries (or if the boundary conditions are described in terms of flux, $\frac{\partial u_{tr}}{\partial \chi} = 0$).
- Impose the initial condition $u(\chi, 0) = u_{ss}(\chi) + u_{tr}(\chi, 0)$ to obtain a value for the last constant

Note: We have seen that the solution of this equation blows up when we attempt to solve it as is. We will therefore make a transformation and solve the equation where $\chi \to 1 - \chi$ and we will reverse the situation at the end.

F.1 Steady State Solution

We start with the steady state solution then: The steady state form of the differential equation is

$$\frac{\partial^2 u}{\partial \chi^2} - \beta \frac{\partial u}{\partial \chi} - \gamma u = 0 \tag{F.1}$$

This is a second order partial differential equation with constant coefficients. The general solution is given by

$$u_{ss} = e^{-a\chi} \left[A \cosh(b\chi) + B \sinh(b\chi) \right] \tag{F.2}$$

where $a = \frac{\beta}{2}$ and $b = (\frac{\beta^2}{4} + \gamma)^{\frac{1}{2}}$ and A and B are arbitrary constants. We impose the boundary condition $u(0, \tau) = 1$ and hence obtain a value for A.

$$u_{ss}(0, \tau) = e^0 \left[A \cosh(0) + B \sinh(0) \right] \tag{F.3}$$

$$1 = 1 \left[A + 0 \right] \tag{F.4}$$

Therefore $A = 1$. We impose the second boundary condition $\frac{\partial u}{\partial \chi}_{\chi=1} + \beta u_{\chi=1} = 0$ and obtain a value for the constant B.

$$\frac{\partial u}{\partial \chi} = -ae^{-a\chi} \left[A \cosh(b\chi) + B \sinh(b\chi) \right] + e^{-a\chi} \left[Ab \sinh(b\chi) + Bb \cosh(b\chi) \right] \tag{F.5}$$

$$\frac{\partial u}{\partial \chi}_{\chi=1} + \beta u_{\chi=1} = 0 \tag{F.6}$$

Therefore

$$-ae^{-a}\left[A\cosh(b)+Ba\sinh(b)\right]+be^{-a}\left[A\sinh(b)+B\cosh(b)\right] \\ +2ae^{-a}\left[A\cosh(b)+Ba\sinh(b)\right]=0 \qquad \text{(F.7)}$$

Adding we get

$$ae^{-a}\left[A\cosh(b)+Ba\sinh(b)\right]+be^{-a}\left[A\sinh(b)+B\cosh(b)\right]=0 \qquad \text{(F.8)}$$

We simplify and remembering that A = 1, this becomes

$$a\cosh(b)+Ba\sinh(b)+b\sinh(b)+Bb\cosh(b)=0 \qquad \text{(F.9)}$$

and hence the constant B is given by

$$B=-\frac{a\cosh(b)+b\sinh(b)}{a\sinh(b)+b\cosh(b)} \qquad \text{(F.10)}$$

(We also denote B by the symbol R for future reference.)

We insert the values for A and B into the general solution to obtain:

$$u_{ss}=e^{a\chi}\left[\cosh(b\chi)+\frac{a\cosh(b)+b\sinh(b)}{a\sinh(b)+b\cosh(b)}\sinh(b\chi)\right] \qquad \text{(F.11)}$$

We now solve the transient solution

F.2 Transient Solution

The technique of separation of variables is well documented in appendix B.1 and appendix D.1 and will not be repeated here. The general solution is

$$u_{tr}=\sum_{n=0}^{\infty}e^{a\chi}[C\cos(b_2\chi)+D\sin(b_2\chi)]exp(-\lambda^2\tau) \qquad \text{(F.12)}$$

where $b_2 = (\frac{\beta^2}{4} + \gamma - \lambda^2)^{\frac{1}{2}}$ and C and D are the undetermined constants. We remember that since the steady state solution satisfied the boundary conditions, that the transient values are zero. That is

$$u_{tr}(0,\tau) = 0 \qquad \frac{\partial u_{tr}}{\partial \chi}_{\chi=1} + \beta u_{\chi=1} = 0 \tag{F.13}$$

We impose the first boundary condition

$$u_{tr}(0,\tau) = 0 = \sum_{n=0}^{\infty} e^0 [C\cos(0) + D\sin(0)] exp(-\lambda^2\tau) \tag{F.14}$$

and therefore obtain that $C = 0$.

We impose the second boundary condition to obtain a value for b_2.

$$\frac{\partial u_{tr}}{\partial \chi}_{\chi=1} = \sum_{n=0}^{\infty} e^{-a} D_n exp(-\lambda^2\tau)\,[-a\sin(b_2) + b_2(\cos b_2)] \tag{F.15}$$

Therefore

$$\frac{\partial u_{tr}}{\partial \chi}_{\chi=1} + \beta u_{\chi=1} = \sum_{n=0}^{\infty} e^{-a} D_n exp(-\lambda^2\tau)\,[a\sin(b_2) + b_2(\cos b_2)] = 0 \tag{F.16}$$

Therefore, b_2 is given by the transcendental equation:

$$b_2 = -a\tan b_2 \tag{F.17}$$

The transient solution is now

$$u_{tr} = \sum_{n=0}^{\infty} e^{a\chi} [D\sin(b_2\chi)] exp(-\lambda^2\tau) \tag{F.18}$$

where all constants are determined apart from D, which will now be determined from the initial condition. We impose the initial condition:

$$u(\chi, 0) = 0 \tag{F.19}$$

Therefore

$$u_{ss} + u_{tr}(\chi, 0) = 0 \tag{F.20}$$

Inserting the values for u_{ss} and u_{tr} into the above equation we get

$$e^{-a\chi}\left[\cosh(b\chi) + \frac{-a\cosh(b) - b\sinh(b)}{a\sinh(b) + b\cosh(b)}\sinh(b\chi)\right] = -\sum_{n=0}^{\infty} e^{-a\chi}[D\sin(b_2\chi)]exp(0) \tag{F.21}$$

Simplifying this we get

$$[\cosh(b\chi) + R\sinh(b\chi)] = -\sum_{n=0}^{\infty}[D\sin(b_2\chi)] \tag{F.22}$$

We multiply both sides by $2\sin(b_m\chi)$ and apply orthogonality to get a value for B_n.

$$2\sum_{n=0}^{\infty}[\cosh(b\chi) + R\sinh(b\chi)]\sin(b_m\chi) = -2\sum_{n=0}^{\infty}[D_n\sin(b_2\chi)\sin(b_m\chi)] = D_n \tag{F.23}$$

The summation is replaced by integration and this becomes

$$D_n = 2\int_{n=0}^{\infty}[\cosh(b\chi) + R\sinh(b\chi)]\sin(b_m\chi) \tag{F.24}$$

The integration is carried out in the exact same manner as detailed in appendix D.1. The final value of D_n is given by

$$D_n = \frac{2}{b^2 + b_n^2}\Bigg[(Rb_n\cos(b_n) - b\sin(b_n))\sinh(b) \tag{F.25}$$

$$+\Big(b_n cos(b_n) - Rb\sin(b_n)\Big)\cosh(b) - b_n\Bigg] \tag{F.26}$$

Bibliography

Abramowitz, M. and Stegun, I. A. 1965 *Handbook of Mathematical functions.* Dover Publincations Inc., New York.

Abramson, H. A. and Gorin, H. H. 1940. *J. Phys. Chem.* **44** (1094).

Addicks, W., Weiner, N., Flynn, G., Curl, R. and Topp, E. 1990. *Pharm. Res.* **7** (1048).

Albery, W. J. and Hadgraft, J. 1979a. *J. Pharm. Pharmacol.* **31**(65).

Albery, W. J. and Hadgraft, J. 1979b. *J. Pharm. Pharmacol.* **31**(129).

Albery, W. J. and Hadgraft, J. 1979c. *J. Pharm. Pharmacol.* **31**(140).

Albery, W. J. and Hillman, A. R. 1984. *J. Electroanal. Chem.* **170**(27).

Albery, W.J., Guy, R. H. and Hadgraft, J. 1983. *Int. J. Pharm.* **15**(125).

Andrieux, C. P., Dumas-Bouchat, J. M., M., J. and Saveant, 1978. *J. Electroanal. Chem.* **87**(39).

Andrieux, C. P. and Saveant, J. M. 1992 *Molecular Design of Electrode Surfaces, Techniques of Chemistry, vol XXII p.207-270.* Wiley Interscience, New York.

Atkins, P. W. 1994 *Physical Chemistry 5th edn.* Freeman, New York.

Bannon, Y. 1989 *Ph. D. Thesis, University of Dublin.*

Barrer, R. M. 1951 *Diffusion in and through solids.* Cambridge Univ. Press.

Barrett, J. M. 1986 *Biology.* Prentice-Hall.

Barrett, J. S., DiSanto, A. R., Thomford, P. J., Larsen, E. M., Palazzolo, M. J. and Morales, R. J. 1997a. *Biopharm. Drug Disp.* **18** (165).

Barrett, J. S., Rohatagi, S., DeWitt, K. E., Morales, R. J. and DiSanto, A. R. 1997b. *Am. J. Ther.* **3** (298).

Bartlett, P. N. and Whitaker, R. G. 1987. *J.Electroanal. Chem.* **224**(27).

Barton, S. P. and Edwards, C. ed Marks, R. M., 1988 *The Physical Nature of the Skin.* MTP Press , Lancaster.

Becker, E. B. 1981 *Finite elements: an introduction.* Englewood Cliffs. - London: Prentice-Hall.

Berryman, J. G. 1980. *J. Math. Phys.* **21** (1326).

Berryman, J. G. and Holland, C. J. 1982. *J. Math. Phys.* **23**(983).

Black, F. and Scholes, M. 1973. *J. Political Economy* **3**(133).

Blank, H.I. 1967. *Br. J. Dermatol.* **37**(311).

Bodde, H., Kadir, R. and Mollee, H. 1990 *Prediction of Percutaneous Penetration.* IBC Technical Services, London.

Bodde, H. E. 1989. *Int. Symposium on Preseent Developments and Future Challenges in Transdermal Drug Delibery, Netherlands.*

Brady, A. B. 1991 *Ph. D. Thesis, University of Dublin.*

Bright, F. V. 1999 *Univeristy at Buffalo, State university Of New York.* Online $< http://www.chem.buffalo.edu/Dept_{H}ome_{P}age/Fac_{R}es_{I}nt/Bright/ >$.

Britz, F. 1981 *Digital Simulation in Electrochemistry - Lecture notes in Chemistry vol.23.* Springer-Verlag, Berlin.

Burghes, D., Huntley, I. and McDonald, J. 1982 *Applying Mathematics* . John wiley and Sons.

Burnette, R. R. and Marrero, D. 1986. *J. Pharm. Sci.* **75** (738).

Burnette, R.R. 1988. *Iontophoresis* (**247**).

Burnette, R.R. and Ongpipattanakul, B. 1987. *J. Pharm. Sci.* **76** (765).

Burnette, R.R. and Ongpipattanakul, B. 1988. *J. Pharm. Sci.* **77** (132).

Carlsaw, H.S. and Jaeger, J.C. 1977 *Conduction of Heat in Solids.* Clarendon Press, Oxford.

Carr, M. G., Corish, J. and Corrigan, O. I. 1997. *Int. J. Pharm.* **157**(35).

Cassidy, J. F., Ghoroghchian, J., Sararazi, F. and Pons, S. 1985. *Can. J. Chem.* **63** (3577).

Cassidy, J. F., Pons, S., Hinman, A. S. and Speiser, B. 1983. *Can. J. Chem.* **62** (716).

Chen, J. and Rosenberger, F. 1991. *J.Phys. Chem* **95** (10164).

Churchill, R.V. 1972 *Operational Mathematics.* Mc Graw Hill, New York.

Clar, E. J., Her, C. P. and Sturelle, C. G. 1975. *J. Soc. Cosmetic Chem.* **26** (337).

Clemessy, M., Courraze, G. and Herrenknecht, C. 1991. *S.T.P. Pharma Sciences* **1**(24).

Clough, R. W. 1960. *Proceedings of the ASCE Conference on Electronic Computation, Pittsburgh PA* .

Conaghey, O. M., Corish, J. and Corrigan, O. I. 1998a. *Int. J. Pharm.* **170**(215).

Conaghey, O. M., Corish, J. and Corrigan, O. I. 1998b. *Int. J. Pharm.* **170**(225).

Cooper, E. R. 1976. *J. Pharm. Sci* **65** (1396).

Corish, J. and Corrigan, O. 1990. *J. Chem. Soc, Faraday Trans.* **1990**(1317).

Crank, J. 1975 *The Mathematics of Diffusion.* Clarendon Press, Oxford.

Cross, M. and Moscardini, A. O. 1985 *Learning the art of Mathematical Modelling.* Ellis Horwood Ltd., Chichester.

Cullander, C. and Guy, R. H. 1992. *Solid State Ionics* **53**(197).

Danielson, D. A. 1973. *J. Biomechanics* **6**(539).

Davies, A. J. 1980 *The finite element method : a first approach.* Oxford University Press.

Dennis, J. C. 1968. *J. Chem. Ed.* f45 (432).

DeNuzzio, J.D. and Berner, B. 1990. *Journal of Controlled Release* **11**(105).

Desai, S.J., Simonelli, A. P. and Higuchi, W.I. 1965. *J. Pharm. Sci* **54**(1459).

Doblhofer, K. and Vorotyntsev, M. 1994 *Electroactive Polymer Electrochemistry Part I.* Plenum Press, New York.

Donbrow, M. and Friedman, M. 1975. *J. Pharm. Sci.* **64**(76).

Durrheim, H., Flynn, G. L., Higuchi, W. I. and Behl, C. R. 1980. *J. Phatm. Sci.* **69**(781).

Dym, C. L. and Ivey, E.S. 1980 *Principles of Mathematical Modelling.* Academic Press.

Evans, G.P. 1990 *(Advances in Electrochemical Science and Engineering).* VCH Weinheim.

Eve, H. 1969 *History of Mathematics.* 3rd edn.

Feldberg, S.W. 1969. *Electroana. Chemistry* **3** (199).

Feldberg, S.W. 1981. *J. Electroanal. Chem.* **127** (1).

Flynn, G. L. 1992 *Proceedings of course on Transdermal Drug Delivery.* The Center for Professional Avvancement, Amsterdam and New Jersey.

Foley, D. 1991 *Ph. D. Thesis, University of Dublin.*

Foley, D 1997 Department of Development, Elan Corporation plc, Monksland, Athlone, Co. Westmeath. .

Foley, D. and Corish, J. 1992. *Solid State Ionics* **53**(184).

Frisch, H. L and Mysels, K. J. 1983. *J. Phys. Chem.* **87**(3988).

Goldman, D. D. 1943. *J. Gen. Physiol.* **27**(37).

Goldsmith, L. A., (1989). *J. Invest. Dermat* **92** (1144).

Grztwna, Z. J. and Pertropoulos, J. H. 1983a. *J. Chem. Soc. Faraday Trans.* **79** (571).

Grztwna, Z. J. and Pertropoulos, J. H. 1983b. *J. Chem. Soc. Faraday Trans.* **79** (585).

Guy, R. H. and Hadgraft, J. 1984. *J. Pharm. Sci.* **73** (883).

Guy, R. H. and Hadgraft, J. 1985. *J. Controlled Rel* **1** (177).

Guy, R.H. and Hadgraft, J. 1982. *Int.J.Pharm.* **11** (187).

Guy, R.H. and Hadgraft, J. 1983. *J. Pharmokinetics and Biopharmaceutics* **11** (189).

Guy, R.H. and Hadgraft, J., (1980). *Int. J. Pharm.* **6** (321).

Guy, R.H. and Hadgraft, J., (1982). *Int. J. Pharm.* **11** (187).

Guy, R.H. and Hadgraft, J., (1985)a. *J. Controlled Release* **16** (177).

Guy, R.H. and Hadgraft, J., (1985)b. *Pharm. Res.* (206).

Guy, R.H., Hadgraft, J. and Maibach, H.I., (1982). *Int. J. Pharm.* **11** (119).

Guy, R.H., Hadgraft, J. and Maibach, H.I., (1985). *Toxicology and Appl. Pharm.* **78**(123).

Hadgraft, J. 1979. *Int. J. Pharm.* **2** (265).

Hadgraft, J. 1980. *Int. J. Pharm.* **1980** (229).

Hadgraft, J., (1983). *Int. J. Pharm.* **16** (255).

Harteck, P. and Schmidt, H. W. 1933. *Z. Physik. Chem.* **B 21**(447).

Heubner, K. H. and Thornton, E. A. 1982 *The Finite Element Method for Engineers.* John Wiley & Sons Inc.

Higuchi, T. 1960. *J. Soc. Cosmet. Chem* **11**(85).

Higuchi, T. 1961. *J. Pharm. Sci.* **50**(874).

Higuchi, T. 1963. *J. Pharm. Sci* **52**(1145).

Higuchi, T. and Konishi, R. 1987. *J. Contr. Rel.* **4**(85).

Higuchi, W. I. and Higuchi, T. 1960. *J. Amer. Pharm. Assoc.* **49**(598).

Higuchi, W.I. 1962. *J. Pharm. Sci* **51**(802).

Higuchi, W.I. 1967. *J. Pharm. Sci* **56**(315).

Hilman, A.R. 1987 *Electrochemical Science and Technology of Polymers.* Elsevier Amsterdam.

Honda, H., Morita, T. and Tanabe, A. 1979. *J Theor. Biol.* **81**(144).

Idson, B. 1975. *J.Pharm. Sci* **64**(901).

Ikeda, T. 1983 *Maximum Principle in Finite Element Models for Convective-Diffusion Phenomena.* North-Holland Publishing Company.

Incropera, F.P. and DeWill, D.P. 1996 *Introduction to Heat Transfer.* John Wiley & Sons.

Ito, S. 1992 *Translations of Mathematical Monographs Vol 114, Diffusion Equations.* American Mathematical Society.

Itoh, T., Xia, J., Magavi, R., Nishihata, T. and Rytting, H. 1990. *Pharm. Res.* **7** (1042).

Jenkinson, D.M. and Walton, G.S. 1974. *Vet. Rec.* **5**(8).

Joslin, T. and Pletcher, D. 1974. *J. Electroanal. Chem.* **49** (171).

Jost, W. 1960 *(Diffusion in Solids, Liquids, Gases).* Acad. Press Inc. New York.

Kasting, G. B. and Keister, J. C. 1988. *Journal of Controlled Release* **8**(195).

Keister, J.C. and Kasting, G.B. 1986. *J. Memb. Sci* **29**(155).

Klotz, I. M. and Miller, D. K. 1947. *J. Am. Chem. Soc.* **69**(2557).

Kreyzig, E. 1993 *Advanced Engineering Mathematics.* John Wiley & Sons Inc.

Kuu, W. Y. and Yalkowsky, S. H. 1985. *J. Pharm. Sci.* **74** (926).

Lamm, O. 1939. *Svensk Kem. Tid.* **51**(130).

Lasia, A. 1983. *J. Electroanal. Chem.* **146**(397).

Lasia, A. 1985. *J. Electroanal. Chem.* **191**(185).

Leduc, S. 1900. *Ann. Electrobiol.* **3** (545).

Lewis, P. E. and Ward, J. P. 1991 *The Finite element method : principles and applications and applications* . Addison-Wesley.

Leypoldt, J. K. and Gough, D. A. 1980. *J. Phys. Chem.* **84** (1058).

Lide, D. R. and Frederikse, H. P. R. 1993 *Handbook of Chemistry and Physics.* CRC press.

Ludloph, R. A., Vieth, W. R. and Frisch, H.L. 1979. *J. Phys. Chem.* **83** (2793).

Lyons, M. E. G. 1996. *Adv. Chem. Phys.* **94** (297).

Lyons, M.E.G. 1990. *Annu. Rep. C. R. Soc. Chem.* **87**(119).

Lyons, M.E.G. 1994a. *The Analyst* **119**(805).

Lyons, M.E.G. 1994b *Electroactive Polymer Electrochemistry Part I.* Plenum Press, New York.

Lyons, M.E.G., Bannon, T., Hinds, G. and Rebouillat, S. 1998a. *The Analyst* **123** (1947).

Lyons, M.E.G., Bannon, T. and Rebouillat, S. 1998b. *The Analyst* **123**:1961.

Lyons, M.E.G. and Bartlett, P.N. 1991. *J. Electroanal. Chem.* **1**(316).

Lyons, M.E.G., Cormack, D.E. Mc and Bartlett, P.N. 1989a. *J. Electroanal. Chem.* **261**(51).

Lyons, M.E.G., Cormack, D.E. Mc, Smyth, O. and Bartlett, P.N. 1989b. *Farafay Discuss.* **88**(139).

Lyons, M.E.G., Fitzgerald, C.A. and Smyth, M.R. 1994. *Analyst* **119**(855).

Lyons, M.E.G., Greer, J.C., Fitzgerald, C.A., Bannon, T. and Bartlett, P.N. 1996. *The Analyst* **121** (715).

Lyons, M.E.G., Lyons, C.H., Michas, A. and Bartlett, P.N. 1992. *Analyst* **117** (1271).

Lyons, M.E.G., Murphy, J., Bannon, T. and Rebouillat, S. 1999. *J. Solid State Electrochem.* **3**(154).

Mahmood, I., Peters, D. K. and Mason, W. D. 1994. *Biopharm. Drug Disp.* **15** (653).

Manning, G. S. 1967. *J. Phys. Chem.* **46**(4976).

Manning, G. S. 1980. *J. Phys Chem* **84** (1058).

Masada, T., Higuchi, W. I., Srinivasan, V., Roht, U., Fox, J., Behl, C. and Pons, S. 1989. *Int. J. Pharm.* **49** (57).

Mazer, N. A. 1990. *J. Controlled. Rel.* **11** (343).

McCollum, P. A. 1965 *Laplace Transform tables and theorems.* New York. - London : Holt, Rinehart and Winston.

Meyer, W., Schwarz, R. and Neurand, K. 1978. *Curr. Prob. Dermat.* **7**(39).

Michaels, A. S., Chandrasekaran, S. K. and Shaw, J. E. 1975. *A. I. Ch. E.* **21** (985).

Mishra, D. S. and Yalkowsky, S. H. 1990. *Pharm. Res.* **7** (1195).

Murray, R. W. 1992 *Molecular Design of Electrode Surfaces Vol. XXII.* Wiley-Interscience, New York .

Mysels, K. J. 1982. *J. Phys. Chem.* **86**(4684).

Mysels, K. J. and Frisch, H. L. 1984. *J. Colloid and Interface Sci.* **99**(136).

Nilson, R. R. 1993. *J. Power Sources* **41**(25).

Nolan, L. M. A. 1996 *Ph. D. Thesis, University of Dublin.*

Nolan, L. M. A., Corish, J. and Corrigan, O. I. 1993. *J. Chem Soc. Faraday Trans.* **89**(2839).

Norman, R. S. 1975. *J. Thero. Biol.* **52**(159).

Northrup, J. H. and Anson, M. L. 1929. *J. Gen. Physiol.* **12**(543).

Pan, T. S., Sun, Q. W., Fang, D. G. and Zhu, B. C. 1995. *Chin. J. Chem Eng.* **3**(88).

Parry, G.E., Silcox, A.L. Bungeand G.D., Pershing, L.K. and Pershing, D. W. 1990. *Pharm. Res.* **7**(230).

Pertropoulos, J. H. and Roussis, P. P. 1967. *J. Chem. Phys.* **47**(1496).

Pikal, M. J. 1992. *Adv. Drug Delivery Revs.* **9**(201).

Pikal, M. J. and Shah, S. 1990. *Pharm. Res.* **7** (213).

Planck, M. 1890. *Ann. Phys. Chem.* **39** (161).

Pons, S. 1984. *Electroana. Chem.* **13**(115).

Post, M. 1999 *National Research Council Canada.* Online < *http* : *//www.icpet.nrc.ca/projects/sensor_e.html* >.

Praissman, M., Miller, I. F. and Berkowitz, J. M. 1973. *J. Membr. Biol.* **11**(139).

Prendergast, P. J. 1997a. *Clin. Biomech.* **12** (343).

Prendergast, P. J. 1997b Private communication.

Prenter, P.M. 1975 *Splines and Variational Methods.* John Wiley and Sons.

Press, W. H., Teukolsky, S. A., Vettering, W. T. and Flannery, B. P. 1992 *Numerical Recipes in C.* Cambridge University Press.

Ranade, V. V. and Hollinger, M. A. 1996 *Drug Delivery Systems.* CRC Press.

Reinl, H. M., Hartlinger, A., Dettmar, P. and Bayer, T. M. 1995. *J. Invest. Dermatol* **105** (291).

Rhine, W., Sukhatme, V., Hsieh, D. S. T. and Langer, R. S. 1980 *Controlled Release of Bioactive Agents.* Acad. Press, New York.

Riviere, J. E., Williams, P. L., Hillman, R. S. and Mishky, L. M. 1992. *J. Pharm. Sci.* **81** (504).

Rohatagi, S., Barrett, J. S., DeWitt, K. E. and Morales, R. J. 1997. *Biopharm. Drug Disp.* **18** (567).

Rosen, G. 1979. *Phys. Rev. B* **19**(2398).

Rossi, P. E. 1996 *Modelling Stock Market Volatility.* Academic Press.

Rothman, S. 1954 *(Physiology and Biochemistry of the Skin).* Univ. Chicago Press.

Rougier, A., Lotte, C. and Maibach, H. I. 1987. *J. Pharm. Sci.* **76** (451).

Rougire, A., Dupuis, D., Lotte, C., Rouget, R. and Schaefer, H. 1983. *J Inv. Dermatol.* **81** (275).

Rudolph, M. 1990. *J. Electroanal. Chem.* **292**(1).

Russo, J., Lipman, A. G., Cornstock, T. J. and Page, B. C. 1980. *Am. J. Hosp. Pharm.* **37**(843).

Sanders, H. J. 1985. *Chem. Eng. News* (30).

Scheuplein, R. J. 1967. *J. Invest. Derm.* **1967**(79).

Scheuplein, R. J. and Blank, H.I. 1971. *Physiol. Rev* **51** (702).

Schogl, R. 1954. *J. Phys. Chem.* **1**(305).

Schwartz, J.B., Simonelli, A. P. and Higuchi, W.I. 1968. *J. Pharm. Sci* **57**(274).

Scott, D. C. and Hollenbeck, R. G. 1991. *Pharm. Res.* **8**(156).

Scott, E. R., White, H. S. and Phipps, J. B. 1992. *Solid State Ionics* **53** (176).

Sewell, G. 1988 *The Numerical Solution of Ordinary and Partial Differential Equations.* Academic Press Inc.

Shelly, W.B., McConahy, J. C. and Hesbacher, E. N. 1950. *J. Invest, Dermatol.* **15**(343).

Silcox, G.D., Barge, G. E. Parryand A.E., Pershing, L. K. and Pershing, D. W. 1990. *Pharm. Res.* **7**(352).

Singh, J. and Maibach, H. I. 1993. *Dermatology* **187** (235).

Singh, S. and Singh, J. 1993. *Medical Reserach reviews* **13**(569).

Solomon, E. P. 1996 *Biology.* Saunders College Publishing.

Spanier, J. and Oldham, K. B. 1987 *An atlas of functions.* Hemisphere Publishing Corporation, New York.

Speiser, B. and Pons, S. 1982a. *Can. J. Chem.* **60** (1352).

Speiser, B. and Pons, S. 1982b. *Can. J. Chem.* **60** (2463).

Speiser, B. and Pons, S. 1983. *Can. J. Chem.* **61** (156).

Spiegel, M. R. 1965 *Theory and Problems of Laplace Transforms.* Mc Graw Hill Book Company.

Stephenson, J. 1995. *Physica A* **222**(234).

Traeger, R. T. 1966 *Physical Functions of the skin.* Acad. Press, London and New York.

Tsimillis, K. and Pertropoulos, J. H. 1967. *J. Phys. Chem.* **81**(2185).

Tyle, P. 1986. *Pharm. Res.* **3**(318).

Vickers, C. F. and Wepierre, J. 1980 *Percutaneous Absorption of Steroids.* Academic Press.

Vincent, C. A. 1976. *Journal of Chemical Education* **53**(490).

Wallace, S. M. and Barnett, G. 1978. *J. Pharmokin. and Biopharm* **6** (315).

Walters, K. A. 1990 *Routes of drug administration.* Wright?

Walters, K. A. 1996 *Chemical Apsects of Drug Delivery Systems.* Cambridge, R.S.C. Information Services.

Walters, K.A. 1989. *Drugs Pharm Sci.* **35**(197).

Wilson, R. W. and Nickell, R. E. 1966. *Nuclear Engineering and Design* **4** (276).

Wring, S.A. and Hart, J.P. 1992. *The Analyst* **117** (1215).

Yamamoto, T. and Yamamoto, T. 1976. *Med. biol. Eng. Comput.* **14**(151).

Yap, W.T., Durst, R.A., Blubaugh, E.A. and Blubaugh, D.D. 1983. *J. Electroanal. Chem.* **144**(69).

Yoshida, N. H. and Roberts, M. S. 1995. *J. Pharm. Pharmacol.* **47**(883).

Zienkiewicz, O. C. and Cheung, Y. K. 1965. *The Engineer* (507).